

Silylamido Complexes of Early Transition Metals

by

Tomislav Ilkov Gountchev

B.A. (Cambridge University, England) 1994

A dissertation submitted in partial satisfaction of the
requirements for the degree of

Doctor of Philosophy

in

Chemistry

in the

GRADUATE DIVISION

of the

UNIVERSITY OF CALIFORNIA, BERKELEY

Committee in charge:

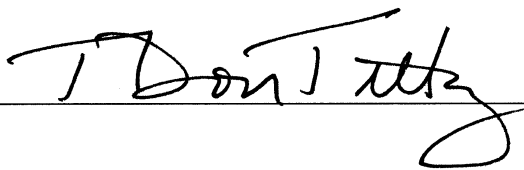
Professor T. Don Tilley, chair


Professor Robert G. Bergman

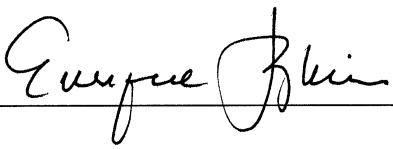
Professor Enrique Iglesia

Fall 1999

The dissertation of Tomislav Ilkov Gountchev is approved:

 9/10/99
Chair Date

 9/14/99
Date

 9/23/99
Date

University of California, Berkeley

Fall 1999

Silylamido Complexes of Early Transition Metals

Copyright © 1999

by

Tomislav Ilkov Gountchev

Abstract

Silylamido Complexes of Early Transition Metals

by

Tomislav Ilkov Gountchev

Doctor of Philosophy in Chemistry

University of California, Berkeley

Professor T. Don Tilley, Chair

This work presents the synthesis, structure, and reactivity of tantalum, yttrium and zirconium complexes with biphenyl and binaphthyl silylamido ligands.

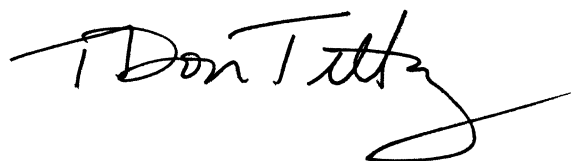
The highly bent imido complex $\text{Cp}^*\text{Ta}[\text{=N}(\text{C}_6\text{H}_3\text{Me})_2\text{NSiMe}_3]\text{Cl}$ and the methyl derivative $\text{Cp}^*\text{Ta}[\text{=N}(\text{C}_6\text{H}_3\text{Me})_2\text{NSiMe}_3]\text{Me}$ were prepared and characterized. $\text{Cp}^*\text{Ta}[\text{=N}(\text{C}_6\text{H}_3\text{Me})_2\text{NSiMe}_3]\text{Me}$ reacts with xylyl isonitrile giving an insertion product, and with MeI giving a cationic complex. Reactions of $\text{Cp}^*\text{Ta}[\text{=N}(\text{C}_6\text{H}_3\text{Me})_2\text{NSiMe}_3]\text{Cl}$ and $\text{Cp}^*\text{Ta}[\text{=N}(\text{C}_6\text{H}_3\text{Me})_2\text{NSiMe}_3]\text{Me}$ with PhSiH_3 afford the hydrides $\text{Cp}^*\text{Ta}[\text{PhSiH}_2\text{N}(\text{C}_6\text{H}_3\text{Me})_2\text{NSiMe}_3](\text{H})\text{Cl}$ and $\text{Cp}^*\text{Ta}[\text{PhSiH}_2\text{N}(\text{C}_6\text{H}_3\text{Me})_2\text{NSiMe}_3](\text{H})\text{Me}$ via addition of the Si–H bond across the Ta=N double bond. In presence of CH_2Cl_2 and PhSiH_3 , $\text{Cp}^*\text{Ta}[\text{=N}(\text{C}_6\text{H}_3\text{Me})_2\text{NSiMe}_3]\text{Cl}$ forms the complex $\text{Cp}^*\text{Ta}[\text{PhSiH}_2\text{N}(\text{C}_6\text{H}_3\text{Me})_2\text{NSiPhHCl}](\text{H})\text{Cl}$, which exhibits a nonclassical interaction between the hydride ligand and a silyl group. Reactions of PhSiH_3 and $(\text{CH}_2)_3\text{SiH}_2$ with $\text{Cp}^*\text{Ta}[\text{=N}(\text{C}_6\text{H}_3\text{Me})_2\text{NSiMe}_3]\text{Cl}$ and $\text{Cp}^*\text{Ta}[\text{=N}(\text{C}_6\text{H}_3\text{Me})_2\text{NSiMe}_3]\text{Me}$ afford the hydrides $\text{Cp}^*\text{Ta}[\text{PhSiH}_2\text{N}(\text{C}_6\text{H}_3\text{Me})_2\text{NSiMe}_3](\text{H})\text{Cl}$ and $\text{Cp}^*\text{Ta}[\text{PhSiH}_2\text{N}(\text{C}_6\text{H}_3\text{Me})_2\text{NSiMe}_3](\text{H})\text{Me}$ via addition of the Si–H bond across the Ta=N double bond. In presence of CH_2Cl_2 and PhSiH_3 , $\text{Cp}^*\text{Ta}[\text{=N}(\text{C}_6\text{H}_3\text{Me})_2\text{NSiMe}_3]\text{Cl}$ forms the complex $\text{Cp}^*\text{Ta}[\text{PhSiH}_2\text{N}(\text{C}_6\text{H}_3\text{Me})_2\text{NSiPhHCl}](\text{H})\text{Cl}$, which exhibits a nonclassical interaction between the hydride ligand and a silyl group. Reactions of PhSiH_3 and $(\text{CH}_2)_3\text{SiH}_2$ with $\text{Cp}^*\text{Ta}[\text{=N}(\text{C}_6\text{H}_3\text{Me})_2\text{NSiMe}_3]\text{Cl}$ and $\text{Cp}^*\text{Ta}[\text{=N}(\text{C}_6\text{H}_3\text{Me})_2\text{NSiMe}_3]\text{Me}$ afford the hydrides $\text{Cp}^*\text{Ta}[\text{PhSiH}_2\text{N}(\text{C}_6\text{H}_3\text{Me})_2\text{NSiMe}_3](\text{H})\text{Cl}$ and $\text{Cp}^*\text{Ta}[\text{PhSiH}_2\text{N}(\text{C}_6\text{H}_3\text{Me})_2\text{NSiMe}_3](\text{H})\text{Me}$ via addition of the Si–H bond across the Ta=N double bond. In presence of CH_2Cl_2 and PhSiH_3 , $\text{Cp}^*\text{Ta}[\text{=N}(\text{C}_6\text{H}_3\text{Me})_2\text{NSiMe}_3]\text{Cl}$ forms the complex $\text{Cp}^*\text{Ta}[\text{PhSiH}_2\text{N}(\text{C}_6\text{H}_3\text{Me})_2\text{NSiPhHCl}](\text{H})\text{Cl}$, which exhibits a nonclassical interaction between the hydride ligand and a silyl group. Reactions of PhSiH_3 and $(\text{CH}_2)_3\text{SiH}_2$ with $\text{Cp}^*\text{Ta}[\text{=N}(\text{C}_6\text{H}_3\text{Me})_2\text{NSiMe}_3]\text{Cl}$ and $\text{Cp}^*\text{Ta}[\text{=N}(\text{C}_6\text{H}_3\text{Me})_2\text{NSiMe}_3]\text{Me}$ afford the hydrides $\text{Cp}^*\text{Ta}[\text{PhSiH}_2\text{N}(\text{C}_6\text{H}_3\text{Me})_2\text{NSiMe}_3](\text{H})\text{Cl}$ and $\text{Cp}^*\text{Ta}[\text{PhSiH}_2\text{N}(\text{C}_6\text{H}_3\text{Me})_2\text{NSiMe}_3](\text{H})\text{Me}$ via addition of the Si–H bond across the Ta=N double bond. In presence of CH_2Cl_2 and PhSiH_3 , $\text{Cp}^*\text{Ta}[\text{=N}(\text{C}_6\text{H}_3\text{Me})_2\text{NSiMe}_3]\text{Cl}$ forms the complex $\text{Cp}^*\text{Ta}[\text{PhSiH}_2\text{N}(\text{C}_6\text{H}_3\text{Me})_2\text{NSiPhHCl}](\text{H})\text{Cl}$, which exhibits a nonclassical interaction between the hydride ligand and a silyl group.

NSiMe₃]Me follow second-order kinetics, with an inverse isotope effect for the PhSiH₃ addition. Elimination of HSiMe₃ from Cp*Ta[PhSiH₂N(C₆H₃Me)₂NSiMe₃](H)Me follows first-order kinetics, with approach to equilibrium, and exhibits inverse isotope effect. The proposed addition / elimination mechanism involves slow formation of pentacoordinate silicon intermediates, coupled with a fast hydride shift between Ta and Si.

The yttrium complex [DADMB]YCl(THF)₂ (DADMB = 2,2'-bis(*tert*-butyldimethylsilylamido)-6,6'-dimethylbiphenyl) and its alkyl derivatives [DADMB]YMe(THF)₂ and [DADMB]Y[CH(SiMe₃)₂](THF)(OEt₂) were prepared. In presence of silicone grease, reaction of [DADMB]YCl(THF)₂ with MeLi produces the trimethylsiloxide [DADMB]Y(OSiMe₃)(THF)₂. [DADMB]YMe(THF)₂ and [DADMB]Y[CH(SiMe₃)₂](THF)(OEt₂) react with phenylsilane or H₂ forming the dimeric hydride {[DADMB]Y(μ-H)(THF)}₂·C₆H₆. This hydride reacts rapidly with olefins via single insertion, and with pyridine, forming two isomeric 1,2- and 1,4-insertion products.

{[DADMB]Y(μ-H)(THF)}₂ catalyzes the hydrosilylation of olefins. Catalyst reactivity and selectivity for different olefins and silanes are investigated. Aliphatic olefins exhibit high preference for terminal addition, while aromatic olefins undergo mostly 2,1 addition. Both primary and secondary silanes can be employed. Using enantiopure catalyst for enantioselective hydrosilylation of norbornene yields 90% ee. Kinetic studies support a mechanism involving fast olefin insertion into the Y–H bond, followed by slow metathesis reaction of the resulting alkyl with silane.

The zirconium complexes {[DADMB]ZrCl₂}₂, [DMBN]ZrCl₂·THF (DMBN = 2,2'-bis(*tert*-butyldimethylsilylamido)-1,1'-binaphthyl), [DBMN]Zr(CH₂Ph)₂ and [DMBN]ZrMe₂·THF were prepared. With B(C₆F₅)₃, [DBMN]Zr(CH₂Ph)₂ produces the zwitterionic complex [DMBN]Zr(CH₂Ph)·[η⁶-PhCH₂B(C₆F₅)₃]. {[DADMB]ZrCl₂}₂ and [DMBN]ZrCl₂·THF are moderately active ethylene polymerization catalysts. [DBMN]Zr(CH₂Ph)₂ activated with Ph₃CB(C₆F₅)₄ polymerizes 1-hexene to low molecular weight oligomers.



To my family

Table of Contents

Title Page	i
Approval Page	ii
Dedication	iii
Table of Contents	iv
List of Figures	vi
List of Tables	viii

Chapter 1: Chelating Imido-Amido Complexes of Tantalum. Mechanistic Studies

on the Addition of Silanes to Ta = N Multiple Bonds.....	1
Introduction	2
Results and Discussion	3
Conclusions.....	30
Experimental Section.....	30
References.....	43

Chapter 2: Yttrium Complexes of the Chelating, C_2 -Symmetric, Bis(silylamido)-

biphenyl Ligand [DADMB] ²⁻ , {[6,6'-Me ₂ -(C ₆ H ₃) ₂](2,2'-NSiMe ₂ ^t Bu) ₂ } ²⁻	49
Introduction	50
Results and Discussion	50
Conclusions.....	64
Experimental Section.....	65
References.....	73

Chapter 3: Hydrosilylation Catalysis by C_2-Symmetric Bis(silylamido) Complexes	
of Yttrium	77
Introduction	78
Results and Discussion	78
Conclusions.....	95
Experimental Section.....	96
References.....	103
Chapter 4: Bis(silylamido) Complexes of Zirconium.....	106
Introduction	107
Results and Discussion	107
Conclusions.....	115
Experimental Section.....	116
References.....	123
Appendix A: Kinetic and Crystallographic Data for Chapter 1	126
Appendix B: Crystallographic Data for Chapter 2	157
Appendix C: Kinetic Data for Chapter 3	180
Appendix D: Crystallographic Data for Chapter 4	183

List of Figures

Chapter 1

- Figure 1.** ORTEP diagram of $\text{Cp}^*\text{Ta}[\text{=N}(\text{C}_6\text{H}_3\text{Me})_2\text{NSiMe}_3]\text{Cl}$ (**4**)..... 5
- Figure 2.** ORTEP diagram of $\text{Cp}^*\text{Ta}[\text{=N}(\text{C}_6\text{H}_3\text{Me})_2\text{NSiMe}_3][\eta^2\text{-(2,6-Me}_2\text{C}_6\text{H}_3)\text{N=CMe}]$ (**6**)..... 9
- Figure 3.** ORTEP diagram of $\{\text{Cp}^*\text{Ta}[\text{MeN}(\text{C}_6\text{H}_3\text{Me})_2\text{NSiMe}_3]\text{Me}\}^+\text{I}^-$ (**7**)..... 11
- Figure 4.** ORTEP diagram of $\text{Cp}^*\text{Ta}[\text{PhSiH}_2\text{N}(\text{C}_6\text{H}_3\text{Me})_2\text{NSiMe}_3](\text{H})\text{Me}$ (**9**). 14
- Figure 5.** ORTEP diagram of $\text{Cp}^*\text{Ta}[\text{PhSiH}_2\text{N}(\text{C}_6\text{H}_3\text{Me})_2\text{NSiPhHCl}](\text{H})\text{Cl}$ (**12**). 16
- Figure 6.** Pseudo-first order plots for disappearance of **5** at different PhSiH_3 concentrations..... 21
- Figure 7.** Observed pseudo-first order rate constant for disappearance of **5** (k_{obs}) as a function of the phenylsilane concentration..... 22
- Figure 8.** Pseudo-first order rate constant for disappearance of **5** as a function of silacyclobutane concentration. 25
- Figure 9.** Plot of concentrations of **9**, **11**, and HSiMe_3 vs. time for the elimination of HSiMe_3 from **9**. ($Q = [\text{11}][\text{HSiMe}_3]/[\text{9}]$). 27
- Figure 10.** Eyring plot for the rate of decomposition of **9** at different temperatures..... 29

Chapter 2

- Figure 1.** ORTEP diagram of $[\text{DADMB}]\text{YCl}(\text{THF})_2$ (**2**)..... 52
- Figure 2.** ORTEP diagram of $[\text{DADMB}]\text{Y}(\text{OSiMe}_3)(\text{THF})_2$ (**4**)..... 53
- Figure 3.** ORTEP diagram of $\{[\text{DADMB}]\text{YH}(\text{THF})\}_2\cdot\text{C}_6\text{H}_6$ (**6**). 58

Figure 4. ORTEP diagram of [DADMB]Y(NC ₅ H ₆)(NC ₅ H ₅) ₂ ·C ₅ H ₁₂ (9).....	62
---	----

Chapter 3

Figure 1. Temperature dependence of the chemical shift of the diastereotopic THF α -protons in 1	84
Figure 2. Pseudo-first order plots for disappearance of 1 at different PhMeSiH ₂ concentrations (298 K, benzene- <i>d</i> ₆).....	87
Figure 3. Pseudo-first order rate constant for disappearance of 1 as a function of phenylmethylsilane concentration (298 K, benzene- <i>d</i> ₆).	88
Figure 4. Pseudo-first order plots for consumption of PhMeSiH ₂ at different concentrations of 1 and 1-hexene (298 K, benzene- <i>d</i> ₆).	89
Figure 5. Observed pseudo-first order rate constant for PhMeSiH ₂ consumption as a function of the 1-hexene concentration, at constant catalyst precursor concentration (298 K, benzene- <i>d</i> ₆).	90
Figure 6. Observed pseudo-first order rate constant for PhMeSiH ₂ consumption as a function of the catalyst precursor concentration, at constant initial 1-hexene concentration (298 K, benzene- <i>d</i> ₆).	91
Figure 7. Pseudo-first order plots for consumption of PhMeSiH ₂ at different concentrations of 1 (298 K, THF- <i>d</i> ₈).....	93
Figure 8. Observed rate constant for consumption of PhMeSiH ₂ (initial rate) as a function of the initial concentration of 1 (298 K, THF- <i>d</i> ₈).	94

Chapter 4

Figure 1. ORTEP diagram of {[DADMB]ZrCl ₂ } ₂ (3).	108
Figure 2. ORTEP diagram of [DMBN]Zr(CH ₂ Ph)[η^6 -PhCH ₂ B(C ₆ F ₅) ₃] (7).....	113

List of Tables

Chapter 3

Table 1. Results from the hydrosilylation of olefins	81
---	----

Appendix A

Table 1. Observed pseudo-first order rate constants for disappearance of 5 at different phenylsilane concentrations.....	127
Table 2. Observed pseudo-first order rate constants for disappearance of 5 at different concentrations of (CH ₂) ₃ SiH ₂	127
Table 3. First order rate constants for decomposition of 9 and 9-d₃ , at different starting concentrations, using initial rates.....	128
Table 4. First order rate constants for decomposition of 9 , at five different temperatures.....	128
Table 5. Crystallographic data for compounds 4 , 6 ·1/2Et ₂ O, and 7	129
Table 5 (cont). Crystallographic data for compounds 9 and 12	131
Table 6. Atomic coordinates and B _{iso} /B _{eq} for Cp*Ta[=N(C ₆ H ₃ Me) ₂ NSiMe ₃]Cl (4).....	133
Table 7. Anisotropic Displacement Parameters for Cp*Ta[=N(C ₆ H ₃ Me) ₂ NSiMe ₃]Cl (4).....	134
Table 8. Bond Lengths (Å) for Cp*Ta[=N(C ₆ H ₃ Me) ₂ NSiMe ₃]Cl (4).....	135
Table 9. Bond Angles (°) for Cp*Ta[=N(C ₆ H ₃ Me) ₂ NSiMe ₃]Cl (4).	135
Table 10. Least Squares Planes for Cp*Ta[=N(C ₆ H ₃ Me) ₂ NSiMe ₃]Cl (4).....	136
Table 11. Atomic coordinates and B _{iso} /B _{eq} for Cp*Ta[=N(C ₆ H ₃ Me) ₂ NSiMe ₃][η ² -(2,6-Me ₂ C ₆ H ₃)N=CMe]·1/2Et ₂ O (6 ·1/2Et ₂ O).	137
Table 12. Anisotropic Displacement Parameters for Cp*Ta[=N(C ₆ H ₃ Me) ₂ NSiMe ₃][η ² -(2,6-Me ₂ C ₆ H ₃)N=CMe]·1/2Et ₂ O (6 ·1/2Et ₂ O).....	138

Table 13. Bond Lengths (Å) for Cp*Ta[=N-(C ₆ H ₃ Me) ₂ NSiMe ₃][η ² -(2,6-Me ₂ C ₆ H ₃)N=CMe]·1/2Et ₂ O (6 ·1/2Et ₂ O)	139
Table 14. Bond Angles (°) for Cp*Ta[=N(C ₆ H ₃ Me) ₂ NSiMe ₃][η ² -(2,6-Me ₂ C ₆ H ₃)N=CMe]·1/2Et ₂ O (6 ·1/2Et ₂ O).	140
Table 15. Least Squares Planes for Cp*Ta[=N-(C ₆ H ₃ Me) ₂ NSiMe ₃][η ² -(2,6-Me ₂ C ₆ H ₃)N=CMe]·1/2Et ₂ O (6 ·1/2Et ₂ O).	141
Table 16. Atomic coordinates and B _{iso} /B _{eq} for {Cp*Ta[MeN(C ₆ H ₃ Me) ₂ NSiMe ₃]Me}+I ⁻ (7).....	142
Table 17. Anisotropic Displacement Parameters for {Cp*Ta[MeN-(C ₆ H ₃ Me) ₂ SiMe ₃]Me}+I ⁻ (7).	143
Table 18. Bond Lengths (Å) for {Cp*Ta[MeN(C ₆ H ₃ Me) ₂ NSiMe ₃]Me}+I ⁻ (7).....	144
Table 19. Bond Angles (°) for {Cp*Ta[MeN(C ₆ H ₃ Me) ₂ NSiMe ₃]Me}+I ⁻ (7).....	145
Table 20. Least Squares Planes for {Cp*Ta[MeN(C ₆ H ₃ Me) ₂ NSiMe ₃]Me}+I ⁻ (7).....	146
Table 21. Atomic coordinates and B _{iso} /B _{eq} for Cp*Ta[PhSiH ₂ N-(C ₆ H ₃ Me) ₂ NSiMe ₃](H)Me (9).....	146
Table 22. Anisotropic Displacement Parameters for Cp*Ta[PhSiH ₂ N-(C ₆ H ₃ Me) ₂ NSiMe ₃](H)Me (9).....	148
Table 23. Bond Lengths (Å) for Cp*Ta[PhSiH ₂ N(C ₆ H ₃ Me) ₂ NSiMe ₃](H)Me (9).	149
Table 24. Bond Angles (°) for Cp*Ta[PhSiH ₂ N(C ₆ H ₃ Me) ₂ NSiMe ₃](H)Me (9).	149
Table 25. Least Squares Planes for Cp*Ta[PhSiH ₂ N(C ₆ H ₃ Me) ₂ NSiMe ₃](H)Me (9).	150

Table 26. Atomic coordinates and B_{iso}/B_{eq} for $Cp^*Ta[PhSiH_2N-(C_6H_3Me)_2NSiPhHCl](H)Cl$ (12).....	151
Table 27. Anisotropic Displacement Parameters for $Cp^*Ta[PhSiH_2N-(C_6H_3Me)_2NSiPhHCl](H)Cl$ (12).....	153
Table 28. Bond Lengths (Å) for $Cp^*Ta[PhSiH_2N(C_6H_3Me)_2NSiPhHCl](H)Cl$ (12).	154
Table 29. Bond Angles (°) for $Cp^*Ta[PhSiH_2N(C_6H_3Me)_2NSiPhHCl](H)Cl$ (12).	154
Table 30. Least Squares Planes for $Cp^*Ta[PhSiH_2N(C_6H_3Me)_2NSiPhHCl](H)Cl$ (12).	155

Appendix B

Table 1. Crystallographic data for compounds 2 , 4 , 6 , and 9	158
Table 2. Atomic coordinates and B_{iso}/B_{eq} for $[DADMB]YCl(THF)_2$ (2).	160
Table 3. Anisotropic Displacement Parameters for $[DADMB]YCl(THF)_2$ (2).....	161
Table 4. Bond Lengths (Å) for $[DADMB]YCl(THF)_2$ (2).....	162
Table 5. Bond Angles (°) for $[DADMB]YCl(THF)_2$ (2).	163
Table 6. Atomic coordinates and B_{iso}/B_{eq} for $[DADMB]Y(OSiMe_3)-(THF)_2$ (4).	164
Table 7. Anisotropic Displacement Parameters for $[DADMB]Y(OSiMe_3)-(THF)_2$ (4).	166
Table 8. Bond Lengths (Å) for $[DADMB]Y(OSiMe_3)(THF)_2$ (4).	167
Table 9. Bond Angles (°) for $[DADMB]Y(OSiMe_3)(THF)_2$ (4).	168
Table 10. Atomic coordinates and B_{iso}/B_{eq} for $\{[DADMB]YH(THF)_2\}_2 \cdot C_6H_6$ (6).	169
Table 11. Anisotropic Displacement Parameters for $\{[DADMB]YH(THF)_2\}_2 \cdot C_6H_6$ (6).	171

Table 12. Bond Lengths (Å) for {[DADMB]YH(THF)} ₂ ·C ₆ H ₆ (6).....	172
Table 13. Bond Angles (°) for {[DADMB]YH(THF)} ₂ ·C ₆ H ₆ (6).....	172
Table 14. Atomic coordinates and B _{iso} /B _{eq} for [DADMB]Y(NC ₅ H ₆)(NC ₅ H ₅) ₂ ·C ₅ H ₁₂ (9).....	173
Table 15. Anisotropic Displacement Parameters for [DADMB]Y(NC ₅ H ₆)(NC ₅ H ₅) ₂ ·C ₅ H ₁₂ (9).....	175
Table 16. Bond Lengths (Å) for [DADMB]Y(NC ₅ H ₆)(NC ₅ H ₅) ₂ ·C ₅ H ₁₂ (9).....	177
Table 17. Bond Angles (°) for [DADMB]Y(NC ₅ H ₆)(NC ₅ H ₅) ₂ ·C ₅ H ₁₂ (9).....	177

Appendix C

Table 1. Observed pseudo-first order rate constants for consumption of 1 at different PhMeSiH ₂ concentration.....	181
Table 2. Observed pseudo-first order rate constants for consumption of 1 at different PhMeSiD ₂ concentration.....	181
Table 3. Observed pseudo-first order rate constants for consumption of PhMeSiH ₂ at different initial concentrations of 1-hexene, PhMeSiH ₂ , and 1 (in benzene- <i>d</i> ₆).	182
Table 4. Observed pseudo-first order rate constants for consumption of PhMeSiH ₂ at different initial concentrations of 1 (in THF- <i>d</i> ₈).	182

Appendix D

Table 1. Crystallographic data for compounds 3 and 7	184
Table 2. Atomic coordinates and B _{iso} /B _{eq} for {[DADMB]ZrCl ₂ } ₂ (3).....	186
Table 3. Anisotropic Displacement Parameters for {[DADMB]ZrCl ₂ } ₂ (3).....	187
Table 4. Bond Lengths (Å) for {[DADMB]ZrCl ₂ } ₂ (3).....	188
Table 5. Bond Angles (°) for {[DADMB]ZrCl ₂ } ₂ (3).....	188

Table 6. Atomic coordinates and $B_{\text{iso}}/B_{\text{eq}}$ for [DMBN]Zr(CH ₂ Ph)[η^6 -PhCH ₂ B(C ₆ F ₅) ₃] \cdot 3.5C ₆ H ₆ (7).....	189
Table 7. Anisotropic Displacement Parameters for [DMBN]Zr(CH ₂ Ph)-[η^6 -PhCH ₂ B(C ₆ F ₅) ₃] \cdot 3.5C ₆ H ₆ (7).....	193
Table 8. Bond Lengths (Å) for [DMBN]Zr(CH ₂ Ph)[η^6 -PhCH ₂ B(C ₆ F ₅) ₃] \cdot 3.5C ₆ H ₆ (7).....	195
Table 9. Bond Angles (°) for [DMBN]Zr(CH ₂ Ph)[η^6 -PhCH ₂ B(C ₆ F ₅) ₃] \cdot 3.5C ₆ H ₆ (7).....	196
Table 10. Least Squares Planes for [DMBN]Zr(CH ₂ Ph)[η^6 -PhCH ₂ B(C ₆ F ₅) ₃] \cdot 3.5C ₆ H ₆ (7).....	197

Chapter 1

**Chelating Imido-Amido Complexes of Tantalum.
Mechanistic Studies on the Addition of Silanes to
Ta = N Multiple Bonds**

Introduction

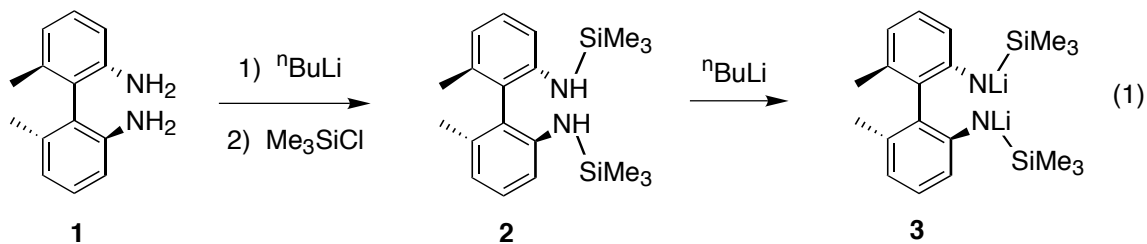
Early transition-metal chemistry has received increased attention in recent years, particularly as new applications in catalysis and polymer chemistry have been developed.¹⁻⁹ Much of this new chemistry involves metal complexes which possess cyclopentadienyl ligand sets. Such complexes are readily modified to adjust electronic and steric properties for the metal center, and therefore activities and selectivities for the catalyst.^{2,3} Many of the systems of interest involve electrophilic and coordinatively unsaturated d^0 metal centers that behave as Lewis acids in their chemistry. For this reason, effort has been devoted to development of alternative ligand sets that may increase the electrophilicity of the metal center.¹⁰⁻¹⁴ One approach involves use of ancillary multidentate amido ligands to support reactive and highly electrophilic metal centers.¹³⁻²⁶

While investigating alternative ancillary ligands for d^0 metal centers, a number of complexes with the bis(triisopropylsilyl)-*o*-phenylenediamido (*o*-C₆H₄(NSi^{*i*}Pr₃)₂) ligand^{27,28} have been synthesized and studied. A common structural feature for these complexes is the presence of a secondary bonding interaction between the aromatic ring and the metal center. While confirming the electron-poor character of the metal center in complexes of this ligand, this donation of electron density from the ligand has the potentially undesirable effect of reducing electrophilicity at the metal. To reduce the possibility of such an interaction, and also to create a chiral environment at the reactive site, an exploration of alternative bis(silylamido) ligands based on *C*₂-symmetric biphenyl backbones was undertaken. The use of similar ligands has recently been reported by Cloke²⁹ and Lappert.³⁰ One aspect of this work, reported in this chapter, concerns a set of tantalum complexes containing both Cp* (η^5 -C₅Me₅) and bis(silylamido) ligands.³¹ This system is characterized by facile cleavage of N–Si bonds in the ligand, and formation of Ta=N double bonds with unusually acute Ta=N–C bond angles. While this reactivity implies that these silylamides cannot always be regarded as innocent spectator ligands, it presents us with the opportunity to explore the chemistry of a reactive d^0 Ta=N bond. The

elimination of silyl groups from silylamido complexes has previously been reported as a limitation in the use of these types of ligands,^{14,23} and the cleavage of N–Si bonds has been employed as a route to transition metal imido species,³²⁻³⁴ but the mechanism of this process has not been investigated. Understanding the reactivity of metal-heteroatom multiple bonds is a subject of both theoretical and practical importance. Transition metal imido species^{32,33,35} are involved or suspected as intermediates in hydrocarbon activation,³⁶⁻⁴⁰ catalytic hydrodenitrogenation,⁴¹ and hydroamination.⁴² In this chapter the synthesis and reactivity of multiply bonded tantalum - nitrogen species are described, supplemented by detailed kinetic and mechanistic studies on the reversible additions of silanes to Ta=N bonds.

Results and Discussion

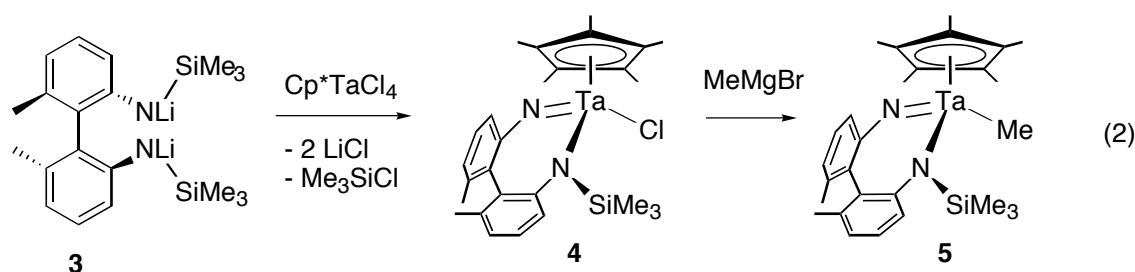
Ligand synthesis. The starting material for the synthesis of the target silylamine ligand, 2,2'-diamino-6,6'-dimethylbiphenyl (**1**), was prepared according to literature procedures.⁴³ N-Silylation of this diamine was achieved via deprotonation of **1** in THF followed by reaction of the resulting dianion with Me₃SiCl (eq 1). N,N'-Bis(trimethylsilyl)-2,2'-diamino-6,6'-dimethylbiphenyl (**2**) was obtained in 84% yield as colorless crystals from pentane. The lithium salt (**3**) was then prepared in 63% yield by treating **2** with two equiv of ⁿBuLi in pentane.



Syntheses and characterization of bent tantalum imido complexes.

Reaction of **3** with Cp^{*}TaCl₄ in refluxing benzene for 4 h yielded a dark red solution.

After evaporation of the solvent and extraction with pentane, compound **4** was isolated in 68% yield as a red crystalline powder. ^1H NMR spectroscopy indicated that loss of one trimethylsilyl group had occurred to afford a tantalum imido complex, as indicated in eq 2. After 3 h (80 °C, benzene- d_6), the reaction had proceeded to >90% conversion with formation of an equimolar mixture of Me_3SiCl and **4**. This reaction therefore differs from that between Cp^*TaCl_4 and $o\text{-C}_6\text{H}_4(\text{NLiSi}^i\text{Pr}_3)_2$, which produces the stable bis(amido) complex $\text{Cp}^*[\text{o-C}_6\text{H}_4(\text{NSi}^i\text{Pr}_3)_2]\text{TaCl}_2$.²⁸



The molecular structure of **4** is shown in Figure 1. The N(1)–Ta–Cl and N(2)–Ta–Cl bond angles are 102.6(2)° and 108.5(2)°, and the bite angle (N(1)–Ta–N(2)) for the imido-amido ligand is 98.8(2)°. The most interesting feature of the molecule is the unusually small Ta–N(1)–C(1) bond angle of 116.3(4)°, which is surprisingly close to the corresponding angle of 114.6(4)° associated with the Ta–N(2)–C(12) amide linkage. The amido N is planar (sum of angles around N(2) = 359.9°), as expected for a metal complex of this type. The Ta=N(1) bond length of 1.830(5) Å is considerably shorter than the Ta–N(2) bond distance of 1.988(6) Å.

The majority of structurally characterized imido complexes exhibit linear, or near linear, geometries with M–N–C bond angles in the range 160–180°.^{32,33} The nature of metal-nitrogen bonding in transition metal imido complexes has been the subject of a number of theoretical studies,^{44–48} which suggest that the metal-ligand bond order is usually intermediate between two and three, and that there is a rather soft potential for bending giving rise to the relatively wide range of observed bond angles. In valence-bond

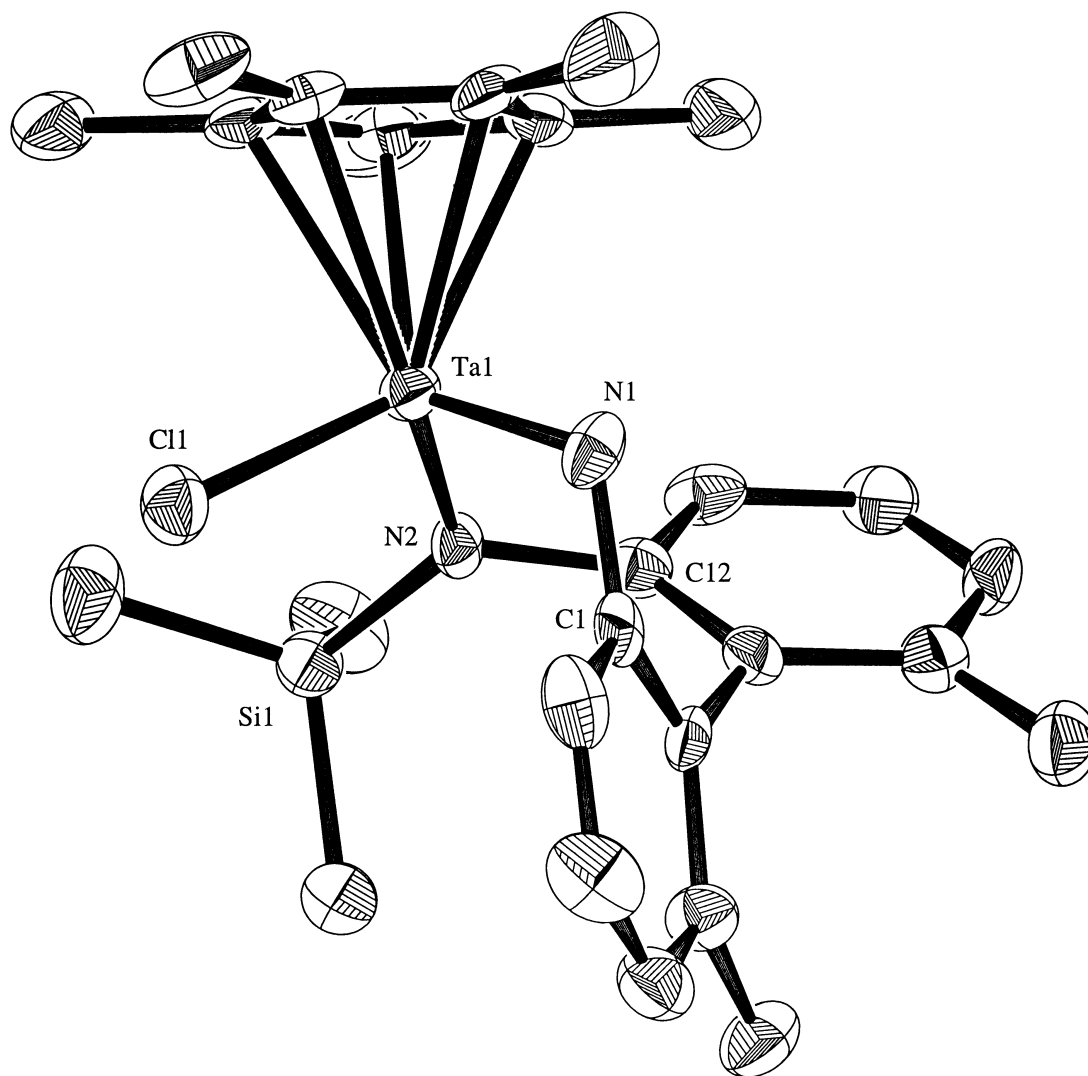


Figure 1. ORTEP diagram of Cp*Ta[=N(C₆H₃Me)₂NSiMe₃]Cl (**4**).

terms, the nitrogen in linear imidos is sp-hybridized, resulting in a formally triple M–N bond. There are only a few reported examples of strongly bent imido complexes, and the bending in these is attributed either to the steric constraints of a chelate ring,^{41,49,50} or to electronic effects (in particular the absence of available empty metal d-orbitals of appropriate symmetry to interact with the nitrogen lone pair).^{51,52} In the limiting case of a strongly bent imido ligand, the N atom would be sp²-hybridized with a formally double M–N bond, and a non-bonding electron pair localized on the nitrogen. There are also a number of linear imidos for which a formally triple M–N bond would result in a violation of the 18-electron rule, and such compounds are best described as possessing a double M–N bond.^{45,47,53}

To the best of our knowledge, compound **4** is the most strongly bent transition metal imido complex reported so far. The observed bending is attributed to the steric restrictions imposed on the imido linkage by the chelating biphenyl ligand. The Ta=N bond is rather long compared to the typical range of 1.6 to 1.8 Å for organoimido complexes of tantalum,^{32,33} but is comparable to the long Ta=N bond of 1.831(10) Å found in Cp*₂Ta(=NC₆H₅)H,^{46,54} which is considered to possess a Ta–N bond order between two and three.

Reaction of **4** with MeMgBr in Et₂O gave the methyl derivative **5**, isolated in 85% yield as orange-red crystals from pentane (eq 2). The TaMe group gives rise to a new singlet at 0.72 ppm in the ¹H NMR spectrum and a signal at 39.5 ppm in the ¹³C NMR spectrum. Unfortunately, Ta=N stretches in infrared spectra of **4** and **5** could not be positively identified, presumably because they are coupled with other vibrations in the molecules.^{33,54}

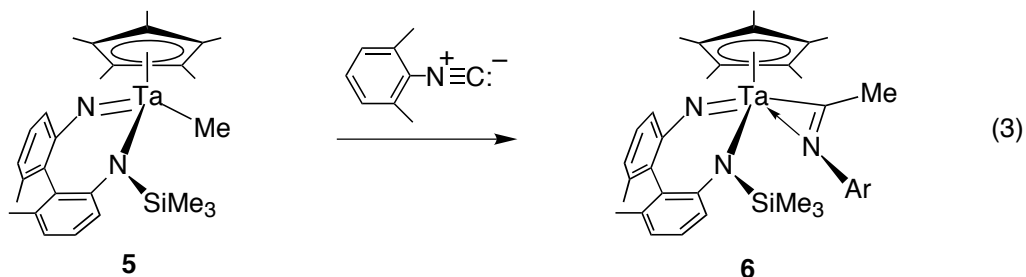
Reactivity of 4 and 5 towards small molecules. While many transition metal imido complexes are stable and unreactive, some exhibit high reactivities towards electrophiles,^{55,56} nucleophiles,⁵⁷ or both.^{33,46,58} Nucleophilic imido ligands tend to be associated with the early transition metals (and more strongly polarized M–N bonds), while

later transition metals exhibit more covalent metal-nitrogen bonding and less nucleophilic imido nitrogen centers.^{33,46} In addition, some imido complexes have been observed to react with unsaturated substrates, to give [2+2] or [2+4] cycloaddition products,^{38,42,56} and certain d^0 imido complexes have been found to activate the C-H bonds in hydrocarbons.^{36,38,40,59} It is expected, according to the bonding model described above, that bending of the imido ligand should lead to a reduced metal-nitrogen bond order and localization of a lone pair on nitrogen. This should lead to increased nucleophilicity of the imido nitrogen atom and increased reactivity of the complex due to a weaker, and more exposed, Ta=N bond.

Contrary to these expectations, compound **4** was found to be rather stable. This compound does not decompose in refluxing toluene- d_8 for 24 h, and does not react with H_2 , CO, C_2H_4 , $PhC\equiv CPh$, or $Me_3SiC\equiv CH$ within 24 h in refluxing benzene- d_6 . The methyl derivative **5** also did not react with H_2 or $Me_3SiC\equiv CH$ under similar conditions. Both **4** and **5** are inert towards the nucleophiles PPh_3 , $PhPH_2$, and *p*-(N,N)-dimethylaminopyridine (24 h, 80 °C, benzene- d_6). Although transition-metal imido complexes typically react readily with organic carbonyl compounds,³³ no reaction was observed between **4** or **5** and benzophenone (4 h, 80 °C, benzene- d_6). Benzaldehyde reacted slowly with **4** (ca. 40% conversion after 20 h) and with **5** (70% conversion after 24 h) at room temperature in benzene- d_6 to give a mixture of products. Complexes **4** and **5** also reacted with weak acids such as PhOH and *p*-toluidine (but not with the more sterically hindered Ph_2NH), giving mixtures of products.

Complex **5** reacts very slowly with carbon monoxide under 40-80 psi, at 80 °C in benzene. However, the accumulation of decomposition products precluded the isolation and identification of the product of this reaction. While **4** did not react with xylol isonitrile, compound **5** was found to undergo a clean reaction at room temperature to give the insertion product **6** (eq 3), isolated as bright yellow crystals in 68% yield. The methyl group of the iminoacyl ligand in **6** appears at 1.26 ppm in the 1H NMR spectrum, and the

^{13}C resonance for the iminoacyl carbon ($\text{N}=\text{CMe}$) was observed at 255.0 ppm, in the low field region of the 195-268 ppm range reported for η^2 -iminoacyl complexes.⁶⁰⁻⁶² In the IR spectrum, the $\text{C}=\text{N}$ stretch appears at 1579 cm^{-1} .



The structure of **6** was determined by X-ray crystallography (Figure 2). The iminoacyl nitrogen N(3) is coordinated to the metal with a Ta–N(3) bond length of 2.259(4) Å, which is longer than the typical values of 2.12-2.17 Å reported for tantalum η^2 -iminoacyl complexes,⁶⁰⁻⁶² but the Ta–C(26) and N(3)–C(26) bond lengths of 2.134(5) Å and 1.273(6) Å are within the typical range for such complexes.⁶² The imido Ta–N(1)–C(1) bond angle of $133.2(3)^\circ$ is considerably expanded relative to the corresponding value for **4**, while the bite angle of the chelating ligand (N(1)–Ta–N(2) = $94.2(2)^\circ$) is slightly reduced from that in **4**. These metrical changes may be attributed to the higher coordination number for the metal center, which leads to increased steric crowding in **6** relative to **4**. The Ta–N(1) bond length, 1.819(4) Å, is slightly shorter than the Ta=N bond in **4**, which is consistent with the greater bond angle at N(1).

The nucleophilic properties of the imido nitrogens in **4** and **5** were demonstrated by their reactions with MeI. Compound **4** did not react with MeI at room temperature in benzene- d_6 , and upon heating the reaction mixture gave a number of decomposition products. The methyl derivative **5**, on the other hand, reacts readily with MeI at room temperature. The product of this reaction (**7**), isolated as yellow crystals in 74% yield, is highly insoluble in nonpolar organic solvents (Et_2O , benzene) but is soluble in CH_2Cl_2 . Reactions of imido complexes with MeI or MeBr have often been observed to result in

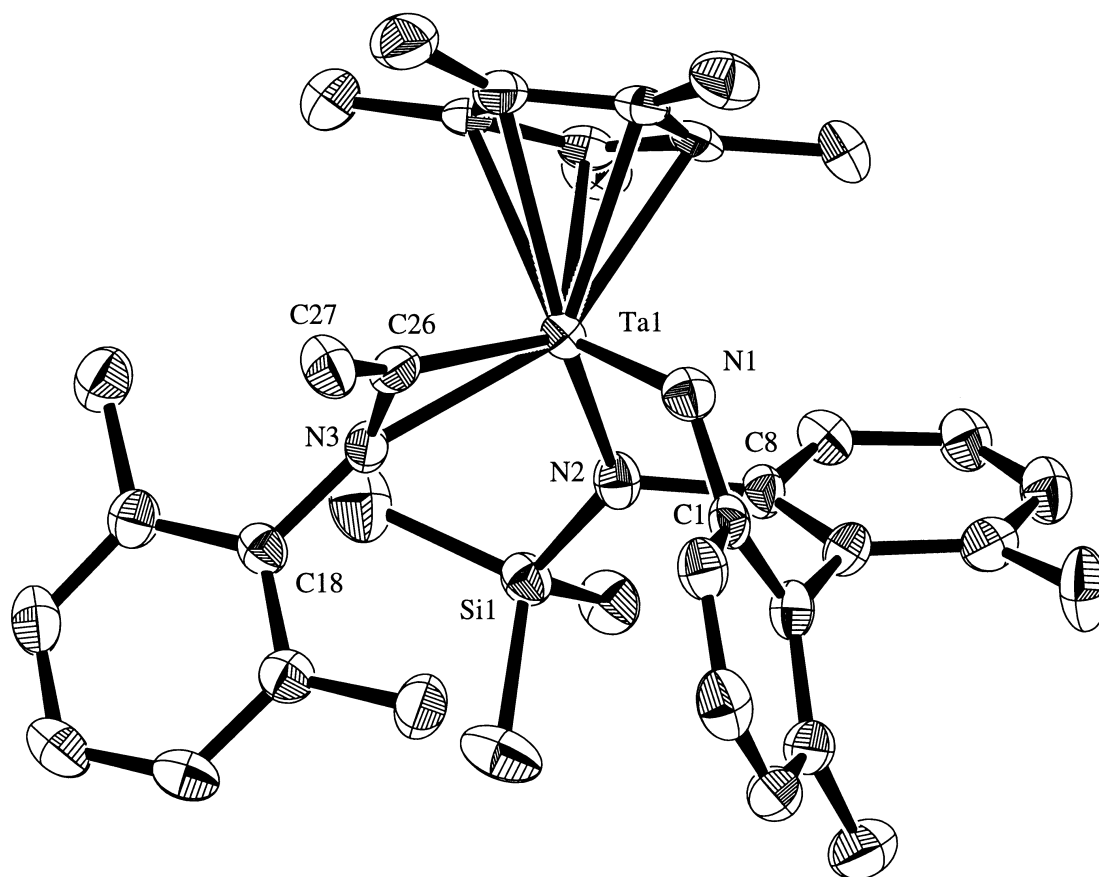
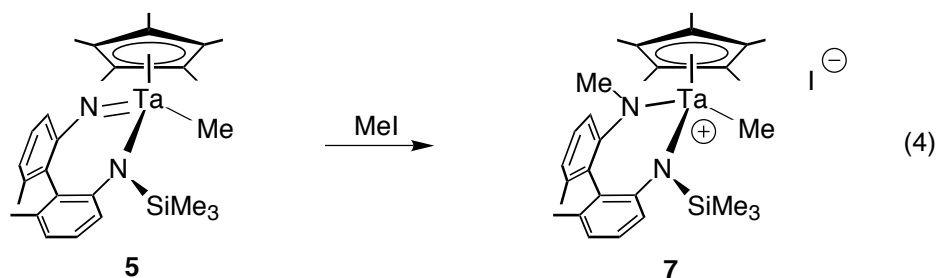


Figure 2. ORTEP diagram of
 $\text{Cp}^*\text{Ta}[\text{=N}(\text{C}_6\text{H}_3\text{Me})_2\text{NSiMe}_3][\eta^2\text{-(2,6-Me}_2\text{C}_6\text{H}_3)\text{N=CMe}]$ (**6**).

complete cleavage of the metal–nitrogen bond to produce ammonium ions,^{55,56} but spectroscopic characterization of **7** revealed that only one equiv of MeI had added to the Ta=N bond (eq 4). Furthermore, the insolubility of **7** in nonpolar solvents and the downfield shifts for the MeN–Ta group in the ¹H (3.39 ppm) and ¹³C (53.4 ppm) NMR spectra suggested that **7** might be cationic, and this formulation was confirmed by X-ray crystallography.

An ORTEP drawing of **7** is shown on Figure 3. The Ta–I distance of 5.311(1) Å, and the undistorted three-legged piano stool geometry about the metal center confirmed that the iodide is not coordinated to Ta. The ligand bite angle in this case is expanded to 104.5(4)°. The Ta–N(Me) bond of 1.92(1) Å is intermediate in length between the multiple Ta=N bonds found in **4** and **6** (1.830(5) and 1.819(4) Å, respectively), and those found for the amido nitrogens in **4**, **6**, **9** and **12**, ranging from 1.988(6) in **4** to 2.105(4) in **6**, while the Ta–N(Si) bond length of 1.99(1) Å is within the latter range. The unusually large Ta–N(1)–C(15) bond angle of 147.2(9)° and the small Ta–N(1)–C(1) angle of 101.8(8)° can be attributed to steric crowding caused by the MeN group interacting with the Cp* ring, and probably the presence of a bonding interaction involving the *ipso* carbon, leading to a close Ta⋯C(1) contact of 2.64(1) Å.



The ionic structure of **7** is attributed to steric crowding about Ta, which prevents coordination of the iodide anion. The stability of the cation can also be rationalized by the possibility for stabilization by donation of π -electron density from the two amido nitrogens.

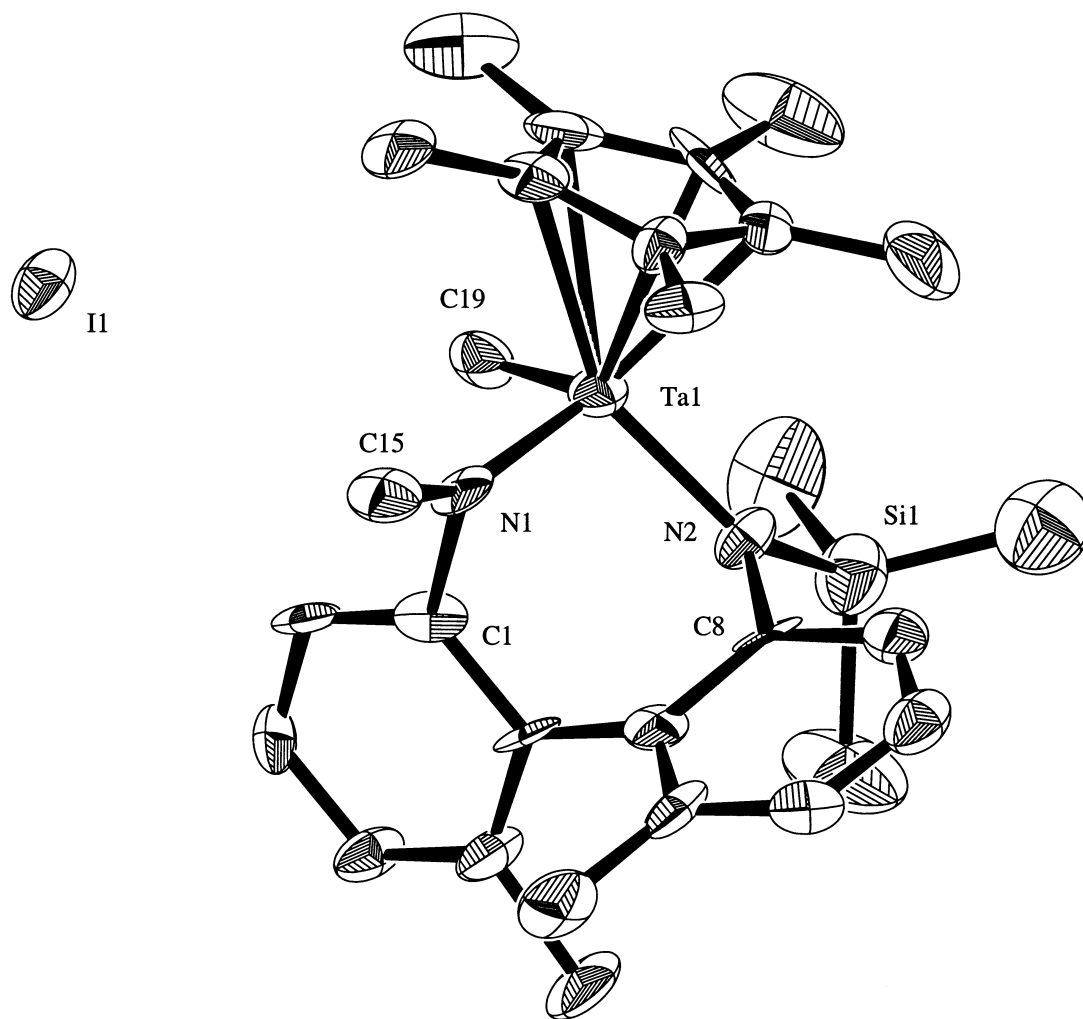
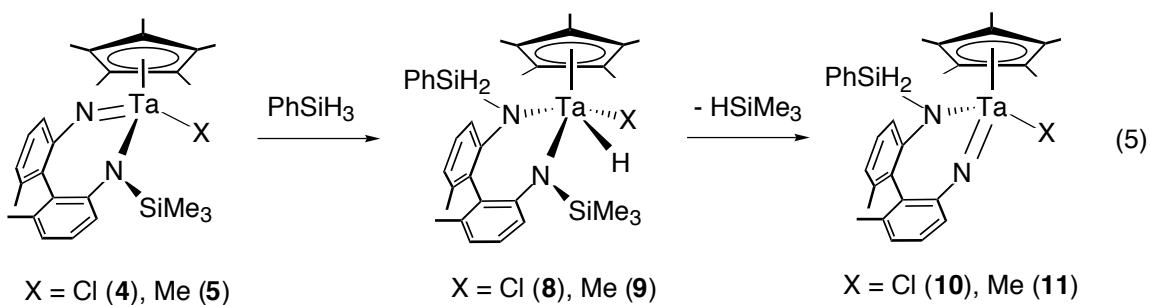


Figure 3. ORTEP diagram of $\{Cp^*Ta[MeN(C_6H_3Me)_2NSiMe_3]Me\}^+I^-$ (**7**).

While coordinatively unsaturated, cationic early transition metal complexes are potentially active as olefin polymerization catalysts, compound **7** did not react with ethene over 24 h (room temperature, dichloromethane- d_2).

Reactions of 4 and 5 with silanes. Compounds **4** and **5** were found to react with hydrosilanes, to form tantalum hydride complexes via addition of the Si–H bond across the Ta=N bond. While the primary silanes PhSiH₃ and PhCH₂SiH₃ reacted at measurable rates at room temperature, reactions with most secondary silanes (such as PhMeSiH₂) could be observed only after prolonged heating, which led to decomposition and the formation of HSiMe₃ (by ¹H NMR spectroscopy). The tertiary silane MeEt₂SiH and the sterically hindered primary silane MesSiH₃ did not react with **4** even at 80 °C over 24 h in benzene- d_6 . Addition of PhSiH₃ to **4** and **5** yielded the hydrido chloride and hydrido methyl complexes **8** and **9**, respectively, as shown in eq 5. The moderate rates of these reactions and the thermal instabilities of the products required use of neat PhSiH₃ and mild reaction conditions (room temperature) for isolation of the products.



The TaH groups in **8** and **9** appear as singlets in the ¹H NMR spectra, at 20.44 and 17.15 ppm, respectively. The methyl ligand in **9** gives rise to a doublet in the ¹H NMR spectrum at 0.88 ppm, with coupling to the hydride ligand (³J_{HH} = 1.9 Hz; coupling was not resolved for the TaH resonance). No significant changes were observed in the ¹H NMR spectrum of **9** on cooling to -80 °C. The Ta–H stretches in the IR spectra of **8** and **9** are observed at 1790 and 1778 cm⁻¹, respectively, and the deuteride **9-d₃**, prepared from **5**

and PhSiD_3 , exhibits a Ta-D stretch at 1278 cm^{-1} . No exchange of the hydride ligand in **9** was observed upon exposure to D_2 (1 atm, $25\text{ }^\circ\text{C}$, 24 h in benzene- d_6). Compound **9** also did not react with ethene under similar conditions.

The structure of **9** was determined by single-crystal X-ray crystallography (Figure 4). The tantalum adopts a four-legged piano stool coordination geometry, with approximately equal Ta-N(amide) distances of 2.060(3) and 2.028(3) Å. The hydride ligand H(1) was located in the Fourier difference map, and its position was refined. Interestingly, it adopts a position that is *trans* to the phenylsilyl group from which it is derived. The Ta-H(1) bond length in **9** is 1.67(3) Å, and the H(1)-Ta-N(2), H(1)-Ta-C(24), and N(1)-Ta-C(24) angles are $74(1)^\circ$, $70(1)^\circ$, and $87.8(1)^\circ$, respectively. The bite angle associated with the chelating diamide ligand is only $88.6(1)^\circ$. Similarly to compound **7**, the angles about N(1) show some deviation from the expected 120° for sp^2 -hybridized N, with a Ta-N(1)-Si(1) angle of $136.0(1)^\circ$ and a Ta-N(1)-C(1) angle of $113.8(2)^\circ$. This distortion is attributed to steric crowding associated with the Cp^* ring. In contrast, the angles about N(2) do not deviate significantly from 120° .

The Ta hydrides **8** and **9** are stable in the solid state under nitrogen and in the dark, but slowly decompose in solution with clean elimination of HSiMe_3 (by ^1H NMR spectroscopy), to give the imido species **10** and **11**, respectively (eq 5). Other potential elimination products (PhSiH_3 , PhSiH_2Cl , PhMeSiH_2 , Me_3SiCl or Me_4Si) were not observed in these decompositions. The hydrido chloride **8** begins to decompose after several hours in benzene- d_6 at room temperature, while the methyl hydride **9** is more stable and exhibits a half-life of a few days in benzene- d_6 . Identification of **10** and **11** was based on their ^1H NMR spectra. Isolation of **11** was not possible as the elimination of HSiMe_3 from **9** did not go to completion but reached equilibrium, and attempts to remove the HSiMe_3 by prolonged reflux in benzene only resulted in production of a mixture of decomposition products.

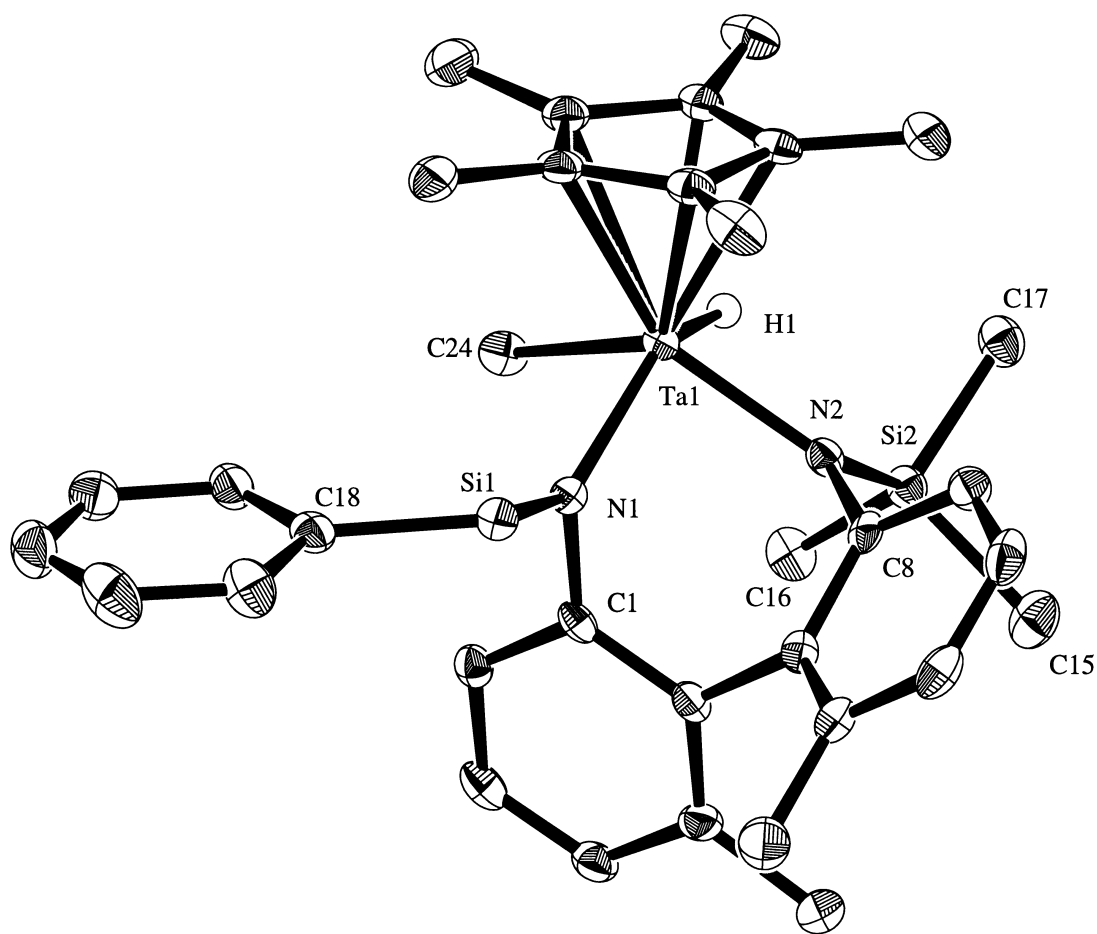


Figure 4. ORTEP diagram of Cp*Ta[PhSiH₂N(C₆H₃Me)₂NSiMe₃](H)Me (**9**).

In dichloromethane solution, the reaction of **4** with PhSiH₃ occurred over four days at room temperature, as the color of the reaction mixture slowly changed from dark red to orange to light yellow. The isolated pale yellow product (**12**) was found to possess a hydride ligand, observed by ¹H NMR spectroscopy as a doublet (*J* = 6.0 Hz) at 14.85 ppm in dichloromethane-*d*₂. Structural characterization of **12** by X-ray crystallography revealed the presence of a diamide ligand containing both -SiH₂Ph and -SiHClPh groups bound to the nitrogens (Figure 5). The structure of **12** is similar to that of the methyl hydride **9**, with angles about Ta of 92.3(1)° (Cl(1)-Ta-N(1)), 89.4(1)° (N(1)-Ta-N(2)), 76(1)° (Cl(1)-Ta-H(1)), and 67(1)° (N(2)-Ta-H(1)). The Ta-N bond lengths of 2.015(3) and 2.016(3) Å are essentially the same. Again, due to the steric hindrance of the Cp* ring, the angles at N(1) show significant deviation from 120°, the Ta-N(1)-Si(1) angle is 140.1(2)° and the Ta-N(1)-C(1) angle is 111.7(2)°. The hydride ligand, located in the Fourier difference map and refined isotropically, is 1.83(4) Å from tantalum (compared to the Ta-H bond length of 1.67(3) Å in **9**). In addition, the distance between H(1) and the neighboring silicon Si(2) in **12**, 1.86(4) Å, is rather small and significantly shorter than the sum of the van der Waals radii (ca. 3.1 Å), suggesting the presence of a nonclassical bonding interaction between these atoms. For comparison, the distance between the hydride H(1) and the silicon Si(2) of the Me₃Si group in **9** is 2.56(3) Å. The Ta-N(2)-Si(2) angle is reduced to 108.8(2)°, while in complexes **4**, **6**, **7**, and **9** the corresponding Ta-N-Si angles are greater than 120°. Further support for a significant H(1)⋯Si(2) interaction is found in the bond distances and angles about Si(2), which suggest a distortion from tetrahedral geometry. The N(2)-Si(2)-C(21) angle of 120.2(2)° is consistent with the nitrogen and the phenyl group occupying equatorial positions in a distorted trigonal bipyramid. The chlorine atom appears to occupy an axial site, with Cl(2)-Si(2)-N(2) and Cl(2)-Si(2)-C(21) angles of 103.1(1)° and 100.5(1)°. The Si(2)-Cl(2) bond length of 2.149(2) Å is also rather long, approaching values observed for axial chlorine in pentacoordinate silicon compounds.⁶³ Similar nonclassical bonding interactions

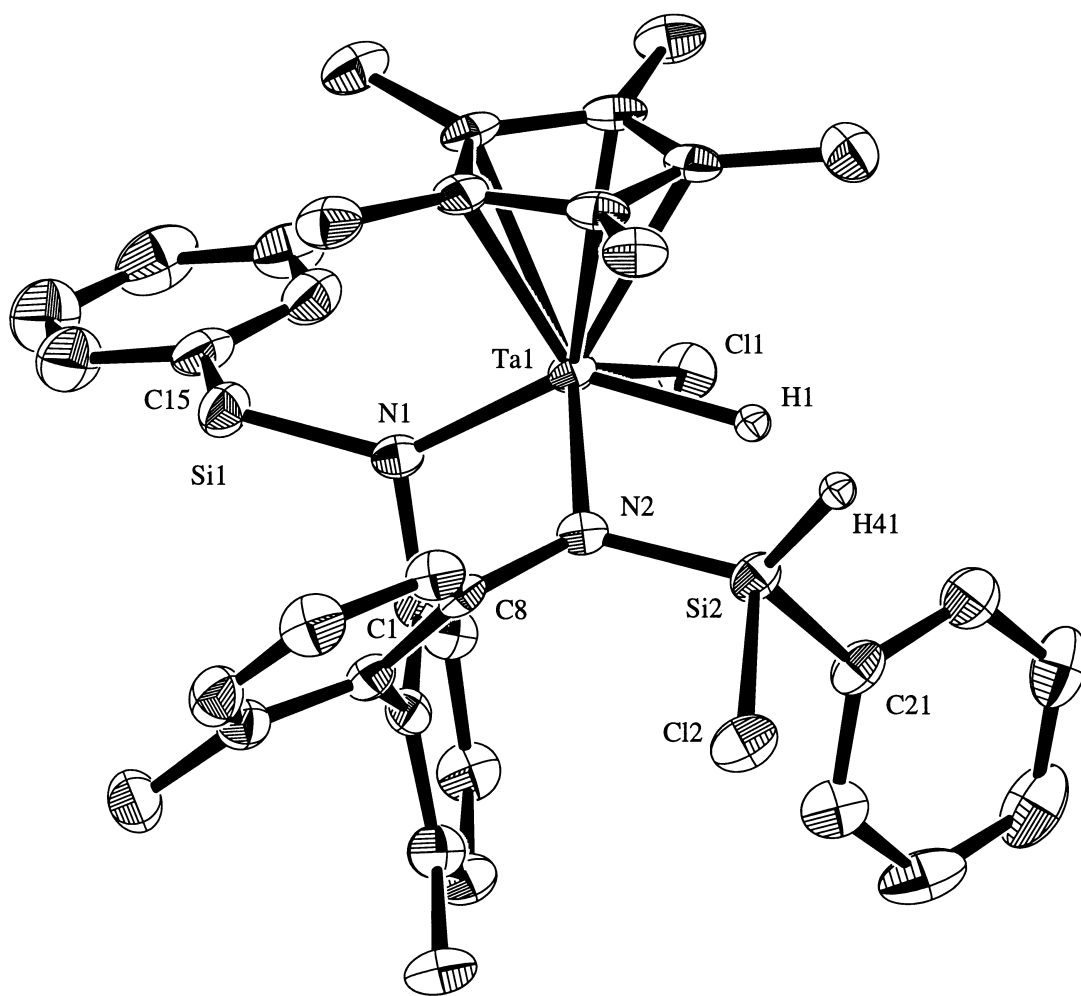
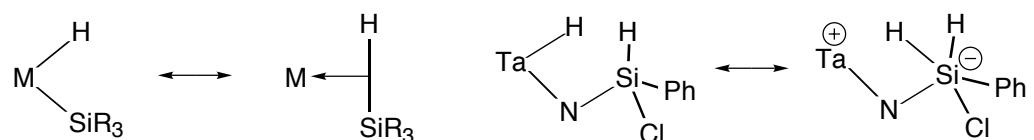


Figure 5. ORTEP diagram of Cp*Ta[PhSiH₂N(C₆H₃Me)₂NSiPhHCl](H)Cl (**12**).

have been characterized for a number of transition metal hydrido silyl complexes,⁶⁴⁻⁷¹ based on short Si–H distances and distorted geometries at silicon. Such complexes can be viewed as exhibiting three-center M–H–Si bonding with limiting metal silyl hydride and σ -H–Si resonance structures.⁷² The bonding situation in compound **12** is different, since the silyl group is not directly bonded to the metal. Thus, the bonding in **12** is probably best described by the resonance structures shown in Scheme 1, involving a pentacoordinate Si center in one of the canonical forms. This interaction may also be differentiated from those found in a number of β -Si–H agostic complexes⁷³⁻⁷⁵ in which an Si–H σ -bond is coordinated to the metal, without an increase of the coordination number at the silicon.

Scheme 1



The existence of a bonding interaction between the hydride ligand and the neighboring silicon atom in **12** may also account for the low Ta–H stretching frequency (1678 cm^{−1} vs. 1790–1778 cm^{−1} for **8**, **9**, and **16**). Finally, evidence for such an interaction is seen in the unusually large ¹H NMR coupling constant (6.0 Hz) between H(1) and H(41) (the hydrogen bonded to Si(2)), which are otherwise separated by four bonds. The magnitude of this coupling and the appearance of the spectrum do not observably change on cooling to −80 °C (in dichloromethane-*d*₂). In the ²⁹Si (¹H coupled) NMR of **12**, the PhSiH(Cl)N silicon appears as a doublet at −66.8 ppm (¹J_{SiH} = 272 Hz), and the PhSiH₂N silicon gives rise to a triplet at −26.9 ppm (¹J_{SiH} = 208 Hz). Unresolved coupling (*J* ≈ 6–7 Hz) to hydrogens of the phenyl groups was observed for both resonances, and this effect on the line width appears to obscure coupling to the hydride ligand.

Monitoring the reaction by ^1H NMR spectroscopy provided evidence for some of the intermediates in this scheme. When **4** was reacted with excess PhSiH_3 (50 equiv) in dichloromethane- d_2 , compound **8** was observed to form as an intermediate (the main TaH-containing species after 12 h), and then gradually disappear (complete conversion to **12** after 2 days). This reaction also produced Me_3SiCl and HSiMe_3 in a 1.2:1 ratio (by ^1H NMR integration). Another tantalum hydride signal, observed to grow and then decay during the reaction, is tentatively assigned to intermediate **13** (vide infra). Reaction of isolated **8** with PhSiH_3 in dichloromethane- d_2 (24 h, room temperature) also produced **12**, along with HSiMe_3 , Me_3SiCl , and CHD_2Cl , identified by ^1H NMR spectroscopy. The formation of CHD_2Cl indicates that solvent is the source of the silicon-bound chlorine in **12**. Compound **10** was observed independently as resulting from the elimination of HSiMe_3 from **8** (benzene- d_6 , room temperature), but the formation of both HSiMe_3 and Me_3SiCl suggests the intermediacy of **14** in an alternative pathway when the reaction occurs in dichloromethane (see Scheme 2). While a number of PhSiH_2 signals are observed during the transformation (some associated with **10** and **13**), it is not possible to unambiguously assign resonances to species such as **14** and **15**.

In an attempt to isolate some of the intermediates in Scheme 2, and also to gain information concerning the silicon-chlorination step, the reaction of **8** with PhSiH_3 in benzene (3 days at room temperature) was examined. Removal of the volatiles from the resulting dark yellow solution and recrystallization of the residue from pentane afforded a yellow solid. The ^1H NMR spectrum (500 MHz, benzene- d_6) of this product mixture revealed a set of signals which represent a major component of the mixture and appear to be associated with **13**, the expected final product in the absence of CH_2Cl_2 . The TaH in **13** appears as a singlet at 19.76 ppm. One of the PhSiH_2 groups gives rise to two doublets ($^2J_{\text{HH}} = 10.1$ Hz), while a set of signals assigned to the other PhSiH_2 group (two doublets of doublets) exhibits further small splittings of 3.1 and 1.5 Hz, presumably due to coupling to the TaH hydride ligand. Other resonances for **13** were obscured by signals from other

species. The elimination product **10** was also identified in this spectrum. Addition of dichloromethane-*d*₂ to this intermediate mixture resulted in its complete conversion to **12** after 16 h at room temperature, implying that **13** lies on the reaction pathway. Finally, a facile ligand exchange between Ta and Si via a pentacoordinate Si intermediate can be invoked to explain the migration of chlorine from tantalum to silicon. Evidence for the involvement of such intermediates in this system also comes from kinetic studies on the silane addition/elimination process (*vide infra*).

Kinetic studies of the silane addition/elimination reactions. The kinetics of the PhSiH₃ addition to the tantalum imido complex **5** was studied by ¹H NMR spectroscopy at 35.0 °C (benzene-*d*₆ solvent). The disappearance of **5** in the presence of a large excess of the silane (25-70 equivalents) was found to be first order in **5**, as shown by the linear decay of ln([**5**]/[**5**]₀) *vs.* time (Figure 6). A plot of the observed pseudo-first order rate constants *k*_{obs} *vs.* PhSiH₃ concentrations (Figure 7) established a second-order rate law for the reaction, and a rate constant of *k*_H = 5.57(6) × 10⁻⁵ L/(mol·s). The measured rate constant (*k*_{obs}) was not affected by addition of one equiv of the product (**9**).

To gain more insight into the mechanism of the reaction of **5** with PhSiH₃, the H/D kinetic isotope effect was measured. The second-order rate constant for the reaction of **5** with PhSiD₃, measured under the same conditions, is *k*_D = 7.15(10) × 10⁻⁵ L/(mol·s), which corresponds to a kinetic isotope effect (KIE) of *k*_H/*k*_D = 0.78(1). This inverse isotope effect suggests that the rate-determining transition state does not involve significant breaking or making of bonds to hydrogen. Although it has been shown⁷⁶ that primary isotope effects can be very small or even inverse in cases of extremely exo- or endothermic reactions, this does not seem likely for the reaction under consideration. Inverse KIEs are usually secondary in nature and associated with changes in the bond strengths and the vibrational frequencies of bonds to H/D in the transition state.^{77,78} The formation of an intermediate adduct, involving a pentacoordinate Si center, is proposed to be the rate-determining step in the addition of the silane to the Ta imido complex **5**, as indicated in

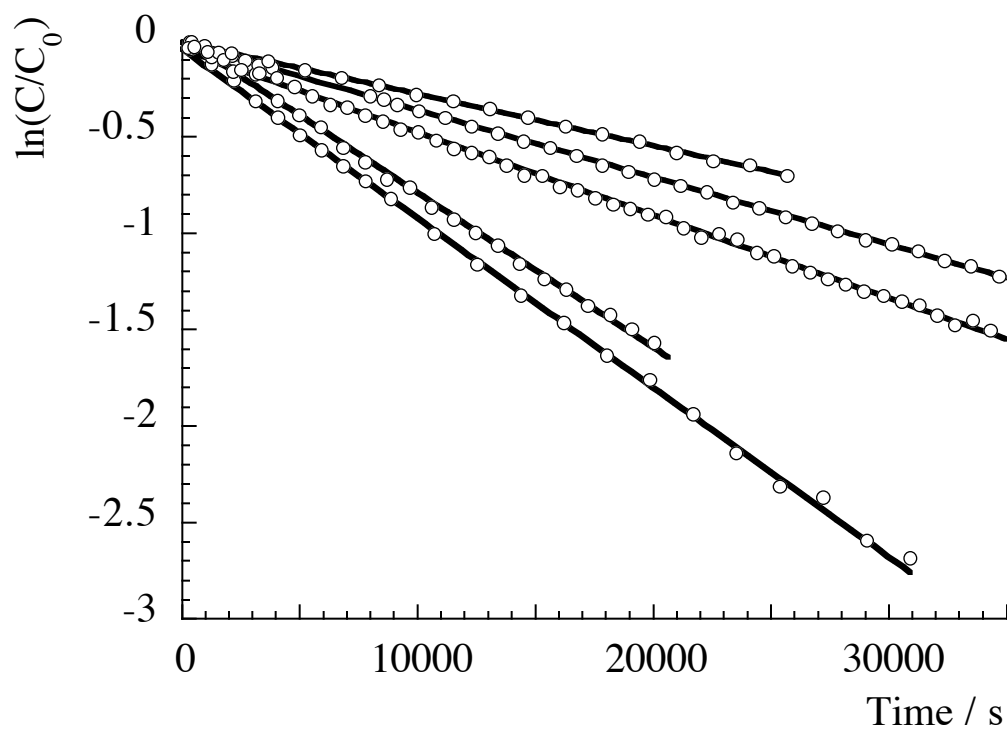


Figure 6. Pseudo-first order plots for disappearance of **5** at PhSiH₃ concentrations of 0.505, 0.668, 0.795^a, 1.483, and 1.588 mol/L; $k_{\text{obs}} \times 10^5 = 2.75, 3.53, 4.67^a, 8.06,$ and 8.90 s^{-1} , respectively. ^a conducted in presence of 1 equiv of **9**

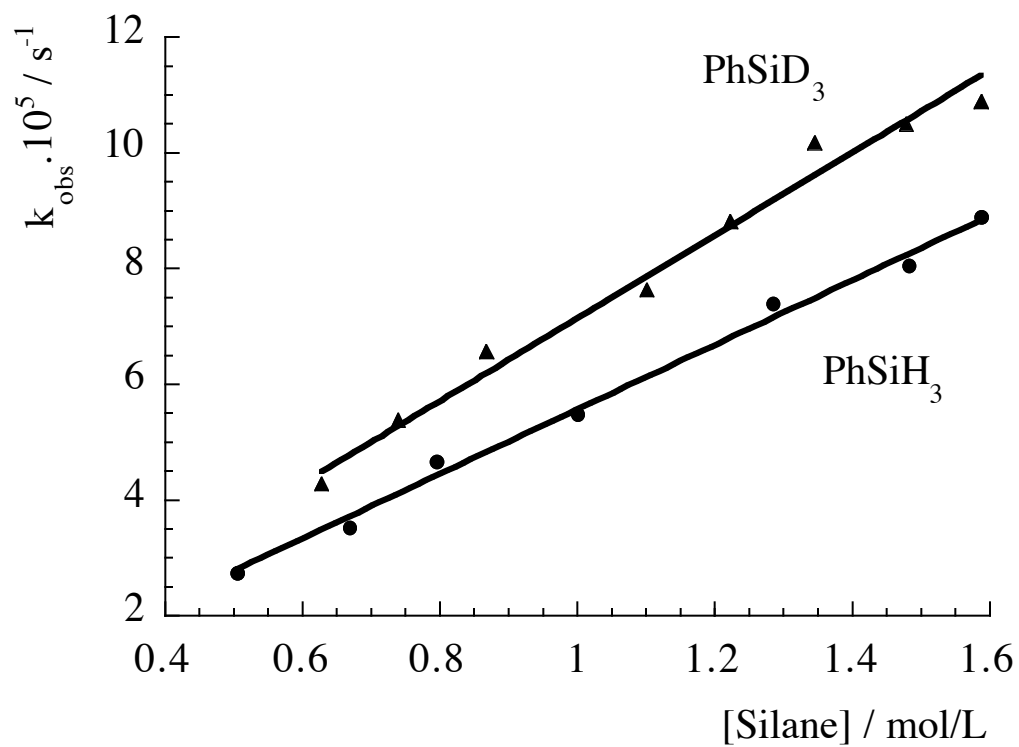
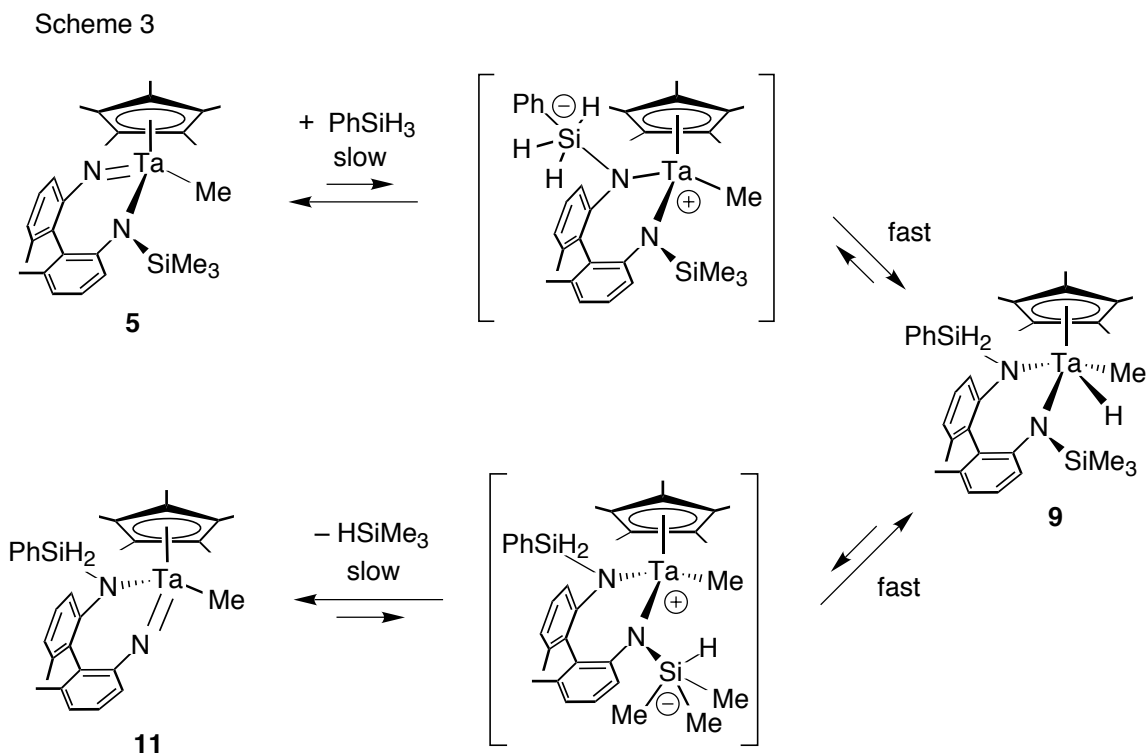


Figure 7. Observed pseudo-first order rate constant for disappearance of **5** (k_{obs}) as a function of the phenylsilane concentration.

Scheme 3. Analogous pentacoordinate silicon species have often been invoked as intermediates in nucleophilic substitution at silicon,^{63,79,80} and the formation of such intermediates has been shown in some cases to be the rate-determining step.⁸¹ While no bonds to H/D are formed or broken in this step, an increase in the Si–H out-of-plane bending frequencies in the pentacoordinate Si intermediate relative to the free silane can lead to a larger zero-point energy difference between the protiated and the deuterated species in the transition state, relative to the zero-point energy difference in the reactants. Such an increase in the Si–H bending force constants can be explained by the increased "tightness" of the transition state relative to the reactants. The resulting lower activation barrier for the deuterated species is consistent with the observed inverse KIE. Related arguments have been used to explain the secondary isotope effects in the very extensively studied S_N2-type reactions at electrophilic sp³ C centers, which proceed through a five-coordinate transition state.^{77,78,82,83} We are not aware, however, of a similar observation of inverse secondary isotope effects for nucleophilic substitution reactions of hydrosilanes, although very small (1-1.3) primary kinetic isotope effects have been reported for nucleophilic substitution of the hydrogen in tertiary silanes with organolithium reagents.⁸¹ Formation of the pentacoordinate Si intermediate is probably followed by a fast intramolecular hydride shift from Si to Ta to give product **9**. The observation of an H···Si bonding interaction in the related complex **12** further supports the idea that such a hydride shift can occur without a significant energy barrier, and thus cleavage of the Si–H bond is not a rate-determining step. Species analogous to **12** probably lie on the reaction coordinate of this migration.

An alternative, one-step mechanism can also be envisaged, involving a concerted [2+2] addition of the Si–H bond to the Ta=N bond, with a transition state resembling the structure of **12**. Such a mechanism, however, would be difficult to reconcile with the observed inverse isotope effect, since it would involve weakening of the bonds to H in the rate-determining transition state.



Additional evidence for rate-determining formation of a pentacoordinate silicon intermediate comes from the observation that silacyclobutane, $(\text{CH}_2)_3\text{SiH}_2$, reacts with **5** much faster than PhSiH_3 , in contrast to other secondary silanes which were unreactive even at elevated temperatures. The disappearance of **5** in the presence of excess silane was followed by ^1H NMR spectroscopy, and the reaction was again found to follow a second-order rate law (Figure 8) with a rate constant ($k' = 1.23(2) \times 10^{-2} \text{ L}/(\text{mol}\cdot\text{s})$ at 35.0°C) which is 220 times greater than that for PhSiH_3 . The product of this reaction, $\text{Cp}^*\text{Ta}[(\text{CH}_2)_3\text{SiHN}(\text{C}_6\text{H}_3\text{Me})_2\text{NSiMe}_3](\text{H})\text{Me}$ (**16**), was isolated and characterized. Its ^1H and ^{13}C NMR spectra suggest a structure analogous to that for **8**, with the strained silacyclobutane ring remaining intact. The higher reactivity of this silane is therefore not due to release of ring strain in the reaction, but rather to the more favored formation of the intermediate with pentacoordinate silicon, which can readily accommodate an imposed 90° bond angle between axial and equatorial substituents in a trigonal bipyramid.

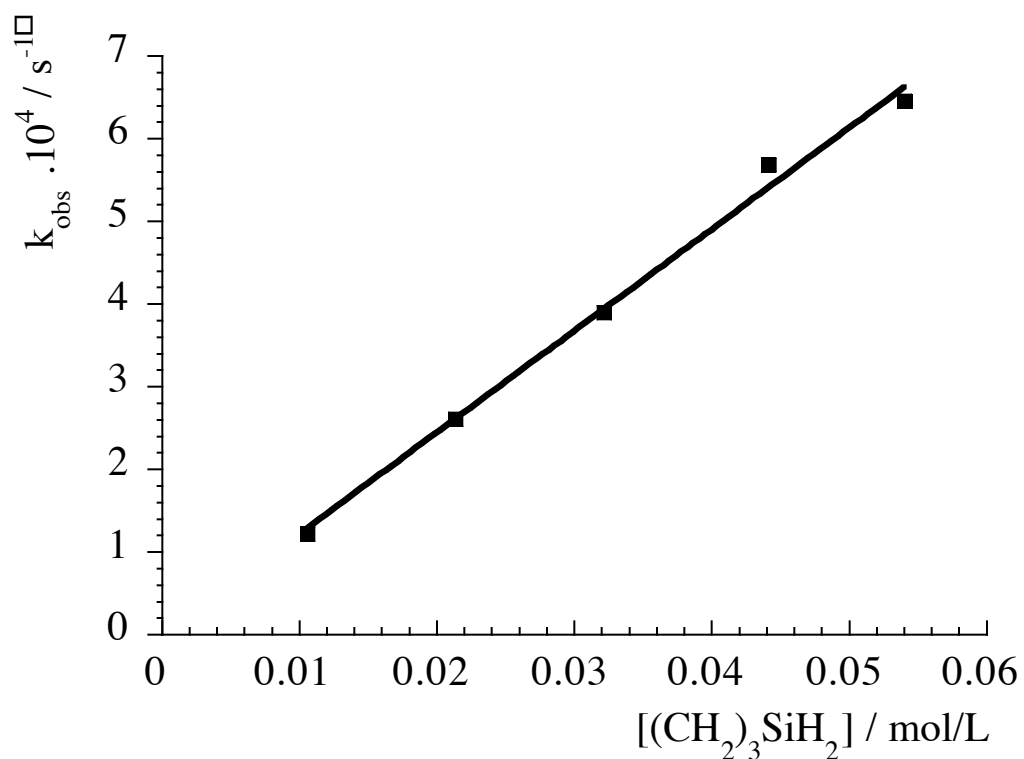
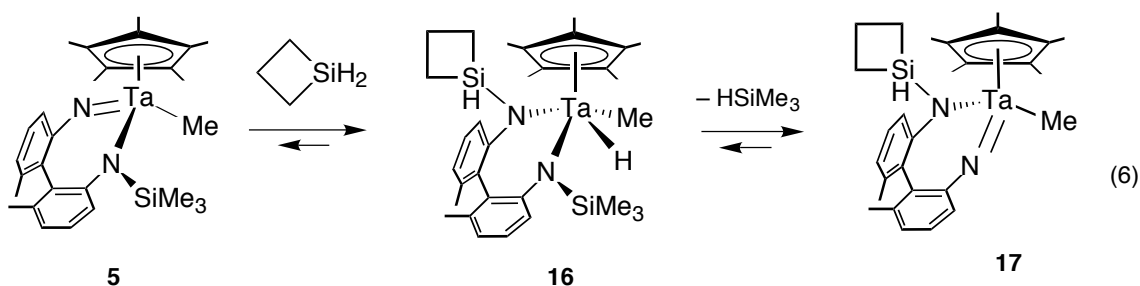


Figure 8. Pseudo-first order rate constant for disappearance of **5** as a function of silacyclobutane concentration. $k_{\text{obs}} \times 10^4 = 1.22 \text{ s}^{-1}$ at $[(\text{CH}_2)_3\text{SiH}_2] = 0.0106 \text{ mol/L}$; 2.61 s^{-1} at 0.0214 mol/L ; 3.90 s^{-1} at 0.0322 mol/L ; 5.69 s^{-1} at 0.0441 mol/L ; 6.46 s^{-1} at 0.0540 mol/L .

The lower kinetic barrier for addition of $(\text{CH}_2)_3\text{SiH}_2$ (compared to PhSiH_3) also results in relatively facile elimination of silacyclobutane from **16**. For comparison, compound **9** thermally decomposes exclusively via HSiMe_3 elimination and no PhSiH_3 was detected. For **16**, two competitive decomposition pathways were observed. Heating **16** for 4 h at 80 °C in benzene- d_6 resulted in about 50% decomposition of **16** to **17** and **5** in a ratio of 1.1:1 (eq 6; identification of **17** is based on its ^1H NMR spectrum). HSiMe_3 was also observed, but no free silacyclobutane could be detected in the reaction mixture, presumably due to its high reactivity leading to further reactions.



The kinetics of the HSiMe_3 elimination from **9**, presumed to occur via the mechanistic reverse of silane addition to **5**, were also studied by ^1H NMR spectroscopy. Figure 9, which is a plot of reactant and product concentrations and the ratio $[\mathbf{11}][\text{HSiMe}_3]/[\mathbf{9}]$ as a function of time, shows that an equilibrium is established after about 7 h. From data taken during the time frame 8-14 h, the equilibrium constant was estimated to be $K_{\text{H}} = 0.025(2)$ mol/L. Note that a more accurate determination of K_{H} is not possible due to the slow decomposition of **11**, which is reflected in an estimated systematic error in K_{H} of ca. 10%. For an initial period (2000-3000 s at 60.6 °C), the plot of $\ln[\mathbf{9}]/[\mathbf{9}]_0$ vs. time gave a straight line with a slope independent of the initial concentration of **9** over a broad concentration range (0.0052-0.041 mol/L). This implies a first order rate law for the forward reaction. The rate constant, calculated from the average of five measurements, was found to be $k_{\text{H}} = 1.09(2) \times 10^{-4} \text{ s}^{-1}$.

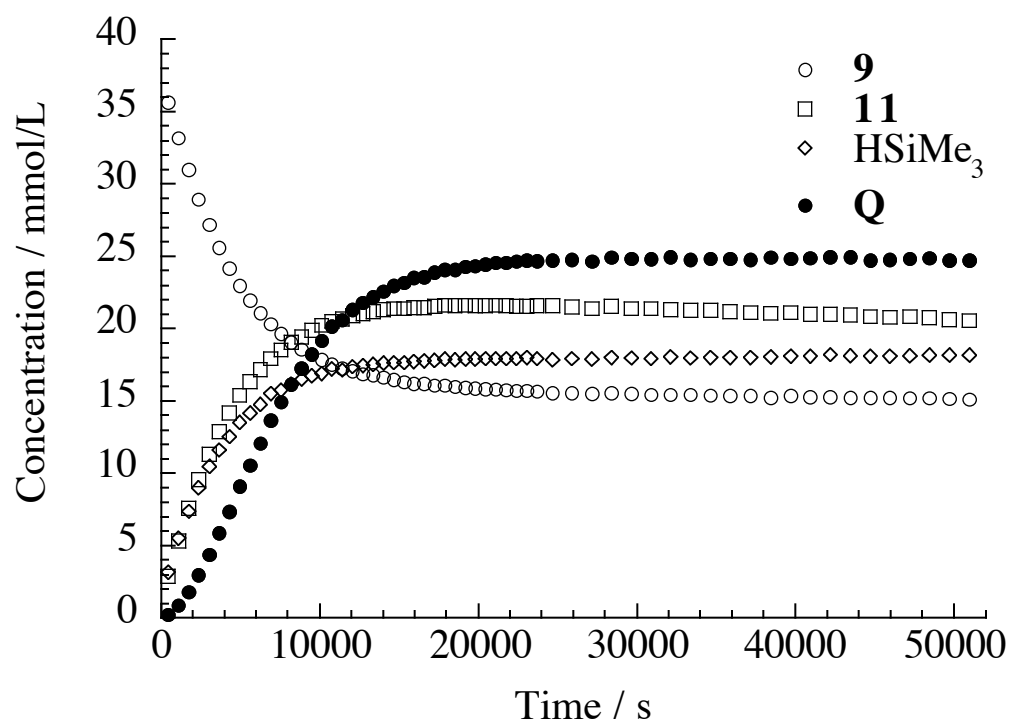


Figure 9. Plot of concentrations of **9**, **11**, and HSiMe₃ vs. time for the elimination of HSiMe₃ from **9**. ($Q = [\mathbf{11}][\text{HSiMe}_3]/[\mathbf{9}]$).

The first-order rate constant for elimination of DSiMe_3 from **9**- d_3 at $60.6\text{ }^\circ\text{C}$ was measured to be $k_{\text{D}} = 1.28(2) \times 10^{-4}\text{ s}^{-1}$ (average of five runs), therefore the deuterium KIE for this reaction is $k_{\text{H}}/k_{\text{D}} = 0.85(2)$. This inverse isotope effect again suggests that no bonds to H/D are being broken in the rate-determining step, which is consistent with our hypothesis of an intermediate pentacoordinate Si species. Such an intermediate is likely formed in a pre-equilibrium with the starting material (**9**), by a rapid hydride shift from Ta to Si. A rate-determining cleavage of the N-Si bond to liberate HSiMe_3 would then lead to product (see Scheme 3). Deuterium substitution appears to shift the pre-equilibrium towards the intermediate, as a result of the stronger Si-H (vs. Ta-H) bond. Thus, the difference in relative zero-point energies for the Si-D and Si-H (vs. the Ta-D and Ta-H) bonds results in an equilibrium isotope effect. The secondary isotope effect for the HSiMe_3 -dissociation step, which is expected to be normal and small, apparently does little to offset the pre-equilibrium isotope effect. The net result is again a lower activation energy for reaction of the deuterated species, in agreement with the observed inverse KIE. The equilibrium constant for the reaction was estimated to be $K_{\text{D}} = 0.026(3)\text{ mol/L}$. While it can be expected that deuterium substitution will shift the equilibrium towards **11** + DSiMe_3 , the difference between K_{H} and K_{D} is clearly within experimental error, and we are therefore prevented from drawing further quantitative conclusions about the equilibrium isotope effect, or the isotope effect for the reverse reaction.

The temperature dependence on the first-order rate constant for elimination of HSiMe_3 from **9** was investigated by conducting the reaction at five different temperatures between 25.0 and $75.0\text{ }^\circ\text{C}$. A plot of $\ln(k/T)$ vs. $1/T$ (Figure 10) produced a straight line from which the activation parameters $\Delta H^\ddagger = 25.5(3)\text{ kcal/mol}$ and $\Delta S^\ddagger = -0.3(1.0)\text{ cal/(mol}\cdot\text{K)}$ were extracted. The very small entropy of activation can be rationalized as resulting from the combined influences of a small positive value for the dissociative, rate-determining step (with an early transition state), and a small negative entropy change for the

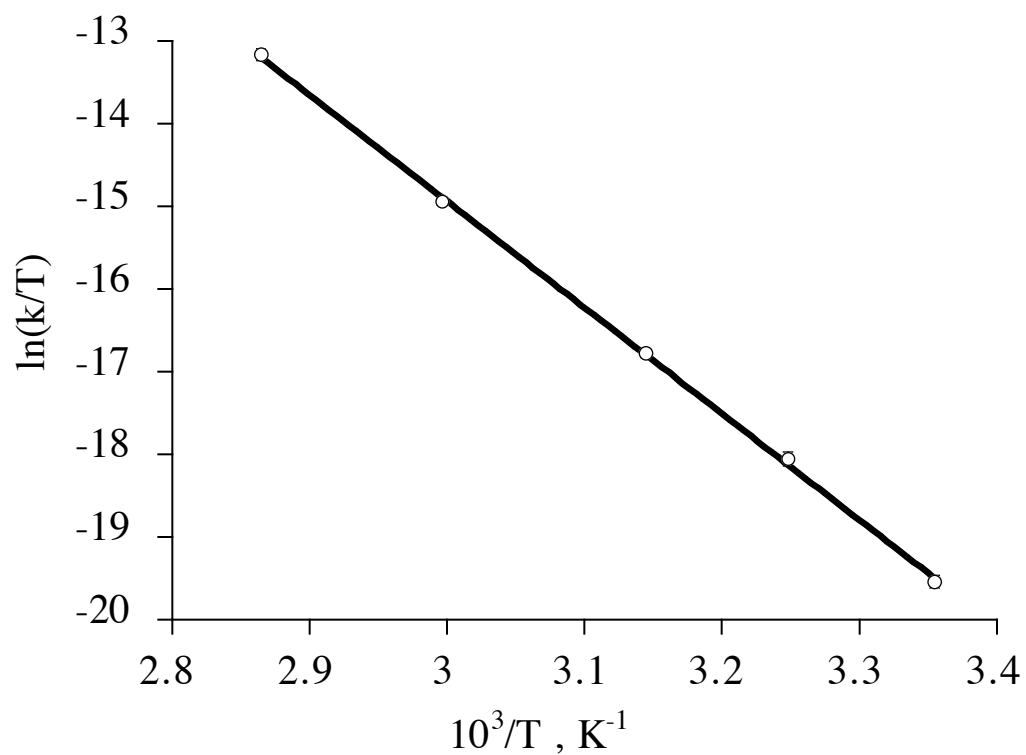


Figure 10. Eyring plot for the rate of decomposition of **9** at different temperatures. $k = 9.8(6) \times 10^{-7} \text{ s}^{-1}$ at $25.0 \text{ }^\circ\text{C}$; $4.5(3) \times 10^{-6} \text{ s}^{-1}$ at $34.8 \text{ }^\circ\text{C}$; $1.66(5) \times 10^{-5} \text{ s}^{-1}$ at $44.8 \text{ }^\circ\text{C}$; $1.09(2) \times 10^{-4} \text{ s}^{-1}$ at $60.6 \text{ }^\circ\text{C}$; $6.7(3) \times 10^{-4} \text{ s}^{-1}$ at $75.9 \text{ }^\circ\text{C}$.

pre-equilibrium (more restricted rotation about the N–Si bond in the intermediate compared to that in the starting material).

Conclusions

In the exploration of the chemistry of some Ta complexes with C_2 -symmetric silylamido ligands, we have observed cleavage of the N–Si bond and loss of a silyl group, to form Ta=N multiply bonded species. These highly bent tantalum imidos are rather stable, but react with silanes via an interesting two-step process involving an intermediate which features a pentacoordinate silicon center. Thus, the bending of an imido ligand in this system appears to enhance the nucleophilicity of the nitrogen center. Formation of pentacoordinate intermediates has often been invoked for reactions of silanes with nucleophiles,^{63,79-81} but this is the first documented example of the involvement of such species in the addition/elimination reactions of silanes with transition metal imidos. The mechanism of these transformations appears to reflect the tendency of silicon to easily expand its coordination sphere, and is thus rather different from that of C–H bond activations by zirconium or tantalum imidos,^{36,40} as might be expected in view of the fundamental differences between carbon and silicon. The tendency of silicon to expand its coordination sphere is also exhibited in the nonclassical bonding interaction found in compound **12**. The loss of silyl groups in such tantalum complexes seems to be facilitated by the sterically crowded coordination environment created by the chelating ligand, and this steric crowding is also reflected in the ease of formation of the cationic complex **7**.

Experimental Section

General. All reactions with air-sensitive compounds were performed under dry nitrogen, using standard Schlenk and glove box techniques. Reagents were obtained from commercial suppliers and used without further purification, unless otherwise noted. Olefin-free pentane, benzene, and toluene were prepared by pretreating with conc. H_2SO_4 ,

0.5 N KMnO_4 in 3 M H_2SO_4 , NaHCO_3 and finally anhydrous MgSO_4 . Solvents (pentane, diethyl ether, benzene, toluene, tetrahydrofuran) were distilled under nitrogen from sodium benzophenone ketyl. Benzene- d_6 was distilled from Na/K alloy. Dichloromethane- d_2 was distilled under nitrogen from calcium hydride. Commercial silanes were distilled and dried over molecular sieves before use. PhSiD_3 was prepared by reduction of PhSiCl_3 with LiAlD_4 (Aldrich, 98% D). ${}^n\text{BuLi}$ was used as a 1.6 M solution in hexanes and MeMgBr as a 1.4 M solution in Et_2O , as supplied by Aldrich. 2,2'-Diamino-6,6'-dimethylbiphenyl (**1**)⁴³ and Cp^*TaCl_4 ⁸⁴ were prepared according to published literature procedures. NMR spectra were recorded at 300 or 500 MHz (${}^1\text{H}$) with Bruker AMX-300 and DRX-500 spectrometers, at 100 MHz (${}^{13}\text{C}\{{}^1\text{H}\}$) with an AMX-400 spectrometer, or at 99.4 MHz (${}^{29}\text{Si}$) with a DRX-500 spectrometer, at ambient temperature and in benzene- d_6 , unless otherwise noted. Signal multiplicities are reported as follows: s - singlet, d - doublet, t - triplet, q - quartet, qn - quintet, m - multiplet. Elemental analyses were performed by the Microanalytical Laboratory at UC Berkeley. Infrared spectra were recorded with a Mattson Instruments Galaxy Series FTIR spectrometer, as Nujol mulls with CsI plates or as KBr pellets.

N,N'-Bis(trimethylsilyl)-2,2'-diamino-6,6'-dimethylbiphenyl (2).

To a cold (0 °C) solution of **1** (7.75 g; 36.5 mmol) in THF (100 mL) was added dropwise 48 mL (76.8 mmol) of 1.6 M ${}^n\text{BuLi}$. A white precipitate formed initially, but dissolved completely after all of the ${}^n\text{BuLi}$ had been added. The solution was stirred at 0 °C for 2 hours, and was then allowed to warm to room temperature, resulting in a color change from pale yellow to green. Me_3SiCl (10.2 mL, 80.4 mmol) was then added dropwise. A white precipitate formed immediately, and the evolution of heat was observed. After 2 h of heating at reflux, the solution was stirred overnight at room temperature. The THF was removed under vacuum to give an oily white solid. Extraction with pentane (2 × 100 mL) gave a bright yellow solution, which was concentrated in vacuo until crystals appeared, and then cooled to -78 °C. The resulting crystalline product was recrystallized from pentane

and dried to afford 10.93 g (30.6 mmol, 84% yield) of the product as colorless crystals, mp 66.5-67.5 °C. ^1H NMR: δ 7.15 (t, overlaps with solvent peak, $J = 7.8$ Hz), 6.87 (d, 2 H, $J = 7.8$ Hz), 6.77 (d, 2 H, $J = 7.5$ Hz biphenyl H's), 3.53 (br s, 2 H, NH), 2.02 (s, 6 H, Me), 0.06 (s, 18 H, SiMe₃). $^{13}\text{C}\{^1\text{H}\}$ NMR: δ 146.3, 138.7, 129.2, 125.2, 120.5, 113.5 (aromatic C's), 20.5 (Me), 0.2 (SiMe₃). IR (Nujol, cm⁻¹): 3371 (m), 1579 (m), 1301 (s), 1252 (s), 962 (m), 868 (s), 840 (s), 773 (m), 750 (m). Anal. Calcd for C₂₀H₃₂N₂Si₂: C, 67.35; H, 9.04; N, 7.85. Found: C, 67.15; H, 9.21; N, 7.78.

Li(Me₃Si)N(C₆H₃Me)₂N(SiMe₃)Li (3). To a solution of 10.87 g (30.48 mmol) of **2** in 150 mL of pentane at 0 °C was added dropwise 40.0 mL (64.0 mmol) of 1.6 M ⁿBuLi. Formation of a white precipitate was observed within 1 h. The mixture was allowed to warm to room temperature and was stirred overnight, during which time the precipitate gradually dissolved. The slightly cloudy solution was filtered, concentrated in vacuo, and cooled to -78 °C to afford 5.02 g of the product as white crystals (mp 120-125 °C, dec). Concentration and cooling of the filtrate afforded another 2.02 g of product, for a total yield of 63%. ^1H NMR: δ 6.98 (t, 2 H, $J = 7.7$ Hz), 6.71 (d, 2 H, $J = 7.8$ Hz), 6.61 (d, 2 H, $J = 7.3$ Hz, biphenyl H's), 1.75 (s, 6 H, Me), 0.06 (s, 18 H, SiMe₃). $^{13}\text{C}\{^1\text{H}\}$ NMR: δ 159.4, 139.2, 133.6, 130.1, 127.1, 120.6 (aromatic C's), 21.0 (Me), 3.7 (SiMe₃). IR (Nujol, cm⁻¹): 3053 (m), 1571 (s), 1562 (s), 1269 (s), 1255 (s), 1245 (s), 1038 (s), 958 (s), 856 (s), 825 (s), 793 (s), 746 (s), 582 (m), 569 (m), 472 (m), 455 (m). Anal. Calcd for C₂₀H₃₀N₂Si₂Li₂: C, 65.18; H, 8.21; N, 7.60. Found: C, 63.84; H, 8.94; N, 5.76. Satisfactory elemental analysis data could not be obtained, even after repeated recrystallization of the spectroscopically pure compound.

Cp^{*}Ta[=N(C₆H₃Me)₂NSiMe₃]Cl (4). Cp^{*}TaCl₄ (3.43 g, 7.48 mmol) and **3** (2.76 g, 7.48 mmol) were dissolved in 150 mL of benzene and the mixture was heated at reflux for 4 h, resulting in a dark red solution. After cooling to room temperature, the solvent was removed under vacuum and the residual solid was extracted with about 200 mL pentane until the extracts were colorless. The dark red pentane solution was

concentrated to about 70 mL, which caused precipitation of red, prism-shaped crystals. After cooling to $-78\text{ }^{\circ}\text{C}$, the solution was filtered, and the isolated crystals were washed with pentane and dried under vacuum to afford 3.21 g of **4** (68%, mp $176\text{-}179\text{ }^{\circ}\text{C}$). ^1H NMR: δ 7.26 (m, 1 H), 7.02 (m, 1 H), 6.91 (m, 1 H), 6.65 (m, 2 H), 6.58 (m, 1 H, aromatic H's), 2.04 (s, 3 H, *Me*), 2.04 (s, 3 H, *Me*), 1.89 (s, 15 H, Me_5C_5), 0.04 (s, 9 H, Me_3Si). $^{13}\text{C}\{^1\text{H}\}$ NMR (dichloromethane- d_2): δ 156.7, 140.1, 138.7, 135.9, 135.4, 128.1, 127.5, 127.3, 127.1, 123.5, 121.5, 121.2, 113.3 (aromatic C's), 21.0 (*Me*, *Me'*), 11.6 (Me_5C_5), 1.8 (Me_3Si). IR (KBr, cm^{-1}): 3049 (w), 2953 (m), 2916 (m), 1574 (m), 1446 (m), 1250 (s), 1211 (m), 1012 (m), 945 (m), 900 (m), 854 (s), 769 (m), 727 (m). Anal. Calcd for $\text{C}_{27}\text{H}_{36}\text{N}_2\text{ClSiTa}$: C, 51.23; H, 5.73; N, 4.43. Found: C, 51.21; H, 5.90; N, 4.34.

$\text{Cp}^*\text{Ta}[\text{=N}(\text{C}_6\text{H}_3\text{Me})_2\text{NSiMe}_3]\text{Me}$ (5**).** To a solution of **4** (1.01 g, 1.59 mmol) in diethyl ether (80 mL) was added 1.20 mL of 1.4 M MeMgBr (1.68 mmol) at room temperature. The color of the solution gradually changed from dark red to light red-orange, with formation of a white precipitate. After stirring for 5 h, the solvent was removed in vacuo and the residue was extracted with about 100 mL pentane, until extracts were colorless. The pentane solution was concentrated to less than 10 mL and left at $-78\text{ }^{\circ}\text{C}$ for 12 h, to obtain 0.83 g of **5** as a bright red-orange crystalline powder (85% yield, mp $114\text{-}118\text{ }^{\circ}\text{C}$). ^1H NMR: δ 7.28 (m, 1 H), 7.05 (m, 1 H), 6.98 (m, 1 H), 6.69 (m, 2 H), 6.59 (m, 1 H, aromatic H's), 2.09 (s, 3 H, *Me*), 2.05 (s, 3 H, *Me*), 1.78 (s, 15 H, Me_5C_5), 0.72 (s, 3 H, *MeTa*), -0.08 (s, 9 H, Me_3Si). $^{13}\text{C}\{^1\text{H}\}$ NMR: δ 159.2, 140.1, 139.5, 135.9, 133.5, 130.6, 128.8, 127.6, 127.4, 124.9, 120.9, 117.9, 113.6 (aromatic C's), 39.5 (*MeTa*), 21.5 (*Me*), 21.3 (*Me*), 11.4 (Me_5C_5), 1.9 (Me_3Si). IR (KBr, cm^{-1}): 3045 (w), 2954 (m), 2912 (m), 1571 (m), 1446 (s), 1377 (w), 1281 (s), 1250 (s), 1207 (m), 1041 (w), 945 (w), 903 (m), 845 (s), 771 (m), 756 (m), 728 (m). Anal. Calcd for $\text{C}_{28}\text{H}_{39}\text{N}_2\text{SiTa}$: C, 54.89; H, 6.42; N, 4.57. Found: C, 54.24; H, 6.47; N, 4.21.

Cp*Ta[=N(C₆H₃Me)₂NSiMe₃][η²-(2,6-Me₂C₆H₃)N=CMe] (6). A solution of xylyl isonitrile (0.12 g, 0.92 mmol) in 20 mL of pentane was added to a solution of **5** (0.57 g, 0.92 mmol) in 40 mL of pentane. The red, transparent solution was stirred for 12 h at room temperature resulting in the formation of a bright yellow, crystalline precipitate which was filtered and dried in vacuo. Cooling the filtrate to -78 °C afforded a second crop of crystals, giving a total yield of 0.47 g of **6** (68% yield). The product was purified by recrystallization from Et₂O, which results in incorporation of 0.5 equiv of solvent in the crystals (mp > 180 °C, dec). ¹H NMR (400 MHz): δ 7.35 (m, 1 H), 7.21 (m, 1 H), 7.03 (m, 2 H), 6.85 (m, 2 H), 6.80 (m, 1 H), 6.52 (d, 1 H), 6.18 (d, 1 H, aromatic H's), 3.25 (q, 2 H, Et₂O), 2.18 (s, 3 H, *Me*), 2.16 (s, 3 H, *Me*), 2.05 (s, 3 H, *Me*), 1.94 (s, 15 H, *Me*₅C₅), 1.86 (t, 3 H, *Me*), 1.26 (s, 3 H, N=C-*Me*), 1.11 (t, 3 H, Et₂O), 0.03 (s, 9 H, *Me*₃Si). ¹³C{¹H} NMR: δ 255.0 (N=C-*Me*), 158.2, 154.7, 145.8, 138.5, 136.1, 135.8, 131.7, 129.9, 129.3, 129.0, 128.5, 127.1, 126.9, 126.6, 125.3, 125.2, 120.5, 116.8, 112.1 (aromatic C's), 66.2 (Et₂O), 23.1, 22.0, 21.3, 19.9, 19.2, 15.9, 12.3 (*Me*'s), 5.2 (*Me*₃Si). IR (KBr, cm⁻¹): 3043 (w), 2953 (m), 2916 (m), 1579 (ν_{N=C}, m), 1446 (s), 1313 (s), 864 (s), 837 (s), 773 (m). Anal. Calcd for C₃₉H₅₃N₃O_{0.5}SiTa: C, 59.99; H, 6.84; N, 5.38. Found: C, 59.88; H, 7.01; N, 5.18.

{Cp*Ta[MeN(C₆H₃Me)₂NSiMe₃]Me}+I⁻ (7). To a solution of **5** (0.46 g, 0.75 mmol) in 20 mL of Et₂O was added 3 mL of MeI at room temperature. The mixture instantly became cloudy. After stirring for 24 h, the yellow precipitate was filtered, washed with 20 mL of Et₂O and then 20 mL of pentane, and finally dried under vacuum to afford 0.42 g (74% yield; mp 240-243 °C, dec, subl) of **7** as a yellow, microcrystalline powder. ¹H NMR (dichloromethane-*d*₂): δ 7.52 (m, 2 H), 7.39 (m, 1 H), 7.29 (m, 1 H), 7.21 (m, 1 H), 6.99 (m, 1 H, aromatic H's), 3.39 (s, 3 H, *Me*N), 2.19 (s, 15 H, *Me*₅C₅), 2.16 (s, 3 H, *Me*), 2.10 (s, 3 H, *Me*), 0.78 (s, 3 H, *TaMe*), -0.08 (s, 9 H, *Me*₃Si). ¹³C{¹H} NMR (dichloromethane-*d*₂): δ 141.1, 138.5, 138.4, 135.0, 134.2, 132.3, 131.7, 131.3, 131.0, 130.0, 128.8, 127.4, 124.0 (aromatic C's), 55.1 (*MeTa*), 53.4

(*MeN*), 21.4 (*Me*), 20.4 (*Me*), 12.4 (*Me*₅C₅), 1.5 (*Me*₃Si). IR (KBr, cm⁻¹): 2953 (m), 2916 (m), 1581 (w), 1443 (m), 1381 (w), 1250 (m), 839 (s). Anal. Calcd for C₂₉H₄₂N₂ISi₂Ta: C, 46.16; H, 5.61; N, 3.71. Found: C, 45.81; H, 5.59 N, 3.75.

Cp^{*}Ta[PhSiH₂N(C₆H₃Me)₂NSiMe₃](H)Cl (8). A solution of **4** (0.56 g, 0.88 mmol) in 1.5 mL of neat PhSiH₃ was stirred at room temperature. The inhomogeneous red mixture turned light yellow after one day. The volatile material was removed under vacuum, the resulting residue was washed with pentane (2 × 20 mL) and extracted with toluene (about 70 mL). The toluene solution was concentrated to 10 mL and cooled to -78 °C, and the resulting precipitate was washed with pentane, to obtain 0.39 g of **8** (in two crops, 60% yield) as a pale yellow powder (mp 138-141 °C, dec). The product is weakly light-sensitive and is best kept in the dark. ¹H NMR: δ 20.44 (s, 1 H, TaH), 7.76 (m, 2 H), 7.60 (m, 1 H), 7.08 (m, 5 H), 6.95 (m, 1 H), 6.80 (m, 2 H, aromatic H's), 5.46 (d, 1 H, ²J_{HH} = 9.8 Hz, ¹J_{HSi} = 195 Hz, PhSiH₂N), 4.80 (d, 1 H, ²J_{HH} = 9.8 Hz, ¹J_{HSi} = 201 Hz, PhSiH₂N), 2.10 (s, 3 H, *Me*), 2.04 (s, 3 H, *Me*), 2.02 (s, 15 H, *Me*₅C₅), 0.03 (s, 9 H, *Me*₃Si). ¹³C{¹H} NMR: δ 156.9, 151.5, 138.6, 136.8, 136.0, 135.7, 134.2, 130.4, 129.7, 128.9, 127.3, 127.1, 126.6, 126.3, 126.1, 123.7, 121.0 (aromatic C's), 21.4 (*Me*), 20.7 (*Me*), 13.3 (*Me*₅C₅), 4.7 (*Me*₃Si). IR (KBr, cm⁻¹): 3055 (w), 2987 (m), 2916 (m), 2216 and 2150 (ν_{Si-H}, s), 1790 (ν_{Ta-H}, m), 1564 (m), 1433 (s), 1238 (s), 1213 (s), 1111 (m), 955 (m), 910 (m), 850 (s). Anal. Calcd for C₃₃H₄₄N₂ClSi₂Ta: C, 53.47; H, 5.98; N, 3.78. Found: C, 53.84; H, 6.10; N, 3.73.

Cp^{*}Ta[PhSiH₂N(C₆H₃Me)₂NSiMe₃](H)Me (9). A solution of **5** (0.37 g, 0.60 mmol) in 0.5 mL of neat PhSiH₃ was stirred at room temperature for one day. The clear, bright red-orange mixture gradually turned pale yellow, with the formation of a precipitate. The volatile material was removed under vacuum and the residue was extracted with Et₂O (80 mL). The extract was filtered, concentrated to about 10 mL and cooled to -78 °C. The resulting white crystalline precipitate was isolated, recrystallized again from Et₂O, washed with cold pentane and dried under vacuum to obtain 0.25 g of **9** (58%; mp

148-149 °C, dec). The product is weakly light-sensitive and is best kept in the dark. ^1H NMR: δ 17.15 (s, 1 H, TaH), 7.49 (m, 2 H), 7.10 (m, 5 H), 6.98 (m, 1 H), 6.94 (m, 1 H), 6.83 (m, 2 H, aromatic H's), 5.29 (d, 1 H, $^2J_{\text{HH}} = 9.6$ Hz, $^1J_{\text{HSi}} = 179$ Hz, PhSiH₂N), 4.68 (d, 1 H, $^2J_{\text{HH}} = 9.6$ Hz, $^1J_{\text{HSi}} = 184$ Hz, PhSiH₂N), 2.11 (s, 3 H, Me), 2.08 (s, 3 H, Me), 1.91 (s, 15 H, Me₅C₅), 0.88 (d, 3 H, $^3J_{\text{HH}} = 1.9$ Hz, MeTa), 0.00 (s, 9 H, Me₃Si). $^{13}\text{C}\{^1\text{H}\}$ NMR: δ 156.3, 153.4, 138.3, 137.3, 136.6, 135.5, 134.7, 134.3, 130.2, 128.5, 127.1, 126.6, 126.6, 126.2, 125.2, 124.6, 116.2 (aromatic C's), 48.4 (MeTa), 21.5 (Me), 21.0 (Me), 12.7 (Me₅C₅), 4.6 (Me₃Si). IR (KBr, cm⁻¹): 3057 (w), 2958 (m), 2922 (m), 2214 and 2150 ($\nu_{\text{Si-H}}$, m), 1778 ($\nu_{\text{Ta-H}}$, m), 1564 (m), 1431 (m), 1236 (s), 948 (m), 910 (m), 870 (m), 845 (s). Characteristic IR bands for **9-d₃**: 1605 and 1565 (ν_{SiD} , m), 1278 (ν_{TaD} , m). Anal. Calcd for C₃₄H₄₇N₂Si₂Ta: C, 56.65; H, 6.57; N, 3.89. Found: C, 57.17; H, 6.68; N, 3.85.

Cp*Ta[=N(C₆H₃Me)₂NSiH₂Ph]Cl (10). A sample of **8** (ca. 10 mg) was dissolved in 0.5 mL benzene-*d*₆ and left at room temperature. After 18 h, about 60% conversion of **8** to **10** and HSiMe₃ was found by ^1H NMR spectroscopy, and after 48 h the conversion was complete. ^1H NMR data for **10**: δ 7.29-7.26 (m, 3 H), 7.21 (m, 2 H), 7.13-6.93 (m, 3 H), 6.68-6.61 (m, 3 H), 5.51 (d, 1 H, $^2J_{\text{HH}} = 10.5$ Hz, PhSiH₂), 5.31 (d, 1 H, $^2J_{\text{HH}} = 10.5$ Hz, PhSiH₂), 2.04 (s 15 H, C₅Me₅), 1.83 (s, 3 H, Me), 1.70 (s, 3 H, Me).

Cp*Ta[=N(C₆H₃Me)₂NSiH₂Ph]Me (11). A sample of **9** (ca. 10 mg) was dissolved in 0.5 mL benzene-*d*₆ and heated to 80 °C for 2 h, to give a mixture of **11** and HSiMe₃. ^1H NMR data for **11**: δ 7.26-7.21 (m, 3 H), 7.12-6.91 (m, 5 H), 6.75-6.65 (m, 3 H, aromatic H's), 5.44 (d, 1 H, $^2J_{\text{HH}} = 10$ Hz, PhSiH₂), 5.33 (d, 1 H, $^2J_{\text{HH}} = 10$ Hz, PhSiH₂), 1.95 (s, 3 H, Me), 1.92 (s, 15 H, C₅Me₅), 1.71 (s, 3 H, Me), 0.34 (s, 3 H, TaMe).

Cp*Ta[PhSiH₂N(C₆H₃Me)₂NSiPhHCl](H)Cl (12). To a solution of **4** (1.00 g, 1.58 mmol) in 25 mL of CH₂Cl₂ was added 1.6 mL of PhSiH₃, and the mixture

was stirred at room temperature. The solution slowly changed color from dark red through orange to yellow over a period of four days. The volatile material was removed under vacuum, and the residual solid was washed with pentane (2×25 mL) and dried to afford 1.08 g of **12** as a pale yellow powder (84%; mp 156-159 °C, dec). The crude product was purified by recrystallization from toluene. ^1H NMR (dichloromethane- d_2): δ 14.85 (d, 1 H, $^4J_{\text{HH}} = 6.0$ Hz, TaH), 7.1 - 7.5 (m, 8 H), 7.03 (m, 5 H), 6.88 (m, 1 H), 6.60 (m, 2 H, aromatic H's), 6.28 (d, 1 H, $^4J_{\text{HH}} = 6.0$ Hz, PhSiH(Cl)N), 5.37 (d, 1 H, $^2J_{\text{HH}} = 10.4$ Hz, PhSiH₂N), 4.54 (d, 1 H, $^2J_{\text{HH}} = 10.4$ Hz, PhSiH₂N), 2.32 (s, 15 H, Me₅C₅), 2.01 (s, 3 H, Me), 1.98 (s, 3 H, Me). $^{13}\text{C}\{^1\text{H}\}$ NMR (benzene- d_6): δ 153.8, 149.8, 140.2, 138.6, 137.9, 135.7, 134.9, 134.2, 133.8, 133.7, 130.7, 129.4, 128.3, 127.9, 127.4, 127.1, 126.2, 126.2, 125.0, 122.3 (aromatic C's), 21.1 (Me), 20.7 (Me), 12.7 (Me₅C₅). ^{29}Si NMR (direct detection, 99.4 MHz, benzene- d_6): δ -26.9 (t, $^1J_{\text{SiH}} = 208$ Hz, PhSiH₂N), -66.8 (d, $^1J_{\text{SiH}} = 272$ Hz, PhSiHClN). IR (KBr, cm^{-1}): 3053 (w), 2999 (w), 2916 (w), 2189 and 2152 ($\nu_{\text{Si-H}}$, m), 1678 ($\nu_{\text{Ta-H}}$, w br), 1585 (w), 1566 (w), 1429 (m), 1113 (m), 835 (s). Anal. Calcd for C₃₆H₄₁N₂Cl₂Si₂Ta: C, 53.40; H, 5.10; N, 3.46. Found: C, 53.44; H, 5.12; N, 3.46.

Cp*Ta[PhSiH₂N(C₆H₃Me)₂NSiH₂Ph](H)Cl (13). A solution of **4** (0.17 g, 0.27 mmol) in 1.5 mL PhSiH₃ was stirred at room temperature for 4 days and the volatiles were removed in vacuo. The crude product (**8**, as identified by ^1H NMR) was redissolved in 10 mL of benzene and 1.0 mL of PhSiH₃ was added. The yellow solution was stirred at room temperature for 3 days. Removal of the volatiles in vacuo followed by extraction of the resulting brown oil with 30 mL of pentane and crystallization at -78 °C gave 0.12 g of yellow powder which was found to contain **13** as a major component, along with unidentified decomposition products. ^1H NMR data for **13**: δ 19.76 (br s, TaH), 6.05 (dd, $J_1 = 3.1$ Hz, $J_2 = 11.4$ Hz, PhSiH₂) and 5.72 (dd, $J_1 = 1.5$ Hz, $J_2 = 11.4$ Hz, PhSiH₂), 5.42 (d, $J = 10.1$ Hz, PhSiH₂), 4.84 (d, $J = 10.1$ Hz, PhSiH₂), 2.01 (s, C₅Me₅).

Cp*Ta[(CH₂)₃SiHN(C₆H₃Me)₂NSiMe₃](H)Me (16). To a solution of **5** (0.37 g, 0.60 mmol) in 25 mL of pentane was added 0.1 mL of (CH₂)₃SiH₂, and the mixture was stirred overnight at room temperature. The solution color changed from orange-red to light yellow. The volatile material was removed in vacuo and the resulting residue was redissolved in pentane (30 mL), concentrated, and crystallized at -78 °C to afford 0.25 g of **16** as a crystalline, off-white powder (60% yield). ¹H NMR: δ 17.02 (s, 1 H, TaH), 7.12-7.04 (m, 3 H), 6.93 (m, 2 H), 6.79 (m, 1 H, aromatic H's), 5.14 (m, 1 H, SiH), 2.13 (s, 3 H, Me), 2.06 (s, 3 H, Me), 1.91 (s, 15 H, Me₅C₅), 1.60-1.40, 1.27-1.22 and 0.86-0.84 (m, 6 H, (CH₂)₃SiH), 0.75 (d, 3 H, ³J_{HH} = 2.1 Hz, MeTa), 0.01 (s, 9 H, Me₃Si). ¹³C{¹H} NMR: δ 156.4, 153.0, 137.7, 137.2, 134.7, 134.4, 127.1, 126.4, 126.2, 125.9, 124.5, 124.3, 116.2 (aromatic C's), 48.4 (MeTa), 21.1 (Me), 20.9 (Me), 20.5, 18.7, 15.1 ((CH₂)₃SiH), 12.6 (Me₅C₅), 4.5 (Me₃Si). IR (KBr, cm⁻¹): 3051 (w), 2960 (m), 2914 (m), 2154 (ν_{Si-H}, w), 1780 (ν_{Ta-H}, m), 1566 (w), 1437 (m), 1236 (s), 1118 (m), 916 (s), 841 (s). Anal. Calcd for C₃₁H₄₇N₂Si₂Ta: C, 54.37; H, 6.92; N, 4.09. Found: C, 54.59; H, 7.23; N, 4.12.

Cp*Ta[=N(C₆H₃Me)₂N(SiH(CH₂)₃)]Me (17). A sample of **16** (ca. 10 mg) was dissolved in 0.5 mL of benzene-*d*₆ and heated at 80 °C. The reaction was monitored by ¹H NMR. After 4 h, 50% of **16** had decomposed to give **17** and **5** in a 1.1:1 ratio, along with some HSiMe₃. After 24 h, **16** had completely decomposed and the ratio of **17** to **5** had decreased to 0.5:1, and after heating for two more days, the reaction mixture was found to contain only **5** and HSiMe₃. ¹H NMR data for **17**: δ 5.33 (m, 1 H, SiH), 2.00 and 2.08 (s, 3 H each, biphenyl Me's), 1.95 (s, 15 H, C₅Me₅), 0.32 (s, 3 H, TaMe), aromatic H's and CH₂'s not assignable.

X-ray structure determinations. X-ray diffraction measurements were made on a Siemens SMART diffractometer with a CCD area detector, using graphite monochromated Mo-K_α radiation. The crystal was mounted on a glass fiber using Paratone N hydrocarbon oil. A hemisphere of data was collected using ω scans of 0.3°.

Cell constants and an orientation matrix for data collection were obtained from a least-squares refinement using the measured positions of reflections in the range $4 < 2\theta < 45^\circ$. The frame data were integrated using the program SAINT (SAX Area-Detector Integration Program; V4.024; Siemens Industrial Automation, Inc.: Madison, WI, 1995). An empirical absorption correction based on measurements of multiply redundant data was performed using the programs XPREP (Part of the SHELXTL Crystal Structure Determination Package; Siemens Industrial Automation, Inc.: Madison, WI, 1995) or SADABS. Equivalent reflections were merged. The data were corrected for Lorentz and polarization effects. A secondary extinction correction was applied if appropriate. The structures were solved using the teXsan crystallographic software package of the Molecular Structure Corporation, using direct methods,^{85,86} and expanded with Fourier techniques.⁸⁷ All non-hydrogen atoms were refined anisotropically and the hydrogen atoms were included in calculated positions but not refined unless otherwise noted. The function minimized in the full-matrix least-squares refinement was $\sum w(|F_o| - |F_c|)^2$. The weighting scheme was based on counting statistics and included a p-factor to downweight the intense reflections.

For 4: Crystals were grown from a dilute pentane solution for 5 days at -40°C . The systematic absences of: $h0l: l = 2n+1$ and $0k0: k = 2n+1$ uniquely determine the space group to be $P2_1/c$ (#14).

For 6·1/2Et₂O: Crystals were grown from a dilute Et₂O solution of **6** for three days at -40°C . The systematic absences of: $h0l: h+l = 2n+1$, $0k0: k = 2n+1$ uniquely determine the space group to be $P2_1/n$ (#14). Non-hydrogen atoms were refined anisotropically, except for those of the solvating Et₂O which was found to be disordered and refined isotropically.

For 7: Crystals were grown by slow vapor diffusion of MeI into a benzene solution of **5** for 6 days, at room temperature. The systematic absences of $h0l: h+l = 2n+1$ and $0k0: k = 2n+1$, uniquely determine the space group to be $P2_1/n$ (#14).

For 9: Crystals were grown from an Et₂O solution of **9** for one week at -40 °C. The systematic absences of: $h0l: l = 2n+1$ and $0k0: k = 2n+1$ uniquely determine the space group to be P2₁/c (#14). Hydrogen atoms were included at calculated positions but not refined, except for H(1) which was refined with a fixed thermal parameter.

For 12: Crystals were grown by slow vapor diffusion of pentane into a concentrated benzene solution of **12**, for 10 days, at room temperature. Inspection of the reflections collected revealed the presence of a second, smaller crystal, with the same unit cell parameters. The set of reflections belonging to that crystal were not included in the unit cell refinement and subsequent structure solution. Based on a statistical analysis of intensity distribution, and the successful solution and refinement of the structure, the space group was determined to be P $\bar{1}$ (#2). The hydrogen atoms were included in calculated positions and not refined, except for H(1) and H(41), which were refined isotropically.

Kinetic measurements. Reactions were monitored by ¹H NMR spectroscopy, with a Bruker AMX300 spectrometer, using 5 mm Wilmad NMR tubes, equipped with J. Young Teflon screw caps. The samples were frozen in liquid N₂ immediately after preparation, and defrosted just before being placed in the preshimmed probe, which was preheated at the required temperature. The probe temperature was calibrated using an ethylene glycol sample,⁸⁸ and monitored with a thermocouple. Repeated calibration showed that the temperature was maintained within ± 0.2 °C of the set value. Single scan spectra were acquired automatically at preset time intervals. The peaks were integrated relative to ferrocene as an internal standard. Rate constants were obtained by non-weighted linear least-squares fits of the integrated first-order rate law in logarithmic form, $\ln C = \ln C_0 - k_{\text{obs}}t$. When several peaks from the same species were monitored, separate plots of $\ln C$ (as calculated from each signal) vs. t were produced, and the rate constants (typically within two standard deviations from each other) were averaged.

Kinetic study of the addition of PhSiH₃ and PhSiD₃ to 5. Samples of **5** (9.5 - 18.7 mg) and Cp₂Fe (2.0-5.0 mg) were weighed in a 1.00 ± 0.01 mL volumetric

flask. The solids were dissolved in a small amount of benzene- d_6 , and known volumes of PhSiH₃ (64-200 μ L) or PhSiD₃ (80-200 μ L) were added using a 100 μ L Hamilton syringe. The exact amount of silane added was determined by weighing the volumetric flask before and after the addition. The solution was diluted with benzene- d_6 to 1.00 mL, mixed quickly, and transferred to the NMR tube. The reaction was followed at 35.0 °C, and the rate of disappearance of **5** was monitored by integrating the C₅(CH₃)₅ and Si(CH₃)₃ peaks relative to Cp₂Fe. Rate constants were calculated using data from the first 1.1-2.9 $\tau_{1/2}$, after which period the accumulating decomposition products caused increased scatter in the data (although linearity was preserved up to 3-4 half-lives).

Kinetic study of the addition of (CH₂)₃SiH₂ to **5.** A 1.15 M solution of (CH₂)₃SiH₂ was prepared by diluting 83.2 mg of the silane with benzene- d_6 up to 1.00 mL. Samples of **5** (1.8 - 5.0 mg) and Cp₂Fe (0.5 - 1.9 mg) were weighed in a 1.00 \pm 0.01 mL volumetric flask. After dissolving the solids in a small amount of benzene- d_6 , a known volume (10 - 50 μ L) of the silane solution was added, the mixture diluted to 1.00 mL, homogenized, and transferred to the NMR tube. (Although the samples were frozen in liquid N₂ immediately, the reaction had typically advanced to 10 - 20% conversion before data acquisition could begin.) The reaction was followed at 35.0 °C, and the rate of disappearance of **5** was monitored for up to 1.5-3.3 $\tau_{1/2}$ by integrating the C₅(CH₃)₅ and Si(CH₃)₃ peaks relative to Cp₂Fe.

Kinetic study of the elimination of trimethylsilane from **9 and **9-*d*₃**.** Samples of **9** (2.8-22.1 mg) or **9-*d*₃** (10.3-28.0 mg) and Cp₂Fe (2-4 mg) were weighed into NMR tubes and dissolved in 0.6-0.8 mL of benzene- d_6 . To determine the exact volume of the solution, the NMR tubes were calibrated by adding known volumes of C₆H₆ with a Hamilton microliter syringe and measuring the resulting height of the solvent. The rate of disappearance of the starting material was followed at 60.6 °C, by integrating the biphenyl CH₃, TaCH₃, and Si(CH₃)₃ signals relative to the Cp₂Fe standard. Initial rates were determined by processing data from the first 2000-3000 s (0.3-0.5 $\tau_{1/2}$) only, where

the deviation from linearity (see Discussion) was negligible. The activation enthalpy and entropy for the reaction were determined by weighted, linear least squares fit of $\ln(k/T)$ vs. $1/T$ at five different temperatures. Only the biphenyl CH_3 and $TaCH_3$ peaks were used at temperatures lower than $60\text{ }^\circ\text{C}$, due to the overlap of the $Si(CH_3)_3$ and $HSi(CH_3)_3$ peaks. Two kinetic runs were performed at each temperature other than $60\text{ }^\circ\text{C}$. The standard deviations in k and T at each data point were calculated based on the random error of the multiple measurements combined with 5% estimated systematic error.

Equilibrium study of the elimination of trimethylsilane from **9 and **9-*d*₃**.** Samples of **9** (27.8 mg) or **9-*d*₃** (23.6 mg) and Cp_2Fe (3-4 mg) were weighed into a 1.00 mL volumetric flask and dissolved in benzene- d_6 . The solutions were heated in J.Young NMR tubes in the spectrometer probe at $60.6\text{ }^\circ\text{C}$ for up to 50 000 s. The concentrations of the starting material and the products were calculated based on the initial concentration of **9** (**9-*d*₃**), relative to the ferrocene internal standard. The biphenyl CH_3 and $TaCH_3$ peaks were used to measure [**11**], and the $HSi(CH_3)_3$ peak was used to determine $[HSi(CH_3)_3]$. The equilibrium constant was calculated as the average value approached by the ratio $[11][HSiMe_3]/[9]$ after 25 000 s.

References:

- (1) Brintzinger, H. H.; Fischer, D.; Mulhaupt, R.; Rieger, B.; Waymouth, R. *Angew. Chem., Int. Ed. Engl.* **1995**, *34*, 1143.
- (2) Kaminsky, W. *Catalysis Today* **1994**, *20*, 257.
- (3) Möhring, P. C.; Coville, N. J. *J. Organomet. Chem.* **1994**, *479*, 1.
- (4) Tilley, T. D. *Acc. Chem. Res.* **1993**, *26*, 22.
- (5) Dioumaev, V. K.; Harrod, J. F. *J. Organomet. Chem.* **1996**, *521*, 133.
- (6) Jordan, R. F. *Adv. Organomet. Chem.* **1991**, *32*, 325.
- (7) Marks, T. J. *Acc. Chem. Res.* **1992**, *25*, 57.
- (8) Visciglio, V. M.; Clark, J. R.; Nguyen, M. T.; Mulford, D. R.; Fanwick, P. E.; Rothwell, I. P. *J. Am. Chem. Soc.* **1997**, *119*, 3490.
- (9) Verdaguer, X.; Lange, U. E. W.; Reding, M. T.; Buchwald, S. L. *J. Am. Chem. Soc.* **1996**, *118*, 6784.
- (10) van der Linden, A.; Schaverien, C. J.; Meijboom, N.; Ganter, C.; Orpen, A. G. *J. Am. Chem. Soc.* **1995**, *117*, 3008.
- (11) Duchateau, R.; van Wee, C. T.; Meetsma, A.; van Duijnen, P. T.; Teuben, J. H. *Organometallics* **1996**, *15*, 2279.
- (12) Rodriguez, G.; Bazan, G. C. *J. Am. Chem. Soc.* **1997**, *119*, 343.
- (13) Baumann, R.; Davis, W. M.; Schrock, R. R. *J. Am. Chem. Soc.* **1997**, *119*, 3830.
- (14) Schrock, R. R. *Acc. Chem. Res.* **1997**, *30*, 9.
- (15) Scollard, J. D.; McConville, D. H.; Payne, N. C.; Vittal, J. J. *Macromolecules* **1996**, *29*, 5241.
- (16) Guérin, F.; McConville, D. H.; Payne, N. C. *Organometallics* **1996**, *15*, 5085.
- (17) Clark, H. C. S.; Cloke, F. G. N.; Hitchcock, P. B.; Love, J. B.; Wainwright, A. P. *J. Organomet. Chem.* **1995**, *501*, 333.
- (18) Scollard, J. D.; McConville, D. H.; Vittal, J. J. *Organometallics* **1995**, *14*, 5478.

- (19) Horton, A. D.; de With, J.; van der Linden, A. J.; van de Weg, H. *Organometallics* **1996**, *15*, 2672.
- (20) Cloke, F. G. N.; Hitchcock, P. B.; Love, J. B. *J. Chem. Soc., Dalton Trans.* **1995**, 25.
- (21) VanderLende, D. D.; Abboud, K. A.; Boncella, J. M. *Organometallics* **1994**, *13*, 3378.
- (22) Deelman, B.-J.; Hitchcock, P. B.; Lappert, M. F.; Lee, H.-K.; Leung, W.-P. *J. Organomet. Chem.* **1996**, *513*, 281.
- (23) Freundlich, J. S.; Schrock, R. R.; Davis, W. M. *J. Am. Chem. Soc.* **1996**, *118*, 3643.
- (24) Duan, Z.; Naiini, A. A.; Lee, J.-H.; Verkade, J. G. *Inorg. Chem.* **1995**, *34*, 5477.
- (25) Findeis, B.; Schubart, M.; Gade, L. H.; Möller, F.; Scowen, I.; McPartlin, M. *J. Chem. Soc., Dalton Trans.* **1996**, 125.
- (26) Schrock, R. R.; Cummins, C. C.; Wilhelm, T.; Lin, S.; Reid, S. M.; Kol, M.; Davis, W. M. *Organometallics* **1996**, *15*, 1470.
- (27) Aoyagi, K.; Gantzel, P. K.; Kalai, K.; Tilley, T. D. *Organometallics* **1996**, *15*, 923.
- (28) Aoyagi, K.; Gantzel, P. K.; Tilley, T. D. *Polyhedron* **1996**, *15*, 4299.
- (29) Cloke, F. G. N.; Geldbach, T. J.; Hitchcock, P. B.; Love, J. B. *J. Organomet. Chem.* **1996**, *506*, 343.
- (30) Drost, C.; Hitchcock, P. B.; Lappert, M. F. *J. Chem. Soc., Dalton Trans.* **1996**, 3595.
- (31) Gountchev, T. I.; Tilley, T. D. *J. Am. Chem. Soc.* **1997**, *119*, 12831.
- (32) Nugent, W. A.; Haymore, B. L. *Coordination Chemistry Reviews* **1980**, *31*, 123.
- (33) Wigley, D. E. *Prog. Inorg. Chem.* **1994**, *42*, 239.
- (34) Herrmann, W. A.; Baratta, W. *J. Organomet. Chem.* **1996**, *506*, 357.
- (35) Nugent, W. A.; Mayer, J. M. *Metal-Ligand Multiple Bonds*; John Wiley and Sons: New York, 1988.

- (36) Schaller, C. P.; Cummins, C. C.; Wolczanski, P. T. *J. Am. Chem. Soc.* **1996**, *118*, 591.
- (37) Arndtsen, B. A.; Bergman, R. G.; Mobley, T. A.; Peterson, T. H. *Acc. Chem. Res.* **1995**, *28*, 154.
- (38) Walsh, P. J.; Hollander, F. J.; Bergman, R. G. *J. Am. Chem. Soc.* **1988**, *110*, 8729.
- (39) de With, J.; Horton, A. D. *Angew. Chem. Int. Ed. Engl.* **1993**, *32*, 903.
- (40) Schaller, C. P.; Wolczanski, P. T. *Inorg. Chem.* **1993**, *32*, 131.
- (41) Weller, K. J.; Gray, S. D.; Briggs, P. M.; Wigley, D. E. *Organometallics* **1995**, *14*, 5588.
- (42) Walsh, P. J.; Baranger, A. M.; Bergman, R. G. *J. Am. Chem. Soc.* **1992**, *114*, 1708.
- (43) Kanoh, S.; Goka, S.; Murose, N.; Kubo, H.; Kondo, M.; Sugino, T.; Motoi, M.; Suda, H. *Polymer Journal* **1987**, *19*, 1047.
- (44) Cundari, T. R. *J. Amer. Chem. Soc.* **1992**, *114*, 7879.
- (45) Jørgensen, K. A. *Inorg. Chem.* **1993**, *32*, 1521.
- (46) Nugent, W. A.; McKinney, R. J.; Kasowski, R. V.; Van-Catledge, F. A. *Inorg. Chim. Acta* **1982**, *65*, L91.
- (47) Schofield, M. H.; Kee, T. P.; Anhaus, J. T.; Schrock, R. R.; Johnson, K. H.; Davis, W. M. *Inorg. Chem.* **1991**, *30*, 3595.
- (48) Anhaus, J. T.; Kee, T. P.; Schofield, M. H.; Schrock, R. R. *J. Am. Chem. Soc.* **1990**, *112*, 1642.
- (49) Herrmann, W. A.; Marz, D. W.; Herdtweck, E. *Z. Naturforsch.* **1991**, *46b*, 747.
- (50) Minelli, M.; Carson, M. R.; Whisenhunt, D. W., Jr.; Imhof, W.; Huttner, G. *Inorg. Chem.* **1990**, *29*, 4801.
- (51) Haymore, B. L.; Maatta, E. A.; Wentworth, R. A. D. *J. Am. Chem. Soc.* **1979**, *101*, 2063.

- (52) Gibson, V. C.; Marshall, E. L.; Redshaw, C.; Clegg, W.; Elsegood, M. R. *J. Chem. Soc. Dalton Trans.* **1996**, 21, 4197.
- (53) Parkin, G. P.; van Asselt, A.; Leahy, D. J.; Whinnery, L.; Hua, N. G.; Quan, R. W.; Henling, L. M.; Schaefer, W. P.; Santarsiero, B. D.; Bercaw, J. E. *Inorg. Chem.* **1992**, 31, 82.
- (54) Korolev, A. V.; Rheingold, A. L.; Williams, D. S. *Inorg. Chem.* **1997**, 36, 2647.
- (55) Maata, E. A.; Wentworth, R. A. D. *Inorg. Chem.* **1979**, 18, 2409.
- (56) Glueck, D. S.; Wu, J.; Hollander, F. J.; Bergman, R. G. *J. Am. Chem. Soc.* **1991**, 113, 2041.
- (57) Arndtsen, B. A.; Sleiman, H. F.; Chang, A. K.; McElwee-White, L. *J. Amer. Chem. Soc.* **1991**, 113, 4871.
- (58) Arndtsen, B. A.; Sleiman, H. F.; McElwee-White, L. *Organometallics* **1993**, 12, 2440.
- (59) Cummins, C. C.; Baxter, S. M.; Wolczanski, P. T. *J. Am. Chem. Soc.* **1988**, 110, 8731.
- (60) Chamberlain, L. R.; Rothwell, I. P.; Huffman, J. C. *J. Chem. Soc. Chem. Commun.* **1986**, 1203.
- (61) Gómez, M.; Gómez-Sal, P.; Jiménez, G.; Martín, A.; Royo, P.; Sánchez-Nieves, J. *Organometallics* **1996**, 15, 3579.
- (62) Durfee, L. D.; Rothwell, I. P. *Chem. Rev.* **1988**, 88, 1059.
- (63) Corriu, R. J. P.; Young, J. C. In *The Chemistry of Organic Silicon Compounds*; S. Patai and Z. Rappoport, Ed.; Wiley: New York, 1989; Vol. 2; pp 1241.
- (64) Nikonov, G. I.; Kuzmina, L. G.; Lemenovskii, D. A.; Kotov, V. V. *J. Am. Chem. Soc.* **1995**, 117, 10133.
- (65) Nikonov, G. I.; Kuzmina, L. G.; Lemenovskii, D. A.; Kotov, V. V. *J. Am. Chem. Soc.* **1996**, 118, 6333.

- (66) Spaltenstein, E.; Palma, P.; Kreutzer, K. A.; Willoughby, C. A.; Davis, W. M.; Buchwald, S. L. *J. Am. Chem. Soc.* **1994**, *116*, 10308.
- (67) Jiang, Q.; Carroll, P. J.; Berry, D. H. *Organometallics* **1991**, *10*, 3648.
- (68) Schubert, U.; Müller, J.; Alt, H. G. *Organometallics* **1987**, *6*, 469.
- (69) Schubert, U.; Ackermann, K.; Wörle, B. *J. Am. Chem. Soc.* **1982**, *104*, 7378.
- (70) Colomer, E.; Corriu, R. J. P.; Marzin, C.; Vioux, A. *Inorg. Chem.* **1982**, *21*, 368.
- (71) Schubert, U. *Adv. Organomet. Chem.* **1990**, *30*, 151.
- (72) Lichtenberger, D. L.; Rai-Chaudhuri, A. *J. Am. Chem. Soc.* **1990**, *112*, 2492.
- (73) Procopio, L. J.; Carroll, P. J.; Berry, D. H. *J. Am. Chem. Soc.* **1994**, *116*, 177.
- (74) Herrmann, W. A.; Huber, N. W.; Behm, J. *Chem. Ber.* **1992**, *125*, 1405.
- (75) Herrmann, W. A.; Eppinger, J.; Spiegler, M.; Runte, O.; Anwander, R. *Organometallics* **1997**, *16*, 1813.
- (76) Melander, L. *Acta Chemica Scandinavica* **1971**, *25*, 3821.
- (77) Streitwieser, A., Jr.; Jagow, R. H.; Fahey, R. C.; Suzuki, S. *J. Am. Chem. Soc.* **1958**, *80*, 2326.
- (78) Melander, L.; Saunders, W. H. *Reaction Rates of Isotopic Molecules*; Wiley: New York, 1980.
- (79) Sommer, L. H. *Stereochemistry, Mechanism and Silicon*; McGraw-Hill: New York, 1965.
- (80) Corriu, R. J. P. *J. Organomet. Chem.* **1990**, *400*, 81.
- (81) Corriu, R. J. P.; Henner, B. J. L. *J. Organomet. Chem.* **1975**, *102*, 407.
- (82) Glad, S. S.; Jensen, F. *J. Am. Chem. Soc.* **1997**, *119*, 227.
- (83) Poirier, R. A.; Wang, Y.; Westaway, K. C. *J. Am. Chem. Soc.* **1994**, *116*, 2526.
- (84) Yasuda, H.; Okamoto, T.; Nakamura, A. In *Organometallic syntheses*; J. J. Eisch and R. B. King, Ed.; Academic Press: New York, 1965; Vol. 4; pp 22.
- (85) Hai-Fu, F. *SAPI91, Structure Analysis Programs with Intelligent Control*, Rigaku Corporation: Tokyo, Japan, 1991

- (86) Altomare, A.; Cascarano, G.; Giacovazzo, C.; Guagliardi, A. *J. Appl. Cryst.* **1993**, *26*, 343.
- (87) Beurskens, P. T.; Admiraal, G.; Beurskens, G.; Bosman, W. P.; Garcia-Granda, S.; Gould, R. O.; Smits, J. M. M.; Smykalla, C. *DIRDIF92, The DIRDIF program system, Technical Report of the Crystallographic Laboratory*, University of Nijmegen: The Netherlands, 1992
- (88) Amman, C.; Meier, P.; Merbach, A. E. *Journal of Magnetic Resonance* **1982**, *46*, 319.

Chapter 2

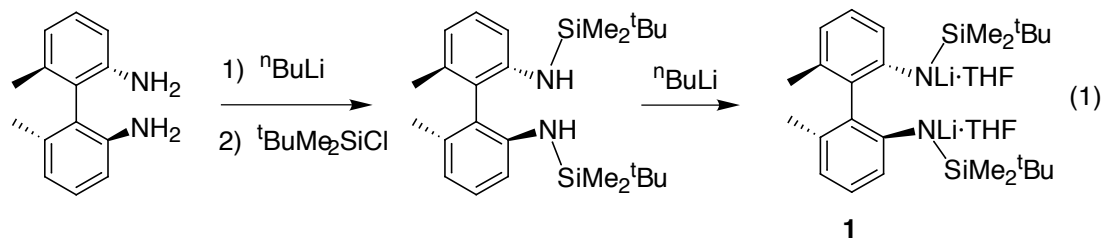
**Yttrium Complexes of the Chelating, C_2 -Symmetric,
Bis(silylamido)biphenyl Ligand [DADMB]²⁻,
{[6,6'-Me₂-(C₆H₃)₂](2,2'-NSiMe₂^tBu)₂}²⁻**

Introduction

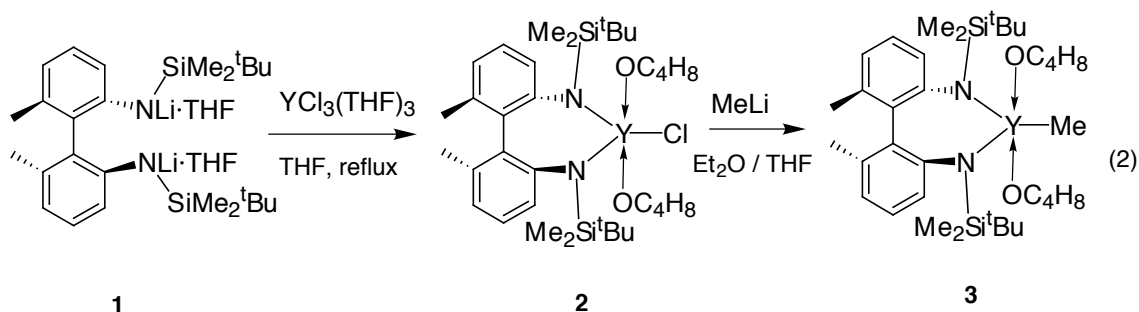
The first chapter described the investigations of the structure and reactivity of a tantalum mixed amido-imido ligand system derived from a bis(trimethylsilylamino)biphenyl ligand.¹ This chapter will present the studies on a series of yttrium complexes with a related bis(silylamido)biphenyl ligand, using more sterically demanding *tert*-butyldimethylsilyl substituents.² Unlike the tantalum system, where reactivity was dominated by reactions of the nitrogen-silicon bond, the yttrium complexes described here appear to possess more robust bis(silylamido) spectator ligands. Asymmetric early transition-metal complexes, usually based on substituted cyclopentadienyl ligands, have found application as olefin polymerization catalysts for control of stereoregularity of the resulting polymer.³⁻⁸ Group 3 and lanthanide metallocene complexes have also been used as regio- and stereoselective hydrosilylation catalysts, and the effect of varying the ancillary Cp-based ligands on the reactivity and selectivity of the catalyst has been studied extensively.⁹⁻¹¹ Even though many alternatives to cyclopentadienyl ligands in early transition metal chemistry have been explored,^{8,12-30} the study of chelating diamides as ligands has been mostly restricted to symmetric systems.

Results and Discussion

The observation of facile cleavage of the nitrogen-silicon bond, described in Chapter 1, suggested that a more sterically demanding substituent be employed. A *tert*-butyldimethylsilyl analogue of the biphenyl diamide ligand was obtained by silylation of the biphenyldiamine anion, as obtained via deprotonation with ⁿBuLi in THF, with ^tBuMe₂SiCl (eq 1). Lithiation of the silylamine *in situ* with ⁿBuLi produced the lithium salt Li₂[DADMB]·2THF (**1**), isolated as a THF adduct in 84% yield from pentane.



Reaction of **1** with $\text{YCl}_3(\text{THF})_3$ in refluxing THF yielded the yttrium complex **2** as a white crystalline solid, in 92% yield (eq 2).



Yttrium complex **2** (Figure 1) adopts a distorted, trigonal-bipyramidal coordination geometry, with the chelating diamide and chloride ligands in the equatorial plane and the two coordinated THF molecules in the axial positions. The molecule has an approximate (noncrystallographic) C_2 -axis coincident with the $\text{Y}-\text{Cl}$ bond. The ligand bite angle is $123.3(2)^\circ$, and the average $\text{Y}-\text{N}$ distance is 2.25 \AA . The dihedral angle between the biphenyl planes is 84.8° . The short $\text{Y}-\text{C}_{\text{ipso}}$ (average 2.75 \AA) and $\text{Y}-\text{C}_{\text{ortho}}$ (average 2.87 \AA) distances, and the small $\text{Y}-\text{N}-\text{C}_{\text{ipso}}$ angles (average 94.6°) suggest the presence of Y -aromatic carbon bonding interactions, which are often observed in complexes of this type.^{31,32}

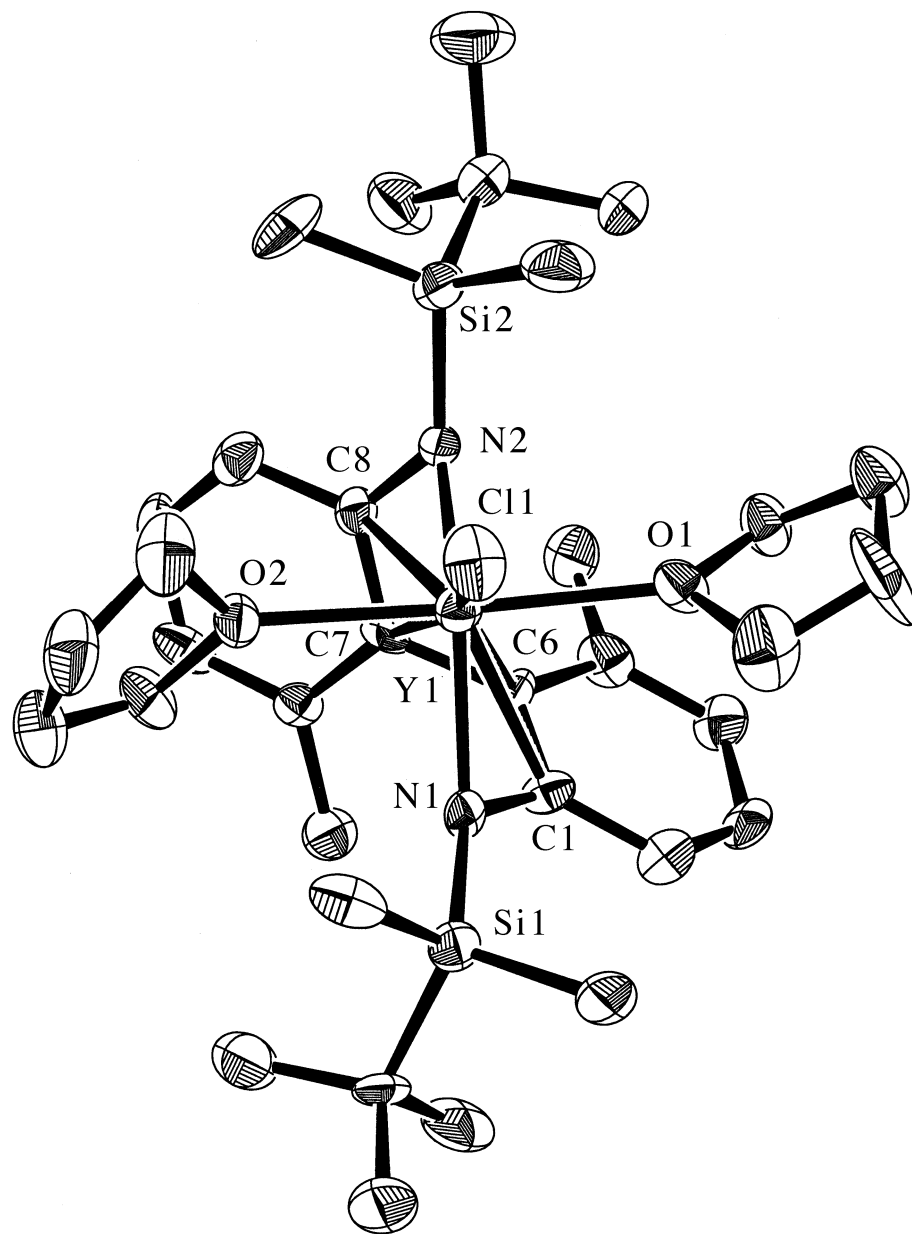


Figure 1. ORTEP diagram of [DADMB]YCl(THF)₂ (2).

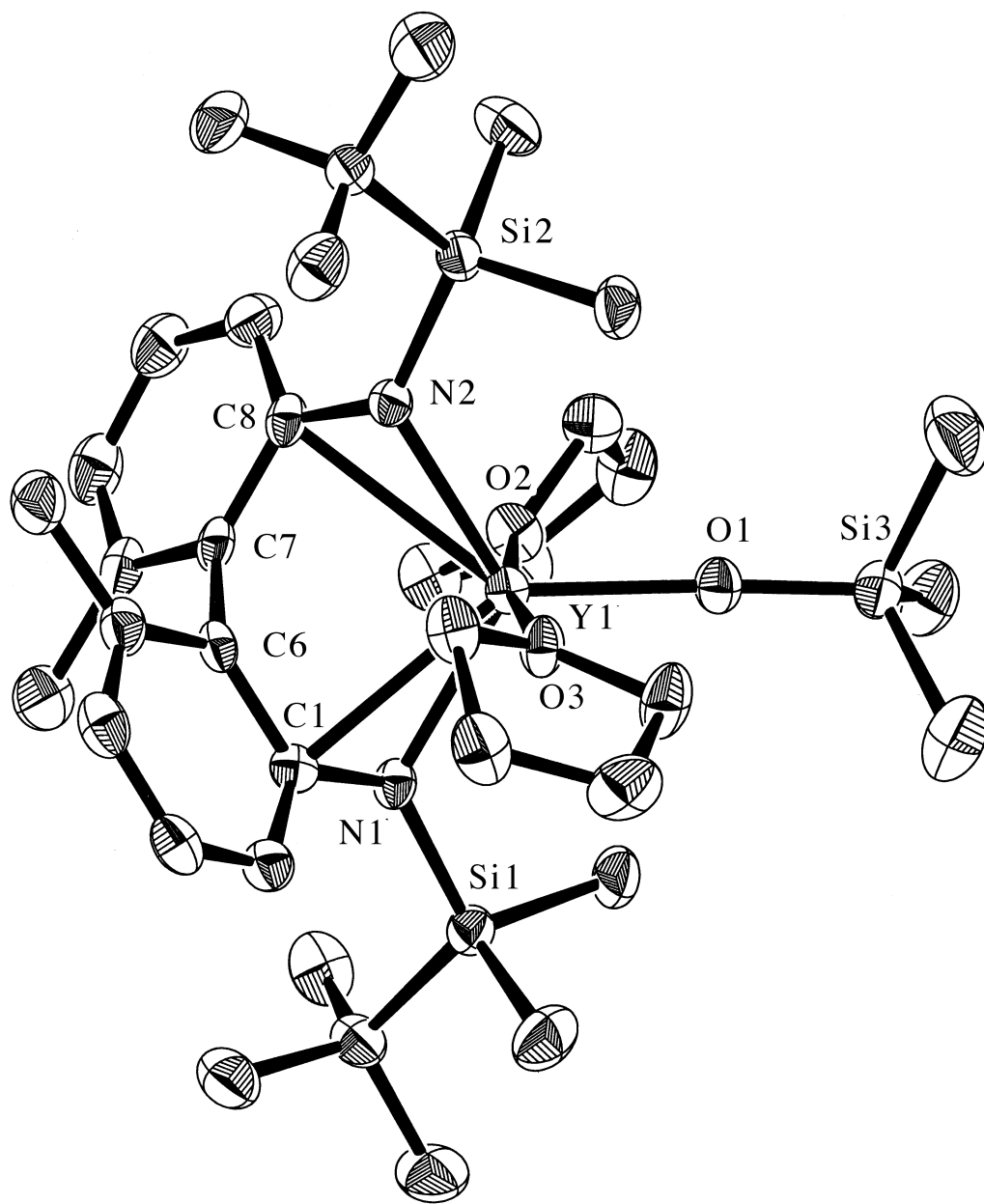


Figure 2. ORTEP diagram of [DADMB]Y(OSiMe₃)(THF)₂ (**4**).

The methyl derivative **3**, an off-white crystalline solid, was synthesized in 60% yield by reaction of **2** with MeLi in Et₂O/THF (eq 2). The methyl group of **3** gives rise to a doublet in the ¹H NMR spectrum at -0.42 ppm, and the coupling constant ²J_{YH} = 1.8 Hz is slightly smaller than those reported for Cp*₂YMe(THF) (²J_{YH} = 2.3 Hz) and related complexes.^{14,33} The ¹J_{CH} = 101 Hz coupling (cf. 108.2 Hz in Cp*₂YMe(THF)³³ and 108 Hz in Cp*Y(OC₆H₃^tBu₂)Me(THF)₂¹⁴) is lower than the typical 120 - 130 Hz for an sp³ CH bond.³⁴⁻³⁶

The synthesis of **3** was found to be very sensitive to the presence of adventitious amounts of silicone grease, such that high yields require exclusive use of hydrocarbon grease in the Schlenkware used for the synthesis. In the presence of Dow Corning silicone grease, the reaction of **2** with MeLi resulted in formation of the yttrium trimethylsiloxide derivative **4** in 50% yield (as the only isolable product). Complex **4** was characterized by X-ray crystallography (Figure 2).

The structure of **4** is very similar to that of the chloride complex **2**, with an Y–N distance of 2.26 Å (average), a ligand bite angle of 118.8(1)°, and an almost linear Y–O–Si linkage of 175.5(2)°. The dihedral angle between the biphenyl planes is 92.0°. The Y–C_{ipso} and Y–C_{ortho} bonding interactions are again present, but the corresponding distances are longer (averages of 2.82 and 3.00 Å, respectively), and the Y–N–C_{ipso} angles are larger (average 98.2°) than those observed for **2**. The mechanism of formation of **4** is unclear, but the methyl complex **3** was found to be unreactive towards silicone grease (benzene-*d*₆, 24 h, room temperature), suggesting that formation of **4** proceeds via trapping by silicone grease of an intermediate in the reaction of **2** with MeLi. Analogous reactivity has been reported for the samarium hydride complex, [(C₅Me₅)₂Sm(μ-H)]₂, which reacts with hexamethylcyclotrisiloxane to afford the dimeric siloxide [(C₅Me₅)₂Sm(THF)]₂(μ-OSiMe₂OSiMe₂O).³⁷

Exposure of **2** to C₂H₄ (80 psi) in the presence of MAO cocatalyst (500 equiv) in toluene produced only 0.06 g of polyethylene. The methyl derivative **3** was also found to

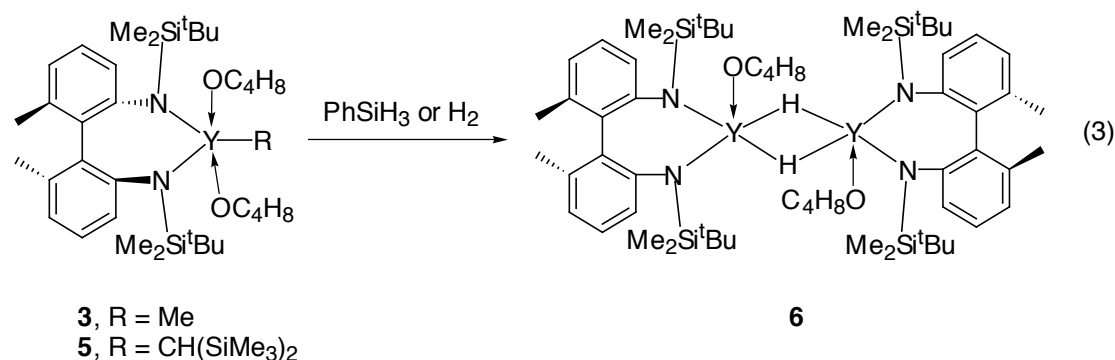
be inert towards olefins, since no reaction was observed between **3** and 1-hexene in benzene-*d*₆ (24 h, room temperature). A benzene-*d*₆ solution of **3** under 5 psi of C₂H₄ appears to react very slowly, as indicated by formation of a cloudy precipitate, presumed to be polyethylene, over the course of a few days. During this time, only a small decrease in the amount of C₂H₄ was observed (by ¹H NMR spectroscopy), **3** remained unchanged after 3 days, and no new organoyttrium species were detected by ¹H NMR spectroscopy.

Reasoning that the coordinated THF ligands may act to greatly diminish the reactivity of **3** toward alkenes, we sought to introduce a bulkier alkyl group which might facilitate dissociation of THF with production of a more coordinatively unsaturated complex. The bis(trimethylsilyl)methyl derivative [DADMB]Y[CH(SiMe₃)₂](THF)(OEt₂) (**5**) was obtained by reaction of **2** with (Me₃Si)₂CHLi in diethyl ether. The incorporation of Et₂O into **5** suggests that the more crowded steric environment in **5** can indeed favor dissociation of coordinated solvent. A similar tendency toward THF dissociation in the presence of a bulky alkyl substituent has been observed for [NON]Y[CH(SiMe₃)₂](THF) ([NON]²⁻ = [tBu-*d*₆-N-*o*-C₆H₄)₂O]²⁻).³⁸ The YCH resonance in the ¹H NMR spectrum appears as a doublet at δ -0.94 (²J_{YH} = 2.1 Hz), and the corresponding resonance in the ¹³C NMR spectrum appears at δ = 39.4 (¹J_{YC} = 35.6 Hz). The downfield chemical shift for the α-carbon is much closer to that reported for [NON]Y[CH(SiMe₃)₂](THF)³⁸ (37.9 ppm) and [PhC(NSiMe₃)₂]₂YCH(SiMe₃)₂¹² (43.5 ppm) than to the one for Cp*₂YCH(SiMe₃)₂³⁹ (25.19 ppm), and can therefore be viewed as an indication of the high electrophilicity of the metal center in **5**. The small C-H coupling for the α C-H bond (¹J_{CH} = 80 Hz, cf. 88 Hz in [PhC(NSiMe₃)₂]₂YCH(SiMe₃)₂,¹² and 84.2 Hz in Cp*₂YCH(SiMe₃)₂³⁹) is consistent with the presence of an α-agostic interaction, as observed for many group 3 and lanthanide bis(trimethylsilyl)methyl complexes.^{34,35}

Reaction of **5** with C₂H₄ (5 psi, benzene-*d*₆) also resulted in the very slow formation of insignificant amounts of polyethylene, with no new organoyttrium species observed in the ¹H NMR spectrum after 5 days. This low olefin polymerization activity for

3 and **5** should be compared to the behavior of other group 3 and lanthanides alkyl derivatives, some of which are reported to be active polymerization catalysts. Thus, $\text{Cp}^*_2\text{YMe}(\text{THF})$,³³ Cp^*_2ScMe ,⁴⁰ $[\text{Tp}^{\text{Me}}\text{YR}_2(\text{THF})]$ (Tp^{Me} = tris(3,5-dimethyl-1-pyrazolyl)borohydride),¹⁸ and $\text{R}_2\text{Si}(\eta^5\text{-C}_5\text{H}_4)(\eta^5\text{-C}_5\text{Me}_4)\text{LuCH}(\text{SiMe}_3)_2$ ⁴¹ are reported to be active as olefin polymerization catalysts, whereas $[\text{PhC}(\text{NSiMe}_3)_2]_2\text{YCH}_2\text{Ph}(\text{THF})$ ⁴² is moderately active and $[\text{Me}_2\text{Si}(\text{NCMe}_3)(\text{OCMe}_3)]_2\text{YCH}(\text{SiMe}_3)_2$ ¹³ and $\text{Cp}^*_2\text{MCH}(\text{SiMe}_3)_2$ ($\text{M} = \text{La}, \text{Nd}, \text{Lu}$),⁴³ and $[\text{NON}]\text{Y}[\text{CH}(\text{SiMe}_3)_2](\text{THF})$ ³⁸ are inactive. The lack of olefin polymerization activity in such systems is usually attributed to either steric hindrance (in the case of $\text{CH}(\text{SiMe}_3)_2$ derivatives), or high ionicity in the bonding which leads to more contracted vacant metal orbitals.^{12,13,42}

To evaluate the activities of **3** and **5** toward σ -bond metathesis processes involving hydrosilanes, their interactions with PhSiH_3 were investigated. Both compounds **3** and **5** were found to react with PhSiH_3 in benzene at room temperature via Si-C bond formation, to give PhMeSiH_2 and $\text{PhSiH}_2\text{CH}(\text{SiMe}_3)_2$,⁹ respectively. These reactions also produced a white crystalline precipitate, insoluble in pentane and benzene but soluble in THF, characterized as an yttrium hydride (eq 3). Hydride **6** was also produced by hydrogenolysis, upon exposure of **3** or **5** to H_2 gas in benzene- d_6 (5 psi, room temperature). The other products of these reactions (methane and $(\text{Me}_3\text{Si})_2\text{CH}_2$,⁴⁴ respectively) were observed to form quantitatively (by NMR spectroscopy).



The hydride resonance for **6** was observed in the ^1H NMR spectrum as a triplet at δ 5.88 ($^1J_{\text{YH}} = 28$ Hz) in THF- d_8 . The Y–H coupling constant is similar to that observed for other yttrium hydride dimers,^{12,13,45,46} and the chemical shift is rather downfield compared to most yttrium hydrides with bis(cyclopentadienyl) ligands (δ 2.02 - 5.45).^{41,45,47,48} However, the shift for **6** is not as low as those reported for bis(benzamidinato)yttrium hydrides (δ 8.28 - 8.31)¹² and $\{[\text{Me}_2\text{Si}(\text{NCMe}_3)(\text{OCMe}_3)]_2\text{Y}(\mu\text{-H})\}_2$ ¹³ (δ 6.80). This hydride signal was observed to decay slowly in intensity, and completely disappear within 4 days at room temperature, indicating exchange with deuterium from the THF- d_8 solvent. In the IR spectrum of **6**, the Y–H absorption at 1240 cm^{-1} was obscured by strong ligand absorptions in the same region, and could be assigned only by comparison with the spectrum of the deuterated analogue **6- d_2** (obtained by hydride exchange with THF- d_8), which exhibits a Y–D absorption at 870 cm^{-1} . This frequency is, however, in good agreement with those reported for other dimeric yttrium hydride species.^{44,45}

X-ray quality crystals of **6** were grown by slow diffusion of PhSiH_3 (in benzene solution) layered above a benzene solution of **5**, and the molecular structure (Figure 3) may be described as a centrosymmetric dimer. The hydride atom, located in the Fourier difference map, was refined isotropically. The Y–H distance is 2.25(4) Å (average), and the Y–H–Y angle is 109(2)°.

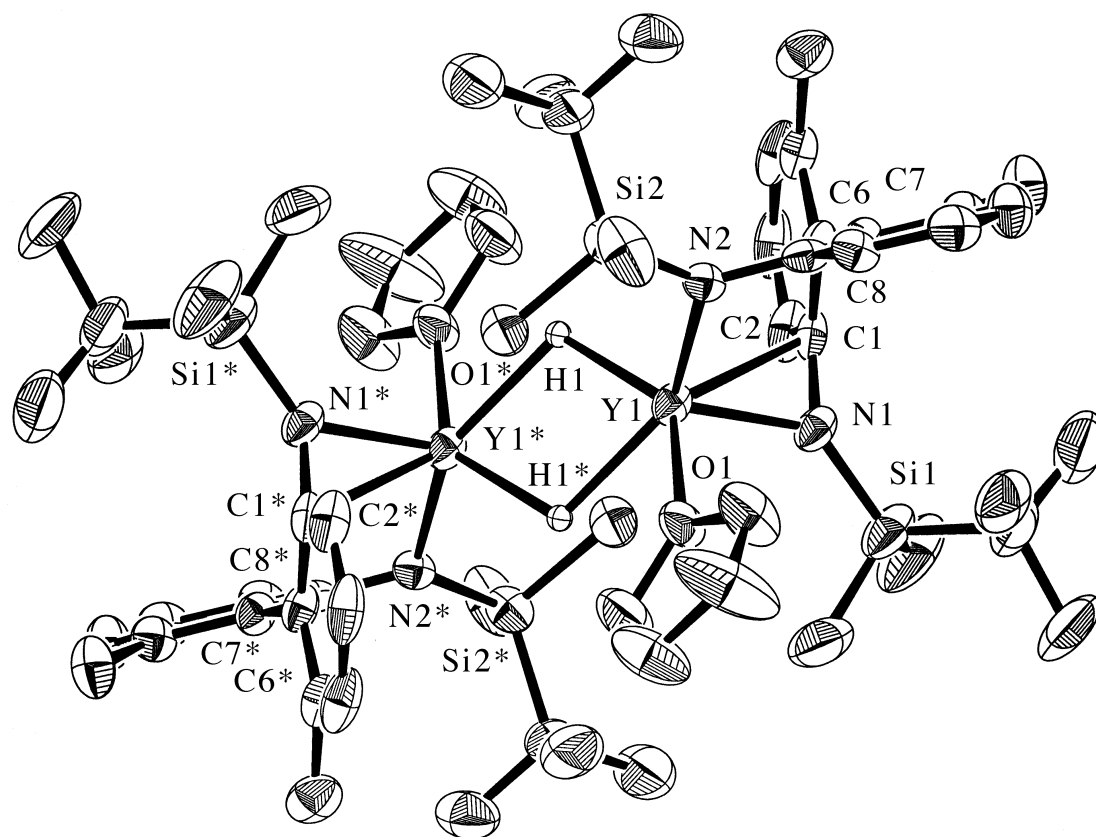
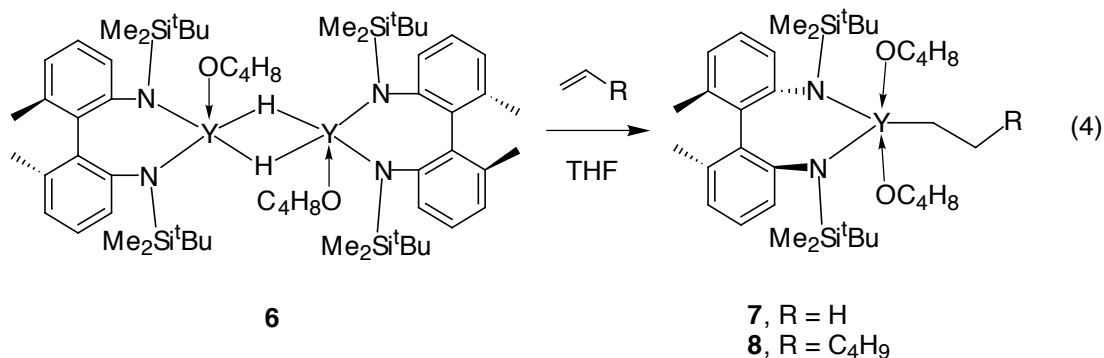


Figure 3. ORTEP diagram of $\{[DADMB]YH(THF)\}_2 \cdot C_6H_6$ (6).

The geometry of the four membered ring is very similar to that found in other structurally characterized dimeric yttrium hydrides, $[(1,3\text{-Me}_2\text{C}_5\text{H}_3)_2\text{Y}(\mu\text{-H})(\text{THF})]_2$ ⁴⁶ (average 2.15(7) Å and 118(3)°), $[(\text{MeC}_5\text{H}_4)_2\text{Y}(\mu\text{-H})(\text{THF})]_2$ ⁴⁵ (2.18(8) Å and 114(3)°), and $\{[\text{PhC}(\text{NSiMe}_3)_2]_2\text{Y}(\mu\text{-H})\}_2$ ¹² (2.14(3) Å and 111.5(15)°). The N–Y–N ligand bite angle in **6** (103.9(1)°) is significantly lower than those of ca. 120° in the 5-coordinate complexes **2** and **4**, and only one of the ligand *ipso* carbons is in a close contact with the yttrium center (Y–C(1) = 2.702(4) Å, Y–C(6) = 3.069(5) Å, Y–N(1)–C(1) = 93.4(2)°, whereas Y–C(8) = 3.098(5) Å, Y–C(7) = 3.409(4) Å, Y–N(2)–C(8) = 114.6(3)°). The dihedral angle between the biphenyl planes is 81.9°. These differences may be attributed to steric crowding in the hydride dimer relative to the monomeric complexes **2** and **4**.

Compound **6** represents a rare example of an yttrium hydride that contains no cyclopentadienyl ligands. We are aware of only one other structurally characterized non-Cp yttrium hydride, the bis(benzamidinato) complex $\{[\text{PhC}(\text{NSiMe}_3)_2]_2\text{Y}(\mu\text{-H})\}_2$ ¹². Other examples of such hydrides are the unstable species $\{[\text{Me}_2\text{Si}(\text{NCMe}_3)(\text{OCMe}_3)]_2\text{Y}(\mu\text{-H})\}_2$ ¹³ and a tris(pyrazolyl)borato yttrium hydride $\text{Tp}^{\text{Me}}\text{YH}_2(\text{THF})_4$ ¹⁸ for which a trimeric solution structure was suggested. All of the structurally characterized yttrium hydrides are dimers^{4,12,41,45,46} or trimers⁴⁶ in the solid state, although more complicated aggregates have also been observed in anionic or heterometallic species.⁴⁸

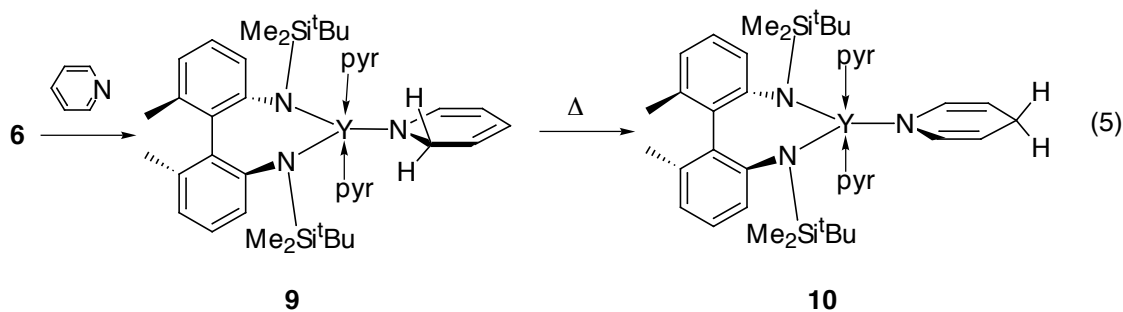
The reactivity of **6** appears to be restricted by its dimeric nature (preserved even in THF solution, as suggested by the ¹H NMR spectrum), and its very low solubility in nonpolar organic solvents. No polymerization activity was observed towards 1-hexene or C₂H₄ (5 psi) in benzene-*d*₆ at room temperature, and heating these mixtures resulted in decomposition of the hydride with precipitation of only a small amount of polyethylene. However, when dissolved in THF, compound **6** was found to rapidly insert ethylene at room temperature, to give the yttrium ethyl complex **7** (eq 4).



At longer reaction times (6-7 h), compound **7** seems to undergo a slow insertion of a second molecule of C₂H₄, but positive identification of multiple insertion products was hindered by their decomposition, and no formation of polyethylene was observed even at elevated pressure (80 psi, THF, 48 h at room temperature). Decomposition of **7** to unidentified products was also found to occur even in solid state, under N₂, over the period of a few months. The ethyl group of **7** gives rise to a broad multiplet at 0.0 ppm (YCH₂CH₃, 2 H) and a triplet of doublets at 1.67 ppm (YCH₂CH₃, 3 H) in the ¹H NMR spectrum. The ³J_{YH} coupling constant of 1.9 Hz for the CH₃ protons of the ethyl ligand is very similar to the related value (³J_{YH} = 1.4 Hz) reported for (η⁵-CH₃C₅H₄)₂Y(CH₂CH₃)-(THF),⁴⁸ and the ¹J_{CH} coupling of 120 Hz is typical for an sp³ C-H bond. Although β-agostic interactions are often observed in early transition metal ethyl complexes,^{34-36,40,49-51} their existence cannot be determined based on the (averaged) ¹J_{CH} coupling constant only. The IR spectrum of **7** doesn't contain evidence for agostic C-H bonds (no low-energy C-H bands were detected). The relatively small ¹J_{CH} coupling of 70-80 Hz (multiplet broadness prevents accurate measurement) for the α protons, however, is consistent with the presence of an α-agostic interaction with the metal center,^{34,35,52-54} analogous to that reported for some bis(trimethylsilyl)methyl yttrium complexes (vide supra). In the ¹³C NMR spectrum of **6**, the α-carbon appeared as a doublet at 35.5 ppm, with a coupling of 50 Hz to yttrium.

In THF-*d*₈ solution, the slower insertion of 1-hexene into the Y–H bond of **6** was observed (eq 4), to give the 1-hexyl derivative **8** (by ¹H NMR spectroscopy). No reaction occurred between **6** and cyclohexene, however. Single insertion of terminal olefins to give yttrium alkyl complexes has been reported for [(η⁵-RC₅H₄)₂YH(THF)]₂ (R = H or Me).⁴⁸ The lack of olefin polymerization activity for compound **6** can be contrasted to the high catalytic activity of certain dimeric group 3 and lanthanide hydrides of the type [Cp*₂MH]₂ (M = La, Nd, Sm, Lu),⁴³ but is similar to the reported low activity for {[PhC(NSiMe₃)₂]₂-Y(μ-H)}₂¹² and {[Me₂Si(NCMe₃)(OCMe₃)]₂Y(μ-H)}₂.¹³ Other dimeric hydrides have been reported to undergo single, reversible olefin insertion to give mixed hydrido-alkyl complexes (e.g., [Cp*Y(OC₆H₃^tBu₂)]₂(μ-H)(μ-alkyl)¹⁴ and [Et₂Si(η⁵-C₅H₄)(η⁵-C₅Me₄)M]₂(μ-H)(μ-CH₂CH₃) for M = Lu, Y),⁴¹ but we have not observed formation of such species in the reactions of **6** with olefins.

As shown in eq 5, yttrium hydride **6** was found to react with pyridine to give a mixture of pyridine insertion products, **9** (major) and **10** (minor), in variable ratios. The structure of **9**, confirmed by X-ray crystallography (Figure 4), is again based on a distorted trigonal bipyramidal geometry, with neutral donors (pyridine) occupying the axial positions.



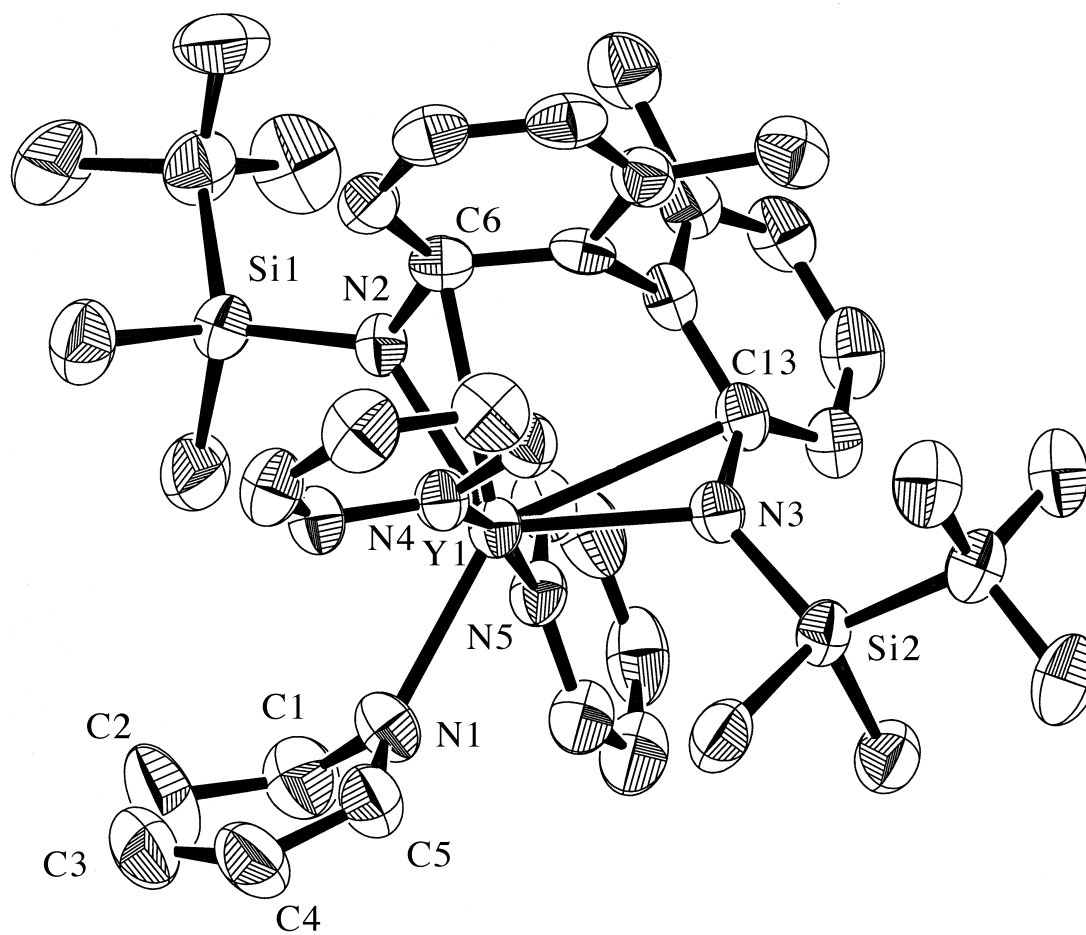


Figure 4. ORTEP diagram of [DADMB]Y(NC₅H₆)(NC₅H₅)₂·C₅H₁₂ (**9**).

The ligand bite angle is 118.9° , and the two *ipso* carbons are in close contact with yttrium (average distance 2.77 \AA). The dihedral angle between the biphenyl planes is 92.8° . The third pyridine unit attached to the metal center has been reduced via 1,2 insertion, as can be deduced from the changes in the C–C bond lengths and a puckering of the pyridine ring.

The identities of the 1,2 and 1,4 insertion products **9** and **10** were further confirmed by 2D NMR studies (TOCSY and HMQC), which revealed a characteristic coupling pattern for the partially hydrogenated pyridine ring,^{48,55,56} and allowed assignment of the ring protons and carbons (see Experimental Section). Heating a solution containing both **9** and **10** to 80°C in benzene-*d*₆ resulted in complete conversion of the mixture within 2 h to compound **10**, as observed by ¹H NMR spectroscopy. This indicates that **10** is the thermodynamically more stable isomer, while **9** is kinetically generated. This reactivity towards pyridine has precedent in a number of previously reported reactions for yttrium hydride and alkyl complexes. Metalation of pyridine via CH activation has been reported for [Cp^*_2YH]₂,⁵⁷ $\text{Cp}^*_2\text{YCH}(\text{SiMe}_3)_2$,⁴⁴ and $\text{Cp}^*_2\text{YMe}(\text{THF})$,⁴⁴ while 1,2-insertion of pyridine followed by rearrangement to the 1,4 insertion product has been reported for $[(\eta^5\text{-C}_5\text{H}_4\text{R})_2\text{YH}(\text{THF})]_2$ (R = H, CH₃).⁴⁸ Also, an analogous 1,2- to 1,4-isomer rearrangement has been observed for the bis(alkoxysilylamido)yttrium derivative $[\text{Me}_2\text{Si}(\text{NCMe}_3)(\text{OCMe}_3)]_2\text{YNC}_5\text{H}_6$.⁵⁵ The bis(trimethylsilyl)benzamidinate complexes $\{[\text{PhC}(\text{NSiMe}_3)_2]_2\text{YH}\}_2$ and $[\text{PhC}(\text{NSiMe}_3)_2]_2\text{YCH}_2\text{Ph}(\text{THF})$ have also been reported to undergo the 1,2-insertion of pyridine,⁴² but no further isomerization was noted in these cases. The reactivity of **6** towards pyridine is thus different from that of similar pentamethylcyclopentadienyl yttrium complexes, and is more similar to that of other known yttrium hydrides and alkyls with monosubstituted Cp, or non-cyclopentadienyl, ligands.

Conclusions

A series of novel yttrium complexes with bis(silylamido)biphenyl ligands have been synthesized and characterized. The structures and reactivities of the chloride, alkyl, and hydrido derivatives have been investigated. In their reactivity, these complexes resemble more closely some benzamidinate¹² and alkoxy-silylamido¹³ yttrium species, rather than the more fully investigated cyclopentadienyl yttrium derivatives.^{39,41,46,48,58} The high degree of ionicity in the yttrium-nitrogen bonding appears to result in a highly electrophilic metal center, which leads to lower reactivity towards olefin polymerization and σ -bond metathesis, perhaps resulting from more contracted vacant metal orbitals which are less effective in substrate binding.^{12,13,42} The reactivity of the hydride is also inhibited by the high stability of the bridged yttrium hydride unit, and the insolubility of the dimer in noncoordinating solvents. Very low olefin polymerization activity is exhibited by the MAO-activated chloride, and the alkyl and the hydride complexes. A single insertion of olefins into the Y-H bond, reminiscent of the reactivity of some monosubstituted-Cp yttrium hydrides,⁴⁸ results in formation of yttrium alkyl species, and the ethyl complex is sufficiently stable to be isolated and characterized. The reactivity of the yttrium hydride **6** towards pyridine also resembles that observed for related hydride derivatives containing benzamidinate and alkoxy-silylamido ancillary ligands.

The yttrium derivatives studied represent another example of non-cyclopentadienyl early transition metal complexes. This study further contributes to an understanding of the factors behind the reactivity of such d^0 complexes. As has been already suggested, in addition to the electrophilicity of the metal center, other possibly important factors include the degree of ionicity in the metal-ligand bonds, and the steric environment created by the ligand. The latter not only affects the accessibility of the metal center by the substrate, but also the ease of dimer formation, which is particularly important in the case of hydride derivatives. Although apparently not promising in terms of olefin polymerization activity,

these silylamido yttrium species exhibit reactivity patterns which are distinct from those known for more traditional cyclopentadienyl derivatives.

Experimental Section

General. All reactions with air-sensitive compounds were performed under dry nitrogen, using standard Schlenk and glove box techniques. Reagents were obtained from commercial suppliers and used without further purification, unless otherwise noted. Olefin-free pentane, benzene, and toluene were prepared by pretreating with conc. H₂SO₄, 0.5 N KMnO₄ in 3 M H₂SO₄, NaHCO₃ and finally anhydrous MgSO₄. Solvents (pentane, diethyl ether, benzene, toluene, tetrahydrofuran) were distilled under nitrogen from sodium benzophenone ketyl. Benzene-*d*₆ was distilled from Na/K alloy. Commercial silanes were distilled and dried over molecular sieves before use. ⁿBuLi was used as a 1.6 M solution in hexanes, as supplied by Aldrich, and MeLi as a 1.6 M solution in Et₂O, as supplied by Alpha Aesar. 2,2'-Diamino-6,6'-dimethylbiphenyl,⁵⁹ YCl₃(THF)₃,³⁹ and LiCH(SiMe₃)₂⁶⁰ were prepared according to published literature procedures. NMR spectra were recorded at 300 or 500 MHz (¹H) with Bruker AMX-300 and DRX-500 spectrometers, or at 100 MHz (¹³C{¹H}) with an AMX-400 spectrometer, at ambient temperature and in benzene-*d*₆, unless otherwise noted. CH coupling constants were obtained from non-decoupled HMQC experiments. Signal multiplicities are reported as follows: s - singlet, d - doublet, t - triplet, q - quartet, qn - quintet, m - multiplet. Elemental analyses were performed by the Microanalytical Laboratory at UC Berkeley, E+R Microanalytical Laboratory, or Desert Analytics. Infrared spectra were recorded with a Mattson Infinity 60 MI FTIR spectrometer, as KBr pellets.

Li₂[DADMB]·2THF (1). To a cold (0 °C) solution of 2,2'-diamino-6,6'-dimethylbiphenyl (4.00 g, 18.8 mmol) in THF (100 mL) was added dropwise 25.0 mL (40 mmol) of 1.6 M ⁿBuLi. A white precipitate formed initially, but dissolved completely after all of the ⁿBuLi had been added. The solution was allowed to warm to room temperature,

and was then stirred for 3 h. A solution of $t\text{BuMe}_2\text{SiCl}$ (6.22 g, 41.2 mmol) in 20 mL of THF was then added dropwise. The mixture was heated at reflux for 5 h, which resulted in the formation of a white precipitate. After cooling to room temperature, a second portion of $n\text{BuLi}$ (25.0 mL, 40 mmol) was added and the mixture was stirred overnight at room temperature. The THF was removed under vacuum to give an oily white solid. Extraction with pentane (2×100 mL) gave a light yellow solution, which was concentrated in vacuo until crystals appeared, and then cooled to -78 °C. The resulting crystalline product was recrystallized from pentane and dried to afford 9.45 g (15.8 mmol, 84% yield) of colorless crystals. ^1H NMR: δ 7.06 (d, 2 H, $J = 7.7$ Hz), 6.95 (t, 2 H, $J = 7.7$ Hz), 6.48 (d, 2 H, $J = 7.1$ Hz biphenyl H's), 3.14 (m, 8 H, THF), 1.99 (s, 6 H, *Me*), 1.25 (m, 8 H, THF), 1.16 (s, 18 H, $t\text{BuMe}_2\text{Si}$), 0.49 (s, 6 H, $t\text{BuMe}_2\text{Si}$), 0.09 (s, 6 H, $t\text{BuMe}_2\text{Si}$). $^{13}\text{C}\{^1\text{H}\}$ NMR: δ 157.5, 140.1, 133.2, 128.0, 121.8, 116.6, 68.6 (THF), 28.7 (CMe_3), 25.4 (THF), 21.8, 21.7 (*Me*; CMe_3), 1.0, -0.5 ($t\text{BuMe}_2\text{Si}$). IR (cm^{-1}): 3039 (w), 2951 (s), 2923 (s), 2879 (s), 2848 (s), 1575 (s), 1559 (s), 1460 (s), 1440 (s), 1288 (s), 1250 (s), 1049 (s), 968 (m), 899 (m), 842 (s), 824 (s), 769 (s), 668 (m), 605 (m), 457 (m), 419 (m). Anal. Calcd for $\text{C}_{34}\text{H}_{58}\text{N}_2\text{Li}_2\text{O}_2\text{Si}_2$: C, 68.42; H, 9.79; N, 4.69. Found: C, 68.18; H, 9.85; N, 4.56.

[DADMB]YCl(THF)₂ (2). A solution of **1** (3.00 g, 5.03 mmol) and $\text{YCl}_3(\text{THF})_3$ (2.10 g, 5.10 mmol) in 100 mL of THF was heated at reflux for 4 h, resulting in formation of a white precipitate. The solvent was removed in vacuo and the resulting white powder was extracted with a mixture of 60 mL of pentane and 25 mL of THF. The filtrate was concentrated to about 15 mL and more pentane (20 mL) was added to initiate crystallization of the product as a white precipitate. After cooling to -78 °C, the solution was filtered and the product was then dried in vacuo to obtain 3.28 g (92% yield) of white crystalline powder. ^1H NMR: δ 7.07 (d, 2 H), 6.95 (t, 2 H), 6.55 d, 2 H, aromatic H), 3.70 - 3.46 (br m, 8 H, THF), 1.88 (s, 6 H, *Me*), 1.24 (m, 8 H, THF), 1.11 (s, 18 H, $t\text{BuMe}_2\text{Si}$), 0.52, 0.50 (s, 6 H each, $t\text{BuMe}_2\text{Si}$). $^{13}\text{C}\{^1\text{H}\}$ NMR: δ 152.4, 142.4, 130.5,

129.9, 123.5, 120.1 (aromatic C), 68 (THF), 28.3 (*Me*₃C), 25.5 (THF), 22.3 (*MeAr*), 21.5 (*Me*₃C), 1.8, -1.6 (*Me*₂Si). IR (cm⁻¹): 3040 (w), 2949 (s), 2925 (s), 2882 (s), 2851 (s), 1578 (m), 1558 (m), 1471 (m), 1461 (m), 1441 (s), 1387 (w), 1356 (w), 1272 (s), 1248 (s), 1085 (w), 1048 (s), 1021 (m), 963 (m), 872 (m), 830 (s), 777 (s), 708 (m), 668 (m), 568 (m), 440 (m). Anal. Calcd for C₃₄H₅₈N₂O₂Si₂YCl: C, 57.73; H, 8.26; N, 3.96. Found: C, 57.61; H, 8.44; N, 3.85.

[DADMB]YMe(THF)₂ (3). Compound **2** (1.16 g, 1.64 mmol) was dissolved in 100 mL of Et₂O, and MeLi (1.10 mL, 1.76 mmol) was added at room temperature. To the reaction mixture was added a small amount of THF, to bring the remaining undissolved **2** into solution. The resulting pale yellow solution was stirred overnight, the solvents were removed in vacuo, and the oily residue was extracted with 2 × 50 mL of pentane. The product was isolated by crystallization at -78°C in two crops (0.67 g, 60% yield) as a white crystalline powder. ¹H NMR: δ 7.07 (m, 2 H), 6.96 (m, 2 H), 6.56 (m, 2 H, aromatic H), 3.43 (m, 8 H, THF), 1.89 (s, 6 H, Me), 1.24 (m, 8 H, THF), 1.14 (s, 18 H, *t*BuMe₂Si), 0.52, 0.40 (s, 6 H each, *t*BuMe₂Si), -0.42 (d, 3 H, ²J_{YH} = 1.8 Hz, ¹J_{CH} = 101 Hz, YMe). ¹³C{¹H} NMR: δ 153.2, 142.1, 131.1, 129.4, 123.4, 119.5, 70.9 (THF), 28.4 (*Me*₃C), 25.5 (THF), 22.4 (*MeAr*), 21.7 (YMe), 21.7 (*Me*₃C), 2.0, -1.9 (*Me*₂Si). IR (cm⁻¹): 3038 (w), 3043 (m), 2951 (s), 2890 (s), 2851 (s), 1906 (w), 1577 (s), 1555 (s), 1460 (s), 1440 (s), 1398 (m), 1358 (m), 1271 (s), 1243 (s), 1085 (m), 1048 (s), 1031 (s), 981 (s), 880 (m), 830 (s), 784 (s), 769 (s), 708 (m), 673 (m), 661 (m), 607 (w), 567 (w), 454 (m), 436 (w). Anal. Calcd for C₃₅H₆₁N₂Si₂O₂Y: C, 61.20; H, 8.95; N, 4.08. Found: C, 59.74; H, 9.48; N, 3.87.

[DADMB]Y(OSiMe₃)(THF)₂ (4). Compound **2** (0.54 g, 0.76 mmol) and 0.3 g of Dow Corning Silicone Grease were dissolved in 100 mL of Et₂O, and MeLi (0.5 mL, 0.8 mmol) was added at room temperature. To the reaction mixture was added a small amount of THF, to bring the remaining undissolved **2** into solution. The resulting pale yellow solution was stirred overnight, the solvents were removed in vacuo, and the oily

residue was extracted with 2×40 mL of pentane. The product was isolated by crystallization from pentane at -78°C (0.29 g, 50% yield) as a white crystalline powder. ^1H NMR: δ 7.04 (m, 2 H), 6.96 (m, 2 H), 6.57 (m, 2 H, aromatic H), 3.46 (m, 8 H, THF), 1.91 (s, 6 H, Me), 1.28 (m, 8 H, THF), 1.14 (s, 18 H, $^t\text{BuMe}_2\text{Si}$), 0.50, 0.29 (s, 6 H each, $^t\text{BuMe}_2\text{Si}$), 0.26 (s, 9 H, Me_3SiO). $^{13}\text{C}\{^1\text{H}\}$ NMR: δ 153.6, 142.2, 131.2, 129.4, 123.2, 119.4, 70.7 (THF), 28.5 (Me_3C), 25.4 (THF), 22.4 (MeAr), 21.6 (Me_3C), 4.0 (Me_3SiO), 1.7, -1.3 (Me_2Si). IR (cm^{-1}): 3078 (w), 3043 (m), 2951 (s), 2890 (s), 2851 (s), 1906 (w), 1577 (s), 1555 (s), 1460 (s), 1440 (s), 1398 (m), 1358 (m), 1271 (s), 1243 (s), 1085 (m), 1048 (s), 1031 (s), 981 (s), 880 (m), 830 (s), 784 (s), 769 (s), 708 (m), 673 (m), 661 (m), 607 (w), 567 (w), 454 (m), 436 (w). Anal. Calcd for $\text{C}_{37}\text{H}_{67}\text{N}_2\text{Si}_3\text{O}_3\text{Y}$: C, 58.39; H, 8.87; N, 3.68. Found: C, 58.66; H, 9.25; N, 3.58.

[DADMB]YCH(SiMe₃)₂(THF)(Et₂O) (5). A mixture of **2** (1.24 g, 1.75 mmol) and $\text{LiCH}(\text{SiMe}_3)_2(\text{Et}_2\text{O})_{0.1}$ (0.30 g, 1.76 mmol) was dissolved in 80 mL of Et_2O . The reaction mixture was kept in an ice bath for 30 min and then allowed to warm to room temperature and was stirred for 8 h. The cloudy yellow solution was filtered, the clear filtrate was concentrated to about 15 mL, and 20 mL of pentane was then added. Further concentration and cooling to -78°C resulted in the formation of a white crystalline precipitate, which was isolated by filtration and dried in vacuo to give 0.59 g of product (43% yield). The product can be purified by recrystallization from pentane. ^1H NMR: δ 7.23 (m, 1 H), 6.85 (m, 3 H), 6.70 (m, 1 H), 6.59 (m, 1 H, aromatic H's), 3.52 (m, broad, 4 H, THF), 3.24 (q, 6 H, Et_2O), 1.88 (s, 3 H, MeAr), 1.84 (s, 3 H, MeAr), 1.38 (m, 4 H, THF), 1.11 (t, 4 H, Et_2O), 1.10 (s, 9 H, Me_3C , overlaps with Et_2O), 1.08 (s, 9 H, Me_3C), 0.60 (s, 3 H, Me_2Si), 0.32 (s, 3 H, Me_2Si), 0.31 (s, 3 H, Me_2Si), 0.29 (s, 9 H, Me_3Si , overlaps Me_2Si), 0.26 (s, 3 H, Me_2Si), 0.25 (s, 9 H, Me_3Si), -0.94 (d, 1 H, $^2J_{\text{YH}} = 2.1$ Hz, $^1J_{\text{CH}} = 80$ Hz, YCH). ^{13}C NMR: δ 150.3, 141.7, 138.6, 129.3, 120.1, 113.4, (biphenyl), 71.7, 68.5, 66.2 (THF, Et_2O), 39.4 (YCH, $^1J_{\text{YC}} = 35.6$ Hz), 28.7, 27.9, 26.0, 25.3 (Me_3C), 26.5 (THF), 22.4 (MeAr), 21.2, 20.6 (Me_3C), 15.9 (Et_2O),

5.7, 4.8 (Me_3Si), 1.28, -0.51 (Me_2Si). IR (cm^{-1}): 3043 (w), 2952 (s), 2887 (s), 2851 (s), 1577 (m), 1559 (m), 1462 (s), 1443 (s), 1387 (w), 1247 (s), 1091 (w), 1044 (s), 1006 (m), 963 (m), 836 (s), 793 (m), 768 (m), 711 (w), 661 (m), 594 (w), 427 (w).
 Anal. Calcd for $C_{41}H_{79}N_2O_2Si_2Y$: C, 63.36; H, 10.25; N, 3.60. Found: C, 63.07; H, 10.45; N, 3.76.

{[DADMB]YH(THF)}₂·C₆H₆ (6). To a solution of **5** (1.05 g, 1.35 mmol) in 50 mL of benzene was added 0.6 mL (5.5 mmol) of $PhSiH_3$. The mixture was left undisturbed at room temperature for 5 days, resulting in formation of a highly crystalline, colorless precipitate. The product was then isolated by filtration, washed with benzene (30 mL) and pentane (30 mL), and briefly dried in vacuo (0.53 g, 61% yield). 1H NMR (THF- d_8): δ 6.99 (m, 4 H, aromatic H), 6.54 (m, 2 H, aromatic H), 5.88 (t, 1 H, $J = 28$ Hz, YH), 3.61 (m, THF), 1.77 (m, THF), 1.69 (s, 6 H, $MeAr$), 0.90 (s, 18 H, Me_3C), 0.35 (s, 6 H, Me_2Si), 0.21 (s, 6 H, Me_2Si). $^{13}C\{^1H\}$ NMR (THF- d_8): δ 152.7, 142.6, 130.8, 130.3, 124.0, 120.3 (aromatic C), 129.2 (C_6H_6), 68.4 (THF), 28.3 (Me_3C), 26.5 (THF), 22.2 ($MeAr$), 21.7 (Me_3C), 1.5 (Me_2Si), -1.7 (Me_2Si). IR (cm^{-1}): 3038 (m), 2949 (s), 2926 (s), 2881 (s), 2850 (s), 2703 (w), 1564 (m), 1462 (s), 1441 (s), 1388 (m), 1359 (m), 1251 (s, broad), 1087 (m), 1047 (s), 1014 (s), 966 (s), 865 (s), 834 (s, broad), 791 (s), 767 (s), 707 (m), 682 (s), 662 (s), 617 (m), 595 (m), 567 (m), 464 (m), 431 (m).
 A sample of the deuterated analogue (**6- d_2**) was obtained by allowing a THF- d_8 solution of **6** stand at room temperature for 4 days, followed by removal of the solvent in vacuo which resulted in complete exchange of the Y-hydride with deuterium. Subtraction of the IR spectrum of **6- d_2** showed the presence of a strong Y-H absorption at 1240 cm^{-1} , overlapping with a strong ligand absorption. Anal. Calcd for $C_{66}H_{108}N_4O_2Si_4Y_2$: C, 61.94; H, 8.51; N, 4.38. Found: C, 61.95; H, 8.55; N, 4.19.

[DADMB]YEt(THF)₂ (7). A sample of the yttrium hydride **6** (0.184 g, 0.144 mmol) was dissolved in 15 mL of THF. The reaction flask was filled with C_2H_4 at 5-10 psi, and the solution was stirred for 30 min. The solvent was removed under vacuum and

the solid residue was extracted into 20 mL of hexane. The extract was filtered, and the filtrate was then concentrated to 5 mL and cooled to -35 °C overnight, to give **7** as a white crystalline solid (0.121 g, 60% yield). ^1H NMR: δ 7.07, 6.95, 6.56 (m, 2 H each, aromatic H), 3.49 (m, 8 H, THF), 1.88 (s, 6 H, *MeAr*), 1.67 (dt, $^3J_{\text{HH}} = 7.4$ Hz, $^3J_{\text{YH}} = 1.9$ Hz, $^1J_{\text{CH}} = 70 - 80$ Hz, 3 H, YCH_2CH_3), 1.25 (m, 8 H, THF), 1.13 (s, 18 H, $t\text{BuMe}_2\text{Si}$), 0.53, 0.37 (s, 6 H each, $t\text{BuMe}_2\text{Si}$), 0.0 (br m, $^1J_{\text{CH}} = 120$ Hz, 2 H, YCH_2CH_3). ^{13}C NMR: δ 153.1, 141.9, 131.4, 129.3, 123.5, 119.7 (biphenyl C), 72 (THF), 35.5, (d, $J = 50$ Hz, YCH_2CH_3), 28.4 (Me_3C), 25.5 (THF), 22.4 (*MeAr*), 21.6 (Me_3C), 15.7 (YCH_2CH_3), 1.7, -1.9 (Me_2Si). IR (cm^{-1}): 3043 (w), 3034 (w), 2953 (s), 2851 (s), 1578 (m), 1555 (m), 1461 (m), 1440 (m), 1268 (s), 1048 (s), 964 (m), 829 (s), 785 (m), 768 (m), 662 (w). Anal. Calcd for $\text{C}_{36}\text{H}_{63}\text{N}_2\text{Si}_2\text{O}_2\text{Y}$: C, 61.68; H, 9.06; N, 4.00. Found: C, 61.08; H, 8.96; N, 4.05.

[DADMB]Y(n-C₆H₁₃)(THF)₂ (8). A sample of **6** (ca. 10 mg) was dissolved in THF-*d*₈ (0.5 mL) and ca. 0.05 mL of 1-hexene was added. After 30 min, the YH signals had nearly disappeared, and after 5 h a complete conversion to product was observed. ^1H NMR: δ 6.9-7.0 (m, 4 H), 6.54 (m, 1 H), 6.47 (m, 1 H, biphenyl H), 1.65 (s, 6 H, *MeAr*), 1.46 (m, 2 H, YCH_2CH_2), 1.33-1.38 (m, overlaps with 1-hexene, $\text{YCH}_2\text{CH}_2(\text{CH}_2)_3\text{CH}_3$), 0.89 (s, 18 H, Me_3C), 0.85 (m, overlaps, $\text{Y}(\text{CH}_2)_5\text{CH}_3$), 0.38 (s, 6 H, Me_2Si), 0.16 (s, 6 H, Me_2Si), -0.32 (m, 2 H, YCH_2).

[DADMB]Y(NC₅H₆)(pyr)₂·C₅H₁₂ (mixture of **9 and **10**).** A sample of **6** (0.36 g, 2.8 mmol) was dissolved in 20 mL of pyridine at room temperature. The dark yellow solution was stirred for 2 days, and the volatile material was then removed by vacuum transfer. The remaining solid was extracted with 2 × 75 mL pentane, and then the combined yellow extracts were concentrated to 20 mL. Cooling the solution to -35 °C produced bright yellow crystals (0.14 g, 30% yield). ^1H NMR: compound **9**: δ 8.23 (m, 4 H, pyr), 7.27 (d, 1 H, NC₅H₆ vinylic), 6.83 - 6.54 (m, pyr and aromatic H), 6.47 (t, 1 H, NC₅H₆ vinylic), 5.40 (m, 1 H, NC₅H₆ vinylic), 5.04 (m, 1 H, NC₅H₆ vinylic), 4.30 (dd,

1 H, NC₅H₆ methylene), 4.04 (dd, 1 H, NC₅H₆ methylene), 2.03 (s, 6 H, *Me*), 1.05 (s, 18 H, *t*BuMe₂Si), 0.23 (s, 6 H, *t*BuMe₂Si), 0.18 (s, 6 H, *t*BuMe₂Si); compound **10**: 8.32 (m, 4 H, pyr), 6.92 (m, 2 H, aromatic H), 6.71 (d, 2 H, NC₅H₆ vinylic), 6.63 - 6.58 (m, pyr and aromatic H), 4.55 (m, 2 H, NC₅H₆ vinylic), 3.69 (m, 2 H, NC₅H₆ methylene), 2.02 (s, 6 H, *Me*), 1.04 (s, 18 H, *t*BuMe₂Si), 0.20 (s, 6 H, *t*BuMe₂Si), 0.13 (s, 6 H, *t*BuMe₂Si). ¹³C{¹H} NMR: compound **9**: δ 152.3, 150.4, 146.4, 141.0, 132.9, 129.3 (aromatic C), 125.8 (NC₅H₆), 124.0, 120.4 (aromatic C), 113.4 (NC₅H₆), 102.2 (NC₅H₆), 96.8 (NC₅H₆), 47.9 (NC₅H₆ methylene), 28.6 (*Me*₃C), 22.3 (*Me*Ar), 21.4 (*Me*₃C), 0.9 (*t*BuMe₂Si), -0.8 (*t*BuMe₂Si); compound **10**: 152.3, 150.5, 141.0 (aromatic C), 137.0 (NC₅H₆), 133.0, 129.7, 129.6, 125.8, 124.1, 120.5 (aromatic C), 95.2 (NC₅H₆), 28.6 (*Me*₃C), 25.5 (NC₅H₆), 21.4 (*Me*₃C), 0.8 (*t*BuMe₂Si), -0.9 (*t*BuMe₂Si). Assignment of the NMR signals is based on 2D NMR studies (TOCSY and HMQC). Heating the NMR sample (product mixture of **9** and **10**) to 80 °C resulted in complete conversion of the mixture within 2 h to compound **10**. IR (cm⁻¹): 3040 (m), 2952 (s), 2926 (s), 2888 (s), 2852 (s), 2795 (m), 1645 (m), 1603 (s), 1579 (s), 1557 (m), 1506 (w), 1489 (w), 1471 (m), 1461 (m), 1443 (s), 1387 (w), 1359 (w), 1304 (w), 1268 (s), 1248 (s), 1231 (m), 1152 (w), 1100 (m), 1067 (m), 1046 (s), 1038 (s), 1007 (m), 998 (m), 965 (s), 932 (w), 867 (w), 829 (s), 786 (m), 769 (m), 752 (m), 702 (s), 661 (w), 627 (m), 567 (w), 536 (w), 432 (w). Anal. Calcd for C₄₆H₇₀N₅Si₂Y: C, 65.92; H, 8.42; N, 8.36. Found: C, 65.21; H, 8.03; N, 8.31.

X-ray structure determinations. X-ray diffraction measurements were made on a Siemens SMART diffractometer with a CCD area detector, using graphite monochromated Mo-K_α radiation. The crystal was mounted on a glass fiber using Paratone N hydrocarbon oil. A hemisphere of data was collected using ω scans of 0.3°. Cell constants and an orientation matrix for data collection were obtained from a least-squares refinement using the measured positions of reflections in the range 4 < 2θ < 45°. The frame data were integrated using the program SAINT (SAX Area-Detector Integration

Program; V4.024; Siemens Industrial Automation, Inc.: Madison, WI, 1995). An empirical absorption correction based on measurements of multiply redundant data was performed using the programs XPREP (Part of the SHELXTL Crystal Structure Determination Package; Siemens Industrial Automation, Inc.: Madison, WI, 1995) or SADABS. Equivalent reflections were merged. The data were corrected for Lorentz and polarization effects. A secondary extinction correction was applied if appropriate. The structures were solved using the teXsan crystallographic software package of the Molecular Structure Corporation, using direct methods, and expanded with Fourier techniques. All non-hydrogen atoms were refined anisotropically and the hydrogen atoms were included in calculated positions but not refined unless otherwise noted. The function minimized in the full-matrix least-squares refinement was $\Sigma w(|F_o| - |F_c|)^2$. The weighting scheme was based on counting statistics and included a p-factor to downweight the intense reflections.

For 2: Crystals were grown from a 10:1 pentane/THF solution of **2** at -35 °C. The Flack parameter of the structure was 0.009(2), suggesting that the correct enantiomorph was chosen. The other enantiomorph was also tested, but this structure resulted in R = 9.64% with a Flack parameter of 0.88.

For 4: Crystals were grown from a pentane solution of **4** at -35 °C.

For 6: Crystals were grown by slow diffusion of PhSiH₃ (0.3 mL dissolved in 20 mL benzene) into a solution of **5** (0.16 g in 20 mL benzene), the two solutions being separated with a layer of neat benzene, at room temperature for 4 days. The non-hydrogen atoms were refined anisotropically. The hydride H was located on the Fourier difference map and refined isotropically, the rest of the hydrogen atoms were included in calculated positions.

For 9: Crystals were grown from a pentane solution of a mixture of **9** and **10** at -15 °C. The single crystal selected was found to be compound **9**. The non-hydrogen atoms were refined anisotropically, except for those of the solvating pentane which were disordered and refined isotropically.

References:

- (1) Gountchev, T. I.; Tilley, T. D. *J. Am. Chem. Soc.* **1997**, *119*, 12831.
- (2) Gountchev, T. I.; Tilley, T. D. *Organometallics* **1999**, *18*, 2896.
- (3) Kaminsky, W. *Catalysis Today* **1994**, *20*, 257.
- (4) Mitchell, J. P.; Hajela, S.; Brookhart, S. K.; Hardcastle, K. I.; Henling, L. M.; Bercaw, J. E. *J. Am. Chem. Soc.* **1996**, *118*, 1045.
- (5) Marks, T. J. *Acc. Chem. Res.* **1992**, *25*, 57.
- (6) Schaverien, C. J. *Adv. Organomet. Chem.* **1994**, *36*, 283.
- (7) Möhring, P. C.; Coville, N. J. *J. Organomet. Chem.* **1994**, *479*, 1.
- (8) van der Linden, A.; Schaverien, C. J.; Meijboom, N.; Ganter, C.; Orpen, A. G. *J. Am. Chem. Soc.* **1995**, *117*, 3008.
- (9) Fu, P.-F.; Brard, L.; Li, Y.; Marks, T. J. *J. Am. Chem. Soc.* **1995**, *117*, 7157.
- (10) Molander, G. A.; Julius, M. *J. Org. Chem.* **1992**, *57*, 6347.
- (11) Molander, G. A.; Nichols, P. J. *J. Am. Chem. Soc.* **1995**, *117*, 4415.
- (12) Duchateau, R.; van Wee, C. T.; Meetsma, A.; van Duijnen, P. T.; Teuben, J. H. *Organometallics* **1996**, *15*, 2279.
- (13) Duchateau, R.; Tuinstra, T.; Brussee, E. A. C.; Meetsma, A.; van Duijnen, P. T.; Teuben, J. H. *Organometallics* **1997**, *16*, 3511.
- (14) Schaverien, C. J. *Organometallics* **1994**, *13*, 69.
- (15) Rodriguez, G.; Bazan, G. C. *J. Am. Chem. Soc.* **1997**, *119*, 343.
- (16) Baumann, R.; Davis, W. M.; Schrock, R. R. *J. Am. Chem. Soc.* **1997**, *119*, 3830.
- (17) Schrock, R. R. *Acc. Chem. Res.* **1997**, *30*, 9.
- (18) Long, D. P.; Bianconi, P. A. *J. Am. Chem. Soc.* **1996**, *118*, 12453.
- (19) Scollard, J. D.; McConville, D. H.; Payne, N. C.; Vittal, J. J. *Macromolecules* **1996**, *29*, 5241.
- (20) Guérin, F.; McConville, D. H.; Payne, N. C. *Organometallics* **1996**, *15*, 5085.

- (21) Clark, H. C. S.; Cloke, F. G. N.; Hitchcock, P. B.; Love, J. B.; Wainwright, A. P. *J. Organomet. Chem.* **1995**, *501*, 333.
- (22) Scollard, J. D.; McConville, D. H.; Vittal, J. J. *Organometallics* **1995**, *14*, 5478.
- (23) Horton, A. D.; de With, J.; van der Linden, A. J.; van de Weg, H. *Organometallics* **1996**, *15*, 2672.
- (24) Cloke, F. G. N.; Hitchcock, P. B.; Love, J. B. *J. Chem. Soc., Dalton Trans.* **1995**, 25.
- (25) VanderLende, D. D.; Abboud, K. A.; Boncella, J. M. *Organometallics* **1994**, *13*, 3378.
- (26) Deelman, B.-J.; Hitchcock, P. B.; Lappert, M. F.; Lee, H.-K.; Leung, W.-P. *J. Organomet. Chem.* **1996**, *513*, 281.
- (27) Freundlich, J. S.; Schrock, R. R.; Davis, W. M. *J. Am. Chem. Soc.* **1996**, *118*, 3643.
- (28) Duan, Z.; Naiini, A. A.; Lee, J.-H.; Verkade, J. G. *Inorg. Chem.* **1995**, *34*, 5477.
- (29) Findeis, B.; Schubart, M.; Gade, L. H.; Möller, F.; Scowen, I.; McPartlin, M. *J. Chem. Soc., Dalton Trans.* **1996**, 125.
- (30) Schrock, R. R.; Cummins, C. C.; Wilhelm, T.; Lin, S.; Reid, S. M.; Kol, M.; Davis, W. M. *Organometallics* **1996**, *15*, 1470.
- (31) Aoyagi, K.; Gantzel, P. K.; Kalai, K.; Tilley, T. D. *Organometallics* **1996**, *15*, 923.
- (32) Aoyagi, K.; Gantzel, P. K.; Tilley, T. D. *Polyhedron* **1996**, *15*, 4299.
- (33) den Haan, K. H.; Wielstra, Y.; Eshuis, J. J. W.; Teuben, J. H. *J. Organomet. Chem.* **1987**, *323*, 181.
- (34) Brookhart, M.; Green, M. L. H.; Wong, L.-L. *Progr. Inorg. Chem.* **1988**, *36*, 1.
- (35) Brookhart, M.; Green, M. L. H. *J. Organomet. Chem.* **1983**, *250*, 395.
- (36) Crabtree, R. H. *Angew. Chem. Int. Ed. Engl.* **1993**, *32*, 789.
- (37) Evans, W. J.; Ulibarri, T. A.; Ziller, J. W. *Organometallics* **1991**, *10*, 134.
- (38) Graf, D. D.; Davis, W. M.; Schrock, R. R. *Organometallics* **1998**, *17*, 5820.

- (39) den Haan, K. H.; de Boer, J. L.; Teuben, J. H.; Spek, A. L.; Kojic-Prodic, B.; Hays, G. R.; Huis, R. *Organometallics* **1986**, *5*, 1726.
- (40) Burger, B. J.; Thompson, M. E.; Cotter, W. D.; Bercaw, J. E. *J. Am. Chem. Soc.* **1990**, *112*, 1566.
- (41) Stern, D.; Sabat, M.; Marks, T. J. *J. Am. Chem. Soc.* **1990**, *112*, 9558.
- (42) Duchateau, R.; Wee, C. T. v.; Teuben, J. H. *Organometallics* **1996**, *15*, 2291.
- (43) Jeske, G.; Lauke, H.; Mauermann, H.; Swepston, P. N.; Schumann, H.; Marks, T. *J. Am. Chem. Soc.* **1985**, *107*, 8091.
- (44) den Haan, K. H.; Wielstra, Y.; Teuben, J. H. *Organometallics* **1987**, *6*, 2053.
- (45) Evans, W. J.; Meadows, J. H.; Wayda, A. L.; Hunter, W. E. *J. Am. Chem. Soc.* **1982**, *104*, 2008.
- (46) Evans, W. J.; Drummond, D. K.; Hanusa, T. P.; Doedens, R. J. *Organometallics* **1987**, *6*, 2279.
- (47) Booiij, M.; Deelman, B.-J.; Duchateau, R.; Postma, D. S.; Meetsma, A.; Teuben, J. H. *Organometallics* **1993**, *12*, 3531.
- (48) Evans, W. J.; Meadows, J. H.; Hunter, W. E.; Atwood, J. L. *J. Am. Chem. Soc.* **1984**, *106*, 1291.
- (49) Dawoodi, Z.; Green, M. L. H.; Mtetwa, V. S. B.; Prout, K.; Schultz, A. J.; Williams, J. M.; Koetzle, T. F. *J. Chem. Soc., Dalton Trans.* **1986**, 1629.
- (50) Crackness, R. B.; Orpen, A. G.; Spencer, J. L. *J. Chem. Soc., Chem. Commun.* **1984**, 326.
- (51) Haaland, A.; Scherer, W.; Ruud, K.; McGrady, G. S.; Downs, A. J.; Swang, O. *J. Am. Chem. Soc.* **1998**, *120*, 3762.
- (52) Bruno, J. W.; Smith, G. M.; Marks, T. J.; Fair, C. K.; Schultz, A. J.; Williams, J. M. *J. Am. Chem. Soc.* **1986**, *108*, 40.
- (53) Mena, M.; Pellinghelli, M. A.; Royo, P.; Serrano, R.; Tiripicchio, A. *J. Chem. Soc., Chem. Commun.* **1986**, *108*, 1118.

- (54) Cayias, J. Z.; Babaian, E. A.; Hrcir, D. C.; Bott, S. G.; Atwood, J. L. *J. Chem. Soc., Dalton Trans.* **1986**, 2743.
- (55) Duchateau, R.; Brussee, E. A. C.; Meetsma, A.; Teuben, J. H. *Organometallics* **1997**, *16*, 5506.
- (56) Woo, H.-G.; Tilley, T. D. *J. Organomet. Chem.* **1990**, *393*, C6.
- (57) Deelman, B.-J.; Stevels, W. M.; Lakin, M. T.; Spek, A. L.; Teuben, J. H. *Organometallics* **1994**, *13*, 3881.
- (58) den Haan, K. H.; Teuben, J. H. *J. Organomet. Chem.* **1987**, *322*, 321.
- (59) Kanoh, S.; Goka, S.; Murose, N.; Kubo, H.; Kondo, M.; Sugino, T.; Motoi, M.; Suda, H. *Polymer Journal* **1987**, *19*, 1047.
- (60) Davidson, P. J.; Harris, D. H.; Lappert, M. F. *J. Chem. Soc., Dalton Trans.* **1976**, 2268.

Chapter 3

Hydrosilylation Catalysis by C_2 -Symmetric Bis(silylamido) Complexes of Yttrium

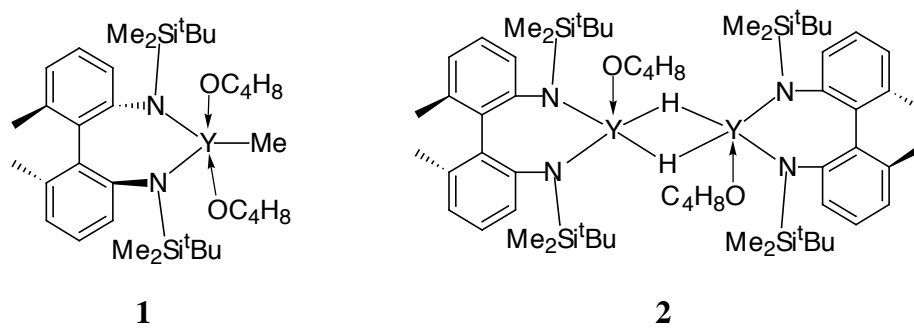
Introduction

The previous chapter described the studies on the structure and reactivity of alkyl and hydride yttrium complexes containing the [DADMB]²⁻ ligand (DADMB = 2,2'-bis(*tert*-butyldimethylsilylamido)-6,6'-dimethylbiphenyl).¹ Early transition metal complexes, including chelating diamide complexes of this type, have been extensively investigated as catalysts for olefin polymerizations,²⁻¹⁷ and we have also been interested in the potential of d⁰ systems to function as silane dehydropolymerization catalysts.¹⁸⁻²² While the yttrium-DADMB complexes were not active as olefin or silane polymerization catalysts, we have found that they can be used as olefin hydrosilylation catalysts.²³ The hydrosilylation of olefins by early transition metal catalysts is a well known process, and recently many studies have been devoted to investigating the reactivity and selectivity of such catalysts towards various unsaturated organic substrates.²⁴⁻³² The mechanism and energetics of the hydrosilylation catalytic cycle has also been investigated extensively.²⁴ As is usually the case in early transition metal chemistry, the ancillary ligands employed in these studies have been based on cyclopentadienide and its derivatives. The potential of non-cyclopentadienyl ligand sets in hydrosilylation catalysis by d⁰ metals has yet to be explored. This chapter describes the hydrosilylation chemistry of [DADMB]Y complexes, and the initial results on the use of a resolved chiral catalyst, (S)-[DADMB]YMe(THF)₂, in the enantioselective hydrosilylation of olefins.

Results and Discussion

The yttrium complexes **1** and **2** were prepared according to previously described methods.¹ While these complexes do not appear to be promising as olefin polymerization catalysts, the yttrium hydride **2** was found to react cleanly with olefins to give single-insertion alkyl products.^{1,23} Further reactions with olefin are very slow, and measurable amounts of polyolefins were not observed. Complexes **1** and **2** were also found to be inactive as dehydropolymerization catalysts, and whereas **2** is inert toward silanes such as

PhSiH₃, the yttrium alkyls **1** and [DADMB]Y[CH(SiMe₃)₂](THF)(OEt₂) react with hydrosilanes in a metathesis-type reaction to form **2** and an alkylsilane. The latter observation of Si–C bond formation prompted us to investigate the possibility of catalytic hydrosilylation, since it was envisioned that the yttrium hydride **2** could react with an olefin via insertion, and then the resulting yttrium alkyl group might be transferred to a silane with regeneration of the yttrium hydride catalyst (Scheme 1). In fact, similar hydrosilylations are known to occur with other group 3 and lanthanide hydrides (e.g., [Cp*₂YH]₂) or their precursors.^{24-27,29}

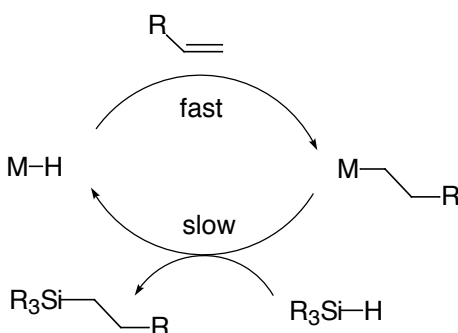


Initial experiments were designed to test the activity of **2** as a hydrosilylation catalyst. Addition of a large excess of PhSiH₃ to a THF-*d*₈ solution of **2** did not result in reaction, but when the mixture was pressurized with ethylene (5 psi, room temperature), the clean formation of PhEtSiH₂ was immediately observed, and within 12 h all the PhSiH₃ had been consumed. 1-Hexene was also found to react with PhSiH₃ in the presence of **2**, to give PhSiH₂(CH₂)₅CH₃ as the major product. Under similar conditions cyclohexene did not undergo hydrosilylation, consistent with its lack of reactivity towards the hydride **2**.

The complete insolubility of the hydride dimer in non-coordinating solvents required the use of THF for the hydrosilylation reactions. However, the yttrium methyl complex **1** can also be used as an active hydrosilylation catalyst, presumably because it first reacts with the silane to give a small concentration of reactive, monomeric hydride. Thus,

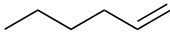
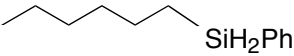
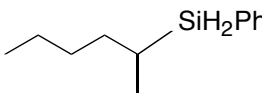
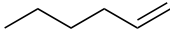
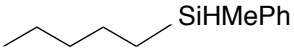
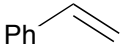
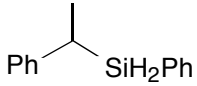
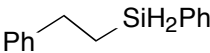
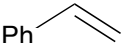
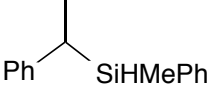
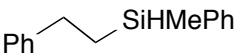

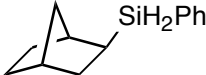
hydrosilylations may be carried out in a nonpolar solvent such as benzene using **1** as the catalyst precursor. The active hydride species under these catalytic conditions has not been observed, as addition of a hydrosilane to **1** led to rapid disappearance of the resonances for **1** (by ^1H NMR spectroscopy) with formation of the methyl silane, but no yttrium hydride resonances could be detected (apparently due to the very low concentration of the active species).

Scheme 1



To probe the selectivity of this catalytic system, a range of olefins was tested, using PhSiH_3 and PhMeSiH_2 as representative primary and secondary silanes. The results are presented in Table 1. The steric bulk of the ligand apparently limits the reactivity of the catalyst such that only terminal olefins react at a measurable rate, and norbornene is the only disubstituted olefin observed to react. With both PhSiH_3 and PhMeSiH_2 , no reaction was observed with cyclohexene, 1-phenyl-1-methylethene (α -methylstyrene), and *trans*-1,2-diphenylethene, and PhMeSiH_2 did not react with norbornene. As has been noted for other lanthanide and yttrium hydrosilylation catalysts,^{24-26,29} both 1,2- and 2,1-additions of the silane to the double bond are observed, the ratio of the two isomers being controlled by steric and electronic effects. Aliphatic olefins give predominantly the terminal addition product, while styrene preferably gives benzylsilane derivatives. The latter effect has been observed with related catalysts, and rationalized in terms of electronic interactions between the metal center and the aromatic ring of styrene, which directs the insertion reaction toward the α -phenylalkyl intermediate.²⁴

Table 1. Results from the hydrosilylation of olefins catalyzed by [DADMB]YMe(THF)₂ (**1**).

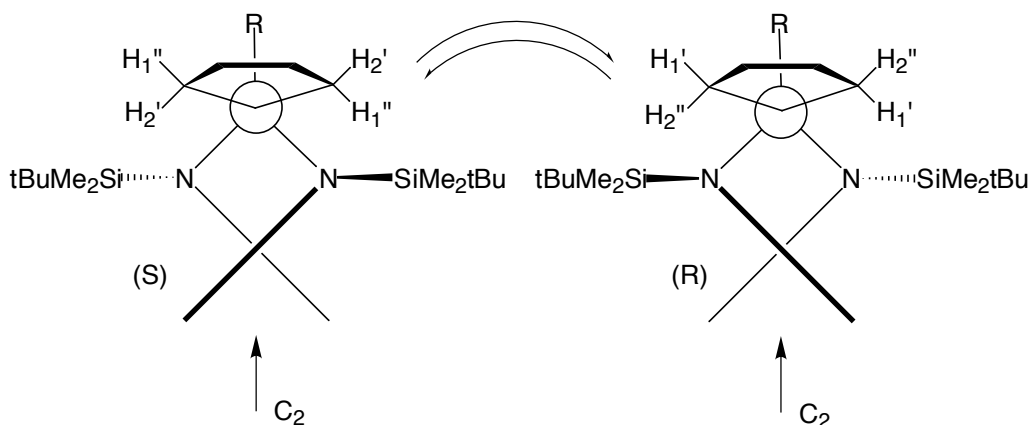
Olefin	Silane	Turnover rate, h ⁻¹	Products	Product ratio
	PhSiH ₃	~100	 SiH ₂ Ph	92%
			 SiH ₂ Ph	8%
	PhMeSiH ₂	4.3	 SiHMePh	>99%
	PhSiH ₃	0.66	 SiH ₂ Ph	76%
			 SiH ₂ Ph	24%
	PhMeSiH ₂	0.12	 SiHMePh	64%
			 SiHMePh	36%
	PhSiH ₃	~30	 SiH ₂ Ph	>99%
				(90% ee)

Our system seems to be less selective towards 2,1 addition in case of aromatic olefins, compared to catalysts such as $\text{Me}_2\text{Si}(\text{C}_5\text{Me}_4)_2\text{SmCH}(\text{SiMe}_3)_2$ ²⁴ which gives near quantitative yields of the 2,1 addition products. In its selectivity towards terminal addition to aliphatic olefins, our catalyst is more similar to $\text{Cp}^*_2\text{YCH}(\text{SiMe}_3)_2$.²⁵ In terms of reactivity, the turnover rates (Table 1) observed for 1-hexene are within the range reported for Cp-based group 3 and lanthanide catalysts, while those for $\text{PhCH}=\text{CH}_2$ are lower (cf. 1-hexene + PhSiH_3 $N_t = 120 \text{ h}^{-1}$, $\text{PhCH}=\text{CH}_2$ + PhSiH_3 $N_t = 25 \text{ h}^{-1}$, both at 23 °C using $\text{Me}_2\text{Si}(\text{C}_5\text{Me}_4)_2\text{SmCH}(\text{SiMe}_3)_2$).²⁴ Most of the literature studies of hydrosilylation with d^0 metal catalysts employ PhSiH_3 as a representative primary silane, with a few reporting successful use of secondary silanes such as PhMeSiH_2 ³⁰ or Ph_2SiH_2 .³¹ In our system, however, the steric bulk of the secondary silane apparently is not a significant hindrance, and most of the olefins tested (norbornene being the only exception) were found to react with both PhSiH_3 and PhMeSiH_2 . As expected, using a secondary (vs. primary) silane favors the terminal addition products.

Since the yttrium species involved in the catalysis are chiral, we examined the enantioselectivity of their catalytic action. A resolved version (**S-1**) of the methyl complex **1** was prepared using a sample of enantiopure (*S*)-2,2'-diamino-6,6'-dimethylbiphenyl,³³ following the previously reported synthetic procedure¹ (see Chapter 2). An unexpected confirmation of the preserved enantiopurity of the prepared complex **S-1** came from its ¹H NMR spectrum. While most chemical shifts for **S-1** were identical to those of racemic **1**,¹ two separate multiplets due to diastereotopic hydrogen atoms were observed for the α -H protons of the coordinated THF in **S-1**, as compared to a single multiplet in **1**. As shown in Scheme 2, coordination of THF to a chiral metal center places the diastereotopic CH₂ protons in two magnetically inequivalent environments. Since all THF coordination sites in an enantiopure system are of the same chirality, exchange of THF between different molecules would preserve the difference in chemical shift between the diastereotopic THF protons. In a racemic mixture, however, an exchange of THF between coordination sites

of opposite chirality would lead to an averaged environment for the same protons. A variable temperature NMR study of **1** further confirmed that the single multiplet observed at room temperature is due to a fast intermolecular exchange of THF. This exchange can apparently be slowed down at lower temperature, so that two separate multiplets are observed (Figure 1).

Scheme 2



The transition temperature in toluene-*d*₈ was determined to be 280 K, from which an activation energy $\Delta G^\ddagger = 54$ kJ/mol (13 kcal/mol) for THF dissociation can be calculated (rate constant $k = 1.8 \times 10^3$ s⁻¹). The rate of THF dissociation is thus faster than any of the kinetically important steps in the catalytic system (*vide infra*).

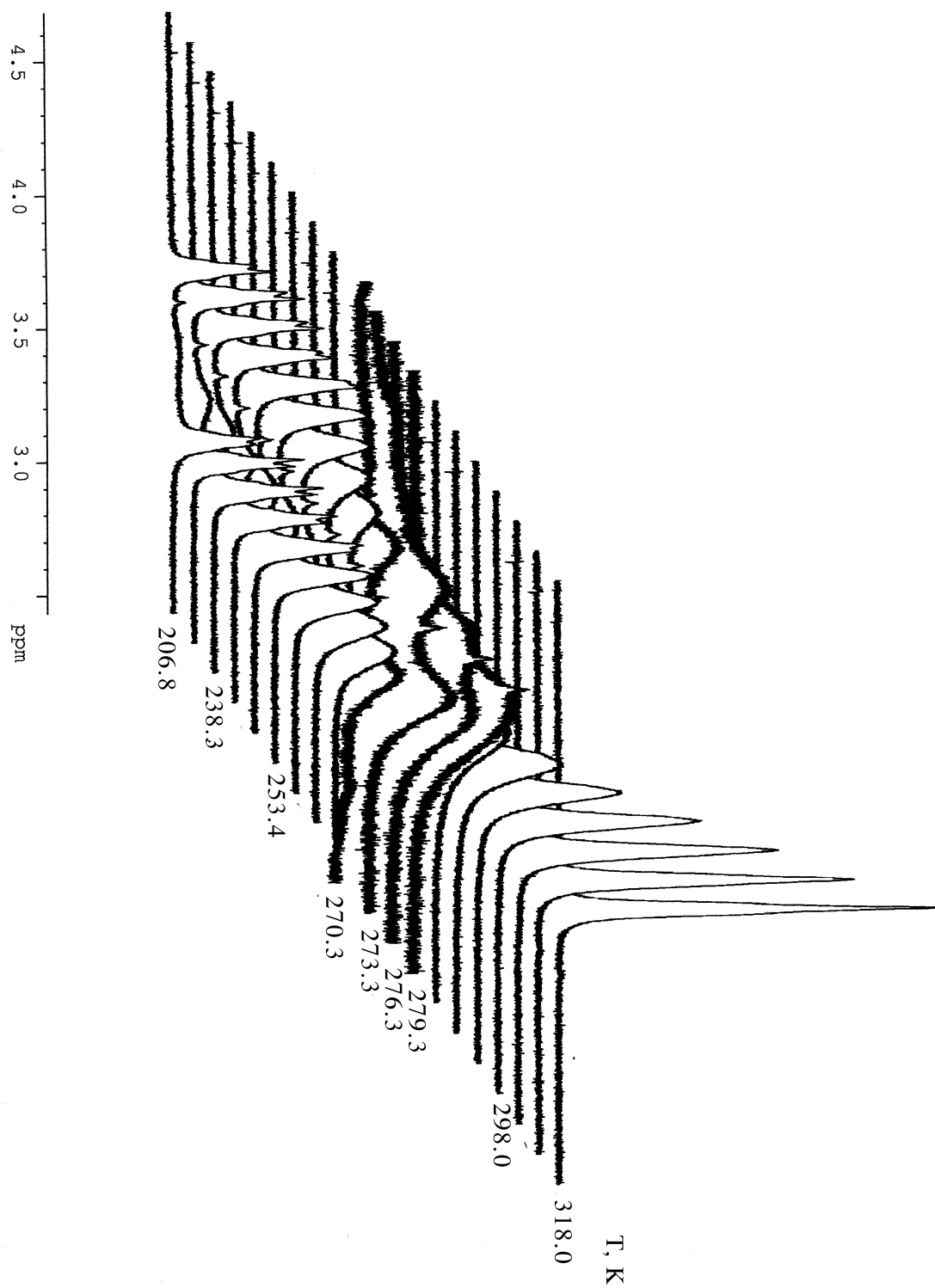
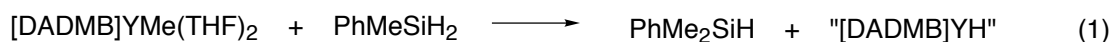


Figure 1. Temperature dependence of the chemical shift of the diastereotopic THF α -protons in **1**.

Evaluation of the catalyst enantioselectivity was hindered by the fact that most of the prochiral olefins tested did not react, or gave a mixture of regioisomers (vide supra). The substrate chosen for enantioselectivity studies was norbornene, since it gives exclusively the exo-dia stereoisomer on reaction with PhSiH₃. The enantiomeric excess of the PhSiH₂-norbornane product was found to be 90.4% (GC analysis with a chiral column), in favor of the 1*S*-enantiomer, as determined by oxidation of the silane to exo-norborneol following standard literature procedures.^{24,26} Highly enantioselective hydrosilylation of norbornene and other olefins using late transition metal (Pd, Pt, Rh) catalysts has been previously reported, with ee's often exceeding 90%.³⁴⁻³⁸ The only other study of enantioselective olefin hydrosilylation by early transition metal or lanthanide catalysts, however, utilized the chiral ansa-cyclopentadienyl complexes (R)-Me₂Si(C₅Me₄)[(-)-menthyl-C₅H₄]SmCH(SiMe₃)₂ and (S)-Me₂Si(C₅Me₅)[(-)-menthyl-C₅H₄]SmCH(SiMe₃)₂, and resulted in observation of enantiomeric excesses of 68% and 65% for the hydrosilylation of PhEtC=CH₂ with PhSiH₃.²⁴

The mechanism of hydrosilylation as catalyzed by early transition metal complexes has been studied for several cyclopentadienyl based systems.^{24,25} The active metal species is thought to be a monomeric d⁰ metal hydride. The catalytic cycle is proposed to occur via fast, irreversible insertion of olefin into the metal-hydrogen bond to give an alkyl species, which then reacts with the silane in a slow, rate-determining step (Scheme 1). The overall reaction rate has been found to be zeroth order in olefin, and first order in silane and catalyst precursor.²⁴

To probe the mechanism of hydrosilylation catalysis by [DADMB]Y complexes, we studied the kinetics of this process. The substrates chosen were 1-hexene and PhMeSiH₂, as that reaction was found to proceed at a rate convenient to follow by NMR spectroscopy.



The mechanism of the catalyst initiation step (eq 1) in benzene solution was studied by monitoring the disappearance of **1** at different concentrations of PhMeSiH₂, the silane being kept in large excess. This reaction should also represent a good model for the product-forming step in the proposed catalytic mechanism (Scheme 1). A linear decrease of ln[**1**] with time was observed, which is consistent with a rate law involving first-order dependence on **1** (Figure 2). A plot of the observed rate constant vs. [PhMeSiH₂] was also found to be linear (Figure 3), consistent with the expected first order dependence on silane concentration. The overall rate constant was found to be $k_H = 3.8(2) \times 10^{-4}$ L/(mol·s) at 298 K. To determine the isotope effect of this σ -bond metathesis process, several kinetic measurements were performed using deuterated silane (PhMeSiD₂), giving a rate constant $k_D = 3.4(3) \times 10^{-4}$ L/(mol·s). An approximate value of $k_H / k_D = 1.1(1)$ can be estimated, but the significant scatter in the experimental data does not allow meaningful conclusions about the isotope effect of this reaction.

The actual hydrosilylation process was studied in benzene by monitoring the consumption of PhMeSiH₂ at different concentrations of 1-hexene (in most cases kept in at least five-fold excess relative to the silane, so that the decrease in olefin concentration during the reaction is insignificant) and the catalyst precursor **1** (typically about 5% relative to PhMeSiH₂). The linear dependence of ln[PhMeSiH₂] vs. time over the whole range of initial concentrations of **1** and 1-hexene (Figure 4) suggests a first order rate law with respect to the silane, as expected from the mechanism of Scheme 1. The dependence of the overall rate on the olefin concentration was probed by conducting several kinetic runs at different 1-hexene concentrations (ranging from 0.33 to 4.01 mol/L). The observed rate constant was found to be practically independent of the olefin concentration (Figure 5), again consistent with the proposed mechanism which implies zeroth order with respect to olefin.

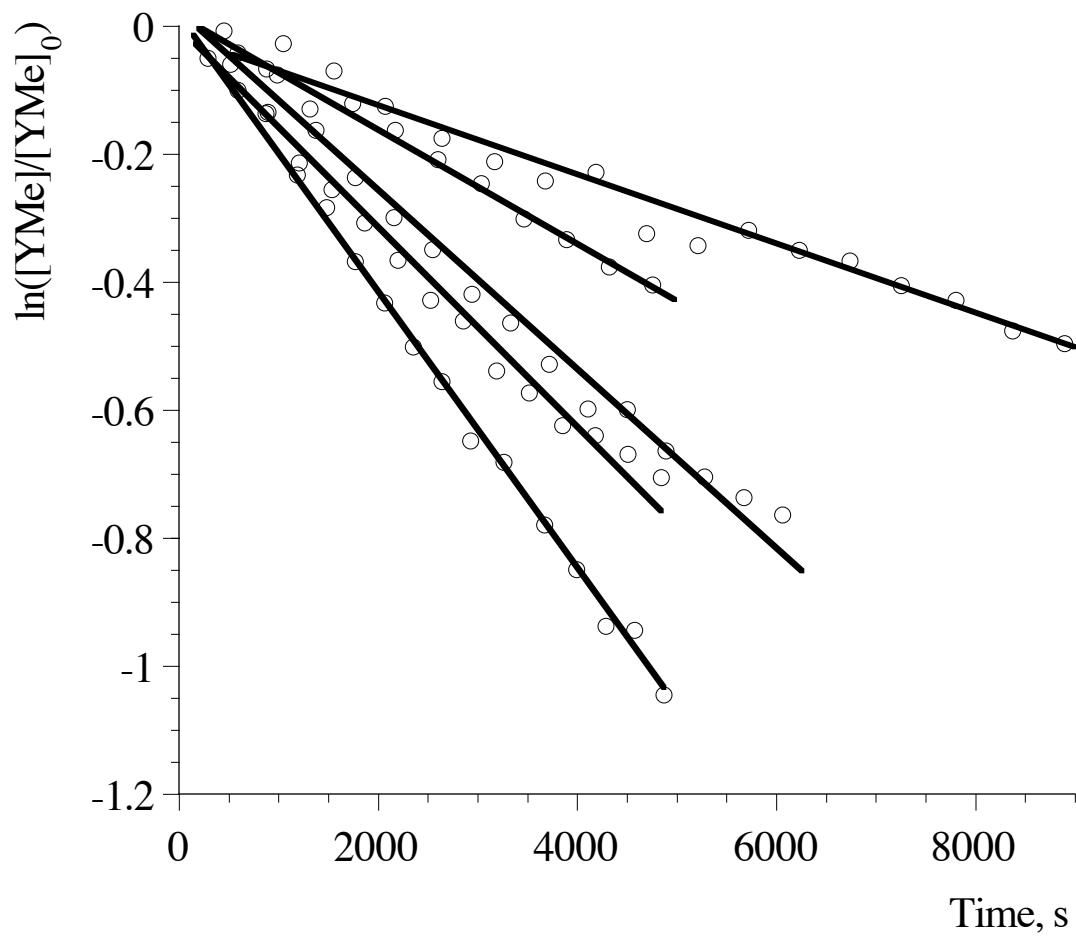


Figure 2. Pseudo-first order plots for disappearance of **1** at different $PhMeSiH_2$ concentrations (298 K, benzene- d_6).

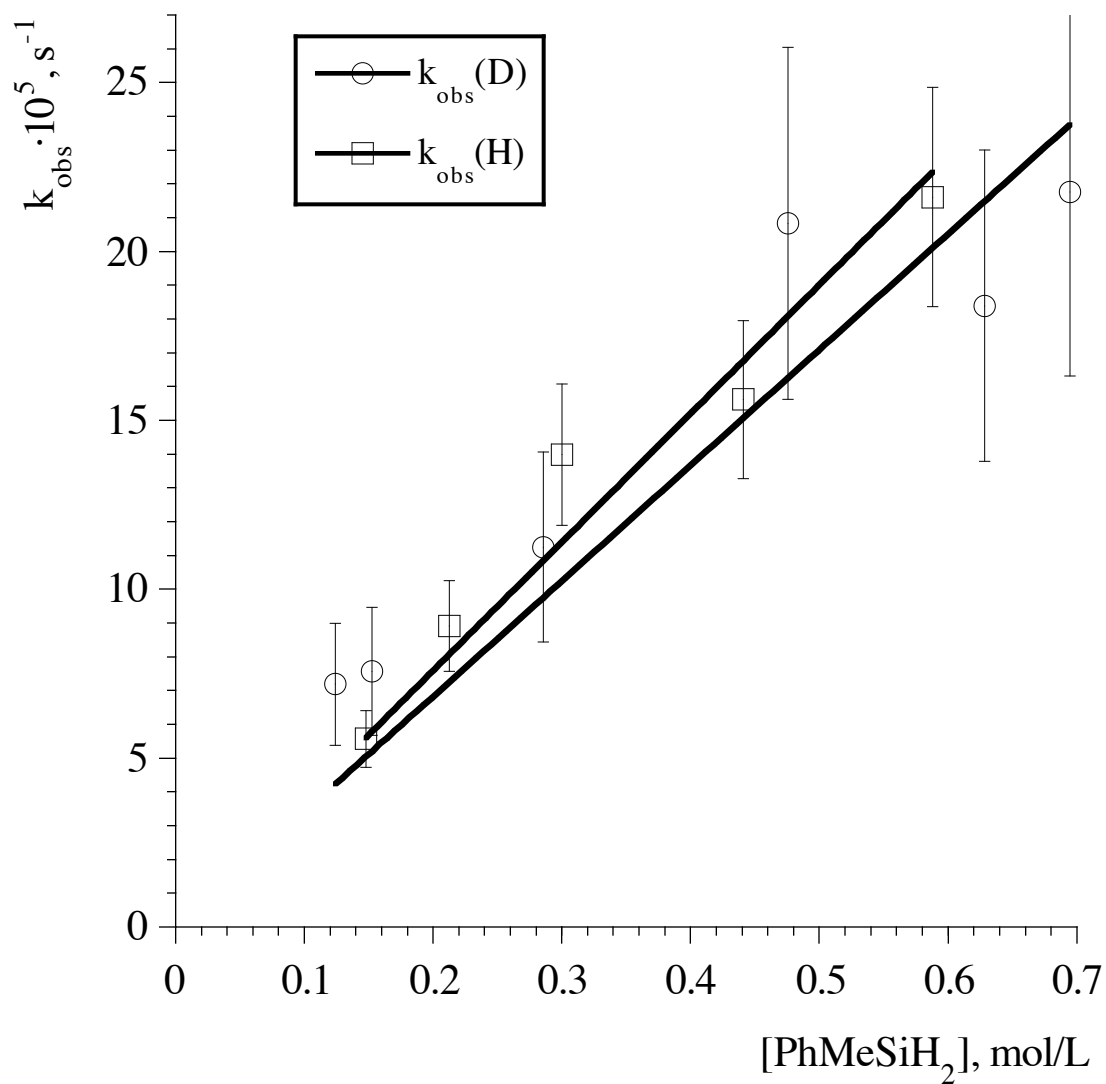


Figure 3. Pseudo-first order rate constant for disappearance of **1** as a function of phenylmethylsilane concentration (298 K, benzene- d_6).

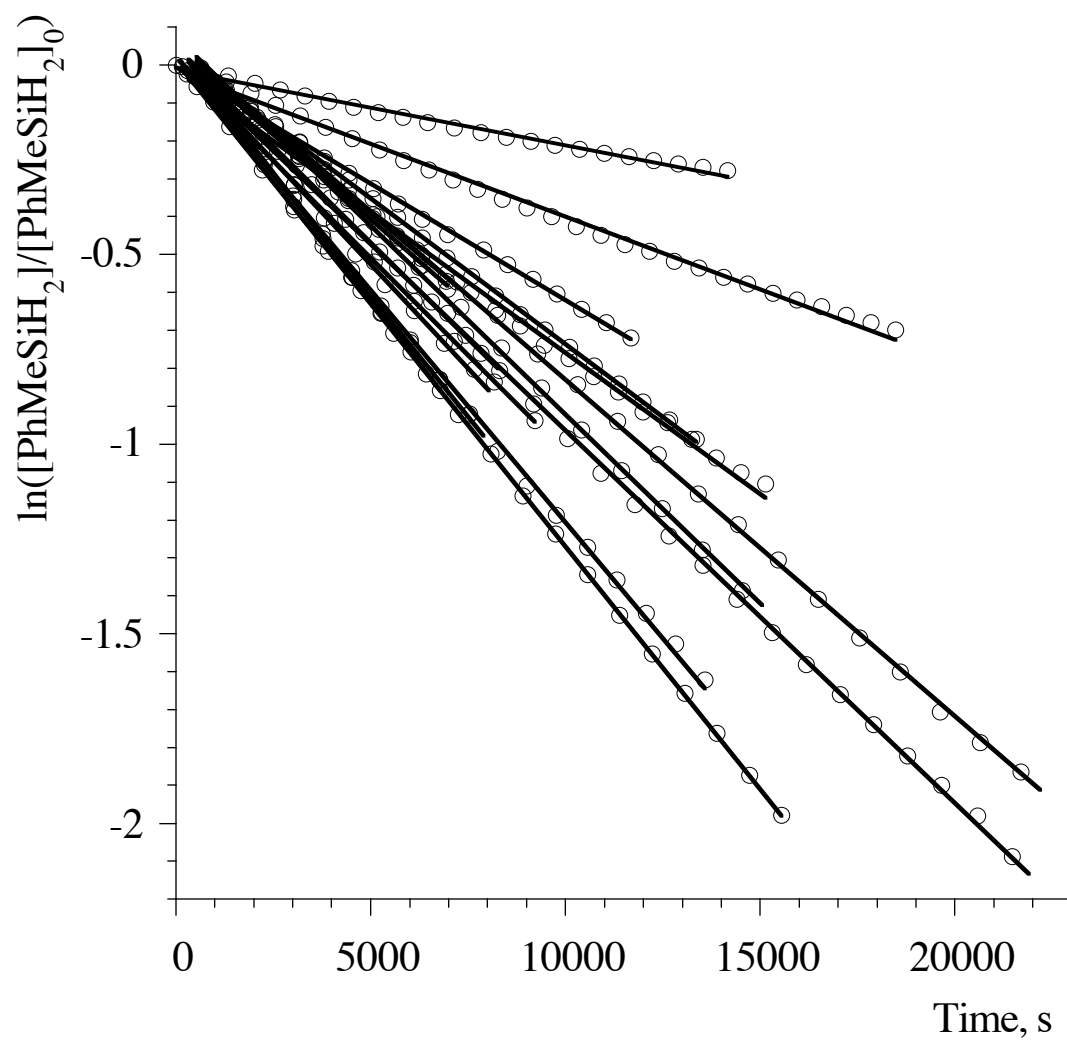


Figure 4. Pseudo-first order plots for consumption of PhMeSiH_2 at different concentrations of **1** and 1-hexene (298 K, benzene- d_6).

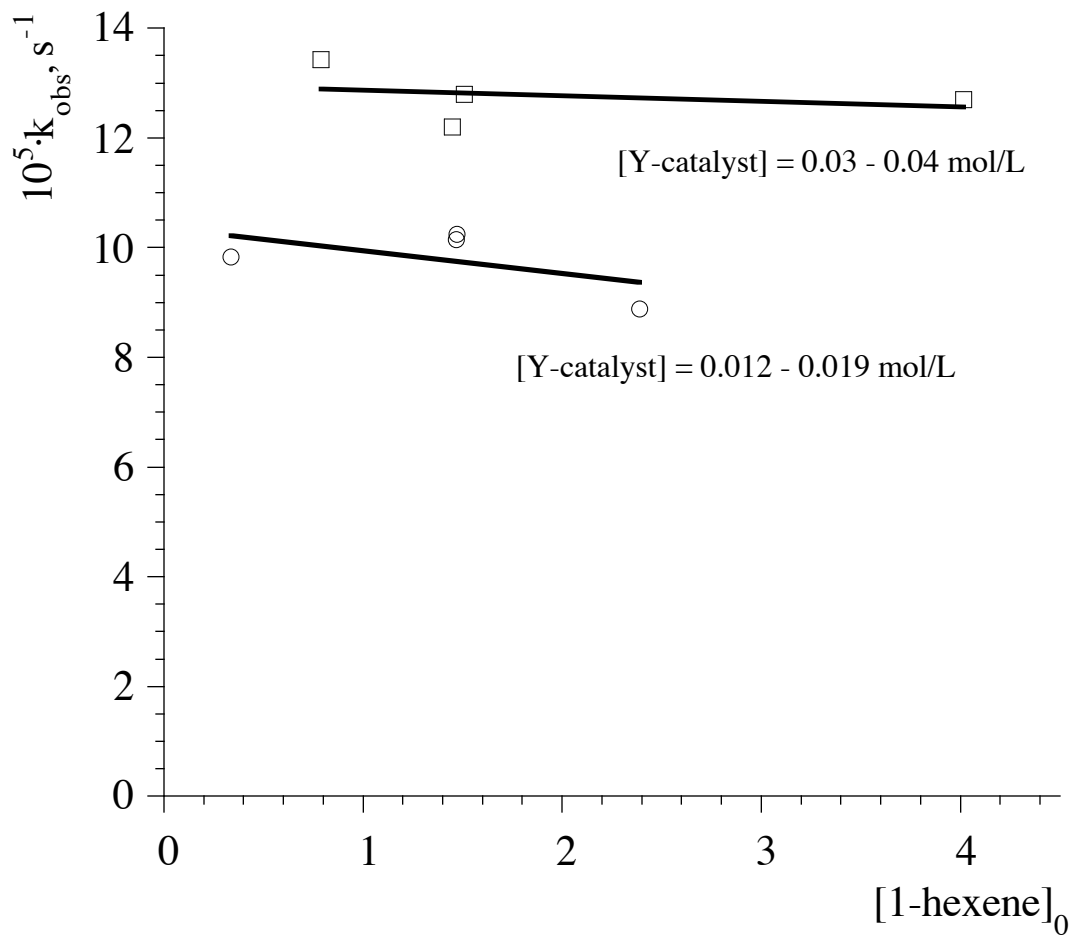


Figure 5. Observed pseudo-first order rate constant for PhMeSiH₂ consumption as a function of the 1-hexene concentration, at constant catalyst precursor concentration (298 K, benzene-*d*₆).

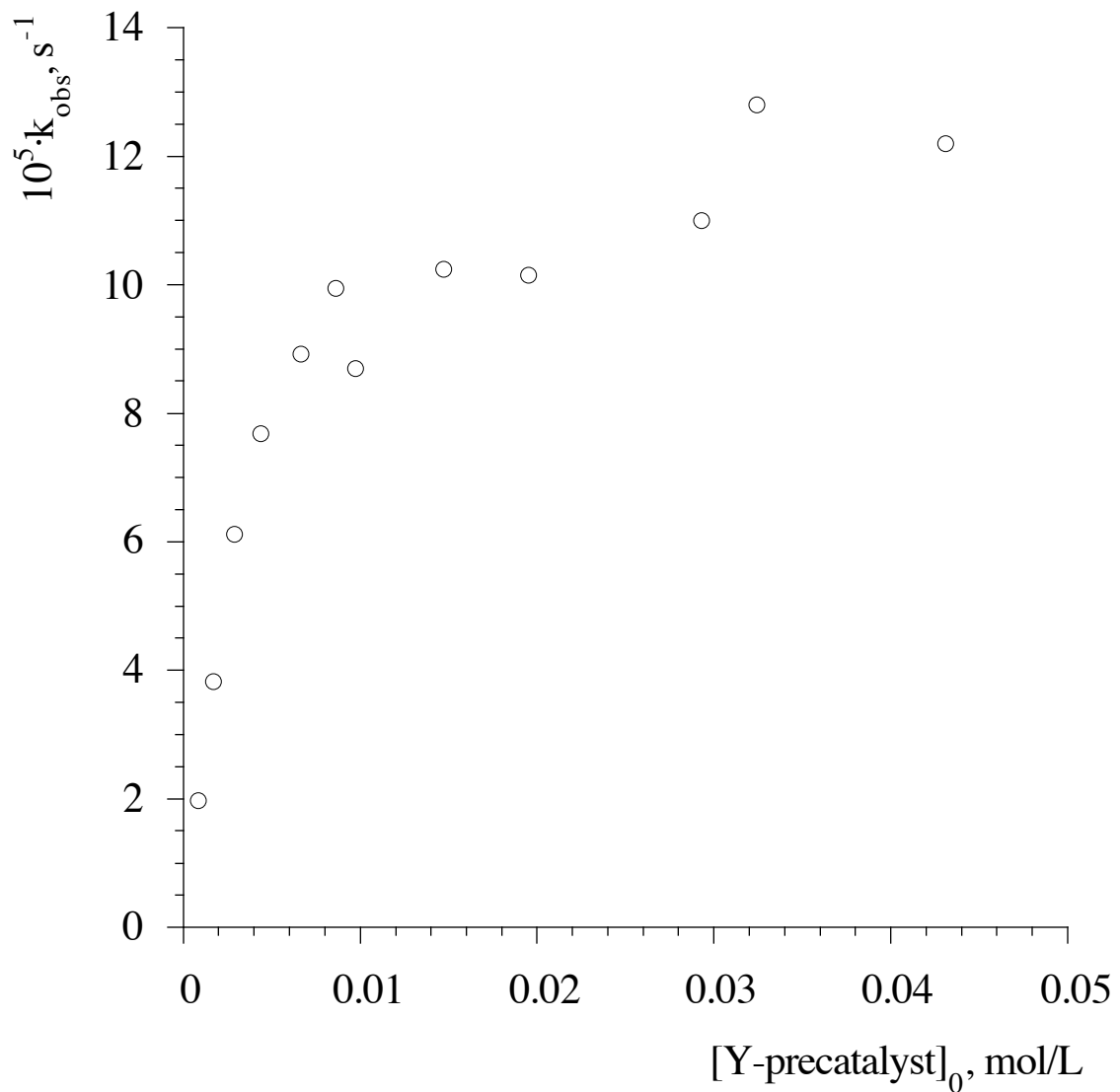


Figure 6. Observed pseudo-first order rate constant for PhMeSiH₂ consumption as a function of the catalyst precursor concentration, at constant initial 1-hexene concentration (298 K, benzene-*d*₆).

The dependence of the observed rate constant on the initial concentration of **1**, however, was found to deviate significantly from the expected linear correlation for a first-order rate law with respect to yttrium catalyst (Figure 6). Precipitation of insoluble yttrium hydride dimer at later stages of the reaction, which can irreversibly remove some of the active catalyst from the solution, is one possible cause of the saturation behavior observed at higher catalyst concentrations. Alternatively, an order of 1/2 would lead to a qualitatively similar behavior, and can be explained if the concentration of the active yttrium species in the rate-determining step is controlled by an equilibrium leading to dimer formation. An example of such half-order dependence on catalyst concentration has been reported for the hydrogenation of olefins catalyzed by Cp^{*}-organolanthanide complexes,³⁹ a mechanistically very similar process. In the latter hydrogenation, the half-order dependence was rationalized by invoking a fast equilibrium between the reactive metal alkyl intermediate and an inactive dimeric (alkyl bridged) species. Interestingly, the corresponding catalytic hydrosilylation process using the same catalysts, is reported to exhibit regular first order dependence on catalyst concentration.²⁴ Although in our system no evidence is available to suggest that **1** itself could form a dimer in solution, the dimeric nature of the hydride **2**, as well as the existence of many examples of dimeric alkyl and mixed hydrido-alkyl yttrium species in the literature,³⁹⁻⁴¹ suggests that such equilibria are not to be ignored. The complexity of the system, however, and uncertainty in the structure of the active species, prevent us from formulating a more detailed mechanistic picture at this time.

To avoid the potential effects of the insolubility of the yttrium hydride dimers in benzene on the kinetics of the hydrosilylation process, several runs were also performed using THF-*d*₈ as a solvent. The consumption of PhMeSiH₂ was followed at different yttrium catalyst precursor concentrations, while keeping the 1-hexene concentration constant. A plot of ln[PhMeSiH₂] vs. time, however, showed that an observable decrease in the reaction rate occurs after some period of time (Figure 7), which is likely due to

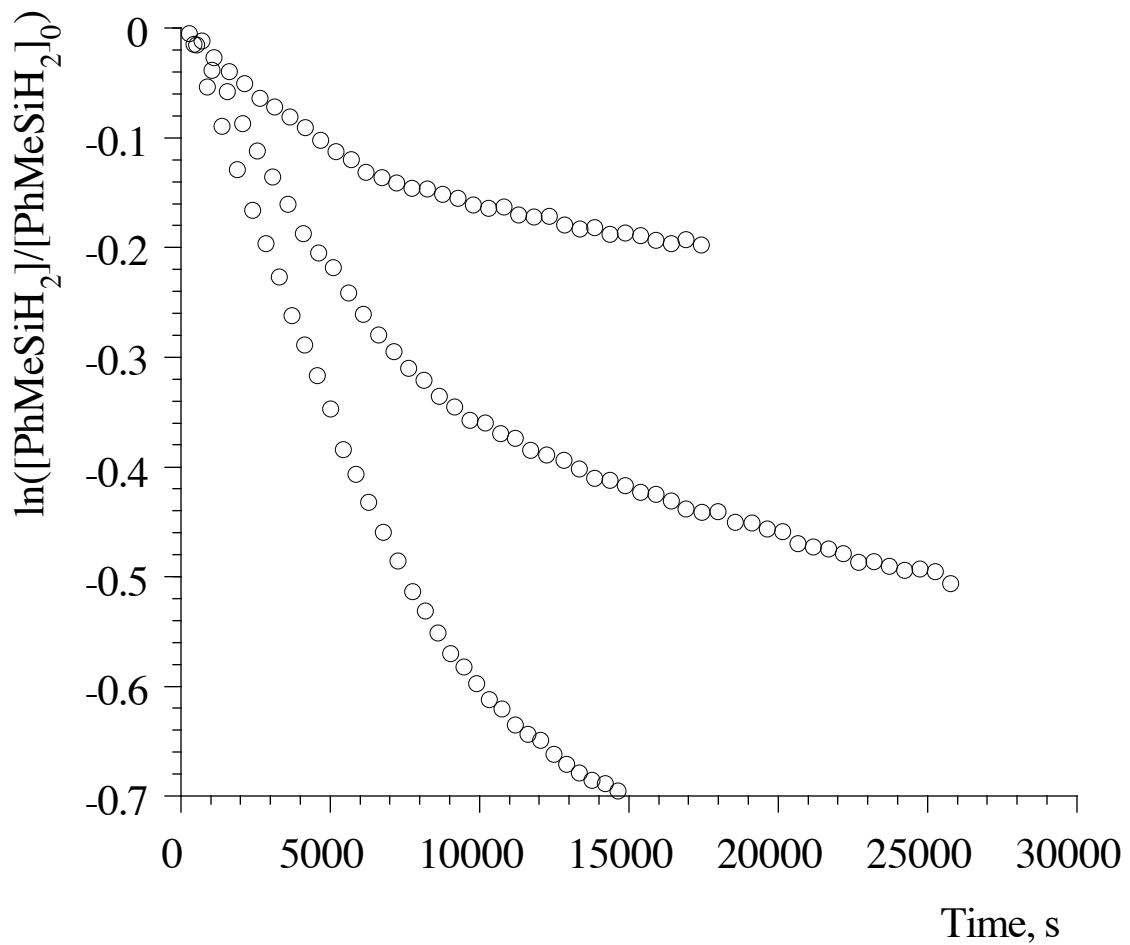


Figure 7. Pseudo-first order plots for consumption of PhMeSiH_2 at different concentrations of **1** (298 K, $\text{THF-}d_8$).

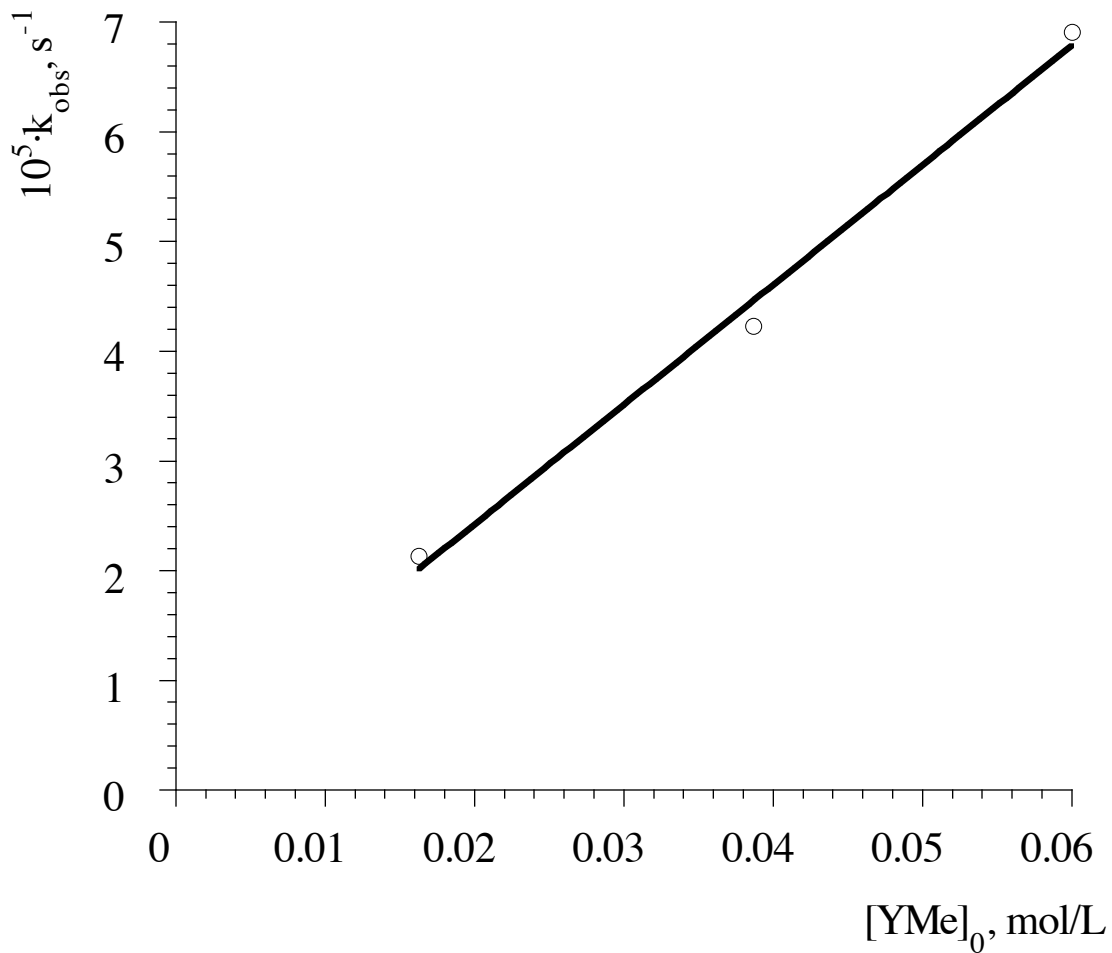


Figure 8. Observed rate constant for consumption of PhMeSiH_2 (initial rate) as a function of the initial concentration of **1** (298 K, $\text{THF-}d_8$).

catalyst decomposition in the THF solvent. Unlike the approximately half-order rate law observed in benzene, however, the dependence of the observed rate constant on the catalyst precursor concentration in the initial period was found to be linear (Figure 8), suggesting a first order rate law ($k = 1.1(1) \times 10^{-3} \text{ L}/(\text{mol}\cdot\text{s})$ at 298 K) with respect to catalyst precursor when the reaction is conducted in THF. The observed rate constants in THF are lower than those in benzene, which is consistent with the idea that the catalytically active species is a coordinatively unsaturated complex, and THF coordination can inhibit its reactivity.

Conclusions

We have explored the hydrosilylation activity of some yttrium complexes with bis(silylamido)biphenyl ligands and have performed kinetic and mechanistic investigations of this catalytic process. Although hydrosilylation catalysis by d^0 transition metal complexes is well known, most of the research on such catalysts has traditionally been done using cyclopentadienyl ligands. The present system is the first to demonstrate the use of non-Cp ligands in the catalytic hydrosilylation of olefins by a d^0 metal. Mechanistic investigations indicate that this hydrosilylation occurs by the mechanism generally accepted to operate for other d^0 systems, involving fast olefin insertion into the reactive metal hydride bond, followed by a slow metathesis reaction with a silane molecule. As with the Cp-based systems studied earlier, the diamido catalyst **1** exhibits a high regioselective preference toward terminal addition in case of aliphatic olefins. However, a lower preference for 2,1-addition in case of aromatic olefins was observed, presumably due to the different steric requirements of the bis(silylamido)biphenyl ligand as compared to the bis-Cp systems. The [DADMB]Y catalyst is also reactive enough to allow a secondary silane such as PhMeSiH_2 to be employed in the hydrosilylation, in addition to the more typically employed PhSiH_3 . Significantly, the enantioselectivity observed with the enantioresolved [DADMB]Y catalyst in the hydrosilylation of norbornene (90% ee) is impressively high for

an unoptimized system, and compares favorably with some of the best late transition metal-based catalysts.

Experimental Section

General. All reactions with air-sensitive compounds were performed under dry nitrogen, using standard Schlenk and glove box techniques. Reagents were obtained from commercial suppliers and used without further purification, unless otherwise noted.

Olefin-free pentane, benzene, and toluene were prepared by pretreating with concentrated H₂SO₄, 0.5 N KMnO₄ in 3 M H₂SO₄, NaHCO₃ and finally anhydrous MgSO₄. Solvents (pentane, diethyl ether, benzene, toluene, tetrahydrofuran) were distilled under nitrogen from sodium benzophenone ketyl. Benzene-*d*₆ and tetrahydrofuran-*d*₈ were distilled from Na/K alloy. Commercial silanes, 1-hexene and PhCH=CH₂ were dried over molecular sieves and distilled before use. Deuterated phenylmethylsilane was obtained by reduction of PhMeSiCl₂ with LiAlD₄ (98% D). The syntheses of **1** and **2** have been reported in Chapter 2. Enantiopure (S)-2,2'-diamino-6,6'-dimethylbiphenyl³³ (99.9+% ee as determined by polarimetry and HPLC) was provided by prof. A. Togni (ETH-Zurich). NMR spectra were recorded at 300 or 500 MHz (¹H) with Bruker AMX-300 and DRX-500 spectrometers, or at 100 MHz (¹³C{¹H}) with an AMX-400 spectrometer, at ambient temperature and in benzene-*d*₆, unless otherwise noted. Signal multiplicities are reported as follows: s - singlet, d - doublet, t - triplet, q - quartet, qn - quintet, m - multiplet.

GC/MS data was obtained with a HP 6890 GC/MS system, equipped with a JW DB-XLB column.

(S)-[DADMB]YMe(THF)₂ (S-1). To a cold (0 °C) solution of (S)-2,2'-diamino-6,6'-dimethylbiphenyl (0.68 g, 3.20 mmol) in THF (50 mL) was added dropwise 4.0 mL (6.4 mmol) of 1.6 M ⁿBuLi. A white precipitate formed initially, but dissolved completely after all of the ⁿBuLi had been added. The solution was allowed to warm to room temperature, and was then stirred for 3 h. A solution of ^tBuMe₂SiCl (1.01 g, 6.72

mmol) in 10 mL of THF was then added dropwise. The mixture was heated at reflux for 1 h, which resulted in the formation of a white precipitate. After cooling to room temperature, a second portion of ⁿBuLi (4.0 mL, 6.4 mmol) was added and the mixture was stirred overnight at room temperature. The THF was removed under vacuum to give an oily white solid. Extraction with hexane (2 × 50 mL) gave a light yellow solution, which was concentrated in vacuo until crystals appeared, and then cooled to -78 °C to obtain 1.53 g (83% yield) of (S)-Li₂[DADMB]·(THF)₂ as colorless crystals. ¹H NMR: δ 7.06 (d, 2 H, J = 7.7 Hz), 6.96 (t, 2 H, J = 7.7 Hz), 6.48 (d, 2 H, J = 7.1 Hz biphenyl H's), 3.26 (m, 4 H, THF), 3.06 (m, 4 H, THF), 1.99 (s, 6 H, Me), 1.24 (m, 8 H, THF), 1.17 (s, 18 H, ^tBuMe₂Si), 0.50 (s, 6 H, ^tBuMe₂Si), 0.10 (s, 6 H, ^tBuMe₂Si). ¹³C{¹H} NMR: δ 157.5, 140.1, 133.2, 128.0, 121.8, 116.6, 68.6 (THF), 28.7 (CMe₃), 25.4 (THF), 21.8, 21.7 (Me; CMe₃), 1.0, -0.5 (^tBuMe₂Si). A portion of this product (1.28 g, 2.15 mmol) mixed with 0.91 g (2.22 mmol) of YCl₃(THF)₃ in 50 mL of THF and the solution was heated at reflux for 3 h. The solvent was removed in vacuo and the resulting white powder was extracted with hexane / THF mixture. The filtrate was concentrated to about 15 mL and more hexane (20 mL) was added to initiate crystallization of the product as a white precipitate. After cooling to -78 °C, the solution was filtered and the product was then dried in vacuo to obtain 1.01 g (66% yield) of (S)-[DADMB]YCl(THF)₂ as a white crystalline powder. ¹H NMR: δ 7.07 (d, 2 H), 6.95 (t, 2 H), 6.56 d, 2 H, aromatic H), 3.73 (m, 4 H, THF), 3.42 (m, 4 H, THF), 1.88 (s, 6 H, Me), 1.24 (m, 8 H, THF), 1.11 (s, 18 H, ^tBuMe₂Si), 0.52, 0.50 (s, 6 H each, ^tBuMe₂Si). ¹³C{¹H} NMR: δ 152.4, 142.4, 130.5, 130.0, 123.5, 120.1 (aromatic C), 71.6 (THF), 28.3 (Me₃C), 25.5 (THF), 22.3 (MeAr), 21.5 (Me₃C), 1.8, -1.5 (Me₂Si). A portion of this product (0.82 g, 1.15 mmol) was dissolved in 50 mL of THF, the solution was cooled in ice bath, and MeLi (0.72 mL, 1.15 mmol) was added. The resulting pale yellow solution was allowed to warm to room temperature and was stirred overnight, the solvents were removed in vacuo, and the oily residue was extracted with 2 × 30 mL of hexane. The (S)-

[DADMB]YMe(THF)₂ product was isolated by crystallization at -78 °C (0.34 g, 43% yield) as a white crystalline powder, mp 128 - 132 °C (cf. 145 - 150 °C for racemic **1**). ¹H NMR: δ 7.07 (m, 2 H), 6.96 (m, 2 H), 6.57 (m, 2 H, aromatic H), 3.66 (m, 4 H, THF), 3.29 (m, 4 H, THF), 1.88 (s, 6 H, Me), 1.24 (m, 8 H, THF), 1.14 (s, 18 H, ^tBuMe₂Si), 0.53, 0.41 (s, 6 H each, ^tBuMe₂Si), -0.42 (d, 3 H, YMe). ¹³C{¹H} NMR: δ 153.2, 142.1, 131.1, 129.4, 123.4, 119.5, 70.9 (THF), 28.4 (Me₃C), 25.5 (THF), 22.4 (MeAr), 21.7 (YMe), 21.7 (Me₃C), 2.0, -1.9 (Me₂Si).

Hydrosilylation of ethylene with PhSiH₃. A sample of **1** (ca. 5 mg) was dissolved in benzene-*d*₆ in a J. Young NMR tube. The tube was evacuated briefly and refilled with C₂H₄ (5 - 10 psi) several times. An excess of PhSiH₃ (ca. 50 μL) was added. After 20 min at room temperature, the silane was completely consumed and formation of PhH₂SiCH₂CH₃ was observed. The NMR spectrum of PhH₂SiCH₂CH₃ was consistent with the literature data.⁴² A control sample not containing **1** revealed no reaction between PhSiH₃ and C₂H₄ after 8 h.

Hydrosilylation of 1-hexene with PhSiH₃. A sample of **1** (9.6 mg, 0.014 mmol) was dissolved in 0.8 mL of benzene-*d*₆. To this solution were added 1-hexene (35 μL, 0.28 mmol) and PhSiH₃ (35 μL, 0.28 mmol). Monitoring the reaction by ¹H NMR spectroscopy showed that 80% conversion to products had occurred within the first 10 min after mixing, corresponding to turnover rate of about 100 h⁻¹. The spectrum of the hydrosilylation product was consistent with that reported for the PhH₂Si(CH₂)₅CH₃ isomer.²⁴ Analysis of the products was also performed by GC/MS, after quenching and diluting the reaction mixture with pentane, which revealed the presence of a small amount (ca. 8%) of the PhSiH₂(CH)(CH₃)(CH₂)₃CH₃ isomer.

Hydrosilylation of 1-hexene with PhMeSiH₂. A sample of **1** (10.0 mg, 0.015 mmol) was dissolved in benzene-*d*₆ (0.8 mL). To this solution were added 1-hexene (36 μL, 0.29 mmol) and PhMeSiH₂ (40 μL, 0.29 mmol). An initial turnover rate of 4.3 h⁻¹ was determined by following the disappearance of the starting materials by ¹H

NMR spectroscopy for the first 7000 s. The ^1H NMR spectrum and the GS/MS data indicated exclusive formation of a single hydrosilylation product, identified as $\text{PhMeHSi}(\text{CH}_2)_5\text{CH}_3$. ^1H NMR: δ 7.50 (m, 2 H, Ph), 7.20 (m, 3 H, Ph), 4.58 (m, 1 H, SiH), 1.10 - 1.30 (m, 8 H, CH_2), 0.87 (t, 3 H, CH_3), 0.70 - 0.80 (m, 2 H, CH_2), 0.26 (d, $^3J_{\text{HH}} = 3.8$ Hz, SiMe).

Hydrosilylation of $\text{PhCH}=\text{CH}_2$ with PhSiH_3 . A sample of **1** (9.6 mg, 0.014 mmol) was dissolved in 0.8 mL of benzene- d_6 . To this solution were added $\text{PhCH}=\text{CH}_2$ (34 μL , 0.30 mmol) and PhSiH_3 (35 μL , 0.28 mmol). An initial turnover rate of 0.66 h^{-1} was determined by following the disappearance of the starting materials by ^1H NMR spectroscopy for the first 12,000 s. After 3 days, ca. 80% conversion was observed. Complete consumption of the starting materials was observed after 1 week. The product ratio $\text{PhCH}(\text{CH}_3)\text{SiH}_2\text{Ph}$ to $\text{PhCH}_2\text{CH}_2\text{SiH}_2\text{Ph}$ as determined by ^1H NMR integration was 3.1:1. The NMR spectrum was consistent with the literature data.²⁴ The identity of the products was also confirmed by GC/MS ($m/z = 212$).

Hydrosilylation of $\text{PhCH}=\text{CH}_2$ with PhMeSiH_2 . A sample of **1** (9.3 mg, 0.013 mmol) was dissolved in 0.8 mL of benzene- d_6 . To this solution were added $\text{PhCH}=\text{CH}_2$ (31 μL , 0.27 mmol) and PhMeSiH_2 (37 μL , 0.27 mmol). An initial turnover rate of ca. 0.12 h^{-1} was determined by following the disappearance of the starting materials by ^1H NMR spectroscopy over the first 80,000 s. After 2 days, 50% conversion was observed. Starting materials were still present even after 10 days. The product ratio $\text{PhCH}(\text{CH}_3)\text{SiHMePh}$ to $\text{PhCH}_2\text{CH}_2\text{SiHMePh}$ as determined by ^1H NMR integration was 1.8:1. The identity of the products was also confirmed by GC/MS ($m/z = 226$), which also showed the presence of both diastereoisomers of $\text{PhCH}(\text{CH}_3)\text{SiHMePh}$, in 1.2 : 1 ratio. ^1H NMR (some peaks overlap): δ 7.45 (m, 2 H, Ph), 7.32 (m, 2 H, Ph), 6.95-7.20 (m, 6 H, Ph), 4.50-4.55 (m, 2 H, SiH), 2.60 (t, 2 H, $\text{PhCH}_2\text{CH}_2\text{SiHMePh}$), 2.28-2.35 (m, 1 H, $\text{PhCH}(\text{CH}_3)\text{SiHMePh}$), 1.30 (m, 3 H, $\text{PhCH}(\text{CH}_3)\text{SiHMePh}$), 1.05-1.10 (m, 2 H,

PhCH₂CH₂SiHMePh), 0.19 (d, SiMe(H), overlaps with PhMeSiH₂), 0.12 (d, SiHMe, 3 H).

Preparative scale hydrosilylation of norbornene with PhSiH₃. To a solution of **1** (0.248 g, 0.36 mmol) and norbornene (1.13 g, 12.0 mmol) in 30 mL of C₆H₆ was added 1.50 mL of PhSiH₃ (12.0 mmol) and the mixture was stirred at room temperature for 48 h. The cloudy solution was diluted with 50 mL of Et₂O and the resulting mixture was poured into 75 mL of saturated aqueous NH₄Cl. The organic layer was separated, the aqueous layer was extracted with Et₂O (3 × 50 mL), and the combined Et₂O extracts were dried over MgSO₄ and then concentrated under vacuum. The resulting oil was redissolved in 30 mL of hexane and filtered through a short silica column. Removal of the volatiles with a rotovap produced 2.80 g (quantitative yield) of exo-phenylsilylnorbornane as a colorless oil (pure by ¹H NMR spectroscopy, containing some residual solvents). Only the exo-isomer was produced, as identified by NOESY ¹H NMR spectroscopy and GC/MS (m/z = 202). The NMR spectrum was in agreement with the published literature data.²⁵ Using the same procedure, enantioselective hydrosilylation of norbornene (0.77 g, 8.2 mmol) with PhSiH₃ (1.0 mL, 8.2 mmol) in presence of (S)-[DADMB]YMe(THF)₂ (0.17 g, 0.25 mmol) produced 0.94 g of exo-phenylsilylnorbornane.

Oxidation of exo-phenylsilylnorbornane to exo-norborneol. The racemic product from the hydrosilylation of norbornene (2.80 g, ca. 12.0 mmol) was dissolved in CHCl₃ (140 mL), the solution was cooled in ice bath, and 4.1 mL of HBF₄·Et₂O was added. The reaction mixture was stirred for 3 h, the volatiles were removed in vacuo and the residue redissolved in 1:1 CH₃OH / THF mixture (200 mL). To this solution were added KF (3.75 g), KHCO₃ (6.7 g) and 33 mL of 30% H₂O₂. The mixture was stirred for 1 h at room temperature and then refluxed overnight, which resulted in the formation of copious white precipitate. After reducing the volume of the solution in vacuo, it was poured into 400 mL concentrated aqueous NaCl and the mixture was

extracted with Et₂O (3 × 100 mL). Removal of volatiles produced pale yellow oil, which was purified by flash chromatography on silica using 3:1 pentane / Et₂O mixture to give 0.75 g of racemic exo-norborneol as a white powder. Under the same reaction conditions, oxidation of the enantioenriched exo-phenylsilylnorbornane product (0.94 g) afforded 0.20 g of exo-norborneol. The enantiomeric excess of the produced exo-norborneol was measured to be 90.4 %, as determined by GC analysis with a chiral column (Supelco beta-DEX 120, at 80 °C, He eluent at 1.4 mL/min flow)³⁴ at the laboratory of prof. A. Togni at ETH-Zurich.

Kinetic measurements. Reactions were monitored by ¹H NMR spectroscopy, with a Bruker AMX300 spectrometer, using 5 mm Wilmad NMR tubes, equipped with J. Young Teflon screw caps. Liquid reagents were measured using a 100 µL Hamilton gas-tight syringe. The total volume of the reaction solution was determined by measuring its height in the precalibrated NMR tube. The samples were frozen in liquid N₂ immediately after preparation, and defrosted just before being placed in the preshimmed probe, which was preheated at 25 °C. Single scan spectra were acquired automatically at preset time intervals. The peaks were integrated relative to ferrocene as an internal standard. Rate constants were obtained by non-weighted linear least-squares fits of the integrated first-order rate law in logarithmic form, $\ln C = \ln C_0 - k_{\text{obs}}t$.

Kinetic study of the reaction of **1 with PhMeSiH₂.** Samples of **1** (12.3-15.5 mg, 0.0179-0.0226 mmol) and Cp₂Fe (1.0-3.0 mg) were weighed into an NMR tube and dissolved in benzene-*d*₆ (0.9 mL). To the solution was added a known amount of PhMeSiH₂. The disappearance of the YMe signal as integrated with respect to the ferrocene standard was monitored. Five kinetic runs were performed, using different amounts of silane. The overall rate constant was determined by plotting the observed pseudo-first order rate constant for the consumption of **1** vs. the concentration of PhMeSiH₂.

Kinetic study of the hydrosilylation of 1-hexene with PhMeSiH₂ in benzene-*d*₆. Samples of **1** (9.6-32.7 mg, 0.014-0.048 mmol) and Cp₂Fe (0.5-3.0 mg) were weighed into an NMR tube and dissolved in benzene-*d*₆ (ca 0.6 mL). Alternatively, for accurate measuring of the amount of the catalyst precursor at low concentrations, a standard solution of **1** was prepared by dissolving 30.6 mg (0.0445 mmol) of **1** in 3.0 mL benzene-*d*₆, and aliquots of this solution (50-800 μL) were used to prepare the NMR sample. To the solution were added known volumes of 1-hexene (36.4-500 μL) and PhMeSiH₂ (20-44 μL). The consumption of PhMeSiH₂ was monitored by integrating the SiH₂ signal against ferrocene. The observed pseudo-first order rate constants for silane disappearance were determined at different olefin or yttrium methyl initial concentrations by plotting ln[PhMeSiH₂] vs. time.

Kinetic study of the hydrosilylation of 1-hexene with PhMeSiH₂ in THF-*d*₈. Samples of **1** (8.2-18.6 mg, 0.012-0.042 mmol) and Cp₂Fe (0.5-2.0 mg) were weighed into an NMR tube and dissolved in THF-*d*₈ (ca 0.5 mL). To this solution were added 1-hexene (150 μL, 1.20 mmol) and PhMeSiH₂ (40 μL, 0.29 mmol). The consumption of PhMeSiH₂ was monitored by integrating the CH₃ signal against ferrocene.

References:

- (1) Gountchev, T. I.; Tilley, T. D. *Organometallics* **1999**, *18*, 2896.
- (2) Aoyagi, K.; Gantzel, P. K.; Kalai, K.; Tilley, T. D. *Organometallics* **1996**, *15*, 923.
- (3) Scollard, J. D.; McConville, D. H. *J. Am. Chem. Soc.* **1996**, *118*, 10008.
- (4) Scollard, J. D.; McConville, D. H.; Rettig, S. J. *Organometallics* **1997**, *16*, 1810.
- (5) Horton, A. D.; de With, J. *Organometallics* **1997**, *16*, 5424.
- (6) Baumann, R.; Davis, W. M.; Schrock, R. R. *J. Am. Chem. Soc.* **1997**, *119*, 3830.
- (7) Warren, T. H.; Schrock, R. R.; Davis, W. M. *Organometallics* **1998**, *17*, 308.
- (8) Tsuie, B.; Swenson, D. C.; Jordan, R. F. *Organometallics* **1997**, *16*, 1392.
- (9) Tinkler, S.; Deeth, R. J.; Duncalf, D. J.; McCamley, A. *J. Chem. Soc. Chem. Commun.* **1996**, 2623.
- (10) Gibson, V. C.; Kimberley, B. S.; White, A. J. P.; Williams, D. J.; Howard, P. J. *Chem. Soc. Chem. Commun.* **1998**, 313.
- (11) Male, N. A. H.; Thornton-Pett, M.; Bochmann, M. *J. Chem. Soc., Dalton Trans.* **1997**, 2487.
- (12) Horton, A. D.; de With, J. *J. Chem. Soc. Chem. Commun.* **1996**, 1375.
- (13) Cloke, F. G. N.; Geldbach, T. J.; Hitchcock, P. B.; Love, J. B. *J. Organomet. Chem.* **1996**, *506*, 343.
- (14) Sinnema, P.-J.; Liekelema, K.; Staal, O. K. B.; Hessen, B.; Teuben, J. H. *J. Mol. Catal. A: Chemical* **1998**, *128*, 143.
- (15) Scollard, J. D.; McConville, D. H.; Payne, N. C.; Vittal, J. J. *Macromolecules* **1996**, *29*, 5241.
- (16) Scollard, J. D.; McConville, D. H.; Vittal, J. J. *Organometallics* **1995**, *14*, 5478.
- (17) Guérin, F.; McConville, D. H.; Payne, N. C. *Organometallics* **1996**, *15*, 5085.
- (18) Tilley, T. D. *Acc. Chem. Res.* **1993**, *26*, 22.
- (19) Woo, H.-G.; Tilley, T. D. *J. Am. Chem. Soc.* **1989**, *111*, 8043.
- (20) Woo, H.-G.; Walzer, J. F.; Tilley, T. D. *J. Am. Chem. Soc.* **1992**, *114*, 7047.

- (21) Gauvin, F.; Harrod, J. F.; Woo, H. G. *Adv. Organomet. Chem.* **1998**, *42*, 363.
- (22) Corey, J.; Larson, G., Ed.; JAI Press, Inc.: Greenwich, Conn., 1991; Vol. 1, pp 327.
- (23) Gountchev, T. I.; Tilley, T. D., submitted for publication.
- (24) Fu, P.-F.; Brard, L.; Li, Y.; Marks, T. J. *J. Am. Chem. Soc.* **1995**, *117*, 7157.
- (25) Molander, G. A.; Julius, M. *J. Org. Chem.* **1992**, *57*, 6347.
- (26) Molander, G. A.; Dowdy, E. D.; Noll, B. C. *Organometallics* **1998**, *17*, 3754.
- (27) Koo, K.; Fu, P.-F.; Marks, T. J. *Macromolecules* **1999**, *32*, 981.
- (28) Marciniak, B.; Gulinski, J. *J. Organomet. Chem.* **1993**, *446*, 15.
- (29) Schumann, H.; Keitsch, M. R.; Demtschuk, J.; Molander, G. A. *J. Organomet. Chem.* **1999**, *582*, 70.
- (30) Molander, G. A.; Nichols, P. J. *J. Am. Chem. Soc.* **1995**, *117*, 4415.
- (31) Kesti, M. R.; Waymouth, R. M. *Organometallics* **1992**, *11*, 1095.
- (32) Carter, M. B.; Schiott, B.; Gutierrez, A.; Buchwald, S. L. *J. Am. Chem. Soc.* **1994**, *116*, 11667.
- (33) Kanoh, S.; Goka, S.; Murose, N.; Kubo, H.; Kondo, M.; Sugino, T.; Motoi, M.; Suda, H. *Polymer Journal* **1987**, *19*, 1047.
- (34) Pioda, G.; Togni, A. *Tetrahedron: Asymmetry* **1998**, *9*, 3903.
- (35) Marciniak, B.; Gulinski, J. *J. Organomet. Chem.* **1993**, *446*, 15.
- (36) Uozumi, Y.; Hayashi, T. *J. Am. Chem. Soc.* **1991**, *113*, 9887.
- (37) Bergens, S. H.; Noheda, P.; Whelan, J.; Bosnich, B. *J. Am. Chem. Soc.* **1992**, *114*, 2121.
- (38) Noyori, R. *Asymmetric Catalysis in Organic Synthesis*; Wiley: New York, 1994.
- (39) Giardello, M. A.; Conticello, V. P.; Brard, L.; Gagné, M. R.; Marks, T. J. *J. Am. Chem. Soc.* **1994**, *116*, 10241.
- (40) Stern, D.; Sabat, M.; Marks, T. J. *J. Am. Chem. Soc.* **1990**, *112*, 9558.
- (41) Schaverien, C. J. *Organometallics* **1994**, *13*, 69.

(42) Bissinger, P.; Paul, M.; Jürgen, R.; Schmidbaur, H. *Chem. Ber.* **1993**, *126*, 2579.

Chapter 4

Bis(silylamido) Complexes of Zirconium

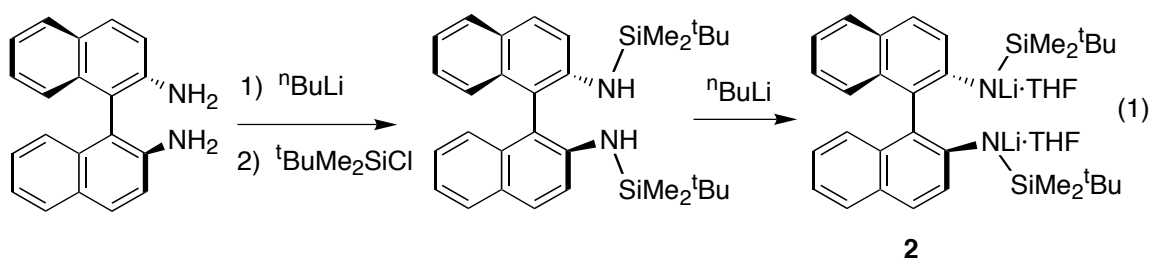
Introduction

Chelating and multidentate amido ligands¹⁻¹⁸ have recently emerged as a viable alternative to the traditionally used cyclopentadienide ligands¹⁹⁻²¹ in the chemistry of early transition metals. Complexes of d^0 metals can be used as catalysts for olefin polymerization,¹⁹⁻²⁷ silane dehydropolymerization,²⁸⁻³² olefin hydrosilylation³³⁻³⁹ and related transformations. It has been recognized that modifying the electronic and steric environment at the metal center affects significantly the reactivity of the complex, and coordinative unsaturation and high electrophilicity have been invoked as a requirement for increased reactivity in d^0 systems.

Chapters 2 and 3 described our studies on the structure and reactivity of silylamido yttrium complexes containing the [DADMB]²⁻ ligand (DADMB = 2,2'-bis(*tert*-butyldimethylsilylamido)-6,6'-dimethylbiphenyl),¹ and their application as olefin hydrosilylation catalysts.³⁹ In a continuing effort to explore the properties of C_2 -symmetric chelating silylamides as ancillary ligands for early transition metals, this chapter describes our investigations of a number of zirconium complexes of these ligands, based on biphenyl or binaphthyl backbones.

Results and Discussion

The lithiated silylamine $\text{Li}_2[\text{DADMB}] \cdot 2\text{THF}$ (**1**) was prepared as previously described.¹ The analogous binaphthyl compound, $\text{Li}_2[\text{DMBN}] \cdot 2\text{THF}$ (**2**), was obtained using the same procedure (eq 1), starting from diaminobinaphthyl (see Experimental Section).



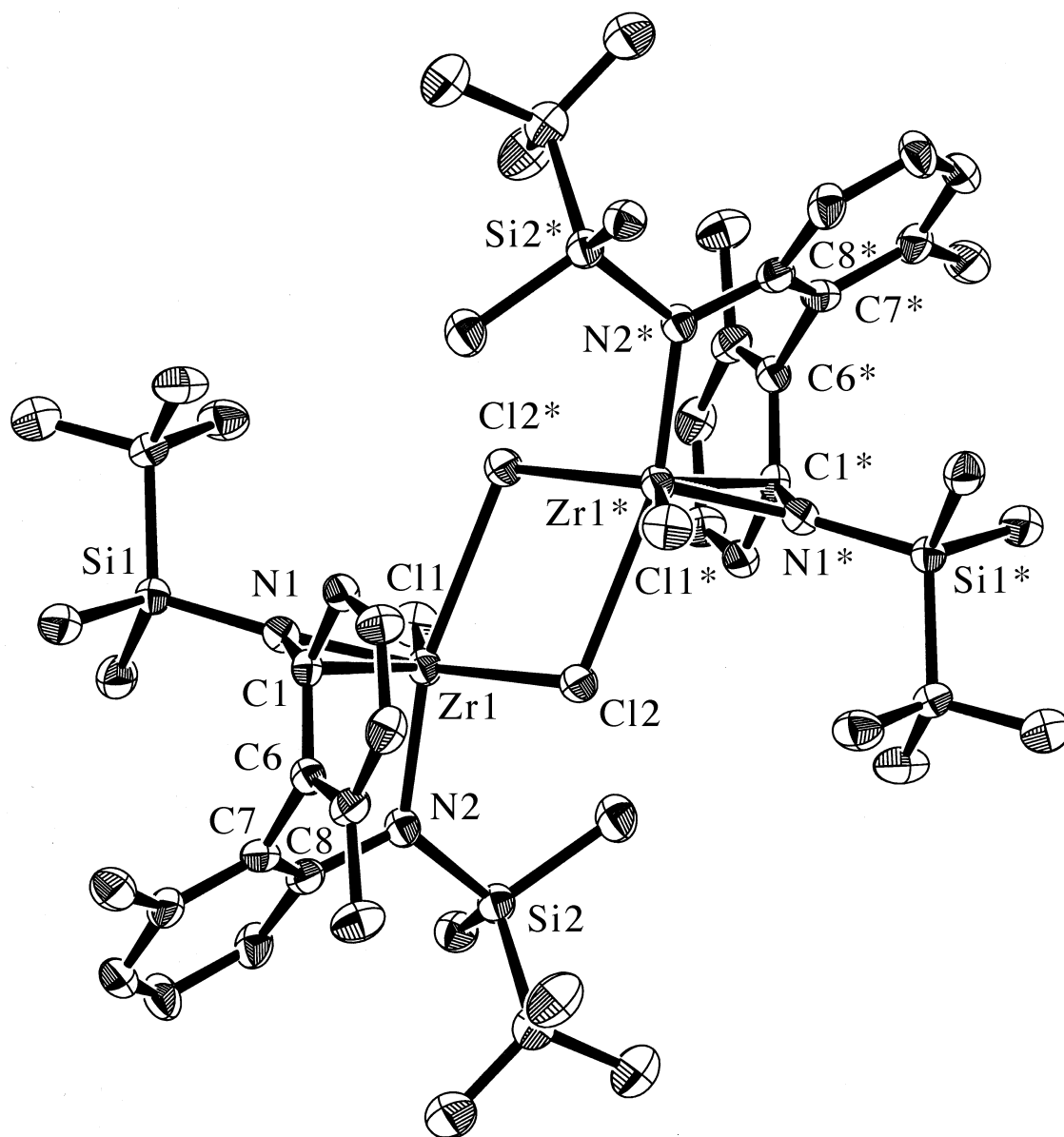
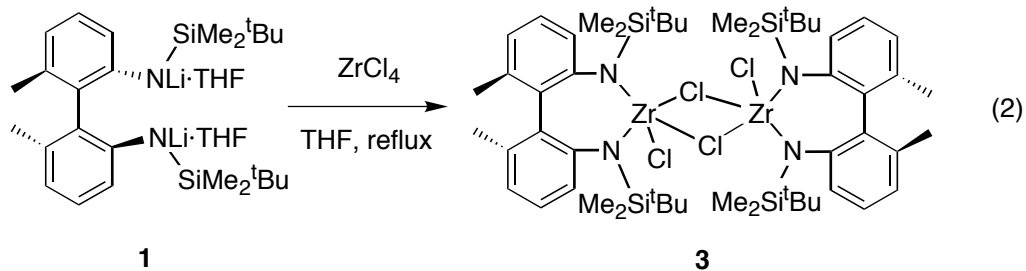


Figure 1. ORTEP diagram of $\{[DADMB]ZrCl_2\}_2$ (**3**).

Reaction of **1** with ZrCl_4 in refluxing THF (eq 2) produced the zirconium complex $\{[\text{DADMB}]\text{ZrCl}_2\}_2$ (**3**), isolated in 82% yield from pentane solution. The solid state structure of **3** (Figure 1) was determined by X-ray crystallography. Compound **3** crystallizes as a centrosymmetric dimer, with two bridging chloride ligands and one terminal chloride per zirconium. The zirconium centers adopt a distorted trigonal-bipyramidal geometry. The two bridging $\mu\text{-Cl}$ ligands asymmetrically bridge the zirconium centers, resulting in inequivalent Zr-Cl_μ bond lengths of 2.575(1) and 2.733(1) Å. For comparison, the terminal Zr-Cl_t bond length is 2.412(1) Å. The close $\text{Zr-C}_{\text{ipso}}$ distance (2.529(4) Å) and the small $\text{Zr-N-C}_{\text{ipso}}$ angle ($93.4(2)^\circ$) suggest the presence of Zr-carbon bonding interactions with one of the biphenyl rings, as is often found in complexes of this type.^{3,4} Similar dimeric chloride bridged structures have often been determined or suggested for zirconium dichloride complexes.^{9,12,40}

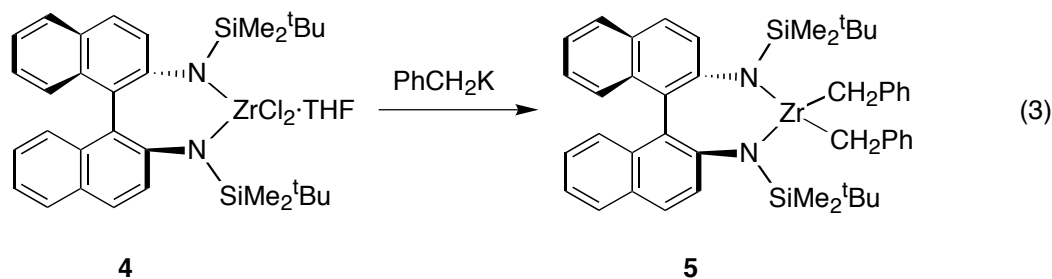


The binaphthyl analogue, $[\text{DMBN}]\text{ZrCl}_2\cdot\text{THF}$ (**4**; $\text{DMBN} = 2,2'$ -bis(*tert*-butyl-dimethylsilylamido)-1,1'-binaphthyl) was prepared in 95% yield from **1** and ZrCl_4 under the same reaction conditions. A notable difference in the properties of **3** and **4** is the tendency of **4** to coordinate one equivalent of THF, which could not be fully removed even after repeated recrystallization.

The reactivity of **3** and **4** as olefin polymerization catalysts when activated with MAO (500 equiv) was investigated. Both complexes were active towards ethylene polymerization (at 40-50 psi C_2H_4 , toluene solution, room temperature), with activities of 4.59 $\text{kg}/(\text{mol}\cdot\text{h}\cdot\text{atm})$ for **3** and 4.17 $\text{kg}/(\text{mol}\cdot\text{h}\cdot\text{atm})$ for **4**, but no measurable polymer

formation was observed with other olefins (1,3-butadiene, propylene) under the same conditions. This rather low reactivity is similar to that of other MAO-activated amido complexes (cf. 64 kg/(mol·h) for $\{\text{Me}_2\text{Si}(\text{NCMe}_3)_2\}\text{ZrCl}_2(\text{THF})_2$,¹² 13 kg/(mol·h·atm) for $\{(C_6H_3)_2-2,2'-(NCH_2C_6H_4^t\text{Bu}-4)_2-6,6'-\text{Me}_2\}\text{Zr}(\text{CH}_2\text{Ph})_2$,⁸ 2.9 kg/(mol·h·atm) for $[\text{Ti}(\text{Me}_3\text{SiNCH}_2\text{CH}_2\text{NSiMe}_3)\text{Cl}_2]$ ⁴¹) but is much lower than the best group 4 metallocene / MAO polymerization catalysts, which show activities often exceeding 1×10^5 kg/(mol·h),^{20,21} and lower than many catalysts with amido or alkoxide ligands (cf. $\{\text{Zr}[\text{RN}(\text{Me}_2\text{SiCH}_2\text{CH}_2\text{SiMe}_2)\text{NR}](\text{NMe}_2)_2\}$ (R = 2,6-Me₂C₆H₃) 990 kg/(mol·h·atm),²⁶ 2,2'-S(4-Me,6-^tBuC₆H₂O)₂TiCl₂ 4740 kg/(mol·h),²⁷ $\{\text{C}_5\text{Me}_4\text{SiMe}_2\text{N}^t\text{Bu}\}\text{ZrCl}_2$ up to 2750 kg/(mol·h)⁴²)

Attempts to isolate alkyl derivatives of **3** by reaction with MeMgBr, MeLi or PhCH₂MgBr resulted in the formation of yellow oils that were difficult to handle and characterize, due apparently to the very high solubility of the alkylated products. The analogous complexes of **4**, however, were found to be less soluble and thus easier to isolate and characterize. The benzyl derivative [DMBN]Zr(CH₂Ph)₂ (**5**) was obtained as a yellow foamy solid by reaction of **4** with two equivalents of PhCH₂K (eq 3).



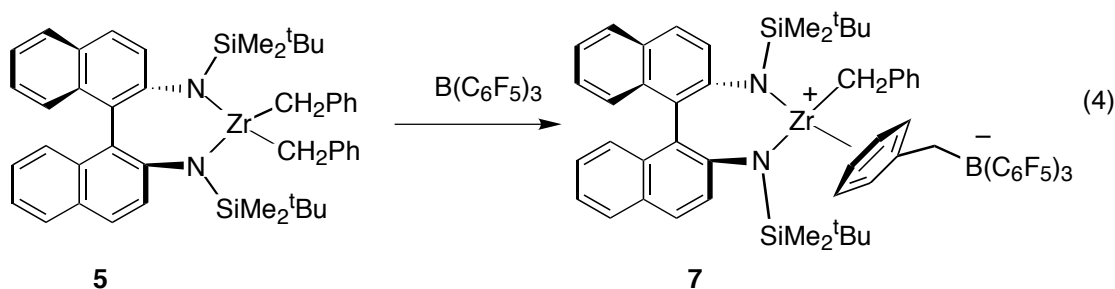
The benzylic protons in **5** give rise to two doublets in the ¹H NMR spectrum at 2.24 and 2.09 ppm (²J_{HH} = 10 Hz), with the ZrCH₂Ph carbon appearing at 72.1 ppm in the ¹³C NMR spectrum (¹J_{CH} = 110 Hz). These NMR shifts are consistent with η¹-coordination of the benzyl group and within the typical range reported for Zr benzyl complexes.^{11-13,24,26,27,42,43}

The methyl derivative [DMBN]ZrMe₂·THF (**6**) was isolated by reaction of **4** with two equivalents of MeLi as a black foamy solid (apparently contaminated with dark colored byproducts, not observable by NMR). The methyl groups in **6** give rise to a singlet at 0.55 ppm in the ¹H NMR spectrum, with the carbon atom appearing at 47.0 ppm (¹J_{CH} = 105 Hz) in the ¹³C NMR spectrum, consistent with the values typically reported for ZrMe species.^{11,13,26,27}

No reaction was observed between **5** or **6** and ethylene (in benzene-*d*₆) after 3 h at room temperature, and heating the reaction mixtures at 80 °C resulted in decomposition with no evidence for polymer formation. Similarly, no reaction was observed between **5** and PhSiH₃ or H₂ (in benzene-*d*₆) after 2 days at room temperature, and heating at 80 °C resulted in decomposition of **5** in both systems.

While the reaction of **6** with B(C₆F₅)₃ gave an intractable mixture of products, the reaction of **5** with B(C₆F₅)₃ resulted in clean benzyl abstraction (eq 4) and formation of the zirconium complex [DMBN]Zr(CH₂Ph)[η⁶-PhCH₂B(C₆F₅)₃] (**7**), isolated in 71% yield. The ¹H NMR spectrum of **7** shows the presence of two inequivalent ^tBu groups, which suggests anion coordination leading to a non-C₂ symmetric structure in solution. Such coordination has been often observed in other analogous zwitterionic zirconium species.^{12,13,24,25,27,42-45} The ZrCH₂Ph group gives rise to two doublets at 2.14 and 1.58 ppm (²J_{HH} = 11 Hz) in the ¹H NMR spectrum, and a signal at 73.6 ppm (¹J_{CH} = 121 Hz) in the ¹³C NMR spectrum of **7** (cf. 1.95 ppm, 52.5 ppm, ¹J_{CH} = 122.5 Hz for the ZrCH₂Ph group in {Me₂Si(NCMe₃)₂}Zr(CH₂Ph)[η⁶-PhCH₂B(C₆F₅)₃]¹²). The BCh₂Ph methylene group appears at 2.8-3.2 ppm (br m) in the ¹H NMR spectrum, and the ¹³C NMR shift for the BCh₂Ph carbon is at 38.5 ppm (cf 3.36 and 36.2 ppm in {Me₂Si(NCMe₃)₂}Zr(CH₂Ph)[η⁶-PhCH₂B(C₆F₅)₃]). A variable temperature NMR study of **7** in toluene-*d*₈ showed that coalescence of the signals from the ^tBu groups occurs at 300 K, which corresponds to an activation energy barrier of 63 kJ mol⁻¹ (15 kcal mol⁻¹) for

anion dissociation. This value is very similar to that of 13.8 kcal/mol reported for [(1,2-Me₂Cp)₂ZrR][CH₃B(C₆F₅)₃] (R = CH₂CMe₃, CH₂SiMe₃).⁴⁶



The solid state structure of **7** was determined by X-ray diffraction (Figure 2). As usually found in such cationic complexes, the borane anion is closely associated with the metal cation, the PhCH₂B group being coordinated to the Zr atom in an η⁶ fashion. The distance between the plane of the C₆ ring and the Zr atom is 2.325(6) Å, similar to that in other related complexes.^{43,47} All Zr–C distances are similar (ranging from 2.675(7) to 2.773(6) Å), which suggests an η⁶ rather than an η⁴ or lower coordination mode. The remaining benzyl group is η¹ coordinated to the metal (Zr–C–C angle of 132.7(4)°), with no evidence for agostic or Zr - aromatic ring interactions. There are close contacts, however, between the Zr atom and the ipso carbons of both binaphthyl rings, with an average Zr–C distance of 2.567(6) Å and a Zr–N–C_{ipso} angle of 91.5(3)°.

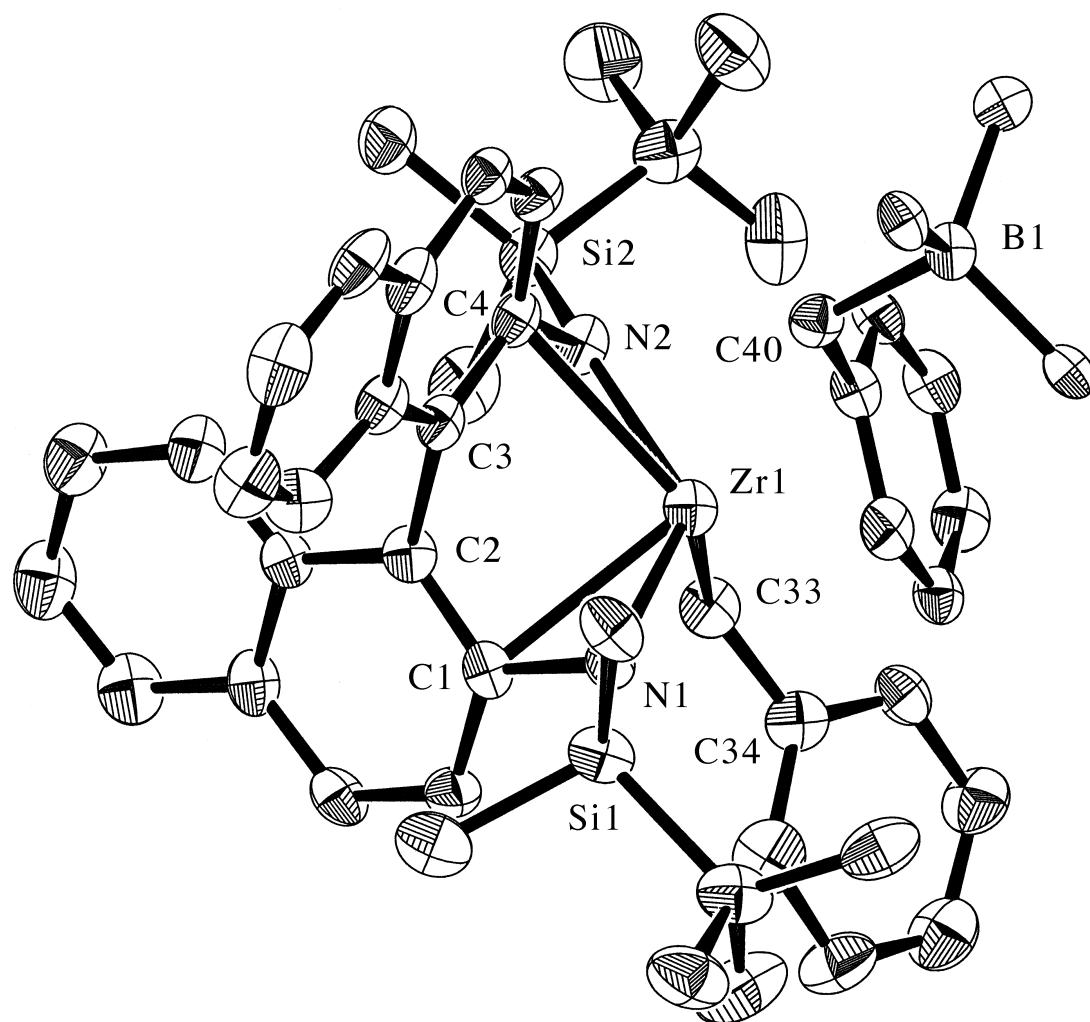


Figure 2. ORTEP diagram of $[\text{DMBN}]\text{Zr}(\text{CH}_2\text{Ph})[\eta^6\text{-PhCH}_2\text{B}(\text{C}_6\text{F}_5)_3]$ (**7**). The C_6F_5 groups of the borane anion have been omitted for clarity.

Reaction of **7** with ethylene (room temperature, 5-10 psi) resulted in fast formation of a new complex within 15 min, presumably an ethylene insertion product, as observed by ^1H NMR (δ 0.84, 0.62 (s, 9 H each, ^tBu), -0.24, -0.26, -0.54, -0.76 (s, 3 H each, Me_2Si), other peaks obscured). The formation of ethylene oligomers was also detected after 3 h (by ^1H NMR spectroscopy). Unlike compounds **3** and **4**, however, complex **7** produced no measurable amount of polyethylene when tested under the same conditions (without MAO cocatalyst). Similar rapid single insertion of α -olefins, but limited polymerization activity has been reported for the analogous complex $\{\text{Me}_2\text{Si}(\text{NCMe}_3)_2\}\text{Zr}(\text{CH}_2\text{Ph})[\eta^6\text{-PhCH}_2\text{B}(\text{C}_6\text{F}_5)_3]$.¹² This may be contrasted to the high polymerization activity reported for $(\text{Me}_2\text{C}_5\text{H}_3)_2\text{ZrMe}[\text{MeB}(\text{C}_6\text{F}_5)_3]$ 6800 kg/(mol·h·atm),^{25,45} $\{\text{Me}_3\text{SiN}(\text{CH}_2\text{CH}_2\text{NSiMe}_3)_2\}\text{Zr}(\text{CH}_2\text{Ph})[\eta^6\text{-PhCH}_2\text{B}(\text{C}_6\text{F}_5)_3]$ 330 kg/(mol·h),¹³ $\text{Cp}^*\text{Zr}(\text{CH}_2\text{Ph})_2[\eta^6\text{-PhCH}_2\text{B}(\text{C}_6\text{F}_5)_3]$ 88 kg/(mol·h),⁴³ and others.^{5,47,48}

Compound **7** was also observed to react rapidly with 1-hexene (by ^1H NMR spectroscopy), presumably forming an insertion product (δ 0.37, 0.78 (s, ^tBu , 9 H each), -0.22, -0.26, -0.40, -0.70 (s, Me_2Si , 3 H each), other peaks obscured), with only a small amount of hexene oligomers found after 1 day. Attempt to conduct the reaction in neat 1-hexene, at room temperature, did not result in formation of measurable amounts of polymer. No reaction occurred between **7** and $\text{PhMeC}=\text{CH}_2$.

An attempt to abstract a methyl group from **6** using $\text{Ph}_3\text{CB}(\text{C}_6\text{F}_5)_4$ in dichloromethane- d_2 solution as observed by ^1H NMR resulted in a new set of peaks, assignable to a cationic zirconium species (δ 0.99, 0.96 (s, 9 H each, ^tBu), 0.25, 0.22, 0.14 (m, 12 H total, Me_2Si), -0.37 (s, 3 H, ZrMe), other peaks obscured). This *in situ* generated cation, however, also did not show observable olefin polymerization activity, as no polymer was formed when excess of 1-hexene was added to the reaction mixture (24 h, room temperature). In addition, no polymer formation occurred on exposure of neat 1-hexene to a mixture of **6** and $\text{Ph}_3\text{CB}(\text{C}_6\text{F}_5)_4$.

The reaction of **5** with $\text{Ph}_3\text{CB}(\text{C}_6\text{F}_5)_4$ in benzene- d_6 or dichloromethane- d_2 resulted in a mixture of products, as observed by ^1H NMR spectroscopy. Addition of an excess 1-hexene to this solution did not result in polymer formation (2 h, room temperature). However, a catalyst generated *in situ* from **5** and $\text{Ph}_3\text{CB}(\text{C}_6\text{F}_5)_4$ (1:1 molar ratio) was found to polymerize hexene when exposed to neat olefin (in the presence of ca. 10% toluene, to improve catalyst solubility). The polymer formed was shown by gel permeation chromatography (GPC) to have an M_w value of 2384 ($M_n = 1720$) and a polydispersity of 1.39. This molecular weight is much lower than those obtained with other recently reported chelating diamide and alkoxide based catalysts (cf. $(\text{MeN}(\text{CH}_2)_3\text{-NMe})\text{Ti}(2,6\text{-}^i\text{Pr}_2\text{C}_6\text{H}_3)_2 + \text{Ph}_3\text{CB}(\text{C}_6\text{F}_5)_4$ and related systems up to $M_w = 239\ 100$,^{10,11,49} $[(\text{tBu-}d_6)\text{N-}o\text{-C}_6\text{H}_4)_2\text{O}]\text{ZrMe}(\text{PhNMe}_2)[\text{B}(\text{C}_6\text{F}_5)_4]$ $M_n = 45\ 000$,⁵ $\{1,1'-(2,2',3,3'\text{-OC}_{10}\text{H}_5\text{SiMePh}_2)\}\text{ZrCl}_2 / \text{MAO}$ $M_w = 674\ 000$ ²⁷). The activity of the **5** / $\text{Ph}_3\text{CB}(\text{C}_6\text{F}_5)_4$ catalyst mixture for ethylene polymerization, 5.10 kg/(mol·h·atm), was not significantly different from those for the MAO-activated dichlorides **3** and **4**.

Conclusions

A series of zirconium chloride and alkyl complexes with chelating silylamido ligands have been synthesized and studied. The polymerization activity of the MAO-activated dichlorides towards ethylene was found to be relatively low, as compared to both Cp and non-Cp based catalytic systems. Reaction of the benzyl and methyl derivatives with Lewis acids results in alkyl abstraction and formation of zwitterionic species. Anion coordination has been shown to occur both in solid state and in solution for the zwitterionic complex **7**. The activity of non-Cp olefin polymerization catalysts has already been seen to depend on multiple factors, including ligand steric bulk and electrophilicity, type of cocatalyst, coordination affinity of the counter-anion in case of cationic species, solvent polarity, etc. It has been observed that MAO-activated catalysts are usually more active than the borane-activated species, in which anion coordination can significantly inhibit

polymerization activity, a non-coordinating anion leading to more reactive catalytic site. While the silylamido complexes presented in this chapter exhibit reactivity in agreement with these general trends, they are apparently not promising in terms of application as olefin polymerization catalysts.

Experimental Section

General. All reactions with air-sensitive compounds were performed under dry nitrogen, using standard Schlenk and glove box techniques. Reagents were obtained from commercial suppliers and used without further purification, unless otherwise noted. Olefin-free pentane, benzene, and toluene were prepared by pretreating with concentrated H_2SO_4 , 0.5 N KMnO_4 in 3 M H_2SO_4 , NaHCO_3 and finally anhydrous MgSO_4 . Solvents (pentane, diethyl ether, benzene, toluene, tetrahydrofuran) were distilled under nitrogen from sodium benzophenone ketyl. Benzene- d_6 was distilled from Na/K alloy. ${}^n\text{BuLi}$ was used as a 1.6 M solution in hexanes, as supplied by Aldrich, and MeLi as a 1.6 M solution in Et_2O , as supplied by Alpha Aesar. $\text{Li}_2[\text{DADMB}]\cdot 2\text{THF}$ (**1**),¹ diaminobinaphthyl,^{50,51} $\text{B}(\text{C}_6\text{F}_5)_3$,⁵² and $\text{Ph}_3\text{CB}(\text{C}_6\text{F}_5)_4$ ⁵³ were prepared according to published literature procedures. NMR spectra were recorded at 300 or 500 MHz (${}^1\text{H}$) with Bruker AMX-300 and DRX-500 spectrometers, or at 100 MHz (${}^{13}\text{C}\{{}^1\text{H}\}$) with an AMX-400 spectrometer, at ambient temperature and in benzene- d_6 , unless otherwise noted. Signal multiplicities are reported as follows: s - singlet, d - doublet, t - triplet, q - quartet, qn - quintet, m - multiplet. Elemental analyses were performed by the Microanalytical Laboratory at UC Berkeley or by Desert Analytics. Infrared spectra were recorded with a Mattson Infinity 60 MI FTIR spectrometer, as KBr pellets. The molecular weight distributions (vs. polystyrene standards) for polyhexene were measured with a Waters Associates chromatograph equipped with a refractive index detector and a PLgel 5μ mixed-D column using THF as a mobile phase.

Li₂[DMBN]·2THF (2). DABN (6.90 g, 24.3 mmol) was dissolved in 250 mL of THF and the solution cooled in ice/water bath. Two equivs of ⁿBuLi (32 mL, 51 mmol) was added dropwise with a syringe, with vigorous stirring. The solution turned cloudy and gradually changed from almost colorless through reddish yellow, to bright yellow-orange, with formation of an orange precipitate. After the mixture was stirred at room temperature overnight, a solution of ^tBuMe₂SiCl (8.31 g, 53.5 mmol) in 70 mL of pentane was added. The solution was heated at reflux for 6 h, which resulted in formation of a white precipitate, and was then left to cool slowly overnight. Removal of the volatiles in vacuo yielded a brownish foamy oil, which was extracted twice with pentane (200 and 50 mL). After filtration, the pentane extracts were concentrated to about 50 mL, and 40 mL of THF was added. ⁿBuLi (32 mL, 51 mmol) was added at room temperature, resulting in the formation of a bright yellow-greenish crystalline precipitate. The volatiles were removed and the solid product was washed with pentane (2 × 50 mL) and dried in vacuo to give 15.0 g (92% yield) of **2**. ¹H NMR: δ 7.53 (m, 6 H), 6.91 (m, 4 H), 6.79 (m, 2 H, binaphthyl H), 2.86 (m, 8 H, THF), 1.11 (s, 18 H, ^tBuMe₂Si), 1.09 (m, 8 H, THF), 0.54 (s, 6 H, ^tBuMe₂Si), 0.13 (s, 6 H, ^tBuMe₂Si). ¹³C{¹H} NMR: δ 155.8, 138.7, 128.6, 128.5, 128.1, 127.7, 127.4, 126.5, 122.0, 120.9 (binaphthyl C), 68.5 (THF), 28.7 ((CH₃)₃C), 25.1 (THF), 21.3 ((CH₃)₃C), 1.1 ((CH₃)₂Si), -0.4 ((CH₃)₂Si). IR (cm⁻¹): 3056 (w), 2952 (s), 2927 (s), 2857 (s), 1618 (s), 1596 (s), 1510 (m), 1469 (s), 1403 (s), 1343 (s), 1285 (s), 1250 (s), 1148 (w), 990 (m), 941 (w), 830 (s), 775 (m), 746 (m). Anal. Calcd. for C₄₀H₅₈N₂Li₂O₂Si₂: C, 71.82; H, 8.74; N, 4.19. Found: C, 71.52; H, 8.76; N, 4.03.

{[DADMB]ZrCl₂}₂ (3). To a mixture of Li₂[DADMB]·2THF (**1**) (3.42 g, 5.72 mmol) and ZrCl₄ (1.40 g, 6.01 mmol) was added 200 mL of THF. The clear, yellow solution was heated at reflux for 20 h. The solvent was removed in vacuo and the resulting oily solid was extracted with pentane (3 × 80 mL). Concentration of the pentane extracts and cooling to -78 °C produced a yellow crystalline precipitate, which was isolated and

dried in vacuo to give 3.16 g (82%) of **3**, containing about 1 equiv of residual THF (by ^1H NMR integration). Recrystallization of 2.88 g of the product from pentane gave 1.35 g of the THF-free complex. ^1H NMR: δ 7.17 (d, 2 H), 7.05 (t, 2 H), 6.80 (d, 2 H, aromatic H), 1.87 (s, 6 H, *MeAr*), 0.96 (s, 18 H, *tBuMe₂Si*), 0.04 (s, 6 H, *tBuMe₂Si*), 0.03 (s, 6 H, *tBuMe₂Si*). $^{13}\text{C}\{^1\text{H}\}$ NMR: δ 139.4, 138.2, 137.0, 130.4, 129.6, 128.1 (aromatic C), 27.6 ((CH_3)₃C), 21.1 ((CH_3)₃C), -1.6 ((CH_3)₂Si), -3.5 ((CH_3)₂Si). IR (cm^{-1}): 3052 (w), 2952 (s), 2927 (s), 2856 (s), 1580 (s), 1465 (s), 1305 (s), 1236 (s), 1036 (m), 960 (m), 830 (s). Anal. Calcd for $\text{C}_{26}\text{H}_{42}\text{N}_2\text{Si}_2\text{Cl}_2\text{Zr}$: C, 51.97; H, 7.05; N, 4.66. Found: C, 51.78; H, 7.24; N, 4.43.

[DMBN]ZrCl₂(THF) (4). A mixture of **2** (2.51 g, 3.75 mmol) and ZrCl_4 (0.92 g, 3.95 mmol) in 80 mL of THF was heated at reflux for 6 h. The volatiles were removed in vacuo and the yellow solid residue was extracted with Et_2O (2 \times 50 mL). The filtrate was concentrated to 15 mL and cooled to -78°C . The resulting crystalline precipitate was washed with pentane and dried in vacuo, to obtain 2.57 g of product in two crops (95% yield). ^1H NMR: δ 7.62 (m, 2 H), 7.51 (m, 2 H), 7.43 (m, 2 H), 7.08 (m, 2 H), 7.01 (m, 2 H), 6.91 (m, 2 H, binaphthyl H), 3.61 (m, 4 H, THF), 1.39 (m, 4 H, THF), 0.994 (s, 18 H, *tBuMe₂Si*), 0.15 (s, 6 H, *tBuMe₂Si*), -0.25 (s, 6 H, *tBuMe₂Si*). $^{13}\text{C}\{^1\text{H}\}$ NMR: δ 138.9, 134.4, 132.8, 131.8, 129.6, 129.0, 128.9, 128.1, 127.6, 126.3 (binaphthyl C), 70.1 (THF), 27.7 ((CH_3)₃C), 25.8 (THF), 19.9 ((CH_3)₃C), -1.6 ((CH_3)₂Si), -2.4 ((CH_3)₂Si). IR (cm^{-1}): 3056 (w), 2953 (s), 2927 (s), 2882 (m), 2855 (s), 1618 (s), 1596 (s), 1509 (m), 1469 (s), 1404 (s), 1391 (s), 1344 (s), 1285 (s), 1250 (s), 1211 (m), 1148 (m), 993 (s), 938 (s), 831 (s), 812 (s), 776 (s), 746 (s), 672 (m). Anal. Calcd. for $\text{C}_{36}\text{H}_{50}\text{N}_2\text{OSi}_2\text{ZrCl}_2$: C, 58.03; H, 6.76; N, 3.76. Found: C, 56.45; H, 6.69; N, 3.50. Satisfactory elemental analysis data could not be obtained due to partial desolvation.

[DBMN]Zr(CH₂Ph)₂ (5). A mixture of **4** (0.60 g, 0.80 mmol) and KCH_2Ph (0.22 g, 1.68 mmol) was dissolved in 25 mL of benzene at room temperature. The red

insoluble KCH_2Ph was consumed within 20 min resulting in the formation of a cloudy yellow solution. After 45 min the benzene was removed in vacuo and the solid residue was extracted with hexanes (2×30 mL). The filtrate was concentrated to 10 mL and cooled to -78 °C to give a voluminous oily yellow precipitate. The product was isolated by filtration at -78 °C and dried in vacuo to give 0.31 g of a yellow foamy solid (50% yield). The lack of crystallinity prevented purification of the product by recrystallization. ^1H NMR: δ 7.61 (m, 4 H), 7.32 (m, 2 H), 7.22 (m, 3 H), 7.06 (m, 4 H), 6.99 (m, 2 H), 6.89 (m, 2 H, aromatic H), 2.24 (d, 2 H, $^2J_{\text{HH}} = 10$ Hz, ZrCH_2Ph), 2.09 (d, 2 H, $^2J_{\text{HH}} = 10$ Hz, ZrCH_2Ph), 0.68 (s, 18 H, $^t\text{BuMe}_2\text{Si}$), -0.06 (s, 6 H, $^t\text{BuMe}_2\text{Si}$), -0.19 (s, 6 H, $^t\text{BuMe}_2\text{Si}$). $^{13}\text{C}\{^1\text{H}\}$ NMR: δ 144.8, 140.1, 134.7, 131.5, 131.1, 130.2, 130.0, 129.2, 128.7, 128.7, 127.9, 127.0, 125.6, 123.4 (aromatic C), 72.1 (ZrCH_2Ph , $^1J_{\text{CH}} = 110$ Hz), 27.3 ($(\text{CH}_3)_3\text{C}$), 19.9 ($(\text{CH}_3)_3\text{C}$), -1.2 ($(\text{CH}_3)_2\text{Si}$), -2.3 ($(\text{CH}_3)_2\text{Si}$). IR (cm^{-1}): 3055 (w), 3016 (w), 2951 (s), 2927 (s), 2881 (m), 2854 (s), 1617 (w), 1593 (s), 1470 (m), 1389 (w), 1343 (m), 1249 (s), 1207 (s), 1146 (m), 1030 (m), 991 (s), 938 (m), 865 (m), 834 (s), 810 (s), 744 (s), 697 (m), 670 (m). Anal. Calcd. for $\text{C}_{46}\text{H}_{56}\text{N}_2\text{Si}_2\text{Zr}$: C, 70.44; H, 7.20; N, 3.57. Found: C, 67.70; H, 7.16; N 3.78.

[DMBN]ZrMe₂(THF) (6). To a solution of **4** (0.60 g, 0.80 mmol) in 30 mL of Et_2O was added 1.1 mL of MeLi (1.7 mmol) at room temperature. The mixture turned dark brown within 30 min. After stirring for 1 h, the volatiles were removed in vacuo and the resulting black solid was extracted with a 1:1 hexanes / benzene mixture (75 mL). The filtrate was dried in vacuo to obtain 0.41 g of dark brown foamy solid. The lack of crystallinity prevented purification of the product by recrystallization. ^1H NMR: δ 7.6 (m, 6 H), 7.0 (m, 4 H, binaphthyl H), 3.56 (m, 4 H, THF), 1.24 (m, 4 H, THF), 0.98 (s, 18 H, $^t\text{BuMe}_2\text{Si}$), 0.55 (s, 6 H, ZrMe_2), 0.22 (s, 6 H, $^t\text{BuMe}_2\text{Si}$), -0.30 (s, 6 H, $^t\text{BuMe}_2\text{Si}$). $^{13}\text{C}\{^1\text{H}\}$ NMR: δ 138.6, 134.6, 131.9, 131.1, 129.7, 128.9, 128.7, 128.5, 128.3, 127.9, 127.6, 127.4, 125.6, 124.5 (binaphthyl C), 69.3 (THF), 47.0 ($\text{Zr}(\text{CH}_3)_2$, $^1J_{\text{CH}} = 105$ Hz), 27.6 ($(\text{CH}_3)_3\text{C}$), 25.6 (THF), 19.6 ($(\text{CH}_3)_3\text{C}$), -1.4 ($(\text{CH}_3)_2\text{Si}$), -2.8

$((\text{CH}_3)_2\text{Si})$. IR (cm^{-1}): 3056 (w), 2951 (s), 2928 (s), 2880 (s), 2853 (s), 1616 (w), 1590 (w), 1500 (w), 1470 (m), 1422 (m), 1345 (m), 1261 (s), 1249 (s), 1224 (s), 1148 (m), 1034 (m), 998 (s), 939 (m), 834 (s), 775 (s), 748 (s), 677 (m). Anal. Calcd. for $\text{C}_{38}\text{H}_{56}\text{N}_2\text{Si}_2\text{ZrO}$: C, 64.80; H, 8.01; N, 3.97. Found: C, 56.95; H, 6.72; N, 3.72.

[DMBN]Zr(CH₂Ph)[η^6 -PhCH₂B(C₆F₅)₃]-3.5C₆H₆ (7). A mixture of **5** (0.169 g, 0.215 mmol) and B(C₆F₅)₃ (0.11 g, 0.215 mmol) was dissolved in 15 mL of benzene. The solution immediately turned bright orange. After the mixture was stirred for 30 min at room temperature, the solvent was removed in vacuo and the remaining orange powder was washed with hexanes and dried to obtain 0.24 g of product (71 % yield). ¹H NMR: δ 8.05 (m, 1 H), 7.70 (m, 2 H), 7.19 - 7.41 (m, 5 H), 7.02 (m, 4 H), 6.90 (m, 3 H), 6.80 (m, 2 H, aromatic H), 2.8 - 3.2 (br m, 2 H, BCH₂Ph), 2.14 (d, 1 H, ²J_{HH} = 11 Hz, ZrCH₂Ph), 1.58 (d, 1 H, ²J_{HH} = 11 Hz, ZrCH₂Ph) 0.83 (br s, 9 H, ^tBuMe₂Si), 0.76 (br s, 9 H, ^tBuMe₂Si), -0.27 (s, 6 H, ^tBuMe₂Si), -0.54 (s, 6 H, ^tBuMe₂Si). ¹³C{¹H} NMR: δ 150.1, 150.0, 150.0, 148.2, 148.1, 140.4, 138.8, 136.9, 129.3, 128.9, 128.7, 128.6, 128.3, 128.2, 128.1, 128.0, 128.0, 128.0, 127.9, 127.2, 124.2 (aromatic C), 73.6 (ZrCH₂Ph, ¹J_{CH} = 121 Hz), 28.0 ((CH₃)₃C), 27.5 ((CH₃)₃C), 20.0 ((CH₃)₃C), 38.5 (BCH₂Ph), 0.24 ((CH₃)₂Si), -0.72((CH₃)₂Si). IR (cm^{-1}): 3050 (w), 2956 (s), 2932 (s), 2898 (m), 2859 (s), 1640 (w), 1598 (s), 1458 (s), 1382 (w), 1263 (s), 1208 (m), 1151 (m), 1084 (s), 981 (s), 935 (m), 835 (s), 814 (s), 776 (m), 750 (m), 677 (m). Anal. Calcd. for $\text{C}_{85}\text{H}_{77}\text{N}_2\text{Si}_2\text{ZrBF}_{15}$: C, 65.04; H, 4.94; N, 1.78. Found: C, 58.93; H, 4.46; N 2.16. Loss of solvent of crystallization is likely responsible for deviation in the elemental analysis data.

Ethylene polymerization. A sample of the zirconium complex (ca. 0.03 mmol) and a 500-fold excess of MAO (ca. 15 mmol) were dissolved in 20 mL of toluene and the solution was transferred to a high-pressure glass reaction vessel. The mixture was pressurized with ethylene at 40-50 psi for 1 h at room temperature. The reaction was stopped by venting the ethylene gas and pouring the solution into a mixture of 100 mL

CH₃OH, 100 mL H₂O and 50 mL conc. HCl. The precipitated polyethylene was separated by filtration, washed several times with CH₃OH, H₂O and acetone, and dried under vacuum overnight.

1-hexene polymerization. A sample of **5** (7.0 mg, 0.01 mmol) and Ph₃CB(C₆F₅)₄ (10 mg, 0.01 mmol) was dissolved in 0.2 mL of toluene. To the resulting bright orange solution was added 1.0 g of neat 1-hexene. The mixture spontaneously heated up. The reaction was stopped after 90 min by addition of 5 mL of THF containing a few drops of conc. HCl. The polymer formed was washed twice with 30 mL of H₂O and dried in vacuo for 24 h at room temperature to give 0.78 g of polyhexene (78% isolated yield) as viscous colorless oil. ¹H NMR (chloroform-*d*): δ 1.26 (m), 1.07 (m), 1.01 (m), 0.90 (m), olefinic signals at 5.36, 4.70. ¹³C{¹H} NMR (chloroform-*d*): δ 40.46, 34.81, 32.60, 28.93, 23.46, 14.41, olefinic signals at 125.5, 128.4, 129.2.

X-ray structure determinations. X-ray diffraction measurements were made on a Siemens SMART diffractometer with a CCD area detector, using graphite monochromated Mo-K_α radiation. The crystal was mounted on a glass fiber using Paratone N hydrocarbon oil. A hemisphere of data was collected using ω scans of 0.3°. Cell constants and an orientation matrix for data collection were obtained from a least-squares refinement using the measured positions of reflections in the range 4 < 2θ < 45°. The frame data were integrated using the program SAINT (SAX Area-Detector Integration Program; V4.024; Siemens Industrial Automation, Inc.: Madison, WI, 1995). An empirical absorption correction based on measurements of multiply redundant data was performed using the programs XPREP (Part of the SHELXTL Crystal Structure Determination Package; Siemens Industrial Automation, Inc.: Madison, WI, 1995) or SADABS. Equivalent reflections were merged. The data were corrected for Lorentz and polarization effects. A secondary extinction correction was applied if appropriate. The structures were solved using the teXsan crystallographic software package of the Molecular Structure Corporation, using direct methods, and expanded with Fourier techniques. All

non-hydrogen atoms were refined anisotropically and the hydrogen atoms were included in calculated positions but not refined unless otherwise noted. The function minimized in the full-matrix least-squares refinement was $\Sigma w(|F_o| - |F_c|)^2$. The weighting scheme was based on counting statistics and included a p-factor to downweight the intense reflections.

References:

- (1) Gountchev, T. I.; Tilley, T. D. *Organometallics* **1999**, *18*, 2896.
- (2) Gountchev, T. I.; Tilley, T. D. *J. Am. Chem. Soc.* **1997**, *119*, 12831.
- (3) Aoyagi, K.; Gantzel, P. K.; Kalai, K.; Tilley, T. D. *Organometallics* **1996**, *15*, 923.
- (4) Aoyagi, K.; Gantzel, P. K.; Tilley, T. D. *Polyhedron* **1996**, *15*, 4299.
- (5) Baumann, R.; Davis, W. M.; Schrock, R. R. *J. Am. Chem. Soc.* **1997**, *119*, 3830.
- (6) Schrock, R. R. *Acc. Chem. Res.* **1997**, *30*, 9.
- (7) Guérin, F.; McConville, D. H.; Payne, N. C. *Organometallics* **1996**, *15*, 5085.
- (8) Cloke, F. G. N.; Geldbach, T. J.; Hitchcock, P. B.; Love, J. B. *J. Organomet. Chem.* **1996**, *506*, 343.
- (9) Cloke, F. G. N.; Hitchcock, P. B.; Love, J. B. *J. Chem. Soc., Dalton Trans.* **1995**, 25.
- (10) Scollard, J. D.; McConville, D. H. *J. Am. Chem. Soc.* **1996**, *118*, 10008.
- (11) Scollard, J. D.; McConville, D. H.; Vittal, J. J. *Organometallics* **1997**, *16*, 4415.
- (12) Horton, A. D.; de With, J. *Organometallics* **1997**, *16*, 5424.
- (13) Horton, A. D.; de With, J.; van der Linden, A. J.; van de Weg, H. *Organometallics* **1996**, *15*, 2672.
- (14) Deelman, B.-J.; Hitchcock, P. B.; Lappert, M. F.; Lee, H.-K.; Leung, W.-P. *J. Organomet. Chem.* **1996**, *513*, 281.
- (15) Duan, Z.; Naiini, A. A.; Lee, J.-H.; Verkade, J. G. *Inorg. Chem.* **1995**, *34*, 5477.
- (16) Freundlich, J. S.; Schrock, R. R.; Davis, W. M. *J. Am. Chem. Soc.* **1996**, *118*, 3643.
- (17) Findeis, B.; Schubart, M.; Gade, L. H.; Möller, F.; Scowen, I.; McPartlin, M. *J. Chem. Soc., Dalton Trans.* **1996**, 125.
- (18) Nomura, K.; Naga, N.; Takaoki, K.; Imai, A. *J. Mol. Catalysis A: Chemical* **1998**, *130*, L209.

- (19) Brintzinger, H. H.; Fischer, D.; Mulhaupt, R.; Rieger, B.; Waymouth, R. *Angew. Chem., Int. Ed. Engl.* **1995**, *34*, 1143.
- (20) Kaminsky, W. *Catalysis Today* **1994**, *20*, 257.
- (21) Möhring, P. C.; Coville, N. J. *J. Organomet. Chem.* **1994**, *479*, 1.
- (22) Marks, T. J. *Acc. Chem. Res.* **1992**, *25*, 57.
- (23) Schaverien, C. J. *Organometallics* **1994**, *13*, 69.
- (24) Horton, A. D.; de With, J. J. *Chem. Soc. Chem. Commun.* **1996**, 1375.
- (25) Deck, P. A.; Beswick, C. L.; Marks, T. J. *J. Am. Chem. Soc.* **1998**, *120*, 1772.
- (26) Gibson, V. C.; Kimberley, B. S.; White, A. J. P.; Williams, D. J.; Howard, P. J. *Chem. Soc. Chem. Commun.* **1998**, 313.
- (27) van der Linden, A.; Schaverien, C. J.; Meijboom, N.; Ganter, C.; Orpen, A. G. *J. Am. Chem. Soc.* **1995**, *117*, 3008.
- (28) Tilley, T. D. *Acc. Chem. Res.* **1993**, *26*, 22.
- (29) Woo, H.-G.; Tilley, T. D. *J. Am. Chem. Soc.* **1989**, *111*, 8043.
- (30) Woo, H.-G.; Walzer, J. F.; Tilley, T. D. *J. Am. Chem. Soc.* **1992**, *114*, 7047.
- (31) Forsyth, C. M.; Nolan, S. P.; Marks, T. J. *Organometallics* **1991**, *10*, 2543.
- (32) Aitken, C.; Harrod, J. F.; Samuel, E. *Journal of Organometallic Chemistry* **1985**, *279*, C11.
- (33) Fu, P.-F.; Brard, L.; Li, Y.; Marks, T. J. *J. Am. Chem. Soc.* **1995**, *117*, 7157.
- (34) Molander, G. A.; Julius, M. *J. Org. Chem.* **1992**, *57*, 6347.
- (35) Molander, G. A.; Dowdy, E. D.; Noll, B. C. *Organometallics* **1998**, *17*, 3754.
- (36) Koo, K.; Fu, P.-F.; Marks, T. J. *Macromolecules* **1999**, *32*, 981.
- (37) Marciniak, B.; Gulinski, J. *J. Organomet. Chem.* **1993**, *446*, 15.
- (38) Schumann, H.; Keitsch, M. R.; Demtschuk, J.; Molander, G. A. *J. Organomet. Chem.* **1999**, *582*, 70.
- (39) Gountchev, T. I.; Tilley, T. D., manuscript in preparation.

- (40) Berno, P.; Floriani, C.; Chiesi-Villa, A.; Rizzoli, C. *J. Chem. Soc. Dalton Trans.* **1991**, 3093.
- (41) Tinkler, S.; Deeth, R. J.; Duncalf, D. J.; McCamley, A. *J. Chem. Soc. Chem. Commun.* **1996**, 2623.
- (42) Sinnema, P.-J.; Liekelema, K.; Staal, O. K. B.; Hessen, B.; Teuben, J. H. *J. Mol. Catal. A: Chemical* **1998**, *128*, 143.
- (43) Pellecchia, C.; Immirzi, A.; Grassi, A.; Zambelli, A. *Organometallics* **1993**, *12*, 4473.
- (44) Bochmann, M.; Jaggar, A. J.; Nicholls, J. C. *Angew. Chem. Int. Ed. Engl.* **1990**, *29*, 780.
- (45) Yang, X.; Stern, C. L.; Marks, T. J. *J. Am. Chem. Soc.* **1994**, *116*, 10015.
- (46) Beswick, C. L.; Marks, T. J. *Organometallics* **1999**, *18*, 2410.
- (47) Pellecchia, C.; Grassi, A.; Immirzi, A. *J. Am. Chem. Soc.* **1993**, *115*, 1160.
- (48) Li, L.; Marks, T. J. *Organometallics* **1998**, *17*, 3996.
- (49) Scollard, J. D.; McConville, D. H.; Vittal, J. J.; Payne, N. C. *J. Mol. Catal. A: Chemical* **1998**, *128*, 201.
- (50) Brown, K. J.; Berry, M. S.; Murdoch, J. R. *J. Org. Chem.* **1985**, *50*, 4345.
- (51) Drost, C.; Hitchcock, P. B.; Lappert, M. F. *J. Chem. Soc., Dalton Trans.* **1996**, 3595.
- (52) Massey, A. G.; Park, A. J. *J. Organomet. Chem.* **1964**, *2*, 245.
- (53) Chien, J. C. W.; Tsai, W.; Rausch, M. D. *J. Am. Chem. Soc.* **1991**, *113*, 8570.

Appendix A

Kinetic and Crystallographic Data for Chapter 1

Table 1. Observed pseudo-first order rate constants for disappearance of **5** at different phenylsilane concentrations.

[PhSiH ₃] or [PhSiD ₃], mol/L	10 ⁵ × k _{obs} (H), s ⁻¹	10 ⁵ × k _{obs} (D), s ⁻¹
0.5052	2.750	-
0.6278	-	4.283
0.6683	3.530	-
0.7395	-	5.388
0.7951 ^a	4.674	-
0.8676	-	6.573
1.0000	5.485	-
1.1011	-	7.639
1.2230	-	8.818
1.2846	7.394	-
1.3454	-	10.176
1.4786	-	10.501
1.4830	8.056	-
1.5873	-	10.890
1.5880	8.901	-

a) Conducted in presence of 1 equiv of **9**.

Table 2. Observed pseudo-first order rate constants for disappearance of **5** at different concentrations of (CH₂)₃SiH₂.

[(CH ₂) ₃ SiH ₂], mol/L	10 ⁵ × k _{obs} , s ⁻¹
0.01058	12.23
0.02136	26.15
0.03217	39.04
0.04414	56.85
0.05399	64.58

Table 3. First order rate constants for decomposition of **9** and **9-d₃**, at different starting concentrations, using initial rates. (The data point in brackets was rejected as an outlier.)

[9] or [9-d₃], mol/L	$10^4 \times k_{\text{obs}}(\text{H}), \text{s}^{-1}$	$10^4 \times k_{\text{obs}}(\text{D}), \text{s}^{-1}$
0.00524	1.106	-
0.0168	1.087	-
0.0210	-	1.305
0.0214	-	1.296
0.0256	-	1.267
0.0262	1.107	-
0.0302	-	1.292
0.0359	1.073	-
0.0413	1.076	-
{0.0425}	-	{1.172}
0.0581	-	1.260
Average:	1.090(16)	1.284(19)

Table 4. First order rate constants for decomposition of **9**, at five different temperatures. Each value of k is an average of two measurements, except that at 60.6 °C, for which five measurements were available.

T, °C	k, s^{-1}
24.95	$9.81(55) \times 10^{-7}$
34.75	$4.47(28) \times 10^{-6}$
44.84	$1.657(49) \times 10^{-5}$
60.60	$1.090(16) \times 10^{-4}$
75.93	$6.73(29) \times 10^{-4}$

Table 5. Crystallographic data for compounds **4**, **6**·1/2Et₂O, and **7**.

Compound	4	6 ·1/2Et ₂ O	7
(a) Crystal Parameters:			
Formula	C ₂₇ H ₃₆ N ₂ ClSiTa	C ₃₉ H ₅₃ N ₃ O _{0.5} SiTa	C ₂₉ H ₄₂ N ₂ ISiTa
Formula weight	633.08	780.90	754.60
Color, habit	red prisms	yellow prisms	yellow feathers
Size (mm)	0.1 × 0.1 × 0.05	0.2 × 0.15 × 0.2	0.20 × 0.06 × 0.03
Crystal system	monoclinic	monoclinic	monoclinic
Space group	P2 ₁ /c (#14)	P2 ₁ /n (#14)	P2 ₁ /n (#14)
Reflections used for unit cell refinement	6427	5758	5209
a (Å)	8.4514(2)	11.1996(3)	9.7141(3)
b (Å)	35.9638(7)	19.8252(6)	18.5350(5)
c (Å)	8.8435(1)	16.7141(4)	17.0915(3)
α (°)	90	90	90
β (°)	103.489(1)	103.039(1)	102.968(1)
γ (°)	90	90	90
V (Å ³)	2613.78(8)	3615.4(2)	2998.9(1)
Z	4	4	4
D _{calc} (g·cm ⁻³)	1.609	1.435	1.671
F ₀₀₀	1264.00	1596.00	1480.00
μ(MoK _α) (cm ⁻¹)	43.64	31.01	47.49

(b) Data Collection:

Temp. (°C)	-93	-140	-112
Measuring time per frame (s)	30	30	20
Total reflection	10611	15068	12447
Unique reflections	3864	5865	4419
R_{int}	0.047	0.038	0.066
Empirical absorption correction:	0.04	0.1	0.2
μR , $T_{\text{min}} - T_{\text{max}}$	0.832 - 0.944	0.717 - 0.825	0.618 - 0.862
Secondary extinction coeff.	1.7×10^{-7}	1.9×10^{-7}	None

(c) Refinement:

Observations ($I > 3\sigma(I)$)	2919	4796	2402
Variables	290	400	307
Reflection / parameters ratio	10.07	11.99	7.82
$R = \sum F_o - F_c / \sum F_o $	0.032	0.031	0.041
$R_w = [(\sum \omega (F_o - F_c)^2 / \sum \omega F_o^2)]^{1/2}$	0.039	0.041	0.043
Goodness of fit ($[\sum w (F_o - F_c)^2 / (N_o - N_v)]^{1/2}$)	1.50	1.73	1.22
p-factor	0.031	0.030	0.030
Max and min peaks in final diff. map ($e^-/\text{\AA}^3$)	0.57 / -0.65	0.76 / -1.12	1.38 / -1.36

Table 5 (cont). Crystallographic data for compounds **9** and **12**.

Compound	9	12
(a) Crystal Parameters:		
Formula	C ₃₄ H ₄₇ N ₂ Si ₂ Ta	C ₃₆ H ₄₁ N ₂ Si ₂ TaCl ₂
Formula weight	720.88	809.79
Color, habit	colorless needles	yellow plates
Size (mm)	0.15 × 0.15 × 0.2	0.22 × 0.1 × 0.1
Crystal system	monoclinic	triclinic
Space group	P2 ₁ /c(#14)	P $\bar{1}$ (#2)
Reflections used for unit cell refinement	6170	6295
a (Å)	10.3865(3)	10.8920(2)
b (Å)	15.4846(5)	11.0713(2)
c (Å)	20.2605(6)	15.7408(1)
α (°)	90	70.675(1)
β (°)	99.563(1)	76.885(1)
γ (°)	90	76.588(1)
V (Å ³)	3213.2(2)	1718.89(4)
Z	4	2
D _{calc} (g·cm ⁻³)	1.490	1.564
F ₀₀₀	1464.00	812.00
μ (MoK α) (cm ⁻¹)	35.15	34.46

(b) Data Collection:

Temp. (°C)	-146	-110
Measuring time per frame (s)	30	30
Total reflection	15451	7320
Unique reflections	5895	4855
R_{int}	0.026	0.032
Empirical absorption correction:	0.3	None
$\mu R, T_{min} - T_{max}$	0.417 - 0.478	
Secondary extinction coeff.	6.3×10^{-8}	None

(c) Refinement:

Observations ($I > 3\sigma(I)$)	4934	4528
Variables	356	396
Reflection / parameters ratio	13.86	11.43
$R = \sum F_o - F_c / \sum F_o $	0.019	0.024
$R_w = [(\sum \omega (F_o - F_c)^2) / \sum \omega F_o^2]^{1/2}$	0.030	0.033
Goodness of fit ($[\sum w (F_o - F_c)^2 / (N_o - N_v)]^{1/2}$)	1.29	1.37
p-factor	0.030	0.030
Max and min peaks in final diff. map ($e^- / \text{\AA}^3$)	0.77 / -0.52	1.20 / -0.62

Structural data for Cp*Ta[=N(C₆H₃Me)₂NSiMe₃]Cl (**4**)**Table 6.** Atomic coordinates and B_{iso}/B_{eq} for Cp*Ta[=N(C₆H₃Me)₂NSiMe₃]Cl (**4**).

atom	x	y	z	B _{eq}
Ta(1)	0.34738(4)	0.085581(8)	0.73296(3)	1.841(8)
Cl(1)	0.5848(2)	0.05118(6)	0.7409(2)	2.81(5)
Si(1)	0.4270(3)	0.13497(6)	0.4313(2)	2.14(5)
N(1)	0.3913(8)	0.1082(2)	0.9235(6)	2.3(1)
N(2)	0.3501(7)	0.1303(2)	0.6012(6)	1.9(1)
C(1)	0.5280(9)	0.1320(2)	0.9570(8)	2.0(2)
C(2)	0.673(1)	0.1203(2)	1.0593(8)	2.8(2)
C(3)	0.8082(10)	0.1428(3)	1.0903(9)	3.4(2)
C(4)	0.8052(9)	0.1767(2)	1.0196(9)	3.0(2)
C(5)	0.6654(9)	0.1896(2)	0.9195(9)	2.3(2)
C(6)	0.5236(8)	0.1677(2)	0.8904(7)	1.7(2)
C(7)	0.3642(8)	0.1814(2)	0.7968(8)	2.0(2)
C(8)	0.2847(9)	0.2123(2)	0.8499(9)	2.5(2)
C(9)	0.1354(9)	0.2238(2)	0.7646(9)	2.8(2)
C(10)	0.0638(9)	0.2078(2)	0.6250(10)	2.6(2)
C(11)	0.1373(9)	0.1779(2)	0.5720(9)	2.5(2)
C(12)	0.2854(8)	0.1637(2)	0.6560(8)	2.0(2)
C(13)	0.3589(10)	0.2312(2)	1.0012(9)	3.3(2)
C(14)	0.6693(10)	0.2261(2)	0.8389(9)	3.3(2)
C(15)	0.6098(10)	0.1650(2)	0.4778(9)	3.3(2)
C(16)	0.279(1)	0.1559(3)	0.2650(9)	3.5(2)
C(17)	0.479(1)	0.0882(2)	0.3726(9)	3.9(2)
C(18)	0.1479(9)	0.0504(2)	0.8463(8)	2.4(2)
C(19)	0.2172(9)	0.0236(2)	0.7667(8)	2.3(2)
C(20)	0.1767(9)	0.0327(2)	0.6061(8)	2.4(2)
C(21)	0.0823(8)	0.0652(2)	0.5844(8)	2.1(2)
C(22)	0.0674(9)	0.0773(2)	0.7357(9)	2.4(2)
C(23)	0.150(1)	0.0514(3)	1.0178(10)	4.5(3)
C(24)	0.308(1)	-0.0104(2)	0.837(1)	3.7(2)
C(25)	0.221(1)	0.0094(2)	0.4799(9)	3.6(2)
C(26)	0.000(1)	0.0826(2)	0.4325(10)	3.6(2)
C(27)	-0.030(1)	0.1095(2)	0.774(1)	3.6(2)
H(1)	0.6770	0.0966	1.1074	3.3448
H(2)	0.9044	0.1347	1.1613	4.0337
H(3)	0.9007	0.1916	1.0396	3.6209
H(4)	0.7552	0.2259	0.7861	3.9697
H(5)	0.6866	0.2456	0.9134	3.9697
H(6)	0.5686	0.2298	0.7659	3.9697
H(7)	0.4337	0.2147	1.0653	3.9060
H(8)	0.2757	0.2377	1.0522	3.9060
H(9)	0.4144	0.2530	0.9817	3.9060
H(10)	0.0805	0.2433	0.8035	3.3509
H(11)	-0.0362	0.2172	0.5649	3.1490
H(12)	0.0860	0.1667	0.4758	2.9543
H(13)	0.1812	0.1419	0.2445	4.2269
H(14)	0.3236	0.1557	0.1757	4.2269
H(15)	0.2572	0.1808	0.2895	4.2269
H(16)	0.5795	0.1893	0.5017	3.9642
H(17)	0.6578	0.1660	0.3909	3.9642
H(18)	0.6859	0.1551	0.5648	3.9642
H(19)	0.3939	0.0714	0.3772	4.6882
H(20)	0.4941	0.0891	0.2694	4.6882

H(21)	0.5772	0.0800	0.4410	4.6882
H(22)	0.1870	0.0750	1.0592	5.3772
H(23)	0.2208	0.0326	1.0705	5.3772
H(24)	0.0431	0.0471	1.0312	5.3772
H(25)	0.3453	-0.0072	0.9457	4.4774
H(26)	0.3990	-0.0143	0.7920	4.4774
H(27)	0.2383	-0.0314	0.8163	4.4774
H(28)	0.3338	0.0037	0.5080	4.3228
H(29)	0.1975	0.0229	0.3849	4.3228
H(30)	0.1596	-0.0129	0.4674	4.3228
H(31)	0.0747	0.0843	0.3676	4.3723
H(32)	-0.0903	0.0677	0.3831	4.3723
H(33)	-0.0369	0.1068	0.4506	4.3723
H(34)	-0.1299	0.1006	0.7918	4.3721
H(35)	-0.0516	0.1265	0.6891	4.3721
H(36)	0.0299	0.1217	0.8644	4.3721

$$B_{eq} = 8/3 \pi^2 (U_{11}(aa^*)^2 + U_{22}(bb^*)^2 + U_{33}(cc^*)^2 + 2U_{12}(aa^*bb^*)\cos\gamma + 2U_{13}(aa^*cc^*)\cos\beta + 2U_{23}(bb^*cc^*)\cos\alpha)$$

Table 7. Anisotropic Displacement Parameters for Cp*Ta[=N(C₆H₃Me)₂NSiMe₃]Cl (**4**).

atom	U ₁₁	U ₂₂	U ₃₃	U ₁₂	U ₁₃	U ₂₃
Ta(1)	0.0257(2)	0.0213(2)	0.0243(2)	-0.0022(1)	0.0065(1)	-0.0004(2)
Cl(1)	0.034(1)	0.033(1)	0.042(1)	0.0068(9)	0.0096(9)	-0.0028(9)
Si(1)	0.033(1)	0.027(1)	0.025(1)	-0.0025(9)	0.011(1)	0.0015(9)
N(1)	0.045(4)	0.022(4)	0.020(3)	-0.001(3)	0.006(3)	-0.002(3)
N(2)	0.025(3)	0.027(4)	0.017(3)	0.001(3)	0.005(3)	-0.005(3)
C(1)	0.036(5)	0.032(5)	0.014(4)	0.002(4)	0.012(3)	-0.006(3)
C(2)	0.044(5)	0.045(5)	0.020(4)	0.014(4)	0.010(4)	0.004(4)
C(3)	0.032(5)	0.068(7)	0.035(5)	0.006(5)	-0.003(4)	0.009(5)
C(4)	0.035(5)	0.047(6)	0.033(5)	-0.004(4)	0.013(4)	-0.003(4)
C(5)	0.027(4)	0.029(4)	0.034(5)	0.000(4)	0.003(4)	0.002(4)
C(6)	0.030(4)	0.018(4)	0.020(4)	0.001(3)	0.008(3)	-0.005(3)
C(7)	0.026(4)	0.025(4)	0.030(4)	-0.001(3)	0.014(3)	0.001(3)
C(8)	0.031(5)	0.028(5)	0.039(5)	-0.001(4)	0.013(4)	0.000(4)
C(9)	0.044(5)	0.017(4)	0.044(5)	0.004(4)	0.018(4)	-0.002(4)
C(10)	0.027(5)	0.022(4)	0.059(6)	0.006(4)	0.011(4)	0.008(4)
C(11)	0.026(4)	0.024(5)	0.039(5)	-0.002(3)	0.000(4)	0.008(4)
C(12)	0.025(4)	0.024(4)	0.027(4)	-0.001(3)	0.006(3)	0.004(3)
C(13)	0.054(6)	0.035(5)	0.038(5)	0.001(4)	0.021(4)	-0.003(4)
C(14)	0.053(5)	0.025(5)	0.040(5)	-0.007(4)	0.011(4)	0.000(4)
C(15)	0.047(6)	0.041(5)	0.050(6)	-0.009(4)	0.025(4)	-0.007(4)
C(16)	0.052(6)	0.068(7)	0.028(5)	0.000(5)	0.013(4)	0.014(4)
C(17)	0.080(7)	0.040(5)	0.038(5)	0.000(5)	0.029(5)	-0.003(4)
C(18)	0.044(5)	0.023(4)	0.028(4)	-0.017(4)	0.013(4)	-0.005(4)
C(19)	0.031(4)	0.023(4)	0.028(4)	-0.012(3)	0.002(3)	0.000(3)
C(20)	0.028(4)	0.035(5)	0.028(4)	-0.017(4)	0.003(3)	-0.007(4)
C(21)	0.024(4)	0.026(5)	0.030(4)	-0.005(3)	0.003(3)	0.001(4)
C(22)	0.019(4)	0.025(5)	0.052(5)	-0.002(3)	0.012(4)	0.001(4)
C(23)	0.093(8)	0.065(7)	0.029(5)	-0.030(6)	0.024(5)	-0.015(5)
C(24)	0.050(6)	0.031(5)	0.057(6)	-0.013(4)	-0.003(5)	0.009(5)

C(25)	0.060(6)	0.046(5)	0.037(5)	-0.024(5)	0.026(4)	-0.010(4)
C(26)	0.037(5)	0.046(6)	0.049(5)	-0.015(4)	-0.012(4)	0.007(5)
C(27)	0.038(5)	0.033(5)	0.082(7)	-0.001(4)	0.029(5)	-0.003(5)

Table 8. Bond Lengths (Å) for Cp*Ta[=N(C₆H₃Me)₂NSiMe₃]Cl (4).

atom	atom	distance	atom	atom	distance
Ta(1)	Cl(1)	2.344(2)	Ta(1)	N(1)	1.830(5)
Ta(1)	N(2)	1.988(6)	Ta(1)	C(18)	2.497(7)
Ta(1)	C(19)	2.534(7)	Ta(1)	C(20)	2.489(7)
Ta(1)	C(21)	2.431(7)	Ta(1)	C(22)	2.391(7)
Si(1)	N(2)	1.779(6)	Si(1)	C(15)	1.851(8)
Si(1)	C(16)	1.852(8)	Si(1)	C(17)	1.845(9)
N(1)	C(1)	1.414(9)	N(2)	C(12)	1.450(9)
C(1)	C(2)	1.406(10)	C(1)	C(6)	1.409(9)
C(2)	C(3)	1.38(1)	C(3)	C(4)	1.37(1)
C(4)	C(5)	1.38(1)	C(5)	C(6)	1.406(10)
C(5)	C(14)	1.50(1)	C(6)	C(7)	1.491(9)
C(7)	C(8)	1.433(10)	C(7)	C(12)	1.419(10)
C(8)	C(9)	1.374(10)	C(8)	C(13)	1.50(1)
C(9)	C(10)	1.37(1)	C(10)	C(11)	1.38(1)
C(11)	C(12)	1.395(9)	C(18)	C(19)	1.40(1)
C(18)	C(22)	1.43(1)	C(18)	C(23)	1.51(1)
C(19)	C(20)	1.420(9)	C(19)	C(24)	1.50(1)
C(20)	C(21)	1.40(1)	C(20)	C(25)	1.51(1)
C(21)	C(22)	1.440(10)	C(21)	C(26)	1.50(1)
C(22)	C(27)	1.50(1)			

Table 9. Bond Angles (°) for Cp*Ta[=N(C₆H₃Me)₂NSiMe₃]Cl (4).

atom	atom	atom	angle	atom	atom	atom	angle
Cl(1)	Ta(1)	N(1)	102.6(2)	Cl(1)	Ta(1)	N(2)	108.5(2)
Cl(1)	Ta(1)	C(18)	112.0(2)	Cl(1)	Ta(1)	C(19)	85.7(2)
Cl(1)	Ta(1)	C(20)	90.7(2)	Cl(1)	Ta(1)	C(21)	122.1(2)
Cl(1)	Ta(1)	C(22)	140.9(2)	N(1)	Ta(1)	N(2)	98.8(2)
N(1)	Ta(1)	C(18)	82.3(2)	N(1)	Ta(1)	C(19)	106.4(2)
N(1)	Ta(1)	C(20)	136.6(3)	N(1)	Ta(1)	C(21)	126.5(3)
N(1)	Ta(1)	C(22)	92.0(3)	N(2)	Ta(1)	C(18)	138.2(2)
N(2)	Ta(1)	C(19)	147.6(2)	N(2)	Ta(1)	C(20)	115.9(2)
N(2)	Ta(1)	C(21)	93.5(2)	N(2)	Ta(1)	C(22)	104.7(2)
C(18)	Ta(1)	C(19)	32.3(2)	C(18)	Ta(1)	C(20)	54.5(2)
C(18)	Ta(1)	C(21)	56.0(2)	C(18)	Ta(1)	C(22)	33.9(2)
C(19)	Ta(1)	C(20)	32.8(2)	C(19)	Ta(1)	C(21)	55.1(2)
C(19)	Ta(1)	C(22)	55.3(2)	C(20)	Ta(1)	C(21)	33.1(2)
C(20)	Ta(1)	C(22)	55.8(3)	C(21)	Ta(1)	C(22)	34.8(2)
N(2)	Si(1)	C(15)	108.5(3)	N(2)	Si(1)	C(16)	113.4(3)
N(2)	Si(1)	C(17)	108.0(3)	C(15)	Si(1)	C(16)	108.2(4)
C(15)	Si(1)	C(17)	110.6(4)	C(16)	Si(1)	C(17)	108.0(4)
Ta(1)	N(1)	C(1)	116.3(4)	Ta(1)	N(2)	Si(1)	128.9(3)

Ta(1)	N(2)	C(12)	114.6(4)	Si(1)	N(2)	C(12)	116.4(4)
N(1)	C(1)	C(2)	119.9(7)	N(1)	C(1)	C(6)	121.6(7)
C(2)	C(1)	C(6)	118.5(7)	C(1)	C(2)	C(3)	120.7(8)
C(2)	C(3)	C(4)	120.5(7)	C(3)	C(4)	C(5)	120.9(7)
C(4)	C(5)	C(6)	119.6(7)	C(4)	C(5)	C(14)	119.3(7)
C(6)	C(5)	C(14)	121.1(7)	C(1)	C(6)	C(5)	119.7(7)
C(1)	C(6)	C(7)	117.7(6)	C(5)	C(6)	C(7)	122.5(6)
C(6)	C(7)	C(8)	120.4(6)	C(6)	C(7)	C(12)	121.1(6)
C(8)	C(7)	C(12)	118.5(6)	C(7)	C(8)	C(9)	119.5(7)
C(7)	C(8)	C(13)	120.8(7)	C(9)	C(8)	C(13)	119.6(7)
C(8)	C(9)	C(10)	121.7(7)	C(9)	C(10)	C(11)	119.7(7)
C(10)	C(11)	C(12)	121.7(7)	N(2)	C(12)	C(7)	122.0(6)
N(2)	C(12)	C(11)	119.2(6)	C(7)	C(12)	C(11)	118.7(7)
Ta(1)	C(18)	C(19)	75.3(4)	Ta(1)	C(18)	C(22)	69.0(4)
Ta(1)	C(18)	C(23)	122.7(5)	C(19)	C(18)	C(22)	108.0(6)
C(19)	C(18)	C(23)	127.7(8)	C(22)	C(18)	C(23)	124.2(8)
Ta(1)	C(19)	C(18)	72.4(4)	Ta(1)	C(19)	C(20)	71.9(4)
Ta(1)	C(19)	C(24)	124.8(5)	C(18)	C(19)	C(20)	108.2(7)
C(18)	C(19)	C(24)	126.1(7)	C(20)	C(19)	C(24)	125.6(7)
Ta(1)	C(20)	C(19)	75.3(4)	Ta(1)	C(20)	C(21)	71.2(4)
Ta(1)	C(20)	C(25)	122.6(5)	C(19)	C(20)	C(21)	109.0(7)
C(19)	C(20)	C(25)	124.5(7)	C(21)	C(20)	C(25)	126.3(7)
Ta(1)	C(21)	C(20)	75.7(4)	Ta(1)	C(21)	C(22)	71.1(4)
Ta(1)	C(21)	C(26)	122.4(5)	C(20)	C(21)	C(22)	107.1(6)
C(20)	C(21)	C(26)	126.9(7)	C(22)	C(21)	C(26)	125.8(7)
Ta(1)	C(22)	C(18)	77.1(4)	Ta(1)	C(22)	C(21)	74.1(4)
Ta(1)	C(22)	C(27)	120.1(5)	C(18)	C(22)	C(21)	107.5(6)
C(18)	C(22)	C(27)	124.5(7)	C(21)	C(22)	C(27)	127.6(7)

Table 10. Least Squares Planes for Cp*Ta[=N(C₆H₃Me)₂NSiMe₃]Cl (4).

Atoms defining plane	Distance
C(18)	-0.014(7)
C(19)	0.005(7)
C(20)	0.006(7)
C(21)	-0.012(7)
C(22)	0.016(7)
Additional Atoms	Distance
Ta(1)	2.149
mean deviation	χ^2
0.0107	13.2

Structural data for

Cp*Ta[=N(C₆H₃Me)₂NSiMe₃][η^2 -(2,6-Me₂C₆H₃)N=CMe]·1/2Et₂O (6·1/2Et₂O)

Table 11. Atomic coordinates and $B_{\text{iso}}/B_{\text{eq}}$
for $\text{Cp}^*\text{Ta}[\text{=N}(\text{C}_6\text{H}_3\text{Me})_2\text{NSiMe}_3][\eta^2\text{-(2,6-Me}_2\text{C}_6\text{H}_3)\text{N=CMe}]\cdot 1/2\text{Et}_2\text{O}$ ($6\cdot 1/2\text{Et}_2\text{O}$).

atom	x	y	z	B_{eq}
Ta(1)	-0.32349(2)	-0.086525(9)	-0.266503(10)	1.841(6)
Si(1)	-0.3221(1)	-0.25207(7)	-0.18799(7)	2.19(3)
O(1)	-0.465(1)	-0.5141(7)	0.0112(9)	5.6(3)
N(1)	-0.1735(4)	-0.0663(2)	-0.2848(2)	2.26(9)
N(2)	-0.2876(4)	-0.1906(2)	-0.2530(2)	1.99(9)
N(3)	-0.3206(4)	-0.0804(2)	-0.1311(2)	1.83(9)
C(1)	-0.0564(5)	-0.0870(2)	-0.2485(3)	1.6(1)
C(2)	0.0292(5)	-0.0426(3)	-0.2017(3)	2.9(1)
C(3)	0.1390(5)	-0.0672(3)	-0.1546(3)	3.0(1)
C(4)	0.1651(4)	-0.1359(3)	-0.1544(3)	2.7(1)
C(5)	0.0847(5)	-0.1804(3)	-0.2039(3)	2.7(1)
C(6)	-0.0250(4)	-0.1564(3)	-0.2539(3)	2.4(1)
C(7)	-0.1053(5)	-0.1987(2)	-0.3181(3)	2.3(1)
C(8)	-0.2279(5)	-0.2158(2)	-0.3157(3)	2.1(1)
C(9)	-0.2953(5)	-0.2565(3)	-0.3792(3)	2.4(1)
C(10)	-0.2449(5)	-0.2796(3)	-0.4426(3)	2.7(1)
C(11)	-0.1289(5)	-0.2607(3)	-0.4465(3)	3.1(1)
C(12)	-0.0585(5)	-0.2201(3)	-0.3855(3)	2.9(1)
C(13)	0.0668(5)	-0.1956(3)	-0.3959(3)	3.6(1)
C(14)	0.1171(5)	-0.2548(3)	-0.2010(3)	3.6(1)
C(15)	-0.1888(6)	-0.2668(3)	-0.1001(3)	3.5(1)
C(16)	-0.3601(5)	-0.3366(3)	-0.2372(3)	2.9(1)
C(17)	-0.4603(6)	-0.2301(3)	-0.1489(3)	3.7(1)
C(18)	-0.2992(5)	-0.0941(2)	-0.0446(3)	2.3(1)
C(19)	-0.1795(5)	-0.1059(3)	0.0014(3)	2.6(1)
C(20)	-0.1618(5)	-0.1217(3)	0.0843(3)	3.1(1)
C(21)	-0.2612(6)	-0.1243(3)	0.1226(3)	3.1(1)
C(22)	-0.3772(6)	-0.1109(3)	0.0764(3)	3.0(1)
C(23)	-0.3997(5)	-0.0948(2)	-0.0065(3)	2.5(1)
C(24)	-0.5255(5)	-0.0768(3)	-0.0536(3)	3.3(1)
C(25)	-0.0711(5)	-0.1015(3)	-0.0383(3)	3.2(1)
C(26)	-0.3056(4)	-0.0230(2)	-0.1615(3)	2.0(1)
C(27)	-0.2659(5)	0.0405(3)	-0.1159(3)	2.7(1)
C(28)	-0.5183(5)	-0.1100(3)	-0.3715(3)	2.7(1)
C(29)	-0.4289(5)	-0.0821(3)	-0.4116(3)	2.5(1)
C(30)	-0.4075(4)	-0.0142(3)	-0.3850(3)	2.4(1)
C(31)	-0.4814(5)	-0.0006(3)	-0.3284(3)	2.4(1)
C(32)	-0.5498(4)	-0.0588(3)	-0.3208(3)	2.3(1)
C(33)	-0.5780(5)	-0.1779(3)	-0.3867(3)	3.2(1)
C(34)	-0.3755(5)	-0.1130(3)	-0.4773(3)	3.2(1)
C(35)	-0.3254(5)	0.0337(3)	-0.4162(3)	3.4(1)
C(36)	-0.4978(6)	0.0675(3)	-0.2915(4)	3.9(1)
C(37)	-0.6503(5)	-0.0650(4)	-0.2743(4)	3.9(1)
C(38)	-0.557(3)	-0.431(2)	-0.084(2)	9.1(8)
C(39)	-0.567(3)	-0.485(2)	-0.037(2)	11(1)
C(40)	-0.480(3)	-0.554(1)	0.085(2)	7.9(7)
C(41)	-0.368(2)	-0.5877(9)	0.116(1)	6.7(4)
H(1)	0.0122	0.0043	-0.2022	3.4273
H(2)	0.1964	-0.0371	-0.1224	3.6413
H(3)	0.2386	-0.1526	-0.1202	3.2606
H(4)	-0.3773	-0.2684	-0.3786	2.9335
H(5)	-0.2909	-0.3087	-0.4834	3.2968
H(6)	-0.0959	-0.2753	-0.4911	3.7324

H(7)	0.0566	-0.1695	-0.4446	4.3408
H(8)	0.1174	-0.2335	-0.3996	4.3408
H(9)	0.1042	-0.1689	-0.3499	4.3408
H(10)	0.0539	-0.2790	-0.2369	4.2679
H(11)	0.1257	-0.2711	-0.1465	4.2679
H(12)	0.1921	-0.2607	-0.2177	4.2679
H(13)	-0.1695	-0.2262	-0.0697	4.2169
H(14)	-0.1200	-0.2808	-0.1203	4.2169
H(15)	-0.2090	-0.3009	-0.0654	4.2169
H(16)	-0.2931	-0.3521	-0.2584	3.5368
H(17)	-0.3755	-0.3678	-0.1975	3.5368
H(18)	-0.4308	-0.3329	-0.2807	3.5368
H(19)	-0.4484	-0.1875	-0.1222	4.4382
H(20)	-0.4731	-0.2636	-0.1110	4.4382
H(21)	-0.5298	-0.2280	-0.1935	4.4382
H(22)	-0.0814	-0.1309	0.1154	3.7687
H(23)	-0.2488	-0.1351	0.1792	3.6868
H(24)	-0.4444	-0.1128	0.1023	3.5664
H(25)	-0.5529	-0.0376	-0.0303	3.9614
H(26)	-0.5798	-0.1131	-0.0512	3.9614
H(27)	-0.5237	-0.0681	-0.1092	3.9614
H(28)	-0.0295	-0.1436	-0.0328	3.8537
H(29)	-0.0168	-0.0673	-0.0121	3.8537
H(30)	-0.0990	-0.0909	-0.0949	3.8537
H(31)	-0.1867	0.0345	-0.0815	3.2026
H(32)	-0.3224	0.0518	-0.0833	3.2026
H(33)	-0.2634	0.0759	-0.1539	3.2026
H(34)	-0.6629	-0.1724	-0.4102	3.8922
H(35)	-0.5411	-0.2027	-0.4234	3.8922
H(36)	-0.5676	-0.2017	-0.3363	3.8922
H(37)	-0.4021	-0.0885	-0.5269	3.8291
H(38)	-0.4018	-0.1585	-0.4855	3.8291
H(39)	-0.2886	-0.1116	-0.4611	3.8291
H(40)	-0.3254	0.0760	-0.3896	4.0448
H(41)	-0.3543	0.0394	-0.4738	4.0448
H(42)	-0.2445	0.0161	-0.4051	4.0448
H(43)	-0.4839	0.0634	-0.2335	4.6372
H(44)	-0.4410	0.0986	-0.3051	4.6372
H(45)	-0.5789	0.0832	-0.3128	4.6372
H(46)	-0.6542	-0.0248	-0.2442	4.7009
H(47)	-0.6333	-0.1021	-0.2375	4.7009
H(48)	-0.7265	-0.0721	-0.3120	4.7009

Table 12. Anisotropic Displacement Parameters for Cp*Ta[=N(C₆H₃Me)₂NSiMe₃][η²-(2,6-Me₂C₆H₃)N=CMe]·1/2Et₂O (6·1/2Et₂O).

atom	U ₁₁	U ₂₂	U ₃₃	U ₁₂	U ₁₃	U ₂₃
Ta(1)	0.0244(2)	0.0247(1)	0.0189(1)	0.00041(8)	0.00432(9)	0.00046(8)
Si(1)	0.0352(8)	0.0239(7)	0.0239(7)	-0.0014(6)	0.0069(6)	0.0000(5)
N(1)	0.036(3)	0.021(2)	0.029(2)	0.000(2)	0.010(2)	0.003(2)
N(2)	0.028(2)	0.029(2)	0.024(2)	-0.004(2)	0.008(2)	-0.005(2)
N(3)	0.028(2)	0.023(2)	0.025(2)	0.003(2)	0.012(2)	0.001(2)
C(1)	0.030(3)	0.026(3)	0.023(2)	-0.001(2)	0.014(2)	0.003(2)

C(2)	0.032(3)	0.035(3)	0.031(3)	-0.007(2)	0.014(2)	0.000(2)
C(3)	0.032(3)	0.051(3)	0.034(3)	-0.016(3)	0.011(2)	-0.007(3)
C(4)	0.019(3)	0.048(3)	0.032(3)	-0.002(2)	0.005(2)	0.003(2)
C(5)	0.025(3)	0.038(3)	0.032(3)	0.001(2)	0.011(2)	0.005(2)
C(6)	0.029(3)	0.030(3)	0.029(3)	-0.004(2)	0.014(2)	-0.002(2)
C(7)	0.032(3)	0.024(3)	0.030(3)	0.006(2)	0.010(2)	-0.004(2)
C(8)	0.032(3)	0.023(3)	0.024(2)	0.002(2)	0.010(2)	-0.003(2)
C(9)	0.034(3)	0.032(3)	0.025(2)	-0.002(2)	0.005(2)	0.001(2)
C(10)	0.041(3)	0.035(3)	0.028(3)	-0.002(2)	0.009(2)	-0.005(2)
C(11)	0.046(3)	0.037(3)	0.032(3)	0.000(3)	0.015(2)	-0.006(2)
C(12)	0.030(3)	0.031(3)	0.036(3)	0.002(2)	0.008(2)	0.002(2)
C(13)	0.040(3)	0.066(4)	0.042(3)	-0.016(3)	0.023(3)	-0.017(3)
C(14)	0.038(3)	0.040(3)	0.055(3)	0.007(3)	0.012(3)	0.007(3)
C(15)	0.060(4)	0.034(3)	0.032(3)	-0.007(3)	-0.011(3)	0.004(2)
C(16)	0.047(3)	0.030(3)	0.034(3)	-0.004(3)	0.007(3)	-0.006(2)
C(17)	0.062(4)	0.036(3)	0.051(3)	-0.012(3)	0.027(3)	-0.001(3)
C(18)	0.034(3)	0.021(3)	0.022(2)	-0.001(2)	0.006(2)	-0.002(2)
C(19)	0.032(3)	0.026(3)	0.031(3)	-0.001(2)	0.006(2)	0.001(2)
C(20)	0.037(3)	0.043(3)	0.028(3)	0.001(3)	-0.004(2)	0.004(2)
C(21)	0.053(4)	0.039(3)	0.025(3)	-0.001(3)	0.005(3)	0.005(2)
C(22)	0.050(4)	0.036(3)	0.034(3)	0.000(3)	0.021(3)	-0.003(2)
C(23)	0.032(3)	0.028(3)	0.031(3)	-0.002(2)	0.009(2)	-0.006(2)
C(24)	0.033(3)	0.045(3)	0.042(3)	0.001(3)	0.010(3)	-0.007(3)
C(25)	0.034(3)	0.047(3)	0.039(3)	0.004(3)	0.013(3)	-0.006(3)
C(26)	0.022(3)	0.028(3)	0.030(3)	0.005(2)	0.005(2)	-0.001(2)
C(27)	0.049(3)	0.032(3)	0.028(3)	-0.002(3)	0.011(2)	-0.001(2)
C(28)	0.026(3)	0.038(3)	0.024(2)	0.003(2)	-0.004(2)	0.002(2)
C(29)	0.034(3)	0.037(3)	0.016(2)	0.008(2)	-0.003(2)	0.005(2)
C(30)	0.027(3)	0.033(3)	0.023(2)	0.007(2)	0.000(2)	0.009(2)
C(31)	0.031(3)	0.033(3)	0.025(2)	0.009(2)	0.000(2)	0.000(2)
C(32)	0.022(3)	0.046(3)	0.019(2)	0.011(3)	-0.003(2)	0.004(2)
C(33)	0.031(3)	0.049(3)	0.037(3)	-0.009(3)	-0.003(2)	0.000(3)
C(34)	0.047(3)	0.048(3)	0.022(3)	0.002(3)	0.010(2)	0.000(2)
C(35)	0.047(4)	0.039(3)	0.040(3)	0.000(3)	0.007(3)	0.012(2)
C(36)	0.051(4)	0.043(3)	0.041(3)	0.017(3)	0.001(3)	-0.004(3)
C(37)	0.037(3)	0.070(4)	0.046(3)	0.016(3)	0.015(3)	0.008(3)

The general temperature factor expression:

$$\exp(-2\pi^2(a^2U_{11}h^2 + b^2U_{22}k^2 + c^2U_{33}l^2 + 2a*b*U_{12}hk + 2a*c*U_{13}hl + 2b*c*U_{23}kl))$$

Table 13. Bond Lengths (Å)

for Cp*Ta[=N(C₆H₃Me)₂NSiMe₃][η²-(2,6-Me₂C₆H₃)N=CMe]·1/2Et₂O (6·1/2Et₂O).

atom	atom	distance	atom	atom	distance
Ta(1)	N(1)	1.819(4)	Ta(1)	N(2)	2.105(4)
Ta(1)	N(3)	2.259(4)	Ta(1)	C(26)	2.134(5)
Ta(1)	C(28)	2.516(5)	Ta(1)	C(29)	2.447(4)
Ta(1)	C(30)	2.453(4)	Ta(1)	C(31)	2.504(5)
Ta(1)	C(32)	2.552(5)	Si(1)	N(2)	1.733(4)
Si(1)	C(15)	1.866(5)	Si(1)	C(16)	1.874(5)
Si(1)	C(17)	1.863(6)	O(1)	O(1)	0.97(2)
O(1)	C(38)	1.60(4)	O(1)	C(39)	1.37(3)
O(1)	C(39)	0.50(4)	O(1)	C(40)	1.51(3)

N(1)	C(1)	1.377(7)	N(2)	C(8)	1.452(6)
N(3)	C(18)	1.437(6)	N(3)	C(26)	1.273(6)
C(1)	C(2)	1.402(7)	C(1)	C(6)	1.429(7)
C(2)	C(3)	1.390(8)	C(3)	C(4)	1.393(8)
C(4)	C(5)	1.391(7)	C(5)	C(6)	1.404(7)
C(5)	C(14)	1.517(8)	C(6)	C(7)	1.492(7)
C(7)	C(8)	1.424(7)	C(7)	C(12)	1.410(7)
C(8)	C(9)	1.411(7)	C(9)	C(10)	1.387(7)
C(10)	C(11)	1.367(7)	C(11)	C(12)	1.395(7)
C(12)	C(13)	1.531(7)	C(18)	C(19)	1.406(7)
C(18)	C(23)	1.413(7)	C(19)	C(20)	1.391(7)
C(19)	C(25)	1.510(7)	C(20)	C(21)	1.406(8)
C(21)	C(22)	1.379(8)	C(22)	C(23)	1.388(7)
C(23)	C(24)	1.493(7)	C(26)	C(27)	1.487(7)
C(28)	C(29)	1.435(7)	C(28)	C(32)	1.416(7)
C(28)	C(33)	1.500(8)	C(29)	C(30)	1.421(7)
C(29)	C(34)	1.495(7)	C(30)	C(31)	1.417(7)
C(30)	C(35)	1.495(7)	C(31)	C(32)	1.407(7)
C(31)	C(36)	1.512(8)	C(32)	C(37)	1.510(7)
C(38)	C(39)	1.33(5)	C(38)	C(40)	0.51(5)
C(38)	C(41)	0.97(3)	C(39)	C(39)	1.82(6)
C(39)	C(40)	1.30(5)	C(40)	C(41)	1.41(4)

Table 14. Bond Angles (°) for Cp*Ta[=N(C₆H₃Me)₂NSiMe₃][η²-(2,6-Me₂C₆H₃)N=CMe]·1/2Et₂O (6·1/2Et₂O).

atom	atom	atom	angle	atom	atom	atom	angle
N(1)	Ta(1)	N(2)	94.2(2)	C(28)	Ta(1)	C(29)	33.6(2)
N(1)	Ta(1)	N(3)	110.6(2)	C(28)	Ta(1)	C(30)	55.3(2)
N(1)	Ta(1)	C(26)	95.1(2)	N(1)	Ta(1)	N(2)	94.2(2)
C(28)	Ta(1)	C(29)	33.6(2)	N(1)	Ta(1)	N(3)	110.6(2)
C(28)	Ta(1)	C(30)	55.3(2)	N(1)	Ta(1)	C(26)	95.1(2)
C(28)	Ta(1)	C(31)	54.4(2)	N(1)	Ta(1)	C(28)	127.8(2)
C(28)	Ta(1)	C(32)	32.4(2)	N(1)	Ta(1)	C(29)	94.8(2)
C(29)	Ta(1)	C(30)	33.7(2)	N(1)	Ta(1)	C(30)	86.4(2)
C(29)	Ta(1)	C(31)	55.2(2)	N(1)	Ta(1)	C(31)	112.0(2)
C(29)	Ta(1)	C(32)	54.6(2)	N(1)	Ta(1)	C(32)	140.7(2)
C(30)	Ta(1)	C(31)	33.2(2)	N(2)	Ta(1)	N(3)	89.2(1)
C(30)	Ta(1)	C(32)	54.4(2)	N(2)	Ta(1)	C(26)	120.7(2)
C(31)	Ta(1)	C(32)	32.3(2)	N(2)	Ta(1)	C(28)	90.5(2)
N(2)	Si(1)	C(15)	110.6(2)	N(2)	Ta(1)	C(29)	100.3(2)
N(2)	Si(1)	C(16)	114.5(2)	N(2)	Ta(1)	C(30)	133.5(2)
N(2)	Si(1)	C(17)	112.1(2)	N(2)	Ta(1)	C(31)	144.2(2)
C(15)	Si(1)	C(16)	105.6(3)	N(2)	Ta(1)	C(32)	113.6(2)
C(15)	Si(1)	C(17)	109.9(3)	N(3)	Ta(1)	C(26)	33.5(2)
C(16)	Si(1)	C(17)	103.8(3)	N(3)	Ta(1)	C(28)	121.5(2)
O(1)	O(1)	C(38)	131(2)	N(3)	Ta(1)	C(29)	152.3(2)
O(1)	O(1)	C(39)	15(2)	N(3)	Ta(1)	C(30)	133.9(2)
O(1)	O(1)	C(39)	136(7)	N(3)	Ta(1)	C(31)	103.1(1)
O(1)	O(1)	C(40)	113(2)	N(3)	Ta(1)	C(32)	97.7(1)
C(38)	O(1)	C(39)	134(2)	C(26)	Ta(1)	C(28)	126.1(2)
C(38)	O(1)	C(39)	50(6)	C(26)	Ta(1)	C(29)	136.8(2)
C(38)	O(1)	C(40)	19(2)	C(26)	Ta(1)	C(30)	105.5(2)

C(39)	O(1)	C(39)	151(5)	C(26)	Ta(1)	C(31)	82.2(2)
C(39)	O(1)	C(40)	118(2)	C(26)	Ta(1)	C(32)	93.9(2)
C(39)	O(1)	C(40)	57(6)	Ta(1)	N(1)	C(1)	133.2(3)
C(9)	C(10)	C(11)	120.0(5)	Ta(1)	N(2)	Si(1)	133.8(2)
C(10)	C(11)	C(12)	120.7(5)	Ta(1)	N(2)	C(8)	111.6(3)
C(7)	C(12)	C(11)	120.5(5)	Si(1)	N(2)	C(8)	114.5(3)
C(7)	C(12)	C(13)	120.7(4)	Ta(1)	N(3)	C(18)	163.6(3)
C(11)	C(12)	C(13)	118.8(4)	Ta(1)	N(3)	C(26)	67.8(3)
N(3)	C(18)	C(19)	120.2(4)	C(18)	N(3)	C(26)	124.2(4)
N(3)	C(18)	C(23)	119.1(4)	N(1)	C(1)	C(2)	121.5(4)
C(19)	C(18)	C(23)	120.7(4)	N(1)	C(1)	C(6)	118.9(4)
C(18)	C(19)	C(20)	119.1(5)	C(2)	C(1)	C(6)	119.5(5)
C(18)	C(19)	C(25)	120.8(4)	C(1)	C(2)	C(3)	120.2(5)
C(20)	C(19)	C(25)	120.1(5)	C(2)	C(3)	C(4)	120.2(5)
C(19)	C(20)	C(21)	120.8(5)	C(3)	C(4)	C(5)	120.7(5)
C(20)	C(21)	C(22)	118.8(5)	C(4)	C(5)	C(6)	120.1(5)
C(21)	C(22)	C(23)	122.6(5)	C(4)	C(5)	C(14)	118.6(5)
C(18)	C(23)	C(22)	117.9(5)	C(6)	C(5)	C(14)	121.3(5)
C(18)	C(23)	C(24)	120.8(5)	C(1)	C(6)	C(5)	118.9(5)
C(22)	C(23)	C(24)	121.2(5)	C(1)	C(6)	C(7)	118.0(4)
Ta(1)	C(26)	N(3)	78.6(3)	C(5)	C(6)	C(7)	122.9(5)
Ta(1)	C(26)	C(27)	152.1(4)	C(6)	C(7)	C(8)	122.8(4)
N(3)	C(26)	C(27)	127.2(4)	C(6)	C(7)	C(12)	118.1(5)
Ta(1)	C(28)	C(29)	70.6(3)	C(8)	C(7)	C(12)	119.0(4)
Ta(1)	C(28)	C(32)	75.2(3)	N(2)	C(8)	C(7)	122.9(4)
Ta(1)	C(28)	C(33)	124.6(3)	N(2)	C(8)	C(9)	119.0(4)
C(29)	C(28)	C(32)	107.3(5)	C(7)	C(8)	C(9)	118.1(4)
C(29)	C(28)	C(33)	126.7(5)	C(8)	C(9)	C(10)	121.6(5)
C(32)	C(28)	C(33)	125.7(5)	Ta(1)	C(29)	C(28)	75.8(3)
O(1)	C(38)	C(41)	131(4)	Ta(1)	C(29)	C(30)	73.4(3)
C(39)	C(38)	C(40)	75(6)	Ta(1)	C(29)	C(34)	122.0(4)
C(39)	C(38)	C(41)	118(4)	C(28)	C(29)	C(30)	107.7(4)
C(40)	C(38)	C(41)	144(8)	C(28)	C(29)	C(34)	128.5(5)
O(1)	C(39)	O(1)	29(5)	C(30)	C(29)	C(34)	123.4(5)
O(1)	C(39)	C(38)	121(3)	Ta(1)	C(30)	C(29)	72.9(3)
O(1)	C(39)	C(39)	8(1)	Ta(1)	C(30)	C(31)	75.4(3)
O(1)	C(39)	C(40)	103(3)	Ta(1)	C(30)	C(35)	119.9(3)
O(1)	C(39)	C(38)	114(7)	C(29)	C(30)	C(31)	107.9(5)
O(1)	C(39)	C(39)	22(3)	C(29)	C(30)	C(35)	124.5(5)
O(1)	C(39)	C(40)	105(6)	C(31)	C(30)	C(35)	127.5(5)
C(38)	C(39)	C(39)	120(4)	Ta(1)	C(31)	C(30)	71.4(3)
C(38)	C(39)	C(40)	22(2)	Ta(1)	C(31)	C(32)	75.7(3)
C(39)	C(39)	C(40)	103(3)	Ta(1)	C(31)	C(36)	125.4(3)
O(1)	C(40)	C(38)	91(7)	C(30)	C(31)	C(32)	108.3(4)
O(1)	C(40)	C(39)	19(2)	C(30)	C(31)	C(36)	125.9(5)
O(1)	C(40)	C(41)	107(2)	C(32)	C(31)	C(36)	125.3(5)
C(38)	C(40)	C(39)	82(6)	Ta(1)	C(32)	C(28)	72.4(3)
C(38)	C(40)	C(41)	24(6)	Ta(1)	C(32)	C(31)	72.0(3)
C(39)	C(40)	C(41)	93(2)	Ta(1)	C(32)	C(37)	126.5(3)
C(38)	C(41)	C(40)	12(3)	C(28)	C(32)	C(31)	108.7(4)
C(28)	C(32)	C(37)	124.4(5)	C(31)	C(32)	C(37)	126.6(5)
O(1)	C(38)	C(39)	17(2)	O(1)	C(38)	C(40)	70(6)

Table 15. Least Squares Planes

for Cp*Ta[=N(C₆H₃Me)₂NSiMe₃][η^2 -(2,6-Me₂C₆H₃)N=CMe]·1/2Et₂O (6·1/2Et₂O).

Atoms defining plane	Distance
C(28)	0.001(5)
C(29)	0.003(5)
C(30)	-0.005(4)
C(31)	0.007(5)
C(32)	-0.003(4)
Additional Atoms	Distance
Ta(1)	2.181
mean deviation	χ^2
0.0039	4.4

Structural data for {Cp*Ta[MeN(C₆H₃Me)₂NSiMe₃]Me}⁺I⁻ (7)

Table 16. Atomic coordinates and B_{iso}/B_{eq} for {Cp*Ta[MeN(C₆H₃Me)₂NSiMe₃]Me}⁺I⁻ (7).

atom	x	y	z	B _{eq}
Ta(1)	0.20367(6)	0.30595(3)	0.58759(4)	2.30(1)
I(1)	0.5972(1)	0.50481(5)	0.68849(6)	3.13(2)
Si(1)	0.0892(5)	0.1383(3)	0.6365(3)	4.3(1)
N(1)	0.376(1)	0.3171(5)	0.5514(6)	2.5(3)
N(2)	0.163(1)	0.2006(6)	0.5779(6)	2.6(3)
C(1)	0.468(1)	0.2640(7)	0.6012(7)	2.0(3)
C(2)	0.567(1)	0.2880(7)	0.6680(8)	2.5(3)
C(3)	0.657(1)	0.2379(8)	0.7123(9)	3.3(4)
C(4)	0.645(2)	0.1645(8)	0.6936(8)	2.9(4)
C(5)	0.550(2)	0.1412(7)	0.6267(9)	3.0(4)
C(6)	0.456(1)	0.1897(7)	0.5775(8)	2.4(3)
C(7)	0.350(1)	0.1673(7)	0.5072(8)	2.5(3)
C(8)	0.204(2)	0.1694(6)	0.5099(8)	2.4(3)
C(9)	0.104(1)	0.1425(8)	0.4457(9)	3.0(4)
C(10)	0.140(2)	0.1156(8)	0.3780(9)	3.3(4)
C(11)	0.281(2)	0.1163(8)	0.3745(8)	3.1(4)
C(12)	0.386(2)	0.1430(7)	0.4366(9)	2.8(4)
C(13)	0.539(2)	0.1444(8)	0.4269(9)	4.0(4)
C(14)	0.547(2)	0.0615(8)	0.607(1)	4.6(5)
C(15)	0.448(1)	0.3526(8)	0.4964(9)	2.7(4)
C(16)	0.089(2)	0.180(1)	0.736(1)	6.6(6)
C(17)	-0.092(2)	0.108(1)	0.588(1)	5.7(6)
C(18)	0.204(2)	0.056(1)	0.649(1)	7.4(7)
C(19)	0.272(1)	0.3279(8)	0.7132(9)	2.8(4)
C(20)	0.143(1)	0.4291(7)	0.5273(9)	2.5(4)
C(21)	0.085(2)	0.4228(9)	0.5948(9)	3.5(4)
C(22)	-0.013(1)	0.3676(9)	0.584(1)	3.3(4)
C(23)	-0.022(1)	0.3379(7)	0.5076(10)	2.7(4)

C(24)	0.080(1)	0.3728(7)	0.4725(8)	2.3(3)
C(25)	0.101(2)	0.3583(8)	0.3900(9)	3.6(4)
C(26)	0.242(2)	0.4871(7)	0.5132(9)	3.4(4)
C(27)	0.118(2)	0.475(1)	0.665(1)	5.7(6)
C(28)	-0.111(2)	0.349(1)	0.639(1)	6.0(6)
C(29)	-0.129(2)	0.2846(10)	0.467(1)	5.3(5)
H(1)	0.573	0.338	0.683	3.014
H(2)	0.729	0.254	0.756	3.981
H(3)	0.703	0.130	0.727	3.484
H(4)	0.007	0.143	0.448	3.576
H(5)	0.070	0.097	0.335	3.913
H(6)	0.307	0.098	0.328	3.753
H(7)	0.548	0.113	0.384	4.827
H(8)	0.600	0.128	0.475	4.827
H(9)	0.563	0.192	0.415	4.827
H(10)	0.506	0.036	0.644	5.542
H(11)	0.492	0.054	0.554	5.542
H(12)	0.641	0.045	0.610	5.542
H(13)	0.465	0.319	0.458	3.195
H(14)	0.535	0.372	0.526	3.195
H(15)	0.391	0.391	0.470	3.195
H(16)	0.021	0.156	0.759	7.861
H(17)	0.066	0.229	0.729	7.861
H(18)	0.180	0.175	0.770	7.861
H(19)	-0.159	0.137	0.607	6.835
H(20)	-0.106	0.114	0.531	6.835
H(21)	-0.103	0.059	0.600	6.835
H(22)	0.197	0.032	0.697	8.929
H(23)	0.174	0.025	0.604	8.929
H(24)	0.299	0.070	0.653	8.929
H(25)	0.356	0.356	0.723	3.403
H(26)	0.290	0.284	0.742	3.403
H(27)	0.200	0.354	0.731	3.403
H(28)	0.017	0.370	0.352	4.261
H(29)	0.124	0.309	0.386	4.261
H(30)	0.177	0.387	0.381	4.261
H(31)	0.258	0.482	0.461	4.120
H(32)	0.329	0.483	0.551	4.120
H(33)	0.201	0.533	0.519	4.120
H(34)	0.207	0.497	0.667	6.894
H(35)	0.121	0.450	0.713	6.894
H(36)	0.046	0.511	0.658	6.894
H(37)	-0.167	0.390	0.645	7.244
H(38)	-0.056	0.335	0.690	7.244
H(39)	-0.171	0.310	0.617	7.244
H(40)	-0.206	0.309	0.433	6.332
H(41)	-0.163	0.258	0.506	6.332
H(42)	-0.088	0.253	0.435	6.332

$$B_{eq} = 8/3 \pi^2 (U_{11}(aa^*)^2 + U_{22}(bb^*)^2 + U_{33}(cc^*)^2 + 2U_{12}(aa^*bb^*)\cos\gamma + 2U_{13}(aa^*cc^*)\cos\beta + 2U_{23}(bb^*cc^*)\cos\alpha)$$

Table 17. Anisotropic Displacement Parameters for {Cp*Ta[MeN(C₆H₃Me)₂NSiMe₃]Me}⁺I⁻ (7).

atom	U ₁₁	U ₂₂	U ₃₃	U ₁₂	U ₁₃	U ₂₃
Ta(1)	0.0314(3)	0.0227(3)	0.0362(3)	0.0045(3)	0.0071(2)	0.0058(4)
I(1)	0.0529(7)	0.0282(6)	0.0393(6)	-0.0073(5)	0.0035(5)	0.0035(5)
Si(1)	0.059(3)	0.048(3)	0.056(3)	-0.009(3)	0.011(3)	0.005(2)
N(1)	0.045(7)	0.008(6)	0.043(7)	0.001(5)	0.007(6)	0.009(6)
N(2)	0.047(7)	0.020(6)	0.024(6)	-0.005(6)	0.007(6)	0.003(6)
C(1)	0.043(9)	0.028(9)	0.012(7)	0.013(7)	0.011(7)	0.016(6)
C(2)	0.040(9)	0.012(8)	0.046(9)	0.012(7)	0.018(8)	0.002(7)
C(3)	0.026(9)	0.04(1)	0.06(1)	-0.009(8)	-0.006(8)	-0.019(9)
C(4)	0.06(1)	0.025(9)	0.023(8)	0.009(7)	-0.006(8)	-0.007(7)
C(5)	0.05(1)	0.018(9)	0.043(10)	0.002(8)	0.007(8)	-0.006(7)
C(6)	0.048(9)	0.005(7)	0.040(8)	0.007(7)	0.017(7)	-0.002(7)
C(7)	0.039(9)	0.020(8)	0.031(9)	0.013(6)	-0.008(7)	0.007(7)
C(8)	0.05(1)	0.004(7)	0.032(9)	0.013(6)	-0.002(8)	-0.001(6)
C(9)	0.038(9)	0.030(9)	0.04(1)	0.007(8)	-0.002(8)	0.004(8)
C(10)	0.05(1)	0.027(9)	0.039(10)	0.001(8)	-0.007(8)	0.002(8)
C(11)	0.046(10)	0.033(9)	0.040(9)	0.011(8)	0.012(8)	0.002(8)
C(12)	0.06(1)	0.012(8)	0.037(9)	-0.003(7)	0.006(8)	-0.002(7)
C(13)	0.07(1)	0.05(1)	0.041(10)	0.002(9)	0.022(9)	-0.022(8)
C(14)	0.08(1)	0.013(9)	0.10(1)	0.004(9)	-0.03(1)	0.001(9)
C(15)	0.045(10)	0.028(9)	0.044(10)	0.012(7)	0.011(8)	0.016(8)
C(16)	0.12(2)	0.09(2)	0.07(1)	-0.04(1)	0.04(1)	0.02(1)
C(17)	0.09(1)	0.07(1)	0.07(1)	0.00(1)	0.01(1)	0.01(1)
C(18)	0.09(2)	0.09(2)	0.15(2)	0.04(1)	0.04(1)	0.07(2)
C(19)	0.027(8)	0.036(10)	0.07(1)	0.002(7)	0.025(8)	0.007(8)
C(20)	0.038(9)	0.024(9)	0.040(10)	0.011(7)	0.011(8)	0.020(7)
C(21)	0.039(10)	0.04(1)	0.05(1)	0.028(9)	0.005(8)	-0.007(9)
C(22)	0.009(7)	0.06(1)	0.08(1)	0.010(8)	0.005(8)	0.04(1)
C(23)	0.028(9)	0.021(8)	0.05(1)	0.006(7)	-0.014(8)	0.013(8)
C(24)	0.036(9)	0.022(9)	0.027(8)	-0.002(7)	-0.001(7)	0.004(7)
C(25)	0.05(1)	0.029(10)	0.06(1)	0.015(8)	0.012(9)	0.003(8)
C(26)	0.06(1)	0.020(9)	0.05(1)	0.007(8)	0.005(8)	0.015(8)
C(27)	0.10(2)	0.07(1)	0.07(1)	0.04(1)	0.03(1)	0.00(1)
C(28)	0.07(1)	0.11(2)	0.09(2)	0.04(1)	0.04(1)	0.05(1)
C(29)	0.04(1)	0.06(1)	0.12(2)	0.008(9)	-0.01(1)	0.03(1)

The general temperature factor expression:

$$\exp(-2\pi^2(a^*2U_{11}h^2 + b^*2U_{22}k^2 + c^*2U_{33}l^2 + 2a^*b^*U_{12}hk + 2a^*c^*U_{13}hl + 2b^*c^*U_{23}kl))$$

Table 18. Bond Lengths (Å) for {Cp*Ta[MeN(C₆H₃Me)₂NSiMe₃]Me}+I⁻ (7).

atom	atom	distance	atom	atom	distance
Ta(1)	N(1)	1.92(1)	Ta(1)	N(2)	1.99(1)
Ta(1)	C(19)	2.14(2)	Ta(1)	C(20)	2.52(1)
Ta(1)	C(21)	2.47(1)	Ta(1)	C(22)	2.39(1)
Ta(1)	C(23)	2.38(1)	Ta(1)	C(24)	2.41(1)
Si(1)	N(2)	1.78(1)	Si(1)	C(16)	1.87(2)
Si(1)	C(17)	1.85(2)	Si(1)	C(18)	1.87(2)
N(1)	C(1)	1.47(1)	N(1)	C(15)	1.45(2)
N(2)	C(8)	1.43(2)	C(1)	C(2)	1.39(2)
C(1)	C(6)	1.43(2)	C(2)	C(3)	1.38(2)

C(3)	C(4)	1.40(2)	C(4)	C(5)	1.37(2)
C(5)	C(6)	1.42(2)	C(5)	C(14)	1.51(2)
C(6)	C(7)	1.45(2)	C(7)	C(8)	1.43(2)
C(7)	C(12)	1.40(2)	C(8)	C(9)	1.39(2)
C(9)	C(10)	1.38(2)	C(10)	C(11)	1.38(2)
C(11)	C(12)	1.39(2)	C(12)	C(13)	1.53(2)
C(20)	C(21)	1.40(2)	C(20)	C(24)	1.44(2)
C(20)	C(26)	1.50(2)	C(21)	C(22)	1.39(2)
C(21)	C(27)	1.52(2)	C(22)	C(23)	1.40(2)
C(22)	C(28)	1.52(2)	C(23)	C(24)	1.43(2)
C(23)	C(29)	1.49(2)	C(24)	C(25)	1.49(2)

Table 19. Bond Angles (°) for {Cp*Ta[MeN(C₆H₃Me)₂NSiMe₃]Me}⁺I⁻ (7).

atom	atom	atom	angle	atom	atom	atom	angle
N(1)	Ta(1)	N(2)	104.5(4)	N(1)	Ta(1)	C(19)	102.0(5)
N(1)	Ta(1)	C(20)	84.9(4)	N(1)	Ta(1)	C(21)	111.8(5)
N(1)	Ta(1)	C(22)	140.2(5)	N(1)	Ta(1)	C(23)	122.9(5)
N(1)	Ta(1)	C(24)	89.5(5)	N(2)	Ta(1)	C(19)	106.3(5)
N(2)	Ta(1)	C(20)	146.1(4)	N(2)	Ta(1)	C(21)	141.0(5)
N(2)	Ta(1)	C(22)	107.9(5)	N(2)	Ta(1)	C(23)	93.2(4)
N(2)	Ta(1)	C(24)	112.6(4)	C(19)	Ta(1)	C(20)	103.3(5)
C(19)	Ta(1)	C(21)	79.9(5)	C(19)	Ta(1)	C(22)	90.5(6)
C(19)	Ta(1)	C(23)	124.4(6)	C(19)	Ta(1)	C(24)	135.1(5)
C(20)	Ta(1)	C(21)	32.6(4)	C(20)	Ta(1)	C(22)	55.3(5)
C(20)	Ta(1)	C(23)	55.9(5)	C(20)	Ta(1)	C(24)	34.0(4)
C(21)	Ta(1)	C(22)	33.1(5)	C(21)	Ta(1)	C(23)	55.3(5)
C(21)	Ta(1)	C(24)	55.7(5)	C(22)	Ta(1)	C(23)	34.1(5)
C(22)	Ta(1)	C(24)	57.0(5)	C(23)	Ta(1)	C(24)	34.6(4)
N(2)	Si(1)	C(16)	109.2(7)	N(2)	Si(1)	C(17)	113.7(7)
N(2)	Si(1)	C(18)	106.7(7)	C(16)	Si(1)	C(17)	109.7(9)
C(16)	Si(1)	C(18)	110(1)	C(17)	Si(1)	C(18)	106.8(10)
Ta(1)	N(1)	C(1)	101.8(8)	Ta(1)	N(1)	C(15)	147.2(9)
C(1)	N(1)	C(15)	110.9(10)	Ta(1)	N(2)	Si(1)	133.4(6)
Ta(1)	N(2)	C(8)	112.1(8)	Si(1)	N(2)	C(8)	114.5(9)
N(1)	C(1)	C(2)	118(1)	N(1)	C(1)	C(6)	118(1)
C(2)	C(1)	C(6)	122(1)	C(1)	C(2)	C(3)	118(1)
C(2)	C(3)	C(4)	121(1)	C(3)	C(4)	C(5)	120(1)
C(4)	C(5)	C(6)	121(1)	C(4)	C(5)	C(14)	117(1)
C(6)	C(5)	C(14)	120(1)	C(1)	C(6)	C(5)	116(1)
C(1)	C(6)	C(7)	120(1)	C(5)	C(6)	C(7)	123(1)
C(6)	C(7)	C(8)	119(1)	C(6)	C(7)	C(12)	122(1)
C(8)	C(7)	C(12)	118(1)	N(2)	C(8)	C(7)	119(1)
N(2)	C(8)	C(9)	120(1)	C(7)	C(8)	C(9)	119(1)
C(8)	C(9)	C(10)	121(1)	C(9)	C(10)	C(11)	118(1)
C(10)	C(11)	C(12)	122(1)	C(7)	C(12)	C(11)	119(1)
C(7)	C(12)	C(13)	121(1)	C(11)	C(12)	C(13)	119(1)
Ta(1)	C(20)	C(21)	71.8(8)	Ta(1)	C(20)	C(24)	68.7(7)
Ta(1)	C(20)	C(26)	128.2(9)	C(21)	C(20)	C(24)	106(1)
C(21)	C(20)	C(26)	125(1)	C(24)	C(20)	C(26)	127(1)
Ta(1)	C(21)	C(20)	75.6(8)	Ta(1)	C(21)	C(22)	70.1(9)
Ta(1)	C(21)	C(27)	125(1)	C(20)	C(21)	C(22)	110(1)
C(20)	C(21)	C(27)	123(1)	C(22)	C(21)	C(27)	126(1)
Ta(1)	C(22)	C(21)	76.8(8)	Ta(1)	C(22)	C(23)	72.9(9)

Ta(1)	C(22)	C(28)	123(1)	C(21)	C(22)	C(23)	108(1)
C(21)	C(22)	C(28)	126(1)	C(23)	C(22)	C(28)	125(1)
Ta(1)	C(23)	C(22)	73.1(8)	Ta(1)	C(23)	C(24)	73.5(7)
Ta(1)	C(23)	C(29)	124(1)	C(22)	C(23)	C(24)	108(1)
C(22)	C(23)	C(29)	125(1)	C(24)	C(23)	C(29)	125(1)
Ta(1)	C(24)	C(20)	77.3(7)	Ta(1)	C(24)	C(23)	71.9(7)
Ta(1)	C(24)	C(25)	121.9(9)	C(20)	C(24)	C(23)	106(1)
C(20)	C(24)	C(25)	127(1)	C(23)	C(24)	C(25)	124(1)

Table 20. Least Squares Planes for {Cp*Ta[MeN(C₆H₃Me)₂NSiMe₃]Me}⁺I⁻ (**7**).

Atoms defining plane	Distance
C(20)	-0.02(1)
C(21)	0.00(1)
C(22)	0.01(1)
C(23)	-0.02(1)
C(24)	0.03(1)
Additional Atoms	Distance
Ta(1)	2.113
mean deviation	χ^2
0.0173	10.7

Structural data for Cp*Ta[PhSiH₂N(C₆H₃Me)₂NSiMe₃](H)Me (**9**)

Table 21. Atomic coordinates and B_{iso}/B_{eq} for Cp*Ta[PhSiH₂N(C₆H₃Me)₂NSiMe₃](H)Me (**9**).

atom	x	y	z	B _{eq}
Ta(1)	0.83407(1)	0.138049(7)	0.722965(6)	1.078(4)
Si(1)	0.52748(8)	0.23624(5)	0.67478(4)	1.41(2)
Si(2)	0.92718(8)	0.07855(6)	0.88169(4)	1.39(2)
N(1)	0.6369(2)	0.1614(2)	0.7153(1)	1.17(5)
N(2)	0.8516(2)	0.1548(2)	0.8233(1)	1.29(5)
C(1)	0.5736(3)	0.1098(2)	0.7608(2)	1.25(6)
C(2)	0.5069(3)	0.0347(2)	0.7382(1)	1.46(6)
C(3)	0.4483(3)	-0.0144(2)	0.7819(2)	1.90(7)
C(4)	0.4542(3)	0.0110(2)	0.8472(2)	1.67(7)
C(5)	0.5184(3)	0.0872(2)	0.8712(1)	1.54(6)
C(6)	0.5778(3)	0.1377(2)	0.8274(2)	1.20(6)
C(7)	0.6479(3)	0.2203(2)	0.8488(1)	1.25(6)
C(8)	0.7832(3)	0.2261(2)	0.8476(1)	1.18(6)
C(9)	0.8501(3)	0.3007(2)	0.8697(2)	1.78(7)
C(10)	0.7837(4)	0.3719(2)	0.8904(2)	1.99(7)

C(11)	0.6506(4)	0.3676(2)	0.8897(2)	1.76(7)
C(12)	0.5812(3)	0.2923(2)	0.8687(2)	1.63(6)
C(13)	0.4357(3)	0.2919(2)	0.8678(2)	2.47(8)
C(14)	0.5209(4)	0.1109(2)	0.9438(2)	2.30(7)
C(15)	0.8967(4)	0.1117(2)	0.9666(2)	2.40(7)
C(16)	0.8533(3)	-0.0309(2)	0.8665(2)	1.94(7)
C(17)	1.1088(3)	0.0755(2)	0.8884(2)	1.97(7)
C(18)	0.4100(3)	0.1929(2)	0.6019(2)	1.75(6)
C(19)	0.2966(3)	0.2403(2)	0.5788(2)	2.40(8)
C(20)	0.2091(4)	0.2135(3)	0.5232(2)	2.82(9)
C(21)	0.2311(4)	0.1380(2)	0.4903(2)	2.63(8)
C(22)	0.3407(3)	0.0905(2)	0.5127(2)	2.11(7)
C(23)	0.4296(3)	0.1173(2)	0.5675(2)	1.80(7)
C(24)	0.7835(3)	0.0100(2)	0.6775(2)	1.66(7)
C(25)	1.0415(3)	0.1485(2)	0.6785(2)	1.52(6)
C(26)	1.0195(3)	0.2272(2)	0.7103(2)	1.35(6)
C(27)	0.9050(3)	0.2667(2)	0.6738(2)	1.43(6)
C(28)	0.8577(3)	0.2123(2)	0.6188(2)	1.57(7)
C(29)	0.9417(3)	0.1397(2)	0.6217(2)	1.60(7)
C(30)	0.9374(4)	0.0719(2)	0.5689(2)	2.48(8)
C(31)	1.1582(3)	0.0912(2)	0.6953(2)	2.16(7)
C(32)	1.1105(3)	0.2672(2)	0.7675(2)	2.19(7)
C(33)	0.8568(4)	0.3560(2)	0.6884(2)	2.22(8)
C(34)	0.7488(3)	0.2299(2)	0.5611(2)	2.08(7)
H(1)	0.943(3)	0.065(2)	0.757(2)	2.0000
H(2)	0.5016	0.0172	0.6929	1.7466
H(3)	0.4036	-0.0660	0.7666	2.2781
H(4)	0.4141	-0.0237	0.8767	1.9990
H(5)	0.9418	0.3037	0.8708	2.1305
H(6)	0.8302	0.4232	0.9048	2.3909
H(7)	0.6059	0.4160	0.9037	2.1152
H(8)	0.3935	0.2638	0.8284	2.9652
H(9)	0.4170	0.2621	0.9061	2.9652
H(10)	0.4050	0.3497	0.8684	2.9652
H(11)	0.5663	0.1639	0.9532	2.7581
H(12)	0.4340	0.1169	0.9521	2.7581
H(13)	0.5639	0.0667	0.9716	2.7581
H(14)	0.9359	0.0710	0.9989	2.8825
H(15)	0.8053	0.1136	0.9667	2.8825
H(16)	0.9334	0.1671	0.9772	2.8825
H(17)	0.8938	-0.0695	0.9001	2.3228
H(18)	0.7625	-0.0278	0.8679	2.3228
H(19)	0.8661	-0.0511	0.8238	2.3228
H(20)	1.1440	0.0347	0.9216	2.3648
H(21)	1.1438	0.1311	0.9006	2.3648
H(22)	1.1311	0.0592	0.8465	2.3648
H(23)	0.2794	0.2916	0.6015	2.8771
H(24)	0.1337	0.2471	0.5077	3.3874
H(25)	0.1707	0.1193	0.4525	3.1580
H(26)	0.3560	0.0385	0.4904	2.5336
H(27)	0.5054	0.0835	0.5820	2.1616
H(28)	0.7449	-0.0246	0.7076	1.9950
H(29)	0.8604	-0.0174	0.6682	1.9950
H(30)	0.7235	0.0170	0.6370	1.9950
H(31)	0.8510	0.0500	0.5580	2.9819
H(32)	0.9631	0.0963	0.5301	2.9819
H(33)	0.9952	0.0263	0.5851	2.9819
H(34)	1.2085	0.0936	0.6602	2.5933

H(35)	1.1305	0.0335	0.7005	2.5933
H(36)	1.2099	0.1102	0.7358	2.5933
H(37)	1.1235	0.2283	0.8043	2.6302
H(38)	1.1919	0.2793	0.7539	2.6302
H(39)	1.0735	0.3194	0.7805	2.6302
H(40)	0.8397	0.3578	0.7330	2.6644
H(41)	0.7789	0.3685	0.6581	2.6644
H(42)	0.9216	0.3976	0.6832	2.6644
H(43)	0.7054	0.2818	0.5693	2.5019
H(44)	0.6884	0.1833	0.5567	2.5019
H(45)	0.7841	0.2355	0.5210	2.5019
H(46)	0.4545	0.2697	0.7217	1.6936
H(47)	0.5996	0.3034	0.6512	1.6936

$$B_{eq} = 8/3 \pi^2 (U_{11}(aa^*)^2 + U_{22}(bb^*)^2 + U_{33}(cc^*)^2 + 2U_{12}(aa^*bb^*)\cos\gamma + 2U_{13}(aa^*cc^*)\cos\beta + 2U_{23}(bb^*cc^*)\cos\alpha)$$

Table 22. Anisotropic Displacement Parameters for $Cp^*Ta[PhSiH_2N(C_6H_3Me)_2NSiMe_3](H)Me$ (**9**).

atom	U_{11}	U_{22}	U_{33}	U_{12}	U_{13}	U_{23}
Ta(1)	0.01304(9)	0.01413(9)	0.01522(9)	-0.00013(4)	0.00252(5)	0.00080(4)
Si(1)	0.0180(4)	0.0163(4)	0.0191(4)	0.0027(3)	0.0022(3)	0.0008(3)
Si(2)	0.0171(4)	0.0188(4)	0.0184(4)	0.0014(3)	0.0006(3)	0.0017(3)
N(1)	0.016(1)	0.018(1)	0.014(1)	-0.001(1)	0.002(1)	0.000(1)
N(2)	0.013(1)	0.017(1)	0.019(1)	0.001(1)	0.001(1)	-0.001(1)
C(1)	0.008(1)	0.018(2)	0.023(2)	0.003(1)	-0.001(1)	0.001(1)
C(2)	0.014(1)	0.019(2)	0.020(2)	0.002(1)	0.001(1)	-0.003(1)
C(3)	0.017(2)	0.018(2)	0.035(2)	-0.004(1)	0.002(1)	-0.001(1)
C(4)	0.018(2)	0.024(2)	0.023(2)	-0.005(1)	0.004(1)	0.005(1)
C(5)	0.015(1)	0.029(2)	0.019(2)	0.002(1)	0.004(1)	0.003(1)
C(6)	0.013(2)	0.018(2)	0.021(2)	-0.001(1)	0.002(1)	-0.002(1)
C(7)	0.019(2)	0.017(2)	0.015(1)	-0.001(1)	0.001(1)	0.000(1)
C(8)	0.020(2)	0.019(2)	0.009(1)	0.001(1)	-0.001(1)	0.004(1)
C(9)	0.022(2)	0.024(2)	0.019(2)	-0.003(1)	0.002(1)	0.002(1)
C(10)	0.040(2)	0.020(2)	0.017(2)	-0.009(1)	0.000(1)	-0.001(1)
C(11)	0.037(2)	0.018(2)	0.016(2)	0.007(1)	0.004(1)	0.000(1)
C(12)	0.026(2)	0.023(2)	0.014(1)	0.001(1)	0.003(1)	0.000(1)
C(13)	0.023(2)	0.039(2)	0.032(2)	0.006(2)	0.004(1)	-0.008(2)
C(14)	0.029(2)	0.040(2)	0.020(2)	-0.008(2)	0.007(1)	0.000(2)
C(15)	0.033(2)	0.032(2)	0.021(2)	0.009(2)	-0.001(1)	0.005(1)
C(16)	0.026(2)	0.022(2)	0.030(2)	0.001(1)	0.001(1)	0.002(1)
C(17)	0.022(2)	0.025(2)	0.025(2)	0.000(1)	-0.001(1)	0.003(1)
C(18)	0.020(2)	0.023(2)	0.020(2)	-0.003(1)	0.003(1)	0.006(1)
C(19)	0.027(2)	0.027(2)	0.035(2)	0.003(2)	-0.002(2)	0.004(2)
C(20)	0.023(2)	0.042(2)	0.047(2)	0.004(2)	-0.008(2)	0.013(2)
C(21)	0.030(2)	0.041(2)	0.024(2)	-0.006(2)	-0.005(2)	0.006(2)
C(22)	0.031(2)	0.027(2)	0.027(2)	-0.008(2)	0.005(1)	0.002(1)
C(23)	0.020(2)	0.027(2)	0.023(2)	-0.003(1)	0.001(1)	0.003(1)
C(24)	0.022(2)	0.015(2)	0.027(2)	0.002(1)	0.007(1)	-0.001(1)
C(25)	0.016(2)	0.020(2)	0.021(2)	-0.002(1)	0.005(1)	0.002(1)
C(26)	0.015(1)	0.017(2)	0.025(2)	-0.001(1)	0.007(1)	0.005(1)
C(27)	0.018(2)	0.020(2)	0.022(2)	0.000(1)	0.006(1)	0.007(1)

C(28)	0.017(2)	0.026(2)	0.020(2)	-0.003(1)	0.007(1)	0.005(1)
C(29)	0.019(2)	0.024(2)	0.020(2)	-0.001(1)	0.007(1)	0.004(1)
C(30)	0.035(2)	0.033(2)	0.026(2)	-0.004(2)	0.012(2)	-0.003(2)
C(31)	0.019(2)	0.030(2)	0.036(2)	0.002(1)	0.008(1)	0.007(2)
C(32)	0.024(2)	0.028(2)	0.030(2)	-0.007(1)	0.005(1)	-0.003(1)
C(33)	0.024(2)	0.020(2)	0.043(2)	0.001(1)	0.003(2)	0.009(1)
C(34)	0.027(2)	0.037(2)	0.020(2)	-0.002(2)	0.004(1)	0.007(1)

The general temperature factor expression:

$$\exp(-2\pi^2(a^2U_{11}h^2 + b^2U_{22}k^2 + c^2U_{33}l^2 + 2a*b*U_{12}hk + 2a*c*U_{13}hl + 2b*c*U_{23}kl))$$

Table 23. Bond Lengths (Å) for Cp*Ta[PhSiH₂N(C₆H₃Me)₂NSiMe₃](H)Me (**9**).

atom	atom	distance	atom	atom	distance
Ta(1)	N(1)	2.060(2)	Ta(1)	N(2)	2.028(3)
Ta(1)	C(24)	2.213(3)	Ta(1)	C(25)	2.474(3)
Ta(1)	C(26)	2.418(3)	Ta(1)	C(27)	2.397(3)
Ta(1)	C(28)	2.451(3)	Ta(1)	C(29)	2.495(3)
Ta(1)	H(1)	1.67(3)	Si(1)	N(1)	1.731(3)
Si(1)	C(18)	1.877(3)	Si(2)	N(2)	1.760(3)
Si(2)	C(15)	1.871(4)	Si(2)	C(16)	1.864(3)
Si(2)	C(17)	1.870(3)	N(1)	C(1)	1.456(4)
N(2)	C(8)	1.442(4)	C(1)	C(2)	1.392(4)
C(1)	C(6)	1.410(4)	C(2)	C(3)	1.383(4)
C(3)	C(4)	1.372(4)	C(4)	C(5)	1.402(4)
C(5)	C(6)	1.401(4)	C(5)	C(14)	1.511(4)
C(6)	C(7)	1.501(4)	C(7)	C(8)	1.412(4)
C(7)	C(12)	1.406(4)	C(8)	C(9)	1.384(4)
C(9)	C(10)	1.401(5)	C(10)	C(11)	1.382(5)
C(11)	C(12)	1.399(4)	C(12)	C(13)	1.509(5)
C(18)	C(19)	1.401(4)	C(18)	C(23)	1.394(5)
C(19)	C(20)	1.388(5)	C(20)	C(21)	1.384(5)
C(21)	C(22)	1.367(5)	C(22)	C(23)	1.385(5)
C(25)	C(26)	1.414(4)	C(25)	C(29)	1.422(5)
C(25)	C(31)	1.495(4)	C(26)	C(27)	1.430(4)
C(26)	C(32)	1.502(4)	C(27)	C(28)	1.417(5)
C(27)	C(33)	1.517(4)	C(28)	C(29)	1.419(4)
C(28)	C(34)	1.511(4)	C(29)	C(30)	1.493(5)

Table 24. Bond Angles (°) for Cp*Ta[PhSiH₂N(C₆H₃Me)₂NSiMe₃](H)Me (**9**).

atom	atom	atom	angle	atom	atom	atom	angle
N(1)	Ta(1)	N(2)	88.6(1)	C(27)	Ta(1)	C(29)	55.9(1)
N(1)	Ta(1)	C(24)	87.8(1)	C(28)	Ta(1)	C(29)	33.3(1)
N(1)	Ta(1)	C(25)	151.1(1)	N(1)	Si(1)	C(18)	115.0(1)
N(1)	Ta(1)	C(26)	133.7(1)	N(2)	Si(2)	C(15)	108.0(1)
N(1)	Ta(1)	C(27)	101.1(1)	N(2)	Si(2)	C(16)	111.9(1)

C(25)	-0.005(3)
C(26)	0.004(3)
C(27)	-0.003(3)
C(28)	0.001(3)
C(29)	0.003(3)
Additional Atoms	Distance
Ta(1)	-2.126
mean deviation	χ^2
0.0032	7.0

Structural data for Cp*Ta[PhSiH₂N(C₆H₃Me)₂NSiPhHCl](H)Cl (**12**).

Table 26. Atomic coordinates and B_{iso}/B_{eq} for Cp*Ta[PhSiH₂N(C₆H₃Me)₂NSiPhHCl](H)Cl (**12**).

atom	x	y	z	B _{eq}
Ta(1)	0.71890(1)	-0.26088(1)	0.270153(10)	1.418(4)
Cl(1)	0.7522(1)	-0.2367(1)	0.11116(7)	2.30(2)
Cl(2)	0.5765(1)	0.1548(1)	0.34179(7)	2.52(2)
Si(1)	1.0290(1)	-0.4275(1)	0.31260(8)	2.09(3)
Si(2)	0.5861(1)	0.0117(1)	0.27459(7)	1.70(2)
N(1)	0.9083(3)	-0.2980(3)	0.2726(2)	1.72(7)
N(2)	0.7005(3)	-0.1130(3)	0.3225(2)	1.50(7)
C(1)	0.9672(4)	-0.1842(4)	0.2231(3)	1.96(9)
C(2)	1.0289(4)	-0.1674(4)	0.1326(3)	2.17(9)
C(3)	1.0853(4)	-0.0585(4)	0.0869(3)	2.42(10)
C(4)	1.0777(4)	0.0354(4)	0.1277(3)	2.37(10)
C(5)	1.0162(4)	0.0214(4)	0.2185(3)	2.02(9)
C(6)	0.9643(4)	-0.0918(4)	0.2676(3)	1.71(8)
C(7)	0.9036(4)	-0.1146(4)	0.3654(3)	1.68(8)
C(8)	0.7715(4)	-0.1169(4)	0.3900(3)	1.33(8)
C(9)	0.7110(4)	-0.1245(4)	0.4796(3)	2.12(9)
C(10)	0.7823(5)	-0.1402(5)	0.5458(3)	2.7(1)
C(11)	0.9138(5)	-0.1478(4)	0.5232(3)	2.8(1)
C(12)	0.9762(4)	-0.1341(4)	0.4336(3)	2.22(9)
C(13)	1.1189(4)	-0.1442(5)	0.4129(3)	2.9(1)
C(14)	1.0047(5)	0.1296(4)	0.2591(3)	3.0(1)
C(15)	1.1164(4)	-0.5106(4)	0.2244(3)	2.43(10)
C(16)	1.2388(5)	-0.5815(5)	0.2336(4)	3.2(1)
C(17)	1.3080(5)	-0.6471(5)	0.1713(4)	3.9(1)
C(18)	1.2521(5)	-0.6447(5)	0.0998(4)	3.7(1)
C(19)	1.1314(5)	-0.5766(5)	0.0896(3)	2.8(1)
C(20)	1.0639(4)	-0.5094(4)	0.1516(3)	2.57(10)
C(21)	0.6205(4)	0.1101(4)	0.1523(3)	2.06(9)
C(22)	0.7041(4)	0.1997(5)	0.1234(3)	2.7(1)
C(23)	0.7168(5)	0.2803(5)	0.0346(4)	3.5(1)
C(24)	0.6469(5)	0.2738(5)	-0.0258(3)	3.5(1)

C(25)	0.5640(5)	0.1867(5)	0.0012(3)	3.5(1)
C(26)	0.5520(4)	0.1043(4)	0.0900(3)	2.62(10)
C(27)	0.5456(4)	-0.3387(4)	0.3898(3)	1.76(9)
C(28)	0.6594(4)	-0.4298(4)	0.4079(3)	1.99(9)
C(29)	0.6991(4)	-0.4928(4)	0.3369(3)	1.99(9)
C(30)	0.6100(4)	-0.4385(4)	0.2753(3)	2.00(9)
C(31)	0.5170(4)	-0.3430(4)	0.3061(3)	1.91(9)
C(32)	0.4621(4)	-0.2665(4)	0.4522(3)	2.30(9)
C(33)	0.7163(5)	-0.4620(4)	0.4930(3)	2.49(10)
C(34)	0.7974(5)	-0.6126(4)	0.3358(3)	3.0(1)
C(35)	0.6097(5)	-0.4858(4)	0.1964(3)	2.6(1)
C(36)	0.3999(4)	-0.2698(5)	0.2649(3)	2.5(1)
H(1)	0.595(4)	-0.124(4)	0.228(3)	2.0(8)
H(2)	1.0321	-0.2303	0.1028	2.6082
H(3)	1.1299	-0.0487	0.0263	2.9015
H(4)	1.1143	0.1109	0.0943	2.8481
H(5)	0.6207	-0.1187	0.4949	2.5446
H(6)	0.7413	-0.1459	0.6068	3.2251
H(7)	0.9626	-0.1626	0.5697	3.3253
H(8)	1.1486	-0.1357	0.4626	3.4742
H(9)	1.1416	-0.0769	0.3592	3.4742
H(10)	1.1568	-0.2262	0.4036	3.4742
H(11)	1.0771	0.1161	0.2874	3.6329
H(12)	0.9292	0.1310	0.3033	3.6329
H(13)	1.0006	0.2103	0.2123	3.6329
H(14)	1.2760	-0.5852	0.2837	3.8082
H(15)	1.3923	-0.6928	0.1778	4.6219
H(16)	1.2978	-0.6906	0.0576	4.4746
H(17)	1.0937	-0.5750	0.0403	3.3635
H(18)	0.9804	-0.4620	0.1439	3.0886
H(19)	0.7523	0.2053	0.1648	3.2216
H(20)	0.7743	0.3406	0.0153	4.1766
H(21)	0.6560	0.3299	-0.0866	4.2047
H(22)	0.5152	0.1829	-0.0404	4.2103
H(23)	0.4959	0.0428	0.1082	3.1415
H(24)	0.5103	-0.2609	0.4936	2.7626
H(25)	0.3930	-0.3108	0.4853	2.7626
H(26)	0.4294	-0.1815	0.4175	2.7626
H(27)	0.6525	-0.4839	0.5451	2.9928
H(28)	0.7479	-0.3889	0.4931	2.9928
H(29)	0.7845	-0.5336	0.4946	2.9928
H(30)	0.7573	-0.6795	0.3346	3.6113
H(31)	0.8361	-0.6404	0.3889	3.6113
H(32)	0.8609	-0.5936	0.2831	3.6113
H(33)	0.6953	-0.5083	0.1686	3.1706
H(34)	0.5646	-0.4191	0.1531	3.1706
H(35)	0.5690	-0.5600	0.2177	3.1706
H(36)	0.4208	-0.2475	0.2002	3.0257
H(37)	0.3694	-0.1928	0.2829	3.0257
H(38)	0.3354	-0.3226	0.2854	3.0257
H(39)	0.9727	-0.5194	0.3884	2.5093
H(40)	1.1179	-0.3791	0.3398	2.5093
H(41)	0.460(5)	0.001(5)	0.302(3)	3.4(10)

$$B_{eq} = 8/3 \pi^2 (U_{11}(aa^*)^2 + U_{22}(bb^*)^2 + U_{33}(cc^*)^2 + 2U_{12}(aa^*bb^*)\cos\gamma + 2U_{13}(aa^*cc^*)\cos\beta + 2U_{23}(bb^*cc^*)\cos\alpha)$$

Table 27. Anisotropic Displacement Parameters for $\text{Cp}^*\text{Ta}[\text{PhSiH}_2\text{N}(\text{C}_6\text{H}_3\text{Me})_2\text{NSiPhHCl}](\text{H})\text{Cl}$ (**12**).

atom	U_{11}	U_{22}	U_{33}	U_{12}	U_{13}	U_{23}
Ta(1)	0.0205(1)	0.0161(1)	0.0168(1)	-0.00418(7)	0.00065(7)	-0.00492(7)
Cl(1)	0.0342(6)	0.0349(6)	0.0190(5)	-0.0102(5)	-0.0008(4)	-0.0078(4)
Cl(2)	0.0410(6)	0.0248(6)	0.0303(6)	-0.0030(5)	0.0016(5)	-0.0135(5)
Si(1)	0.0258(6)	0.0220(6)	0.0310(7)	0.0008(5)	-0.0044(5)	-0.0071(5)
Si(2)	0.0234(6)	0.0187(6)	0.0211(6)	-0.0012(5)	0.0000(5)	-0.0055(5)
N(1)	0.024(2)	0.018(2)	0.022(2)	-0.005(1)	-0.001(1)	-0.008(1)
N(2)	0.021(2)	0.019(2)	0.017(2)	-0.006(1)	0.001(1)	-0.007(1)
C(1)	0.022(2)	0.024(2)	0.022(2)	-0.001(2)	-0.001(2)	-0.008(2)
C(2)	0.024(2)	0.028(2)	0.031(2)	-0.004(2)	0.000(2)	-0.013(2)
C(3)	0.030(2)	0.034(3)	0.025(2)	-0.007(2)	0.006(2)	-0.010(2)
C(4)	0.034(3)	0.027(2)	0.026(2)	-0.012(2)	0.003(2)	-0.002(2)
C(5)	0.023(2)	0.027(2)	0.031(2)	-0.003(2)	0.002(2)	-0.012(2)
C(6)	0.015(2)	0.024(2)	0.023(2)	-0.004(2)	-0.001(2)	-0.005(2)
C(7)	0.027(2)	0.016(2)	0.021(2)	-0.002(2)	-0.003(2)	-0.006(2)
C(8)	0.028(2)	0.011(2)	0.017(2)	-0.002(2)	-0.003(2)	-0.003(2)
C(9)	0.033(2)	0.025(2)	0.021(2)	-0.008(2)	0.000(2)	-0.008(2)
C(10)	0.042(3)	0.037(3)	0.017(2)	-0.009(2)	0.002(2)	-0.008(2)
C(11)	0.046(3)	0.029(2)	0.031(3)	-0.002(2)	-0.017(2)	-0.009(2)
C(12)	0.032(2)	0.022(2)	0.030(2)	-0.003(2)	-0.007(2)	-0.010(2)
C(13)	0.031(3)	0.036(3)	0.043(3)	-0.001(2)	-0.014(2)	-0.016(2)
C(14)	0.047(3)	0.023(2)	0.039(3)	-0.014(2)	-0.001(2)	-0.010(2)
C(15)	0.031(2)	0.017(2)	0.037(3)	-0.004(2)	0.002(2)	-0.007(2)
C(16)	0.033(3)	0.033(3)	0.055(3)	0.002(2)	-0.004(2)	-0.018(2)
C(17)	0.030(3)	0.039(3)	0.067(4)	0.007(2)	0.001(3)	-0.024(3)
C(18)	0.046(3)	0.032(3)	0.054(3)	0.001(2)	0.014(3)	-0.018(2)
C(19)	0.042(3)	0.029(3)	0.035(3)	-0.011(2)	0.004(2)	-0.010(2)
C(20)	0.028(2)	0.024(2)	0.037(3)	-0.003(2)	0.001(2)	-0.005(2)
C(21)	0.032(2)	0.020(2)	0.022(2)	0.000(2)	-0.002(2)	-0.007(2)
C(22)	0.036(3)	0.032(3)	0.032(3)	-0.008(2)	0.003(2)	-0.012(2)
C(23)	0.059(3)	0.029(3)	0.041(3)	-0.017(2)	0.014(3)	-0.009(2)
C(24)	0.057(3)	0.042(3)	0.021(2)	0.003(3)	0.003(2)	0.001(2)
C(25)	0.042(3)	0.044(3)	0.029(3)	0.007(2)	-0.006(2)	-0.005(2)
C(26)	0.033(3)	0.030(3)	0.033(3)	-0.001(2)	-0.003(2)	-0.011(2)
C(27)	0.029(2)	0.026(2)	0.021(2)	-0.017(2)	0.006(2)	-0.006(2)
C(28)	0.028(2)	0.022(2)	0.022(2)	-0.015(2)	0.001(2)	0.004(2)
C(29)	0.030(2)	0.014(2)	0.028(2)	-0.009(2)	0.003(2)	-0.002(2)
C(30)	0.031(2)	0.021(2)	0.024(2)	-0.016(2)	0.006(2)	-0.007(2)
C(31)	0.026(2)	0.023(2)	0.027(2)	-0.015(2)	0.000(2)	-0.005(2)
C(32)	0.029(2)	0.029(2)	0.022(2)	-0.012(2)	0.008(2)	-0.010(2)
C(33)	0.043(3)	0.030(3)	0.020(2)	-0.015(2)	0.001(2)	-0.004(2)
C(34)	0.043(3)	0.020(2)	0.041(3)	-0.004(2)	-0.003(2)	-0.009(2)
C(35)	0.044(3)	0.026(2)	0.033(2)	-0.011(2)	0.001(2)	-0.014(2)
C(36)	0.030(2)	0.039(3)	0.029(2)	-0.009(2)	-0.005(2)	-0.009(2)

The general temperature factor expression:

$$\exp(-2\pi^2(a^2U_{11}h^2 + b^2U_{22}k^2 + c^2U_{33}l^2 + 2a*b*U_{12}hk + 2a*c*U_{13}hl + 2b*c*U_{23}kl))$$

Table 28. Bond Lengths (Å) for Cp*Ta[PhSiH₂N(C₆H₃Me)₂NSiPhHCl](H)Cl (**12**).

atom	atom	distance	atom	atom	distance
Ta(1)	Cl(1)	2.378(1)	Ta(1)	N(1)	2.015(3)
Ta(1)	N(2)	2.016(3)	Ta(1)	C(27)	2.433(4)
Ta(1)	C(28)	2.421(4)	Ta(1)	C(29)	2.472(4)
Ta(1)	C(30)	2.493(4)	Ta(1)	C(31)	2.450(4)
Cl(2)	Si(2)	2.149(2)	Si(1)	N(1)	1.756(4)
Si(1)	C(15)	1.877(4)	Si(2)	N(2)	1.723(3)
Si(2)	C(21)	1.873(4)	N(1)	C(1)	1.450(5)
N(2)	C(8)	1.433(5)	C(1)	C(2)	1.402(6)
C(1)	C(6)	1.409(6)	C(2)	C(3)	1.385(6)
C(3)	C(4)	1.370(7)	C(4)	C(5)	1.408(6)
C(5)	C(6)	1.406(6)	C(5)	C(14)	1.505(6)
C(6)	C(7)	1.494(6)	C(7)	C(8)	1.406(6)
C(7)	C(12)	1.407(6)	C(8)	C(9)	1.399(6)
C(9)	C(10)	1.380(6)	C(10)	C(11)	1.385(7)
C(11)	C(12)	1.394(7)	C(12)	C(13)	1.499(6)
C(15)	C(16)	1.393(7)	C(15)	C(20)	1.386(7)
C(16)	C(17)	1.392(7)	C(17)	C(18)	1.386(8)
C(18)	C(19)	1.371(7)	C(19)	C(20)	1.396(7)
C(21)	C(22)	1.397(6)	C(21)	C(26)	1.385(6)
C(22)	C(23)	1.383(7)	C(23)	C(24)	1.375(8)
C(24)	C(25)	1.372(8)	C(25)	C(26)	1.389(7)
C(27)	C(28)	1.422(6)	C(27)	C(31)	1.439(6)
C(27)	C(32)	1.486(6)	C(28)	C(29)	1.442(6)
C(28)	C(33)	1.506(6)	C(29)	C(30)	1.419(6)
C(29)	C(34)	1.501(6)	C(30)	C(31)	1.414(6)
C(30)	C(35)	1.500(6)	C(31)	C(36)	1.501(6)
Ta(1)	H(1)	1.83(4)	Si(2)	H(41)	1.36(5)
Si(2)	H(1)	1.86(4)			

Table 29. Bond Angles (°) for Cp*Ta[PhSiH₂N(C₆H₃Me)₂NSiPhHCl](H)Cl (**12**).

atom	atom	atom	angle	atom	atom	atom	angle
Cl(1)	Ta(1)	N(1)	92.29(9)	C(29)	Ta(1)	C(31)	55.8(1)
Cl(1)	Ta(1)	N(2)	123.89(9)	C(30)	Ta(1)	C(31)	33.2(1)
Cl(1)	Ta(1)	C(27)	129.9(1)	N(1)	Si(1)	C(15)	113.0(2)
Cl(1)	Ta(1)	C(28)	135.0(1)	Cl(2)	Si(2)	N(2)	103.1(1)
Cl(1)	Ta(1)	C(29)	101.7(1)	Cl(2)	Si(2)	C(21)	100.5(1)
Cl(1)	Ta(1)	C(30)	81.1(1)	N(2)	Si(2)	C(21)	120.2(2)
Cl(1)	Ta(1)	C(31)	95.6(1)	Ta(1)	N(1)	Si(1)	140.1(2)
N(1)	Ta(1)	N(2)	89.4(1)	Ta(1)	N(1)	C(1)	111.7(2)
N(1)	Ta(1)	C(27)	129.2(1)	Si(1)	N(1)	C(1)	108.1(3)
N(1)	Ta(1)	C(28)	97.4(1)	Ta(1)	N(2)	Si(2)	108.8(2)
N(1)	Ta(1)	C(29)	92.8(1)	Ta(1)	N(2)	C(8)	123.7(2)
N(1)	Ta(1)	C(30)	119.5(1)	Si(2)	N(2)	C(8)	127.4(3)
N(1)	Ta(1)	C(31)	148.5(1)	N(1)	C(1)	C(2)	120.5(4)
N(2)	Ta(1)	C(27)	87.8(1)	N(1)	C(1)	C(6)	119.4(3)
N(2)	Ta(1)	C(28)	100.2(1)	C(2)	C(1)	C(6)	120.1(4)
N(2)	Ta(1)	C(29)	134.2(1)	C(1)	C(2)	C(3)	119.5(4)

N(2)	Ta(1)	C(30)	142.6(1)	C(2)	C(3)	C(4)	121.0(4)
N(2)	Ta(1)	C(31)	110.8(1)	C(3)	C(4)	C(5)	120.8(4)
C(27)	Ta(1)	C(28)	34.1(1)	C(4)	C(5)	C(6)	119.0(4)
C(27)	Ta(1)	C(29)	56.5(1)	C(4)	C(5)	C(14)	119.0(4)
C(27)	Ta(1)	C(30)	56.0(1)	C(6)	C(5)	C(14)	122.0(4)
C(27)	Ta(1)	C(31)	34.3(1)	C(1)	C(6)	C(5)	119.4(4)
C(28)	Ta(1)	C(29)	34.3(1)	C(1)	C(6)	C(7)	119.3(4)
C(28)	Ta(1)	C(30)	56.0(1)	C(5)	C(6)	C(7)	121.3(4)
C(28)	Ta(1)	C(31)	56.5(1)	C(6)	C(7)	C(8)	119.5(3)
C(29)	Ta(1)	C(30)	33.2(1)	C(6)	C(7)	C(12)	121.1(4)
C(8)	C(7)	C(12)	119.3(4)	Ta(1)	C(27)	C(28)	72.5(2)
N(2)	C(8)	C(7)	119.2(3)	Ta(1)	C(27)	C(31)	73.5(2)
N(2)	C(8)	C(9)	120.7(4)	Ta(1)	C(27)	C(32)	125.9(3)
C(7)	C(8)	C(9)	120.1(4)	C(28)	C(27)	C(31)	107.3(4)
C(8)	C(9)	C(10)	120.1(4)	C(28)	C(27)	C(32)	126.2(4)
C(9)	C(10)	C(11)	119.8(4)	C(31)	C(27)	C(32)	126.0(4)
C(10)	C(11)	C(12)	121.5(4)	Ta(1)	C(28)	C(27)	73.4(2)
C(7)	C(12)	C(11)	118.9(4)	Ta(1)	C(28)	C(29)	74.8(2)
C(7)	C(12)	C(13)	121.7(4)	Ta(1)	C(28)	C(33)	122.9(3)
C(11)	C(12)	C(13)	119.4(4)	C(27)	C(28)	C(29)	108.3(4)
Si(1)	C(15)	C(16)	118.8(4)	C(27)	C(28)	C(33)	124.0(4)
Si(1)	C(15)	C(20)	123.4(3)	C(29)	C(28)	C(33)	127.4(4)
C(16)	C(15)	C(20)	117.7(4)	Ta(1)	C(29)	C(28)	70.9(2)
C(15)	C(16)	C(17)	121.7(5)	Ta(1)	C(29)	C(30)	74.2(2)
C(16)	C(17)	C(18)	119.1(5)	Ta(1)	C(29)	C(34)	130.2(3)
C(17)	C(18)	C(19)	120.4(5)	C(28)	C(29)	C(30)	107.4(4)
C(18)	C(19)	C(20)	119.9(5)	C(28)	C(29)	C(34)	127.7(4)
C(15)	C(20)	C(19)	121.2(4)	C(30)	C(29)	C(34)	123.7(4)
Si(2)	C(21)	C(22)	121.9(3)	Ta(1)	C(30)	C(29)	72.6(2)
Si(2)	C(21)	C(26)	119.4(3)	Ta(1)	C(30)	C(31)	71.7(2)
C(22)	C(21)	C(26)	118.4(4)	Ta(1)	C(30)	C(35)	126.1(3)
C(21)	C(22)	C(23)	120.2(5)	C(29)	C(30)	C(31)	108.7(4)
C(22)	C(23)	C(24)	120.4(5)	C(29)	C(30)	C(35)	124.5(4)
C(23)	C(24)	C(25)	120.3(4)	C(31)	C(30)	C(35)	126.6(4)
C(24)	C(25)	C(26)	119.5(5)	Ta(1)	C(31)	C(27)	72.2(2)
C(21)	C(26)	C(25)	121.1(4)	Ta(1)	C(31)	C(30)	75.0(2)
Ta(1)	C(31)	C(36)	124.1(3)	C(27)	C(31)	C(30)	108.3(4)
C(27)	C(31)	C(36)	125.5(4)	C(30)	C(31)	C(36)	125.8(4)
Cl(1)	Ta(1)	H(1)	76(1)	N(1)	Ta(1)	H(1)	139(1)
N(2)	Ta(1)	H(1)	67(1)	C(27)	Ta(1)	H(1)	84(1)
C(28)	Ta(1)	H(1)	118(1)	C(29)	Ta(1)	H(1)	128(1)
C(30)	Ta(1)	H(1)	97(1)	C(31)	Ta(1)	H(1)	72(1)
Cl(2)	Si(2)	H(41)	95(2)	N(2)	Si(2)	H(41)	119(2)
C(21)	Si(2)	H(41)	112(2)	H(41)	Si(2)	N(2)	119(2)
H(41)	Si(2)	H(1)	84(2)	H(41)	Si(2)	Cl(2)	95(2)
H(41)	Si(2)	C(21)	112(2)	N(2)	Si(2)	H(1)	73(1)
H(1)	Si(2)	C(21)	85(1)	H(1)	Si(2)	Cl(2)	174(1)

Table 30. Least Squares Planes
for Cp*Ta[PhSiH₂N(C₆H₃Me)₂NSiPhHCl](H)Cl (**12**).

Atoms defining plane	Distance
C(27)	-0.009(4)
C(28)	0.006(4)

C(29)	-0.001(4)
C(30)	-0.006(4)
C(31)	0.010(4)
Additional Atoms	Distance
Ta(1)	2.132
mean deviation	χ^2
0.0063	16.9

Appendix B

Crystallographic Data for Chapter 2

Table 1. Crystallographic data for compounds **2**, **4**, **6**, and **9**.

Compound	2	4	6	9
(a) Crystal Parameters:				
Formula	$C_{34}H_{58}N_2ClO_2Si_2Y$	$C_{37}H_{67}N_2O_3Si_3Y$	$C_{33}H_{54}N_2Si_2OY$	$C_{46}H_{70}N_5Si_2Y$
Formula weight	707.37	761.11	639.88	838.17
Size (mm)	0.1 × 0.07 × 0.06	0.2 × 0.1 × 0.08	0.1 × 0.1 × 0.1	0.2 × 0.15 × 0.25
Crystal system	orthorhombic	monoclinic	monoclinic	monoclinic
Space group	Pca2 ₁ (#29)	P2 ₁ /n (#14)	P2 ₁ /c (#14)	C2/c(#15)
a (Å)	17.1765(5)	11.3639(2)	10.7444(5)	23.8332(1)
b (Å)	10.5593(3)	17.3411(2)	19.0747(8)	11.8922(1)
c (Å)	20.7010(7)	21.7183(3)	17.7776(8)	33.2391(3)
α, β, γ (°)	90, 90, 90	90, 102.836(1), 90	90, 106.838(1), 90	90, 91.062(1), 90
V (Å ³)	3754.6(2)	4172.9(1)	3487.2(2)	9419.3(1)
Z	4	4	4	8
D _{calc} (g·cm ⁻³)	1.251	1.211	1.219	1.182
F ₀₀₀	1504.00	1632.00	1364.00	3584.00
μ(MoK _α) (cm ⁻¹)	17.20	15.19	17.69	13.26
(b) Data Collection:				
Temp. (°C)	-120	-110	-155	-110
Unique/ Total reflection	5472 / 12491	7636 / 19613	5153 / 14444	7098 / 19732
R _{int}	0.067	0.047	0.049	0.052
Empirical absorption correction:	0.05	0.07	0.3	0.5
μR, T _{min} - T _{max}	0.828 - 0.886	0.786 - 0.879	0.473 - 0.547	0.216 - 0.270

	(c) Refinement:			
Observations ($I > 3\sigma(I)$)	3431	4655	3213	4366
Variables	379	416	357	488
Reflection / parameters ratio	9.05	11.19	9.00	8.95
$R = \frac{\sum F_o - F_c }{\sum F_o }$	0.047	0.042	0.038	0.045
$R_w = \left[\frac{\sum w(F_o - F_c)^2}{\sum w F_o^2} \right]^{1/2}$	0.052	0.047	0.044	0.055
Goodness of fit $\left[\frac{\sum w(F_o - F_c)^2}{(N_o - N_v)} \right]^{1/2}$	1.63	1.66	1.51	1.79
Max and min peaks in final diff. map ($e^{-\text{\AA}^3}$)	0.41 / -0.54	0.41 / -0.47	0.51 / -0.37	0.48 / -0.41

Structural data for [DADMB]YCl(THF)₂ (**2**).**Table 2.** Atomic coordinates and B_{iso}/B_{eq} for [DADMB]YCl(THF)₂ (**2**).

atom	x	y	z	B _{eq}
Y(1)	-0.47592(4)	-0.16953(7)	-0.314	1.98(2)
Cl(1)	-0.5616(1)	0.0192(2)	-0.2802(1)	3.74(6)
Si(1)	-0.5965(1)	-0.2571(2)	-0.4463(1)	2.54(6)
Si(2)	-0.3271(1)	-0.1208(3)	-0.1972(1)	2.50(6)
O(1)	-0.5479(3)	-0.2782(7)	-0.2338(3)	2.3(2)
O(2)	-0.4191(4)	-0.0220(5)	-0.3875(3)	2.6(1)
N(1)	-0.5196(4)	-0.2906(7)	-0.3954(3)	2.0(2)
N(2)	-0.3630(4)	-0.2063(6)	-0.2618(3)	2.1(2)
C(1)	-0.5008(5)	-0.4060(8)	-0.3648(4)	2.6(2)
C(2)	-0.5551(5)	-0.5062(8)	-0.3533(4)	2.1(2)
C(3)	-0.5353(5)	-0.6090(7)	-0.3189(5)	2.6(2)
C(4)	-0.4615(5)	-0.6218(8)	-0.2908(4)	2.3(2)
C(5)	-0.4060(5)	-0.5302(8)	-0.3023(4)	2.5(2)
C(6)	-0.4230(5)	-0.4202(8)	-0.3392(4)	1.0(2)
C(7)	-0.3556(5)	-0.3379(9)	-0.3593(4)	1.8(2)
C(8)	-0.3229(4)	-0.2452(7)	-0.3177(5)	2.1(2)
C(9)	-0.2510(5)	-0.1905(7)	-0.3364(4)	2.7(2)
C(10)	-0.2142(5)	-0.2259(9)	-0.3912(4)	2.3(2)
C(11)	-0.2476(5)	-0.3144(8)	-0.4329(4)	2.5(2)
C(12)	-0.3187(4)	-0.3692(8)	-0.4175(4)	1.7(2)
C(13)	-0.3517(5)	-0.4680(8)	-0.4605(4)	2.7(2)
C(14)	-0.3237(5)	-0.5464(8)	-0.2763(4)	2.8(2)
C(15)	-0.5844(5)	-0.3300(9)	-0.5299(4)	3.4(2)
C(16)	-0.5749(6)	-0.474(1)	-0.5248(4)	3.9(3)
C(17)	-0.6579(6)	-0.302(1)	-0.5711(5)	5.2(3)
C(18)	-0.5121(6)	-0.276(1)	-0.5637(5)	3.7(3)
C(19)	-0.5994(6)	-0.080(1)	-0.4566(5)	4.1(3)
C(20)	-0.6955(5)	-0.300(1)	-0.4150(5)	3.4(3)
C(21)	-0.2539(6)	-0.2135(9)	-0.1476(5)	2.7(2)
C(22)	-0.1855(6)	-0.265(1)	-0.1884(5)	4.0(3)
C(23)	-0.2202(7)	-0.129(1)	-0.0932(5)	5.1(3)
C(24)	-0.2968(5)	-0.327(1)	-0.1155(5)	4.0(3)
C(25)	-0.4138(6)	-0.079(1)	-0.1459(5)	3.9(3)
C(26)	-0.2831(6)	0.0353(9)	-0.2192(5)	4.1(3)
C(27)	-0.5204(5)	-0.3736(9)	-0.1869(4)	2.9(2)
C(28)	-0.5755(6)	-0.363(1)	-0.1304(5)	3.8(3)
C(29)	-0.6511(7)	-0.314(2)	-0.1618(5)	6.9(4)
C(30)	-0.6324(6)	-0.278(1)	-0.2272(6)	5.2(3)
C(31)	-0.4125(7)	0.1141(9)	-0.3799(5)	4.8(3)
C(32)	-0.4296(6)	0.1659(9)	-0.4462(5)	5.1(3)
C(33)	-0.3955(6)	0.0645(9)	-0.4912(5)	3.8(3)
C(34)	-0.3862(5)	-0.0527(9)	-0.4489(5)	2.3(2)
H(1)	-0.606	-0.500	-0.370	2.499
H(2)	-0.572	-0.675	-0.313	3.171
H(3)	-0.450	-0.693	-0.264	2.790
H(4)	-0.228	-0.127	-0.310	3.248
H(5)	-0.165	-0.190	-0.401	2.819
H(6)	-0.222	-0.337	-0.472	3.035
H(7)	-0.320	-0.477	-0.498	3.206
H(8)	-0.403	-0.444	-0.473	3.206
H(9)	-0.354	-0.546	-0.438	3.206
H(10)	-0.300	-0.618	-0.296	3.323

H(11)	-0.326	-0.558	-0.231	3.323
H(12)	-0.294	-0.473	-0.286	3.323
H(13)	-0.619	-0.509	-0.504	4.642
H(14)	-0.570	-0.509	-0.567	4.642
H(15)	-0.530	-0.493	-0.500	4.642
H(16)	-0.702	-0.336	-0.550	6.275
H(17)	-0.652	-0.340	-0.613	6.275
H(18)	-0.664	-0.213	-0.576	6.275
H(19)	-0.507	-0.315	-0.605	4.485
H(20)	-0.518	-0.187	-0.569	4.485
H(21)	-0.467	-0.294	-0.538	4.485
H(22)	-0.552	-0.053	-0.476	4.891
H(23)	-0.642	-0.058	-0.484	4.891
H(24)	-0.605	-0.041	-0.416	4.891
H(25)	-0.705	-0.257	-0.376	4.116
H(26)	-0.698	-0.389	-0.408	4.116
H(27)	-0.734	-0.277	-0.446	4.116
H(28)	-0.205	-0.323	-0.220	4.844
H(29)	-0.160	-0.197	-0.210	4.844
H(30)	-0.149	-0.307	-0.161	4.844
H(31)	-0.194	-0.058	-0.112	6.128
H(32)	-0.184	-0.176	-0.068	6.128
H(33)	-0.261	-0.100	-0.066	6.128
H(34)	-0.262	-0.369	-0.087	4.750
H(35)	-0.340	-0.296	-0.092	4.750
H(36)	-0.314	-0.383	-0.148	4.750
H(37)	-0.450	-0.032	-0.171	4.638
H(38)	-0.438	-0.155	-0.131	4.638
H(39)	-0.397	-0.030	-0.110	4.638
H(40)	-0.265	0.077	-0.181	4.861
H(41)	-0.240	0.022	-0.248	4.861
H(42)	-0.321	0.086	-0.240	4.861
H(43)	-0.469	-0.356	-0.174	3.467
H(44)	-0.523	-0.456	-0.205	3.467
H(45)	-0.556	-0.304	-0.099	4.618
H(46)	-0.583	-0.443	-0.111	4.618
H(47)	-0.670	-0.243	-0.139	8.322
H(48)	-0.689	-0.379	-0.162	8.322
H(49)	-0.652	-0.195	-0.236	6.255
H(50)	-0.655	-0.337	-0.257	6.255
H(51)	-0.449	0.144	-0.349	5.804
H(52)	-0.362	0.137	-0.366	5.804
H(53)	-0.405	0.245	-0.453	6.105
H(54)	-0.484	0.175	-0.453	6.105
H(55)	-0.430	0.048	-0.526	4.583
H(56)	-0.347	0.091	-0.508	4.583
H(57)	-0.413	-0.122	-0.468	2.819
H(58)	-0.333	-0.073	-0.444	2.819

$$B_{eq} = 8/3 \pi^2 (U_{11}(aa^*)^2 + U_{22}(bb^*)^2 + U_{33}(cc^*)^2 + 2U_{12}(aa^*bb^*)\cos \gamma + 2U_{13}(aa^*cc^*)\cos \beta + 2U_{23}(bb^*cc^*)\cos \alpha)$$

Table 3. Anisotropic Displacement Parameters for [DADMB]YCl(THF)₂ (2).

atom	U ₁₁	U ₂₂	U ₃₃	U ₁₂	U ₁₃	U ₂₃
Y(1)	0.0240(4)	0.0293(4)	0.0276(4)	-0.0010(4)	0.0011(5)	-0.0024(5)
Cl(1)	0.049(2)	0.040(1)	0.054(2)	0.012(1)	0.015(1)	0.001(1)
Si(1)	0.024(1)	0.037(2)	0.034(2)	-0.001(1)	-0.003(1)	0.002(1)
Si(2)	0.032(1)	0.038(2)	0.031(2)	-0.008(1)	0.002(1)	-0.007(1)
O(1)	0.025(4)	0.049(4)	0.026(4)	0.008(3)	0.000(3)	0.003(3)
O(2)	0.044(4)	0.027(4)	0.027(4)	-0.008(3)	0.010(3)	-0.005(3)
N(1)	0.013(4)	0.032(4)	0.026(4)	0.001(4)	0.002(3)	0.004(3)
N(2)	0.029(4)	0.030(4)	0.019(4)	-0.010(4)	0.003(3)	-0.004(3)
C(1)	0.023(5)	0.030(5)	0.033(6)	-0.002(4)	-0.008(4)	-0.002(4)
C(2)	0.028(5)	0.026(5)	0.044(6)	0.003(5)	-0.002(4)	-0.003(4)
C(3)	0.038(5)	0.024(4)	0.037(6)	-0.013(4)	0.008(5)	-0.015(6)
C(4)	0.042(6)	0.018(5)	0.040(7)	-0.001(4)	-0.004(4)	0.004(3)
C(5)	0.025(5)	0.040(6)	0.032(7)	0.010(4)	-0.005(4)	0.007(4)
C(6)	0.022(5)	0.022(5)	0.028(5)	-0.008(4)	0.005(3)	-0.002(4)
C(7)	0.028(5)	0.040(6)	0.013(5)	-0.002(5)	-0.009(4)	0.003(4)
C(8)	0.028(4)	0.021(4)	0.027(5)	-0.003(3)	-0.002(5)	0.005(5)
C(9)	0.033(6)	0.023(5)	0.041(7)	-0.005(4)	-0.006(4)	0.006(4)
C(10)	0.025(5)	0.046(6)	0.040(7)	-0.009(5)	0.002(4)	0.019(5)
C(11)	0.040(6)	0.042(6)	0.021(5)	0.015(5)	-0.006(4)	0.001(4)
C(12)	0.017(5)	0.030(5)	0.025(6)	0.005(4)	-0.004(4)	0.001(4)
C(13)	0.030(5)	0.037(6)	0.033(5)	-0.001(5)	0.003(4)	-0.006(4)
C(14)	0.041(6)	0.027(5)	0.043(6)	0.001(5)	0.000(5)	0.004(4)
C(15)	0.040(6)	0.043(6)	0.028(6)	-0.013(5)	-0.019(4)	0.000(5)
C(16)	0.054(7)	0.068(8)	0.029(6)	0.005(6)	0.003(5)	-0.021(5)
C(17)	0.036(6)	0.083(9)	0.048(7)	-0.009(6)	-0.015(5)	0.005(6)
C(18)	0.046(7)	0.071(7)	0.035(6)	-0.002(6)	-0.003(5)	-0.001(5)
C(19)	0.056(7)	0.061(8)	0.034(6)	0.012(6)	-0.013(5)	-0.007(5)
C(20)	0.022(5)	0.078(8)	0.041(7)	-0.010(6)	-0.006(4)	0.001(5)
C(21)	0.042(6)	0.048(6)	0.040(6)	-0.018(5)	-0.005(5)	0.004(5)
C(22)	0.042(7)	0.072(8)	0.033(7)	0.004(6)	0.002(5)	0.000(6)
C(23)	0.065(8)	0.079(9)	0.056(8)	-0.009(7)	-0.027(6)	-0.007(6)
C(24)	0.038(6)	0.064(7)	0.038(6)	-0.025(6)	-0.004(4)	0.006(6)
C(25)	0.053(7)	0.067(8)	0.039(7)	-0.005(6)	-0.002(5)	-0.022(6)
C(26)	0.039(6)	0.026(6)	0.080(8)	-0.012(5)	0.001(5)	-0.020(5)
C(27)	0.028(5)	0.048(6)	0.032(6)	0.006(5)	0.007(4)	0.007(4)
C(28)	0.032(6)	0.069(8)	0.035(7)	0.015(6)	0.007(5)	0.014(5)
C(29)	0.058(8)	0.17(2)	0.034(8)	0.023(10)	0.021(6)	0.046(8)
C(30)	0.030(6)	0.086(10)	0.074(9)	0.014(7)	0.006(6)	0.023(7)
C(31)	0.093(10)	0.030(5)	0.060(8)	-0.014(6)	0.040(7)	-0.021(6)
C(32)	0.069(7)	0.034(6)	0.070(8)	-0.007(6)	0.022(6)	0.008(6)
C(33)	0.049(7)	0.039(6)	0.050(7)	0.008(5)	0.012(5)	0.014(5)
C(34)	0.040(6)	0.051(6)	0.025(6)	0.011(5)	0.014(4)	-0.005(5)

The general temperature factor expression:

$$\exp(-2\pi^2(a^2U_{11}h^2 + b^2U_{22}k^2 + c^2U_{33}l^2 + 2a*b*U_{12}hk + 2a*c*U_{13}hl + 2b*c*U_{23}kl))$$

Table 4. Bond Lengths (Å) for [DADMB]YCl(THF)₂ (**2**).

atom	atom	distance	atom	atom	distance
Y(1)	Cl(1)	2.574(2)	Y(1)	O(1)	2.365(6)

Y(1)	O(2)	2.388(5)	Y(1)	N(1)	2.247(7)
Y(1)	N(2)	2.252(7)	Y(1)	C(1)	2.745(8)
Y(1)	C(6)	2.847(8)	Y(1)	C(7)	2.884(9)
Y(1)	C(8)	2.749(7)	Si(1)	N(1)	1.726(7)
Si(1)	C(15)	1.904(10)	Si(1)	C(19)	1.88(1)
Si(1)	C(20)	1.876(9)	Si(2)	N(2)	1.727(7)
Si(2)	C(21)	1.895(10)	Si(2)	C(25)	1.88(1)
Si(2)	C(26)	1.870(10)	O(1)	C(27)	1.48(1)
O(1)	C(30)	1.46(1)	O(2)	C(31)	1.45(1)
O(2)	C(34)	1.429(10)	N(1)	C(1)	1.41(1)
N(2)	C(8)	1.41(1)	C(1)	C(2)	1.43(1)
C(1)	C(6)	1.45(1)	C(2)	C(3)	1.34(1)
C(3)	C(4)	1.40(1)	C(4)	C(5)	1.38(1)
C(5)	C(6)	1.42(1)	C(5)	C(14)	1.52(1)
C(6)	C(7)	1.51(1)	C(7)	C(8)	1.42(1)
C(7)	C(12)	1.40(1)	C(8)	C(9)	1.42(1)
C(9)	C(10)	1.35(1)	C(10)	C(11)	1.40(1)
C(11)	C(12)	1.39(1)	C(12)	C(13)	1.49(1)
C(15)	C(16)	1.53(1)	C(15)	C(17)	1.55(1)
C(15)	C(18)	1.53(1)	C(21)	C(22)	1.55(1)
C(21)	C(23)	1.55(1)	C(21)	C(24)	1.55(1)
C(27)	C(28)	1.51(1)	C(28)	C(29)	1.54(1)
C(29)	C(30)	1.44(1)	C(31)	C(32)	1.51(2)
C(32)	C(33)	1.53(1)	C(33)	C(34)	1.52(1)

Table 5. Bond Angles (°) for [DADMB]YCl(THF)₂ (**2**).

atom	atom	atom	angle	atom	atom	atom	angle
Cl(1)	Y(1)	O(1)	83.5(2)	N(2)	Y(1)	C(1)	99.3(2)
Cl(1)	Y(1)	O(2)	84.3(1)	N(2)	Y(1)	C(6)	69.7(2)
Cl(1)	Y(1)	N(1)	116.9(2)	N(2)	Y(1)	C(7)	55.5(2)
Cl(1)	Y(1)	N(2)	119.8(2)	N(2)	Y(1)	C(8)	30.7(2)
Cl(1)	Y(1)	C(1)	136.0(2)	C(1)	Y(1)	C(6)	29.9(2)
Cl(1)	Y(1)	C(6)	162.2(2)	C(1)	Y(1)	C(7)	54.9(2)
Cl(1)	Y(1)	C(7)	167.3(2)	C(1)	Y(1)	C(8)	82.7(2)
Cl(1)	Y(1)	C(8)	141.2(2)	C(6)	Y(1)	C(7)	30.5(2)
O(1)	Y(1)	O(2)	167.9(2)	C(6)	Y(1)	C(8)	54.5(2)
O(1)	Y(1)	N(1)	94.3(2)	C(7)	Y(1)	C(8)	29.1(2)
O(1)	Y(1)	N(2)	91.8(2)	N(1)	Si(1)	C(15)	112.9(4)
O(1)	Y(1)	C(1)	75.3(2)	N(1)	Si(1)	C(19)	107.0(4)
O(1)	Y(1)	C(6)	81.1(2)	N(1)	Si(1)	C(20)	115.6(4)
O(1)	Y(1)	C(7)	107.7(2)	C(15)	Si(1)	C(19)	107.6(5)
O(1)	Y(1)	C(8)	112.3(2)	C(15)	Si(1)	C(20)	108.3(4)
O(2)	Y(1)	N(1)	91.6(2)	C(19)	Si(1)	C(20)	104.9(5)
O(2)	Y(1)	N(2)	93.8(2)	N(2)	Si(2)	C(21)	112.8(4)
O(2)	Y(1)	C(1)	114.3(2)	N(2)	Si(2)	C(25)	106.0(4)
O(2)	Y(1)	C(6)	111.0(2)	N(2)	Si(2)	C(26)	114.6(4)
O(2)	Y(1)	C(7)	84.3(2)	C(21)	Si(2)	C(25)	109.9(5)
O(2)	Y(1)	C(8)	77.3(2)	C(21)	Si(2)	C(26)	108.6(4)
N(1)	Y(1)	N(2)	123.3(2)	C(25)	Si(2)	C(26)	104.5(5)
N(1)	Y(1)	C(1)	30.8(2)	Y(1)	O(1)	C(27)	128.6(5)
N(1)	Y(1)	C(6)	55.9(2)	Y(1)	O(1)	C(30)	125.8(6)
N(1)	Y(1)	C(7)	69.1(2)	C(27)	O(1)	C(30)	105.1(7)
N(1)	Y(1)	C(8)	97.6(3)	Y(1)	O(2)	C(31)	127.5(5)

Y(1)	O(2)	C(34)	125.6(5)	Y(1)	C(7)	C(6)	73.4(5)
C(31)	O(2)	C(34)	106.9(7)	Y(1)	C(7)	C(8)	70.2(5)
Y(1)	N(1)	Si(1)	126.7(4)	Y(1)	C(7)	C(12)	138.7(6)
Y(1)	N(1)	C(1)	94.5(5)	C(6)	C(7)	C(8)	122.3(7)
Si(1)	N(1)	C(1)	128.8(6)	C(6)	C(7)	C(12)	116.7(7)
Y(1)	N(2)	Si(2)	126.0(4)	C(8)	C(7)	C(12)	120.3(8)
Y(1)	N(2)	C(8)	94.6(5)	Y(1)	C(8)	N(2)	54.7(4)
Si(2)	N(2)	C(8)	127.8(6)	Y(1)	C(8)	C(7)	80.7(5)
Y(1)	C(1)	N(1)	54.7(4)	Y(1)	C(8)	C(9)	136.3(5)
Y(1)	C(1)	C(2)	135.3(6)	N(2)	C(8)	C(7)	120.4(7)
Y(1)	C(1)	C(6)	79.0(5)	N(2)	C(8)	C(9)	122.2(7)
N(1)	C(1)	C(2)	124.3(7)	C(7)	C(8)	C(9)	117.3(8)
N(1)	C(1)	C(6)	117.8(7)	C(8)	C(9)	C(10)	121.7(8)
C(2)	C(1)	C(6)	117.7(7)	C(9)	C(10)	C(11)	120.7(8)
C(1)	C(2)	C(3)	121.5(8)	C(10)	C(11)	C(12)	119.9(8)
C(2)	C(3)	C(4)	121.8(8)	C(7)	C(12)	C(11)	119.8(8)
C(3)	C(4)	C(5)	119.1(8)	C(7)	C(12)	C(13)	120.6(8)
C(4)	C(5)	C(6)	121.6(8)	C(11)	C(12)	C(13)	119.4(8)
C(4)	C(5)	C(14)	120.2(8)	Si(1)	C(15)	C(16)	110.5(6)
C(6)	C(5)	C(14)	118.2(7)	Si(1)	C(15)	C(17)	109.5(7)
Y(1)	C(6)	C(1)	71.1(5)	Si(1)	C(15)	C(18)	110.7(6)
Y(1)	C(6)	C(5)	136.6(6)	C(16)	C(15)	C(17)	108.2(8)
Y(1)	C(6)	C(7)	76.1(5)	C(16)	C(15)	C(18)	108.2(9)
C(1)	C(6)	C(5)	118.2(7)	C(17)	C(15)	C(18)	109.7(8)
C(1)	C(6)	C(7)	123.3(7)	Si(2)	C(21)	C(22)	112.9(7)
C(5)	C(6)	C(7)	117.6(7)	Si(2)	C(21)	C(23)	110.0(7)
Si(2)	C(21)	C(24)	108.3(6)	C(22)	C(21)	C(23)	108.5(8)
C(22)	C(21)	C(24)	108.9(8)	C(23)	C(21)	C(24)	108.2(8)
O(1)	C(27)	C(28)	104.8(7)	C(27)	C(28)	C(29)	103.2(8)
C(28)	C(29)	C(30)	107.2(9)	O(1)	C(30)	C(29)	108.0(9)
O(2)	C(31)	C(32)	104.2(8)	C(31)	C(32)	C(33)	103.1(8)
C(32)	C(33)	C(34)	104.9(8)	O(2)	C(34)	C(33)	106.6(7)

Structural data for [DADMB]Y(OSiMe₃)(THF)₂ (**4**).

Table 6. Atomic coordinates and B_{iso}/B_{eq} for [DADMB]Y(OSiMe₃)(THF)₂ (**4**).

atom	x	y	z	B _{eq}
Y(1)	0.85703(4)	0.21349(2)	0.09482(2)	1.686(9)
Si(1)	0.5669(1)	0.28712(8)	0.03117(6)	2.05(3)
Si(2)	1.1176(1)	0.13056(7)	0.19181(6)	2.06(3)
Si(3)	0.9591(1)	0.22446(8)	-0.05574(6)	2.47(3)
O(1)	0.9183(3)	0.2162(2)	0.0099(1)	2.21(7)
O(2)	0.9301(3)	0.3411(2)	0.1082(1)	2.30(7)
O(3)	0.7966(3)	0.0859(2)	0.0647(1)	2.29(7)
N(1)	0.6663(3)	0.2496(2)	0.0959(2)	1.68(8)
N(2)	0.9805(3)	0.1761(2)	0.1861(2)	1.80(8)
C(1)	0.6432(4)	0.1952(2)	0.1394(2)	1.82(9)
C(2)	0.5441(4)	0.1439(3)	0.1262(2)	2.4(1)
C(3)	0.5279(4)	0.0868(3)	0.1671(2)	2.7(1)
C(4)	0.6099(4)	0.0776(3)	0.2246(2)	2.9(1)
C(5)	0.7078(4)	0.1273(3)	0.2410(2)	2.4(1)
C(6)	0.7261(4)	0.1862(2)	0.1991(2)	1.71(9)
C(7)	0.8235(4)	0.2444(2)	0.2254(2)	1.74(9)

C(8)	0.9472(4)	0.2319(2)	0.2257(2)	1.77(10)
C(9)	1.0323(4)	0.2832(3)	0.2637(2)	2.7(1)
C(10)	0.9957(5)	0.3414(3)	0.2966(2)	3.1(1)
C(11)	0.8747(5)	0.3553(3)	0.2941(2)	2.9(1)
C(12)	0.7890(4)	0.3067(3)	0.2592(2)	2.2(1)
C(13)	0.6576(5)	0.3186(3)	0.2604(2)	3.4(1)
C(14)	0.7914(5)	0.1192(3)	0.3048(2)	3.1(1)
C(15)	0.6609(5)	0.3412(3)	-0.0145(2)	3.1(1)
C(16)	0.4820(5)	0.2136(3)	-0.0260(2)	3.7(1)
C(17)	0.4532(4)	0.3566(3)	0.0524(2)	2.6(1)
C(18)	0.3634(5)	0.3844(3)	-0.0083(3)	3.9(1)
C(19)	0.3795(4)	0.3184(3)	0.0957(3)	3.2(1)
C(20)	0.5171(5)	0.4272(3)	0.0861(3)	3.3(1)
C(21)	1.1081(5)	0.0827(3)	0.1139(2)	2.8(1)
C(22)	1.2534(4)	0.1950(3)	0.2037(3)	3.1(1)
C(23)	1.1493(4)	0.0537(3)	0.2552(2)	2.4(1)
C(24)	1.0473(5)	-0.0069(3)	0.2443(2)	3.3(1)
C(25)	1.1615(5)	0.0897(3)	0.3204(2)	3.0(1)
C(26)	1.2679(5)	0.0116(3)	0.2537(3)	3.6(1)
C(27)	1.1044(6)	0.1737(4)	-0.0519(3)	4.5(2)
C(28)	0.8452(6)	0.1831(3)	-0.1227(3)	4.1(2)
C(29)	0.9823(5)	0.3270(3)	-0.0753(3)	3.6(1)
C(30)	1.0491(4)	0.3632(3)	0.1025(2)	2.6(1)
C(31)	1.0347(5)	0.4461(3)	0.0800(2)	3.6(1)
C(32)	0.9283(5)	0.4761(3)	0.1040(3)	4.0(1)
C(33)	0.8796(5)	0.4075(3)	0.1333(2)	3.0(1)
C(34)	0.7783(5)	0.0554(3)	0.0008(2)	3.3(1)
C(35)	0.6824(5)	-0.0051(3)	-0.0040(3)	3.7(1)
C(36)	0.6744(5)	-0.0232(3)	0.0633(3)	3.3(1)
C(37)	0.7762(4)	0.0225(3)	0.1036(2)	2.6(1)
H(1)	0.4864	0.1492	0.0874	2.8668
H(2)	0.4604	0.0532	0.1561	3.2338
H(3)	0.5989	0.0374	0.2526	3.4356
H(4)	1.1161	0.2762	0.2659	3.2603
H(5)	1.0547	0.3735	0.3222	3.7772
H(6)	0.8510	0.3978	0.3162	3.5142
H(7)	0.6506	0.3609	0.2872	4.0958
H(8)	0.6272	0.2733	0.2760	4.0958
H(9)	0.6127	0.3290	0.2189	4.0958
H(10)	0.8717	0.1123	0.2998	3.7484
H(11)	0.7872	0.1644	0.3289	3.7484
H(12)	0.7681	0.0758	0.3259	3.7484
H(13)	0.7022	0.3818	0.0108	3.7350
H(14)	0.7179	0.3072	-0.0260	3.7350
H(15)	0.6104	0.3622	-0.0515	3.7350
H(16)	0.5378	0.1802	-0.0393	4.4608
H(17)	0.4347	0.2392	-0.0617	4.4608
H(18)	0.4308	0.1843	-0.0058	4.4608
H(19)	0.4068	0.4086	-0.0356	4.6847
H(20)	0.3083	0.4202	0.0028	4.6847
H(21)	0.3202	0.3414	-0.0291	4.6847
H(22)	0.3241	0.3548	0.1058	3.7946
H(23)	0.3364	0.2756	0.0746	3.7946
H(24)	0.4325	0.3014	0.1334	3.7946
H(25)	0.5722	0.4115	0.1236	3.9907
H(26)	0.5597	0.4529	0.0591	3.9907
H(27)	0.4591	0.4613	0.0966	3.9907
H(28)	1.1815	0.0564	0.1142	3.3654

H(29)	1.0433	0.0468	0.1064	3.3654
H(30)	1.0945	0.1205	0.0814	3.3654
H(31)	1.2431	0.2315	0.1703	3.6820
H(32)	1.2625	0.2214	0.2428	3.6820
H(33)	1.3233	0.1648	0.2040	3.6820
H(34)	1.0652	-0.0453	0.2763	3.9170
H(35)	1.0408	-0.0302	0.2041	3.9170
H(36)	0.9732	0.0175	0.2459	3.9170
H(37)	1.0879	0.1144	0.3227	3.6443
H(38)	1.1793	0.0507	0.3518	3.6443
H(39)	1.2249	0.1266	0.3274	3.6443
H(40)	1.3327	0.0475	0.2616	4.2624
H(41)	1.2619	-0.0112	0.2133	4.2624
H(42)	1.2823	-0.0273	0.2852	4.2624
H(43)	1.0952	0.1206	-0.0433	5.3693
H(44)	1.1273	0.1789	-0.0912	5.3693
H(45)	1.1649	0.1956	-0.0193	5.3693
H(46)	0.8344	0.1299	-0.1151	4.9072
H(47)	0.7707	0.2094	-0.1264	4.9072
H(48)	0.8725	0.1889	-0.1607	4.9072
H(49)	1.0054	0.3297	-0.1147	4.3223
H(50)	0.9093	0.3548	-0.0779	4.3223
H(51)	1.0439	0.3489	-0.0433	4.3223
H(52)	1.1046	0.3598	0.1422	3.0893
H(53)	1.0759	0.3316	0.0727	3.0893
H(54)	1.0187	0.4484	0.0352	4.2694
H(55)	1.1053	0.4751	0.0972	4.2694
H(56)	0.9534	0.5153	0.1346	4.7645
H(57)	0.8684	0.4961	0.0701	4.7645
H(58)	0.9049	0.4091	0.1780	3.6062
H(59)	0.7939	0.4064	0.1217	3.6062
H(60)	0.7523	0.0950	-0.0293	3.9175
H(61)	0.8508	0.0333	-0.0060	3.9175
H(62)	0.6073	0.0138	-0.0274	4.4350
H(63)	0.7041	-0.0501	-0.0240	4.4350
H(64)	0.6850	-0.0768	0.0717	3.9379
H(65)	0.5988	-0.0072	0.0707	3.9379
H(66)	0.8468	-0.0084	0.1151	3.1373
H(67)	0.7539	0.0407	0.1406	3.1373

$$B_{eq} = 8/3 \pi^2 (U_{11}(aa^*)^2 + U_{22}(bb^*)^2 + U_{33}(cc^*)^2 + 2U_{12}(aa^*bb^*)\cos \gamma + 2U_{13}(aa^*cc^*)\cos \beta + 2U_{23}(bb^*cc^*)\cos \alpha)$$

Table 7. Anisotropic Displacement Parameters for [DADMB]Y(OSiMe₃)(THF)₂ (**4**).

atom	U ₁₁	U ₂₂	U ₃₃	U ₁₂	U ₁₃	U ₂₃
Y(1)	0.0231(2)	0.0194(2)	0.0216(2)	-0.0008(2)	0.0065(2)	-0.0007(2)
Si(1)	0.0274(7)	0.0274(7)	0.0235(6)	0.0021(6)	0.0060(5)	0.0020(6)
Si(2)	0.0260(7)	0.0293(7)	0.0249(7)	0.0044(6)	0.0090(5)	0.0040(6)
Si(3)	0.0367(7)	0.0319(8)	0.0251(7)	0.0021(6)	0.0093(6)	0.0013(6)
O(1)	0.032(2)	0.028(2)	0.026(2)	-0.003(2)	0.010(1)	0.002(1)
O(2)	0.032(2)	0.018(2)	0.038(2)	-0.004(1)	0.012(1)	-0.005(1)
O(3)	0.037(2)	0.024(2)	0.024(2)	-0.005(1)	0.012(1)	-0.007(1)

N(1)	0.027(2)	0.019(2)	0.020(2)	0.002(2)	0.007(2)	0.004(2)
N(2)	0.023(2)	0.026(2)	0.021(2)	-0.001(2)	0.005(2)	-0.004(2)
C(1)	0.025(2)	0.014(2)	0.027(2)	0.007(2)	0.007(2)	0.000(2)
C(2)	0.028(3)	0.031(3)	0.029(3)	0.000(2)	0.007(2)	-0.002(2)
C(3)	0.031(3)	0.033(3)	0.041(3)	-0.004(2)	0.018(2)	0.000(2)
C(4)	0.040(3)	0.025(3)	0.040(3)	0.002(2)	0.021(2)	0.009(2)
C(5)	0.035(3)	0.029(3)	0.027(3)	0.009(2)	0.013(2)	0.003(2)
C(6)	0.025(2)	0.021(2)	0.022(2)	0.003(2)	0.012(2)	0.000(2)
C(7)	0.033(3)	0.022(2)	0.015(2)	0.003(2)	0.009(2)	0.006(2)
C(8)	0.032(2)	0.021(3)	0.018(2)	0.002(2)	0.008(2)	0.006(2)
C(9)	0.032(3)	0.036(3)	0.030(3)	0.001(2)	0.002(2)	-0.001(2)
C(10)	0.047(3)	0.039(3)	0.029(3)	-0.003(3)	0.004(2)	-0.010(2)
C(11)	0.057(3)	0.032(3)	0.030(3)	0.006(3)	0.013(2)	-0.006(2)
C(12)	0.042(3)	0.026(3)	0.019(2)	0.008(2)	0.010(2)	0.001(2)
C(13)	0.046(3)	0.042(3)	0.040(3)	0.014(3)	0.011(3)	-0.011(3)
C(14)	0.042(3)	0.044(3)	0.035(3)	0.005(2)	0.015(2)	0.012(3)
C(15)	0.043(3)	0.053(4)	0.026(3)	0.012(3)	0.013(2)	0.013(2)
C(16)	0.052(3)	0.050(3)	0.033(3)	-0.002(3)	-0.001(2)	-0.010(3)
C(17)	0.028(3)	0.031(3)	0.037(3)	0.006(2)	0.011(2)	0.011(2)
C(18)	0.039(3)	0.050(4)	0.054(4)	0.014(3)	0.006(3)	0.020(3)
C(19)	0.035(3)	0.046(3)	0.049(3)	0.006(2)	0.014(3)	0.001(3)
C(20)	0.053(3)	0.025(3)	0.055(4)	0.005(2)	0.022(3)	-0.001(3)
C(21)	0.044(3)	0.049(3)	0.028(3)	0.021(3)	0.015(2)	0.004(2)
C(22)	0.029(3)	0.044(3)	0.057(4)	0.002(2)	0.016(2)	0.008(3)
C(23)	0.027(3)	0.032(3)	0.026(3)	0.004(2)	0.007(2)	0.003(2)
C(24)	0.053(3)	0.037(3)	0.035(3)	-0.007(3)	0.008(3)	0.007(2)
C(25)	0.046(3)	0.051(3)	0.028(3)	0.000(3)	0.004(2)	0.011(2)
C(26)	0.052(4)	0.045(3)	0.045(3)	0.010(3)	0.013(3)	0.017(3)
C(27)	0.062(4)	0.071(4)	0.061(4)	0.029(3)	0.034(3)	0.016(3)
C(28)	0.082(5)	0.056(4)	0.036(3)	-0.014(3)	0.011(3)	-0.002(3)
C(29)	0.062(4)	0.042(3)	0.040(3)	-0.008(3)	0.012(3)	0.008(3)
C(30)	0.034(3)	0.030(3)	0.037(3)	-0.009(2)	0.007(2)	-0.004(2)
C(31)	0.058(4)	0.034(3)	0.040(3)	-0.016(3)	0.016(3)	0.000(2)
C(32)	0.056(4)	0.028(3)	0.070(4)	0.003(3)	0.022(3)	0.006(3)
C(33)	0.047(3)	0.021(3)	0.048(3)	0.001(2)	0.016(3)	-0.002(2)
C(34)	0.060(4)	0.038(3)	0.027(3)	-0.015(3)	0.013(3)	-0.012(2)
C(35)	0.047(3)	0.044(4)	0.047(4)	-0.017(3)	-0.001(3)	-0.006(3)
C(36)	0.048(3)	0.039(3)	0.048(3)	-0.011(3)	0.021(3)	-0.012(3)
C(37)	0.043(3)	0.023(3)	0.039(3)	-0.006(2)	0.018(2)	0.000(2)

The general temperature factor expression:

$$\exp(-2\pi^2(a^2U_{11}h^2 + b^2U_{22}k^2 + c^2U_{33}l^2 + 2a*b*U_{12}hk + 2a*c*U_{13}hl + 2b*c*U_{23}kl))$$

Table 8. Bond Lengths (Å) for [DADMB]Y(OSiMe₃)(THF)₂ (**4**).

atom	atom	distance	atom	atom	distance
Y(1)	O(1)	2.111(3)	Y(1)	O(2)	2.358(3)
Y(1)	O(3)	2.365(3)	Y(1)	N(1)	2.262(3)
Y(1)	N(2)	2.254(3)	Y(1)	C(1)	2.827(4)
Y(1)	C(8)	2.816(4)	Si(1)	N(1)	1.724(3)
Si(1)	C(15)	1.864(5)	Si(1)	C(16)	1.889(5)
Si(1)	C(17)	1.897(5)	Si(2)	N(2)	1.726(4)
Si(2)	C(21)	1.867(5)	Si(2)	C(22)	1.876(5)

Si(2)	C(23)	1.893(4)	Si(3)	O(1)	1.601(3)
Si(3)	C(27)	1.856(6)	Si(3)	C(28)	1.862(6)
Si(3)	C(29)	1.861(5)	O(2)	C(30)	1.437(5)
O(2)	C(33)	1.448(5)	O(3)	C(34)	1.457(5)
O(3)	C(37)	1.436(5)	N(1)	C(1)	1.400(5)
N(2)	C(8)	1.401(5)	C(1)	C(2)	1.414(6)
C(1)	C(6)	1.431(6)	C(2)	C(3)	1.370(6)
C(3)	C(4)	1.392(7)	C(4)	C(5)	1.390(6)
C(5)	C(6)	1.414(6)	C(5)	C(14)	1.502(6)
C(6)	C(7)	1.513(6)	C(7)	C(8)	1.421(6)
C(7)	C(12)	1.410(6)	C(8)	C(9)	1.434(6)
C(9)	C(10)	1.354(7)	C(10)	C(11)	1.386(7)
C(11)	C(12)	1.381(7)	C(12)	C(13)	1.514(7)
C(17)	C(18)	1.554(7)	C(17)	C(19)	1.540(7)
C(17)	C(20)	1.525(7)	C(23)	C(24)	1.543(7)
C(23)	C(25)	1.526(7)	C(23)	C(26)	1.539(7)
C(30)	C(31)	1.516(7)	C(31)	C(32)	1.511(7)
C(32)	C(33)	1.511(7)	C(34)	C(35)	1.499(7)
C(35)	C(36)	1.517(7)	C(36)	C(37)	1.510(6)

Table 9. Bond Angles (°) for [DADMB]Y(OSiMe₃)(THF)₂ (**4**).

atom	atom	atom	angle	atom	atom	atom	angle
O(1)	Y(1)	O(2)	84.9(1)	O(1)	Y(1)	O(3)	84.9(1)
O(1)	Y(1)	N(1)	120.4(1)	O(1)	Y(1)	N(2)	120.8(1)
O(1)	Y(1)	C(1)	141.0(1)	O(1)	Y(1)	C(8)	139.6(1)
O(2)	Y(1)	O(3)	169.8(1)	O(2)	Y(1)	N(1)	92.9(1)
O(2)	Y(1)	N(2)	91.6(1)	O(2)	Y(1)	C(1)	111.7(1)
O(2)	Y(1)	C(8)	74.4(1)	O(3)	Y(1)	N(1)	92.4(1)
O(3)	Y(1)	N(2)	93.4(1)	O(3)	Y(1)	C(1)	76.7(1)
O(3)	Y(1)	C(8)	113.8(1)	N(1)	Y(1)	N(2)	118.8(1)
N(1)	Y(1)	C(1)	29.4(1)	N(1)	Y(1)	C(8)	95.3(1)
N(2)	Y(1)	C(1)	94.6(1)	N(2)	Y(1)	C(8)	29.5(1)
C(1)	Y(1)	C(8)	79.3(1)	N(1)	Si(1)	C(15)	106.0(2)
N(1)	Si(1)	C(16)	115.3(2)	N(1)	Si(1)	C(17)	113.5(2)
C(15)	Si(1)	C(16)	105.0(2)	C(15)	Si(1)	C(17)	108.2(2)
C(16)	Si(1)	C(17)	108.2(2)	N(2)	Si(2)	C(21)	105.6(2)
N(2)	Si(2)	C(22)	116.0(2)	N(2)	Si(2)	C(23)	113.4(2)
C(21)	Si(2)	C(22)	105.7(2)	C(21)	Si(2)	C(23)	108.0(2)
C(22)	Si(2)	C(23)	107.6(2)	O(1)	Si(3)	C(27)	110.4(2)
O(1)	Si(3)	C(28)	111.8(2)	O(1)	Si(3)	C(29)	111.9(2)
C(27)	Si(3)	C(28)	108.0(3)	C(27)	Si(3)	C(29)	107.1(3)
C(28)	Si(3)	C(29)	107.4(3)	Y(1)	O(1)	Si(3)	175.5(2)
Y(1)	O(2)	C(30)	123.5(3)	Y(1)	O(2)	C(33)	129.4(3)
C(30)	O(2)	C(33)	106.2(3)	Y(1)	O(3)	C(34)	125.1(3)
Y(1)	O(3)	C(37)	129.0(3)	C(34)	O(3)	C(37)	105.9(3)
Y(1)	N(1)	Si(1)	123.5(2)	Y(1)	N(1)	C(1)	98.3(2)
Si(1)	N(1)	C(1)	128.2(3)	Y(1)	N(2)	Si(2)	124.8(2)
Y(1)	N(2)	C(8)	98.1(2)	Si(2)	N(2)	C(8)	129.4(3)
Y(1)	C(1)	N(1)	52.3(2)	Y(1)	C(1)	C(2)	135.1(3)
Y(1)	C(1)	C(6)	83.1(2)	N(1)	C(1)	C(2)	123.1(4)
N(1)	C(1)	C(6)	120.0(4)	C(2)	C(1)	C(6)	116.7(4)
C(1)	C(2)	C(3)	122.6(4)	C(2)	C(3)	C(4)	120.4(4)
C(3)	C(4)	C(5)	119.8(4)	C(4)	C(5)	C(6)	120.5(4)

C(4)	C(5)	C(14)	119.0(4)	C(6)	C(5)	C(14)	120.5(4)
C(1)	C(6)	C(5)	120.0(4)	C(1)	C(6)	C(7)	123.3(4)
C(5)	C(6)	C(7)	116.0(4)	C(6)	C(7)	C(8)	122.7(4)
C(6)	C(7)	C(12)	116.3(4)	C(8)	C(7)	C(12)	120.3(4)
Y(1)	C(8)	N(2)	52.4(2)	Y(1)	C(8)	C(7)	82.9(2)
Y(1)	C(8)	C(9)	134.4(3)	N(2)	C(8)	C(7)	120.3(4)
N(2)	C(8)	C(9)	122.8(4)	C(7)	C(8)	C(9)	116.6(4)
C(8)	C(9)	C(10)	121.3(4)	C(9)	C(10)	C(11)	121.8(5)
C(10)	C(11)	C(12)	119.2(4)	C(7)	C(12)	C(11)	120.7(4)
C(7)	C(12)	C(13)	120.2(4)	C(11)	C(12)	C(13)	119.0(4)
Si(1)	C(17)	C(18)	110.2(3)	Si(1)	C(17)	C(19)	111.6(3)
Si(1)	C(17)	C(20)	110.4(3)	C(18)	C(17)	C(19)	107.9(4)
C(18)	C(17)	C(20)	108.1(4)	C(19)	C(17)	C(20)	108.5(4)
Si(2)	C(23)	C(24)	110.7(3)	Si(2)	C(23)	C(25)	110.5(3)
Si(2)	C(23)	C(26)	110.1(3)	C(24)	C(23)	C(25)	109.4(4)
C(24)	C(23)	C(26)	107.8(4)	C(25)	C(23)	C(26)	108.3(4)
O(2)	C(30)	C(31)	104.2(4)	C(30)	C(31)	C(32)	104.6(4)
C(31)	C(32)	C(33)	105.7(4)	O(2)	C(33)	C(32)	104.7(4)
O(3)	C(34)	C(35)	105.6(4)	C(34)	C(35)	C(36)	106.0(4)
C(35)	C(36)	C(37)	104.4(4)	O(3)	C(37)	C(36)	105.3(4)

Structural data for {[DADMB]YH(THF)}₂·C₆H₆ (**6**).

Table 10. Atomic coordinates and B_{iso}/B_{eq} for {[DADMB]YH(THF)}₂·C₆H₆ (**6**).

atom	x	y	z	B _{eq}
Y(1)	0.44736(4)	0.53415(2)	-0.10063(2)	2.41(1)
Si(1)	0.1375(2)	0.46337(10)	-0.21648(9)	4.32(4)
Si(2)	0.6749(1)	0.65248(8)	-0.11310(8)	3.03(3)
O(1)	0.5332(3)	0.4632(2)	-0.1800(2)	3.40(8)
N(1)	0.2377(3)	0.5276(2)	-0.1644(2)	2.98(9)
N(2)	0.5135(3)	0.6302(2)	-0.1492(2)	2.52(9)
C(1)	0.2056(4)	0.5871(3)	-0.1253(2)	2.6(1)
C(2)	0.1444(4)	0.5789(3)	-0.0660(3)	3.4(1)
C(3)	0.1261(4)	0.6337(4)	-0.0210(3)	3.5(1)
C(4)	0.1721(4)	0.7005(3)	-0.0324(3)	3.6(1)
C(5)	0.2338(4)	0.7115(3)	-0.0896(3)	2.9(1)
C(6)	0.2494(4)	0.6545(3)	-0.1380(2)	2.4(1)
C(7)	0.2908(4)	0.6719(2)	-0.2101(2)	2.5(1)
C(8)	0.4190(4)	0.6608(2)	-0.2134(3)	2.6(1)
C(9)	0.4455(4)	0.6776(3)	-0.2842(3)	2.8(1)
C(10)	0.3523(5)	0.7052(3)	-0.3465(3)	3.3(1)
C(11)	0.2269(5)	0.7166(3)	-0.3427(3)	3.7(1)
C(12)	0.1953(4)	0.7012(3)	-0.2742(3)	2.8(1)
C(13)	0.0613(5)	0.7200(3)	-0.2695(3)	3.9(1)
C(14)	0.2800(5)	0.7840(3)	-0.1014(3)	4.2(1)
C(15)	0.0645(6)	0.4865(4)	-0.3243(3)	5.1(2)
C(16)	-0.0053(8)	0.4226(5)	-0.3706(4)	7.8(2)
C(17)	-0.0356(6)	0.5447(4)	-0.3326(4)	6.6(2)
C(18)	0.1689(6)	0.5118(4)	-0.3602(3)	5.3(2)
C(19)	0.0005(7)	0.4402(4)	-0.1763(4)	7.0(2)
C(20)	0.2382(7)	0.3837(3)	-0.2115(3)	6.0(2)
C(21)	0.6991(5)	0.7354(3)	-0.0528(4)	4.6(1)
C(22)	0.6430(5)	0.7978(3)	-0.1066(4)	5.1(2)

C(23)	0.8459(6)	0.7504(4)	-0.0125(5)	8.2(2)
C(24)	0.6288(7)	0.7309(4)	0.0107(4)	6.6(2)
C(25)	0.7720(5)	0.6599(3)	-0.1856(4)	4.8(2)
C(26)	0.7487(4)	0.5778(3)	-0.0466(3)	3.6(1)
C(27)	0.5358(7)	0.4847(4)	-0.2578(3)	5.6(2)
C(28)	0.6103(9)	0.4393(4)	-0.2836(5)	9.0(3)
C(29)	0.6473(6)	0.3785(3)	-0.2278(4)	5.3(2)
C(30)	0.5975(7)	0.3948(4)	-0.1636(3)	5.5(2)
C(31)	0.5731(7)	0.0405(4)	-0.0341(4)	5.1(2)
C(32)	0.4485(9)	0.0573(4)	-0.0429(4)	5.5(2)
C(33)	0.3737(6)	0.0164(5)	-0.0099(4)	5.5(2)
H(1)	0.481(3)	0.560(2)	0.028(2)	2.0(8)
H(2)	0.1147	0.5337	-0.0569	4.0711
H(3)	0.0824	0.6266	0.0178	4.1605
H(4)	0.1607	0.7385	-0.0005	4.3710
H(5)	0.5302	0.6695	-0.2888	3.3718
H(6)	0.3738	0.7168	-0.3932	3.9768
H(7)	0.1626	0.7349	-0.3869	4.4663
H(8)	0.0550	0.7092	-0.2186	4.6808
H(9)	-0.0019	0.6940	-0.3077	4.6808
H(10)	0.0466	0.7687	-0.2793	4.6808
H(11)	0.3212	0.7830	-0.1420	5.0264
H(12)	0.3401	0.7997	-0.0539	5.0264
H(13)	0.2078	0.8150	-0.1156	5.0264
H(14)	-0.0409	0.4350	-0.4243	9.4085
H(15)	-0.0733	0.4081	-0.3498	9.4085
H(16)	0.0550	0.3854	-0.3662	9.4085
H(17)	-0.0706	0.5565	-0.3865	7.9134
H(18)	-0.1036	0.5290	-0.3124	7.9134
H(19)	0.0047	0.5847	-0.3041	7.9134
H(20)	0.2305	0.4754	-0.3573	6.3413
H(21)	0.1299	0.5241	-0.4136	6.3413
H(22)	0.2114	0.5516	-0.3321	6.3413
H(23)	0.0343	0.4235	-0.1240	8.4271
H(24)	-0.0515	0.4805	-0.1767	8.4271
H(25)	-0.0511	0.4046	-0.2079	8.4271
H(26)	0.3067	0.3934	-0.2339	7.2028
H(27)	0.2738	0.3700	-0.1582	7.2028
H(28)	0.1857	0.3468	-0.2400	7.2028
H(29)	0.6863	0.8018	-0.1460	6.1768
H(30)	0.6552	0.8396	-0.0764	6.1768
H(31)	0.5527	0.7905	-0.1307	6.1768
H(32)	0.8548	0.7939	0.0145	9.8419
H(33)	0.8907	0.7525	-0.0514	9.8419
H(34)	0.8816	0.7140	0.0237	9.8419
H(35)	0.6663	0.6946	0.0467	7.8713
H(36)	0.6372	0.7743	0.0379	7.8713
H(37)	0.5394	0.7211	-0.0132	7.8713
H(38)	0.8607	0.6683	-0.1582	5.7612
H(39)	0.7393	0.6976	-0.2206	5.7612
H(40)	0.7648	0.6174	-0.2146	5.7612
H(41)	0.8388	0.5865	-0.0233	4.3469
H(42)	0.7381	0.5356	-0.0762	4.3469
H(43)	0.7067	0.5734	-0.0066	4.3469
H(44)	0.4499	0.4845	-0.2926	6.6706
H(45)	0.5712	0.5306	-0.2555	6.6706
H(46)	0.5632	0.4225	-0.3341	10.7759
H(47)	0.6869	0.4624	-0.2868	10.7759

H(48)	0.6094	0.3364	-0.2528	6.3583
H(49)	0.7391	0.3735	-0.2100	6.3583
H(50)	0.5368	0.3601	-0.1590	6.6415
H(51)	0.6667	0.3969	-0.1161	6.6415
H(52)	0.6247	0.0690	-0.0572	6.1536
H(53)	0.4121	0.0977	-0.0722	6.6126
H(54)	0.2854	0.0285	-0.0163	6.5648

$$B_{eq} = 8/3 \pi^2 (U_{11}(aa^*)^2 + U_{22}(bb^*)^2 + U_{33}(cc^*)^2 + 2U_{12}(aa^*bb^*)\cos \gamma + 2U_{13}(aa^*cc^*)\cos \beta + 2U_{23}(bb^*cc^*)\cos \alpha)$$

Table 11. Anisotropic Displacement Parameters for {[DADMB]YH(THF)}₂-C₆H₆ (**6**).

atom	U ₁₁	U ₂₂	U ₃₃	U ₁₂	U ₁₃	U ₂₃
Y(1)	0.0383(3)	0.0348(3)	0.0220(2)	-0.0078(2)	0.0088(2)	0.0013(3)
Si(1)	0.065(1)	0.058(1)	0.0415(9)	-0.0350(9)	0.0060(8)	-0.0027(9)
Si(2)	0.0343(8)	0.0381(9)	0.0502(9)	-0.0011(6)	0.0176(7)	0.0086(7)
O(1)	0.074(2)	0.040(2)	0.026(2)	0.016(2)	0.011(2)	0.006(2)
N(1)	0.042(2)	0.038(3)	0.027(2)	-0.016(2)	0.007(2)	0.000(2)
N(2)	0.038(2)	0.028(2)	0.029(2)	0.001(2)	0.013(2)	0.001(2)
C(1)	0.024(2)	0.048(3)	0.022(2)	-0.006(2)	0.000(2)	0.007(2)
C(2)	0.033(3)	0.069(4)	0.030(3)	-0.016(3)	0.007(2)	0.011(3)
C(3)	0.026(3)	0.095(5)	0.023(3)	-0.004(3)	0.007(2)	0.008(3)
C(4)	0.028(3)	0.089(5)	0.028(3)	-0.001(3)	0.009(2)	-0.014(3)
C(5)	0.027(2)	0.055(4)	0.027(3)	-0.002(2)	0.005(2)	-0.004(3)
C(6)	0.029(3)	0.045(3)	0.021(2)	-0.007(2)	0.006(2)	-0.001(2)
C(7)	0.037(3)	0.035(3)	0.024(3)	-0.004(2)	0.010(2)	0.001(2)
C(8)	0.048(3)	0.022(3)	0.029(3)	-0.005(2)	0.018(2)	-0.005(2)
C(9)	0.047(3)	0.032(3)	0.032(3)	0.002(2)	0.021(2)	0.005(2)
C(10)	0.072(4)	0.038(3)	0.027(3)	-0.002(3)	0.023(3)	0.005(2)
C(11)	0.045(3)	0.053(4)	0.035(3)	0.000(3)	0.011(2)	0.010(3)
C(12)	0.046(3)	0.037(3)	0.030(3)	0.000(2)	0.015(2)	0.004(2)
C(13)	0.045(3)	0.069(4)	0.041(3)	0.004(3)	0.008(2)	0.015(3)
C(14)	0.047(3)	0.053(4)	0.058(4)	0.002(3)	0.020(3)	-0.021(3)
C(15)	0.066(4)	0.069(5)	0.047(4)	-0.019(3)	-0.007(3)	-0.008(3)
C(16)	0.130(6)	0.093(6)	0.064(5)	-0.041(5)	-0.020(4)	-0.028(4)
C(17)	0.075(5)	0.100(6)	0.070(5)	-0.019(4)	-0.017(4)	0.000(4)
C(18)	0.096(5)	0.077(5)	0.032(3)	-0.014(4)	0.008(3)	-0.003(3)
C(19)	0.088(5)	0.121(7)	0.070(5)	-0.075(5)	0.011(4)	-0.009(4)
C(20)	0.131(6)	0.048(4)	0.053(4)	-0.032(4)	0.009(4)	-0.006(3)
C(21)	0.048(3)	0.037(4)	0.077(4)	-0.010(3)	-0.001(3)	-0.002(3)
C(22)	0.054(4)	0.042(4)	0.100(5)	-0.004(3)	0.024(3)	-0.001(4)
C(23)	0.063(5)	0.051(5)	0.188(8)	-0.010(4)	-0.039(5)	-0.001(5)
C(24)	0.121(6)	0.061(4)	0.054(4)	-0.002(4)	0.009(4)	-0.016(4)
C(25)	0.043(3)	0.078(5)	0.083(4)	0.006(3)	0.027(3)	0.040(4)
C(26)	0.039(3)	0.047(4)	0.049(3)	-0.002(3)	0.013(2)	0.006(3)
C(27)	0.129(6)	0.075(5)	0.029(3)	0.046(4)	0.034(3)	0.014(3)
C(28)	0.202(9)	0.071(6)	0.146(7)	0.057(6)	0.140(7)	0.052(5)
C(29)	0.075(4)	0.050(4)	0.126(6)	0.017(3)	0.066(4)	0.030(4)
C(30)	0.127(6)	0.058(5)	0.047(4)	0.047(4)	0.009(4)	0.000(3)
C(31)	0.092(5)	0.054(4)	0.060(4)	-0.022(4)	0.037(4)	-0.013(4)
C(32)	0.138(7)	0.058(5)	0.058(4)	0.040(5)	0.039(5)	0.014(4)

C(33) 0.053(4) 0.113(7) 0.046(4) 0.019(4) -0.002(3) -0.015(4)

The general temperature factor expression:

$$\exp(-2\pi^2(a^2U_{11}h^2 + b^2U_{22}k^2 + c^2U_{33}l^2 + 2a*b*U_{12}hk + 2a*c*U_{13}hl + 2b*c*U_{23}kl))$$

Table 12. Bond Lengths (Å) for {[DADMB]YH(THF)}₂·C₆H₆ (6).

atom	atom	distance	atom	atom	distance
Y(1)	Y(1)	3.6652(8)	Y(1)	O(1)	2.329(3)
Y(1)	N(1)	2.213(4)	Y(1)	N(2)	2.228(4)
Y(1)	C(1)	2.702(4)	Si(1)	N(1)	1.714(4)
Si(1)	C(15)	1.900(6)	Si(1)	C(19)	1.865(7)
Si(1)	C(20)	1.853(7)	Si(2)	N(2)	1.719(4)
Si(2)	C(21)	1.887(6)	Si(2)	C(25)	1.883(5)
Si(2)	C(26)	1.875(5)	O(1)	C(27)	1.451(6)
O(1)	C(30)	1.465(7)	N(1)	C(1)	1.425(6)
N(2)	C(8)	1.416(6)	C(1)	C(2)	1.403(6)
C(1)	C(6)	1.411(7)	C(2)	C(3)	1.364(8)
C(3)	C(4)	1.402(8)	C(4)	C(5)	1.381(6)
C(5)	C(6)	1.427(7)	C(5)	C(14)	1.503(7)
C(6)	C(7)	1.511(6)	C(7)	C(8)	1.411(6)
C(7)	C(12)	1.409(6)	C(8)	C(9)	1.405(6)
C(9)	C(10)	1.366(6)	C(10)	C(11)	1.387(7)
C(11)	C(12)	1.387(6)	C(12)	C(13)	1.508(6)
C(15)	C(16)	1.539(9)	C(15)	C(17)	1.522(10)
C(15)	C(18)	1.521(8)	C(21)	C(22)	1.537(8)
C(21)	C(23)	1.558(8)	C(21)	C(24)	1.531(9)
C(27)	C(28)	1.348(9)	C(28)	C(29)	1.502(9)
C(29)	C(30)	1.429(8)	C(31)	C(32)	1.340(9)
C(31)	C(33)	1.363(9)	C(32)	C(33)	1.369(10)
Y(1)	H(1)	2.27(4)	Y(1)	H(1)	2.22(4)

Table 13. Bond Angles (°) for {[DADMB]YH(THF)}₂·C₆H₆ (6).

atom	atom	atom	angle	atom	atom	atom	angle
Y(1)	Y(1)	O(1)	108.68(8)	Y(1)	Y(1)	N(1)	117.44(9)
Y(1)	Y(1)	N(2)	128.87(9)	Y(1)	Y(1)	C(1)	107.54(9)
O(1)	Y(1)	N(1)	100.3(1)	O(1)	Y(1)	N(2)	91.0(1)
O(1)	Y(1)	C(1)	130.5(1)	N(1)	Y(1)	N(2)	103.9(1)
N(1)	Y(1)	C(1)	31.8(1)	N(2)	Y(1)	C(1)	91.7(1)
N(1)	Si(1)	C(15)	112.9(2)	N(1)	Si(1)	C(19)	113.9(3)
N(1)	Si(1)	C(20)	107.1(2)	C(15)	Si(1)	C(19)	107.5(3)
C(15)	Si(1)	C(20)	107.6(3)	C(19)	Si(1)	C(20)	107.6(4)
N(2)	Si(2)	C(21)	112.1(2)	N(2)	Si(2)	C(25)	117.5(2)
N(2)	Si(2)	C(26)	104.1(2)	C(21)	Si(2)	C(25)	108.3(3)
C(21)	Si(2)	C(26)	108.4(2)	C(25)	Si(2)	C(26)	105.8(2)
Y(1)	O(1)	C(27)	122.2(3)	Y(1)	O(1)	C(30)	130.0(3)
C(27)	O(1)	C(30)	107.7(4)	Y(1)	N(1)	Si(1)	134.8(2)

Y(1)	N(1)	C(1)	93.4(2)	Si(1)	N(1)	C(1)	129.0(3)
Y(1)	N(2)	Si(2)	117.3(2)	Y(1)	N(2)	C(8)	114.6(3)
Si(2)	N(2)	C(8)	127.6(3)	Y(1)	C(1)	N(1)	54.8(2)
Y(1)	C(1)	C(2)	118.3(3)	Y(1)	C(1)	C(6)	91.0(3)
N(1)	C(1)	C(2)	120.8(5)	N(1)	C(1)	C(6)	120.6(4)
C(2)	C(1)	C(6)	118.2(5)	C(1)	C(2)	C(3)	122.3(5)
C(2)	C(3)	C(4)	119.7(4)	C(3)	C(4)	C(5)	120.6(5)
C(4)	C(5)	C(6)	119.5(5)	C(4)	C(5)	C(14)	119.4(5)
C(6)	C(5)	C(14)	121.0(4)	C(1)	C(6)	C(5)	119.7(4)
C(1)	C(6)	C(7)	122.0(4)	C(5)	C(6)	C(7)	117.4(4)
C(6)	C(7)	C(8)	122.2(4)	C(6)	C(7)	C(12)	116.6(4)
C(8)	C(7)	C(12)	121.2(4)	N(2)	C(8)	C(7)	120.6(4)
N(2)	C(8)	C(9)	122.2(4)	C(7)	C(8)	C(9)	117.2(4)
C(8)	C(9)	C(10)	121.6(4)	C(9)	C(10)	C(11)	121.0(4)
C(10)	C(11)	C(12)	120.0(4)	C(7)	C(12)	C(11)	119.1(4)
C(7)	C(12)	C(13)	122.3(4)	C(11)	C(12)	C(13)	118.5(4)
Si(1)	C(15)	C(16)	110.5(5)	Si(1)	C(15)	C(17)	110.0(5)
Si(1)	C(15)	C(18)	111.0(4)	C(16)	C(15)	C(17)	107.7(5)
C(16)	C(15)	C(18)	109.3(5)	C(17)	C(15)	C(18)	108.4(6)
Si(2)	C(21)	C(22)	109.3(4)	Si(2)	C(21)	C(23)	111.7(5)
Si(2)	C(21)	C(24)	110.9(4)	C(22)	C(21)	C(23)	107.8(5)
C(22)	C(21)	C(24)	108.3(5)	C(23)	C(21)	C(24)	108.8(6)
O(1)	C(27)	C(28)	108.6(5)	C(27)	C(28)	C(29)	110.0(5)
C(28)	C(29)	C(30)	105.7(5)	O(1)	C(30)	C(29)	107.4(5)
C(32)	C(31)	C(33)	119.8(6)	C(31)	C(32)	C(33)	120.3(6)
C(31)	C(33)	C(32)	119.9(6)	Y(1)	Y(1)	H(1)	34.8(10)
Y(1)	Y(1)	H(1)	35.8(9)	O(1)	Y(1)	H(1)	139.9(9)
O(1)	Y(1)	H(1)	75.3(9)	N(1)	Y(1)	H(1)	111.7(8)
N(1)	Y(1)	H(1)	112.5(9)	N(2)	Y(1)	H(1)	103.6(10)
N(2)	Y(1)	H(1)	142.8(9)	C(1)	Y(1)	H(1)	86.8(9)
C(1)	Y(1)	H(1)	123.7(9)	H(1)	Y(1)	H(1)	70(1)

Structural data for [DADMB]Y(NC₅H₆)(NC₅H₅)₂·C₅H₁₂ (**9**).

Table 14. Atomic coordinates and B_{iso}/B_{eq} for [DADMB]Y(NC₅H₆)(NC₅H₅)₂·C₅H₁₂ (**9**).

atom	x	y	z	B _{eq}
Y(1)	0.17019(2)	0.07021(5)	0.12763(1)	2.52(1)
Si(1)	0.31982(6)	0.0224(1)	0.14288(5)	3.32(4)
Si(2)	0.02718(6)	0.0277(1)	0.09807(5)	3.00(4)
N(1)	0.1680(2)	0.2596(4)	0.1382(1)	3.6(1)
N(2)	0.2516(2)	-0.0241(4)	0.1365(1)	3.0(1)
N(3)	0.0943(2)	-0.0233(4)	0.1040(1)	2.56(10)
N(4)	0.1439(2)	0.0586(4)	0.1994(1)	2.5(1)
N(5)	0.1928(2)	0.1144(4)	0.0566(1)	3.1(1)
C(1)	0.2085(3)	0.3334(6)	0.1215(2)	5.0(2)
C(2)	0.2423(3)	0.3964(7)	0.1508(3)	6.2(2)
C(3)	0.2144(3)	0.4358(6)	0.1834(2)	5.9(2)
C(4)	0.1601(3)	0.4027(5)	0.1897(2)	5.1(2)
C(5)	0.1375(2)	0.3166(5)	0.1674(2)	4.2(2)
C(6)	0.2258(2)	-0.1119(4)	0.1574(2)	2.6(1)
C(7)	0.2385(2)	-0.1358(5)	0.1985(2)	3.2(1)

C(8)	0.2087(2)	-0.2139(5)	0.2199(2)	3.4(1)
C(9)	0.1661(2)	-0.2739(5)	0.2016(2)	3.6(2)
C(10)	0.1520(2)	-0.2553(5)	0.1613(2)	3.4(1)
C(11)	0.1804(2)	-0.1727(4)	0.1390(2)	2.7(1)
C(12)	0.1672(2)	-0.1649(5)	0.0944(2)	2.7(1)
C(13)	0.1220(2)	-0.1004(4)	0.0792(2)	2.7(1)
C(14)	0.1088(2)	-0.1093(5)	0.0378(2)	3.4(1)
C(15)	0.1386(3)	-0.1798(6)	0.0132(2)	3.7(2)
C(16)	0.1827(2)	-0.2443(5)	0.0284(2)	3.6(2)
C(17)	0.1969(2)	-0.2378(5)	0.0690(2)	3.4(1)
C(18)	0.2410(2)	-0.3153(5)	0.0855(2)	4.1(2)
C(19)	0.1072(2)	-0.3277(5)	0.1415(2)	4.3(2)
C(20)	0.3280(3)	0.1464(6)	0.1089(2)	5.2(2)
C(21)	0.3379(2)	0.0784(6)	0.1939(2)	5.0(2)
C(22)	0.3744(2)	-0.0864(6)	0.1282(2)	4.5(2)
C(23)	0.3673(3)	-0.1184(7)	0.0843(2)	5.4(2)
C(24)	0.3692(3)	-0.1911(6)	0.1556(2)	5.6(2)
C(25)	0.4340(3)	-0.0356(6)	0.1345(2)	5.6(2)
C(26)	0.0110(2)	0.1036(5)	0.0500(2)	4.4(2)
C(27)	0.0201(2)	0.1378(6)	0.1376(2)	4.6(2)
C(28)	-0.0303(2)	-0.0820(5)	0.1045(2)	3.6(1)
C(29)	-0.0878(2)	-0.0299(6)	0.0984(2)	4.4(2)
C(30)	-0.0255(2)	-0.1320(6)	0.1474(2)	4.0(2)
C(31)	-0.0239(2)	-0.1788(6)	0.0745(2)	4.3(2)
C(32)	0.2255(2)	0.0493(5)	0.0350(2)	3.5(1)
C(33)	0.2311(3)	0.0587(6)	-0.0062(2)	4.2(2)
C(34)	0.2001(3)	0.1372(7)	-0.0261(2)	4.6(2)
C(35)	0.1651(3)	0.2075(6)	-0.0046(2)	5.1(2)
C(36)	0.1631(2)	0.1939(5)	0.0372(2)	3.6(1)
C(37)	0.1070(2)	-0.0179(5)	0.2132(2)	3.4(1)
C(38)	0.0986(3)	-0.0348(5)	0.2536(2)	4.5(2)
C(39)	0.1302(3)	0.0246(6)	0.2814(2)	4.2(2)
C(40)	0.1682(2)	0.1032(5)	0.2678(2)	3.6(1)
C(41)	0.1731(2)	0.1173(5)	0.2272(2)	3.1(1)
C(42)	0.0000	0.243(1)	0.2500	11.2(5)
C(43)	0.0154(7)	0.343(1)	0.2362(5)	6.6(4)
C(44)	0.0000	0.455(1)	0.2500	7.8(4)
C(45)	0.0184(7)	0.563(1)	0.2354(5)	6.5(4)
C(46)	0.0000	0.677(1)	0.2500	8.2(4)
C(47)	0.0948(8)	0.493(2)	0.0369(6)	8.1(5)
C(48)	-0.068(1)	0.530(2)	-0.0533(8)	11.7(7)
C(49)	0.0000	0.5000	0.0000	14.0(8)
C(50)	0.041(2)	0.457(3)	0.016(1)	15(1)
C(51)	0.043(1)	0.533(3)	0.031(1)	13.0(9)
H(1)	0.2332	0.2897	0.1057	5.9442
H(2)	0.1892	0.3859	0.1048	5.9442
H(3)	0.2812	0.4092	0.1474	7.3805
H(4)	0.2325	0.4859	0.2017	7.1093
H(5)	0.1382	0.4394	0.2094	6.1072
H(6)	0.0998	0.2949	0.1718	5.0948
H(7)	0.2684	-0.0967	0.2116	3.8210
H(8)	0.2176	-0.2263	0.2475	4.0703
H(9)	0.1461	-0.3284	0.2165	4.3722
H(10)	0.0788	-0.0660	0.0267	4.0367
H(11)	0.1288	-0.1844	-0.0146	4.4683
H(12)	0.2030	-0.2925	0.0111	4.2846
H(13)	0.2293	-0.3910	0.0817	4.9480
H(14)	0.2751	-0.3031	0.0718	4.9480

H(15)	0.2466	-0.3009	0.1134	4.9480
H(16)	0.0730	-0.3194	0.1555	5.1004
H(17)	0.1018	-0.3049	0.1143	5.1004
H(18)	0.1186	-0.4042	0.1423	5.1004
H(19)	0.3652	0.1745	0.1113	6.2828
H(20)	0.3206	0.1243	0.0818	6.2828
H(21)	0.3023	0.2036	0.1163	6.2828
H(22)	0.3344	0.0202	0.2133	5.9922
H(23)	0.3754	0.1055	0.1943	5.9922
H(24)	0.3131	0.1382	0.2002	5.9922
H(25)	0.3309	-0.1490	0.0799	6.4523
H(26)	0.3718	-0.0535	0.0680	6.4523
H(27)	0.3948	-0.1728	0.0776	6.4523
H(28)	0.3333	-0.2244	0.1516	6.7538
H(29)	0.3975	-0.2440	0.1491	6.7538
H(30)	0.3736	-0.1692	0.1830	6.7538
H(31)	0.4614	-0.0900	0.1278	6.7691
H(32)	0.4379	0.0286	0.1178	6.7691
H(33)	0.4390	-0.0142	0.1619	6.7691
H(34)	0.0373	0.1627	0.0466	5.2968
H(35)	0.0134	0.0526	0.0281	5.2968
H(36)	-0.0258	0.1340	0.0508	5.2968
H(37)	0.0255	0.1047	0.1634	5.4821
H(38)	0.0475	0.1946	0.1338	5.4821
H(39)	-0.0164	0.1700	0.1358	5.4821
H(40)	-0.0930	0.0280	0.1177	5.3312
H(41)	-0.0908	0.0011	0.0721	5.3312
H(42)	-0.1158	-0.0859	0.1015	5.3312
H(43)	-0.0540	-0.1868	0.1508	4.8430
H(44)	0.0103	-0.1663	0.1510	4.8430
H(45)	-0.0297	-0.0738	0.1667	4.8430
H(46)	-0.0524	-0.2330	0.0787	5.1152
H(47)	-0.0271	-0.1505	0.0478	5.1152
H(48)	0.0119	-0.2130	0.0783	5.1152
H(49)	0.2464	-0.0076	0.0486	4.1948
H(50)	0.2561	0.0112	-0.0202	5.0928
H(51)	0.2022	0.1440	-0.0545	5.5552
H(52)	0.1431	0.2633	-0.0179	6.1013
H(53)	0.1399	0.2426	0.0523	4.3642
H(54)	0.0860	-0.0616	0.1943	4.0778
H(55)	0.0712	-0.0871	0.2623	5.4294
H(56)	0.1260	0.0119	0.3094	5.0574
H(57)	0.1903	0.1463	0.2862	4.2679
H(58)	0.1989	0.1722	0.2181	3.7139

$$B_{eq} = 8/3 \pi^2 (U_{11}(aa^*)^2 + U_{22}(bb^*)^2 + U_{33}(cc^*)^2 + 2U_{12}(aa^*bb^*)\cos\gamma + 2U_{13}(aa^*cc^*)\cos\beta + 2U_{23}(bb^*cc^*)\cos\alpha)$$

Table 15. Anisotropic Displacement Parameters for [DADMB]Y(NC₅H₆)(NC₅H₅)₂·C₅H₁₂ (**9**).

atom	U ₁₁	U ₂₂	U ₃₃	U ₁₂	U ₁₃	U ₂₃
Y(1)	0.0337(3)	0.0371(3)	0.0269(3)	-0.0036(3)	0.0007(2)	-0.0004(3)

Si(1)	0.0341(9)	0.047(1)	0.0431(9)	-0.0013(8)	-0.0015(7)	-0.0003(8)
Si(2)	0.0340(9)	0.048(1)	0.0352(8)	-0.0011(8)	-0.0031(6)	-0.0051(7)
N(1)	0.055(3)	0.040(3)	0.040(3)	-0.010(3)	0.007(2)	-0.002(2)
N(2)	0.032(3)	0.040(3)	0.035(2)	-0.006(2)	-0.001(2)	0.000(2)
N(3)	0.039(3)	0.038(3)	0.025(2)	-0.001(2)	0.001(2)	-0.007(2)
N(4)	0.035(3)	0.037(3)	0.031(2)	-0.003(2)	0.001(2)	-0.003(2)
N(5)	0.040(3)	0.046(3)	0.031(3)	-0.005(2)	-0.003(2)	0.004(2)
C(1)	0.068(5)	0.064(5)	0.063(4)	-0.009(4)	0.002(3)	0.000(4)
C(2)	0.076(6)	0.079(6)	0.108(7)	-0.037(4)	0.023(5)	-0.037(5)
C(3)	0.074(5)	0.057(5)	0.095(6)	-0.004(4)	-0.014(4)	-0.029(5)
C(4)	0.067(5)	0.046(4)	0.082(5)	-0.005(4)	0.007(4)	-0.020(4)
C(5)	0.053(4)	0.048(4)	0.055(4)	-0.007(3)	0.000(3)	-0.009(3)
C(6)	0.035(3)	0.036(3)	0.032(3)	0.007(3)	0.011(2)	-0.003(3)
C(7)	0.039(3)	0.043(4)	0.039(3)	0.003(3)	-0.002(2)	-0.001(3)
C(8)	0.053(4)	0.049(4)	0.037(3)	0.011(3)	0.005(3)	0.010(3)
C(9)	0.053(4)	0.040(4)	0.052(4)	0.008(3)	0.014(3)	0.021(3)
C(10)	0.040(3)	0.036(3)	0.048(4)	0.002(3)	0.004(3)	-0.003(3)
C(11)	0.043(3)	0.024(3)	0.038(3)	0.008(3)	0.007(2)	-0.001(2)
C(12)	0.034(3)	0.039(3)	0.033(3)	-0.009(3)	0.008(2)	-0.008(3)
C(13)	0.037(3)	0.041(4)	0.029(3)	-0.008(3)	0.004(2)	-0.006(3)
C(14)	0.038(3)	0.047(4)	0.042(3)	-0.006(3)	0.001(3)	-0.006(3)
C(15)	0.056(4)	0.076(5)	0.038(4)	-0.015(4)	0.008(3)	-0.019(3)
C(16)	0.050(4)	0.050(4)	0.044(4)	-0.004(3)	0.018(3)	-0.018(3)
C(17)	0.040(3)	0.045(4)	0.045(4)	-0.003(3)	0.005(3)	-0.006(3)
C(18)	0.056(4)	0.056(4)	0.053(4)	0.002(3)	0.011(3)	-0.017(3)
C(19)	0.053(4)	0.048(4)	0.058(4)	-0.010(3)	0.013(3)	0.008(3)
C(20)	0.052(4)	0.062(5)	0.092(5)	-0.016(4)	-0.013(3)	0.022(4)
C(21)	0.044(4)	0.078(5)	0.069(4)	0.000(4)	-0.001(3)	-0.019(4)
C(22)	0.037(3)	0.065(5)	0.065(4)	0.007(3)	0.009(3)	-0.008(4)
C(23)	0.081(5)	0.092(6)	0.061(5)	-0.007(5)	0.029(4)	-0.019(4)
C(24)	0.061(5)	0.052(5)	0.114(6)	0.017(4)	0.013(4)	0.021(4)
C(25)	0.034(4)	0.092(6)	0.104(6)	0.013(4)	0.011(3)	-0.001(5)
C(26)	0.049(4)	0.058(4)	0.050(4)	-0.003(3)	-0.008(3)	0.005(3)
C(27)	0.042(4)	0.066(5)	0.060(4)	0.014(4)	-0.013(3)	-0.019(4)
C(28)	0.038(3)	0.061(4)	0.037(3)	-0.002(3)	-0.003(2)	0.000(3)
C(29)	0.034(3)	0.093(6)	0.056(4)	-0.007(4)	0.003(3)	-0.001(4)
C(30)	0.051(4)	0.075(5)	0.045(4)	-0.014(4)	0.007(3)	0.004(4)
C(31)	0.050(4)	0.070(5)	0.050(4)	-0.020(3)	0.000(3)	-0.005(4)
C(32)	0.052(4)	0.050(4)	0.038(3)	-0.010(3)	0.005(3)	-0.001(3)
C(33)	0.073(5)	0.067(5)	0.040(4)	-0.023(4)	0.013(3)	-0.013(4)
C(34)	0.066(5)	0.089(6)	0.035(4)	-0.030(4)	-0.001(3)	-0.002(4)
C(35)	0.058(4)	0.072(5)	0.056(4)	-0.020(4)	-0.010(3)	0.029(4)
C(36)	0.046(4)	0.056(4)	0.039(3)	-0.009(3)	0.001(3)	0.011(3)
C(37)	0.041(3)	0.045(4)	0.039(3)	0.000(3)	-0.001(2)	-0.003(3)
C(38)	0.060(4)	0.061(4)	0.042(4)	-0.004(3)	0.015(3)	0.004(3)
C(39)	0.070(4)	0.077(5)	0.026(3)	0.003(4)	0.004(3)	-0.003(3)
C(40)	0.046(4)	0.066(5)	0.029(3)	-0.001(3)	-0.001(2)	-0.006(3)
C(41)	0.039(3)	0.044(4)	0.043(4)	-0.008(3)	0.001(3)	-0.001(3)
C(42)	0.28(2)	0.08(1)	0.09(1)	0.0000	0.00(1)	0.0000
C(44)	0.16(1)	0.11(1)	0.039(6)	0.0000	-0.017(7)	0.0000
C(46)	0.12(1)	0.076(9)	0.11(1)	0.0000	-0.002(8)	0.0000
C(49)	0.13(2)	0.25(2)	0.18(2)	0.02(2)	-0.06(1)	0.04(2)

The general temperature factor expression:

$$\exp(-2\pi^2(a^*2U_{11}h^2 + b^*2U_{22}k^2 + c^*2U_{33}l^2 + 2a^*b^*U_{12}hk + 2a^*c^*U_{13}hl + 2b^*c^*U_{23}kl))$$

Table 16. Bond Lengths (Å) for [DADMB]Y(NC₅H₆)(NC₅H₅)₂·C₅H₁₂ (**9**).

atom	atom	distance	atom	atom	distance
Y(1)	N(1)	2.280(5)	Y(1)	N(2)	2.254(4)
Y(1)	N(3)	2.253(4)	Y(1)	N(4)	2.481(4)
Y(1)	N(5)	2.486(4)	Y(1)	C(6)	2.717(5)
Y(1)	C(13)	2.822(5)	Si(1)	N(2)	1.728(4)
Si(1)	C(20)	1.870(7)	Si(1)	C(21)	1.866(6)
Si(1)	C(22)	1.905(6)	Si(2)	N(3)	1.718(4)
Si(2)	C(26)	1.869(6)	Si(2)	C(27)	1.865(6)
Si(2)	C(28)	1.906(6)	N(1)	C(1)	1.424(7)
N(1)	C(5)	1.397(7)	N(2)	C(6)	1.403(6)
N(3)	C(13)	1.408(6)	N(4)	C(37)	1.352(7)
N(4)	C(41)	1.343(7)	N(5)	C(32)	1.320(7)
N(5)	C(36)	1.340(7)	C(1)	C(2)	1.459(9)
C(2)	C(3)	1.365(9)	C(3)	C(4)	1.372(9)
C(4)	C(5)	1.369(8)	C(6)	C(7)	1.422(7)
C(6)	C(11)	1.429(7)	C(7)	C(8)	1.375(7)
C(8)	C(9)	1.375(8)	C(9)	C(10)	1.393(7)
C(10)	C(11)	1.410(7)	C(10)	C(19)	1.514(8)
C(11)	C(12)	1.513(7)	C(12)	C(13)	1.408(7)
C(12)	C(17)	1.411(7)	C(13)	C(14)	1.407(7)
C(14)	C(15)	1.378(8)	C(15)	C(16)	1.388(8)
C(16)	C(17)	1.387(8)	C(17)	C(18)	1.493(8)
C(22)	C(23)	1.514(9)	C(22)	C(24)	1.550(9)
C(22)	C(25)	1.553(8)	C(28)	C(29)	1.516(8)
C(28)	C(30)	1.546(8)	C(28)	C(31)	1.533(8)
C(32)	C(33)	1.383(8)	C(33)	C(34)	1.356(9)
C(34)	C(35)	1.387(9)	C(35)	C(36)	1.400(8)
C(37)	C(38)	1.377(7)	C(38)	C(39)	1.375(8)
C(39)	C(40)	1.382(8)	C(40)	C(41)	1.367(7)
C(42)	C(43)	1.33(2)	C(42)	C(43)	1.33(2)
C(43)	C(43)	1.19(3)	C(43)	C(44)	1.46(2)
C(44)	C(45)	1.44(2)	C(44)	C(45)	1.44(2)
C(45)	C(45)	1.32(3)	C(45)	C(46)	1.50(2)
C(47)	C(48)	0.89(3)	C(47)	C(50)	1.52(5)
C(47)	C(51)	1.34(4)	C(48)	C(50)	1.40(5)
C(48)	C(51)	1.22(4)	C(49)	C(50)	1.21(4)
C(49)	C(50)	1.21(4)	C(49)	C(51)	1.47(4)
C(49)	C(51)	1.47(4)	C(50)	C(51)	1.03(4)

Table 17. Bond Angles (°) for [DADMB]Y(NC₅H₆)(NC₅H₅)₂·C₅H₁₂ (**9**).

atom	atom	atom	angle	atom	atom	atom	angle
N(1)	Y(1)	N(2)	119.5(2)	N(1)	Y(1)	N(3)	121.4(2)
N(1)	Y(1)	N(4)	84.2(1)	N(1)	Y(1)	N(5)	86.8(2)
N(1)	Y(1)	C(6)	138.0(2)	N(1)	Y(1)	C(13)	142.0(2)
N(2)	Y(1)	N(3)	118.9(1)	N(2)	Y(1)	N(4)	94.5(1)
N(2)	Y(1)	N(5)	91.6(1)	N(2)	Y(1)	C(6)	31.0(1)
N(2)	Y(1)	C(13)	93.3(2)	N(3)	Y(1)	N(4)	95.3(1)

N(3)	Y(1)	N(5)	87.7(1)	N(3)	Y(1)	C(6)	96.7(2)
N(3)	Y(1)	C(13)	29.6(1)	N(4)	Y(1)	N(5)	170.8(2)
N(4)	Y(1)	C(6)	74.7(1)	N(4)	Y(1)	C(13)	113.7(1)
N(5)	Y(1)	C(6)	113.6(1)	N(5)	Y(1)	C(13)	72.7(1)
C(6)	Y(1)	C(13)	79.9(2)	N(2)	Si(1)	C(20)	106.6(3)
N(2)	Si(1)	C(21)	115.3(2)	N(2)	Si(1)	C(22)	113.4(3)
C(20)	Si(1)	C(21)	104.1(3)	C(20)	Si(1)	C(22)	107.6(3)
C(21)	Si(1)	C(22)	109.1(3)	N(3)	Si(2)	C(26)	116.4(2)
N(3)	Si(2)	C(27)	105.2(2)	N(3)	Si(2)	C(28)	114.4(2)
C(26)	Si(2)	C(27)	104.2(3)	C(26)	Si(2)	C(28)	106.9(3)
C(27)	Si(2)	C(28)	109.0(3)	Y(1)	N(1)	C(1)	122.1(4)
Y(1)	N(1)	C(5)	126.9(4)	C(1)	N(1)	C(5)	109.6(5)
Y(1)	N(2)	Si(1)	131.5(2)	Y(1)	N(2)	C(6)	93.0(3)
Si(1)	N(2)	C(6)	126.6(4)	Y(1)	N(3)	Si(2)	127.3(2)
Y(1)	N(3)	C(13)	98.2(3)	Si(2)	N(3)	C(13)	127.5(3)
Y(1)	N(4)	C(37)	122.8(3)	Y(1)	N(4)	C(41)	119.7(3)
C(37)	N(4)	C(41)	116.6(4)	Y(1)	N(5)	C(32)	122.2(4)
Y(1)	N(5)	C(36)	119.0(4)	C(32)	N(5)	C(36)	117.5(5)
N(1)	C(1)	C(2)	115.2(6)	C(1)	C(2)	C(3)	115.8(6)
C(2)	C(3)	C(4)	119.8(6)	C(3)	C(4)	C(5)	119.6(6)
N(1)	C(5)	C(4)	122.3(6)	Y(1)	C(6)	N(2)	56.0(2)
Y(1)	C(6)	C(7)	127.0(4)	Y(1)	C(6)	C(11)	83.5(3)
N(2)	C(6)	C(7)	122.6(5)	N(2)	C(6)	C(11)	119.9(5)
C(7)	C(6)	C(11)	117.0(5)	C(6)	C(7)	C(8)	122.0(5)
C(7)	C(8)	C(9)	120.3(5)	C(8)	C(9)	C(10)	120.4(5)
C(9)	C(10)	C(11)	120.4(5)	C(9)	C(10)	C(19)	118.9(5)
C(11)	C(10)	C(19)	120.7(5)	C(6)	C(11)	C(10)	119.7(5)
C(6)	C(11)	C(12)	122.1(5)	C(10)	C(11)	C(12)	117.6(5)
C(11)	C(12)	C(13)	122.1(4)	C(11)	C(12)	C(17)	116.8(5)
C(13)	C(12)	C(17)	120.5(5)	Y(1)	C(13)	N(3)	52.2(2)
Y(1)	C(13)	C(12)	83.4(3)	Y(1)	C(13)	C(14)	133.8(4)
N(3)	C(13)	C(12)	120.5(5)	N(3)	C(13)	C(14)	121.5(5)
C(12)	C(13)	C(14)	117.8(5)	C(13)	C(14)	C(15)	121.1(5)
C(14)	C(15)	C(16)	121.1(5)	C(15)	C(16)	C(17)	119.5(5)
C(12)	C(17)	C(16)	120.0(5)	C(12)	C(17)	C(18)	121.1(5)
C(16)	C(17)	C(18)	118.7(5)	Si(1)	C(22)	C(23)	110.7(5)
Si(1)	C(22)	C(24)	109.4(4)	Si(1)	C(22)	C(25)	109.2(4)
C(23)	C(22)	C(24)	110.8(6)	C(23)	C(22)	C(25)	108.3(5)
C(24)	C(22)	C(25)	108.5(5)	Si(2)	C(28)	C(29)	110.8(4)
Si(2)	C(28)	C(30)	109.1(4)	Si(2)	C(28)	C(31)	111.1(4)
C(29)	C(28)	C(30)	109.5(5)	C(29)	C(28)	C(31)	108.6(5)
C(30)	C(28)	C(31)	107.7(5)	N(5)	C(32)	C(33)	124.1(6)
C(32)	C(33)	C(34)	118.4(6)	C(33)	C(34)	C(35)	119.4(6)
C(34)	C(35)	C(36)	118.2(6)	N(5)	C(36)	C(35)	122.2(6)
N(4)	C(37)	C(38)	122.5(5)	C(37)	C(38)	C(39)	119.4(6)
C(38)	C(39)	C(40)	118.8(5)	C(39)	C(40)	C(41)	118.3(5)
N(4)	C(41)	C(40)	124.2(5)	C(43)	C(42)	C(43)	53(1)
C(42)	C(43)	C(43)	63.4(7)	C(42)	C(43)	C(44)	129(1)
C(43)	C(43)	C(44)	66.0(6)	C(43)	C(44)	C(43)	47(1)
C(43)	C(44)	C(45)	128.8(8)	C(43)	C(44)	C(45)	176.4(9)
C(43)	C(44)	C(45)	176.4(9)	C(43)	C(44)	C(45)	128.8(8)
C(45)	C(44)	C(45)	54(1)	C(44)	C(45)	C(45)	62.7(6)
C(44)	C(45)	C(46)	126(1)	C(45)	C(45)	C(46)	63.9(6)
C(45)	C(46)	C(45)	52(1)	C(48)	C(47)	C(50)	65(2)
C(48)	C(47)	C(51)	62(2)	C(50)	C(47)	C(51)	41(1)
C(47)	C(48)	C(50)	79(2)	C(47)	C(48)	C(51)	77(2)
C(50)	C(48)	C(51)	45(2)	C(50)	C(49)	C(50)	180.0
C(50)	C(49)	C(51)	43(1)	C(50)	C(49)	C(51)	136(1)

C(50)	C(49)	C(51)	136(1)
C(51)	C(49)	C(51)	180.0
C(47)	C(50)	C(49)	138(3)
C(48)	C(50)	C(49)	133(3)
C(49)	C(50)	C(51)	81(3)
C(47)	C(51)	C(49)	129(2)
C(48)	C(51)	C(49)	126(2)
C(49)	C(51)	C(50)	54(3)

C(50)	C(49)	C(51)	43(1)
C(47)	C(50)	C(48)	35(1)
C(47)	C(50)	C(51)	60(3)
C(48)	C(50)	C(51)	57(3)
C(47)	C(51)	C(48)	40(1)
C(47)	C(51)	C(50)	78(3)
C(48)	C(51)	C(50)	76(3)

Appendix C

Kinetic Data for Chapter 3

Table 1. Observed pseudo-first order rate constants for consumption of **1** at different PhMeSiH₂ concentration.

[PhMeSiH ₂], mol/L	$10^5 \times k_{\text{obs}}, \text{ s}^{-1}$
0.1474	5.6(1)
0.2122	8.9(2)
0.2999	14.0(3)
0.4407	15.6(4)
0.5878	21.6(2)

Table 2. Observed pseudo-first order rate constants for consumption of **1** at different PhMeSiD₂ concentration.

[PhMeSiD ₂], mol/L	$10^5 \times k_{\text{obs}}, \text{ s}^{-1}$
0.1237	7.2(1)
0.1523	7.6(2)
0.2856	11.3(3)
0.4752	20.8(7)
0.6280	18.4(6)
0.6943	21.8(6)

Table 3. Observed pseudo-first order rate constants for consumption of PhMeSiH₂ at different initial concentrations of 1-hexene, PhMeSiH₂, and **1** (in benzene-*d*₆).

[1-hexene], mol/L	[PhMeSiH ₂], mol/L	[1], mol/L	10 ⁵ × k _{obs} , s ⁻¹
0.335	0.335	0.0168	9.83(3)
0.786	0.315	0.0381	13.43(2)
1.470	0.295	0.0147	10.25(4)
2.390	0.239	0.0120	8.88(2)
4.014	0.322	0.0428	12.7(1)
1.481	0.297	0.0086	9.95(4)
1.467	0.294	0.0195	10.15(4)
1.508	0.302	0.0324	12.80(1)
1.447	0.290	0.0431	12.2(1)
1.443	0.131	0.0293	11.0(1)
1.795	0.359	0.000833	1.98(3)
1.523	0.305	0.00170	3.83(3)
1.538	0.308	0.00286	6.12(3)
1.568	0.314	0.00437	7.69(2)
1.428	0.286	0.00663	8.93(5)
1.311	0.262	0.00974	8.7(1)
1.707	0.342	0.0323 ^a	7.46(6)

a) using S-**1** instead of racemic **1**.

Table 4. Observed pseudo-first order rate constants for consumption of PhMeSiH₂ at different initial concentrations of **1** (in THF-*d*₈).

[1-hexene], mol/L	[PhMeSiH ₂], mol/L	[1], mol/L	10 ⁵ × k _{obs} , s ⁻¹ (initial rate)
1.632	0.396	0.0162	2.13
1.713	0.416	0.0387	4.23
1.693	0.411	0.0600	6.91

Appendix D

Crystallographic Data for Chapter 4

Table 1. Crystallographic data for compounds **3** and **7**.

Compound	3	7
(a) Crystal Parameters:		
Formula	C ₂₆ H ₄₂ N ₂ Si ₂ Cl ₂ Zr	C ₈₅ H ₇₇ N ₂ Si ₂ ZrBF ₁₅
Formula weight	600.93	1569.73
Size (mm)	0.10 × 0.04 × 0.06 mm	0.17 × 0.26 × 0.10 mm
Crystal system	monoclinic	triclinic
Space group	C2/c (#15)	P $\bar{1}$ (#2)
a (Å)	30.6339(4)	15.023(1)
b (Å)	11.2771(2)	16.254(1)
c (Å)	21.7039(3)	18.377(1)
α, β, γ (°)	90, 128.042(1), 90	73.647(1), 73.426(1), 63.245(1)
V (Å ³)	5905.0(2)	3778.4(4)
Z	8	2
D _{calc} (g.cm ⁻³)	1.352	1.380
F ₀₀₀	2512	1618.00
μ (MoK α) (cm ⁻¹)	6.51	2.61
(b) Data Collection:		
Temp. (°C)	-136	-130
Unique/ Total reflection	4466 / 12111	12772 / 18308
R _{int}	0.045	0.049
Empirical absorption correction:	0.06	0.025
μ R, T _{min} - T _{max}	0.884 - 0.986	0.732 - 0.978

	(c) Refinement:	
Observations ($I > 3\sigma(I)$)	3330	5948
Variables	299	955
Reflection / parameters ratio	11.14	6.23
$R = \sum F_o - F_c / \sum F_o $	0.036	0.053
$R_w = [(\sum w(F_o - F_c)^2 / \sum w F_o^2)]^{1/2}$	0.046	0.050
Goodness of fit $([\sum w(F_o - F_c)^2 / (N_o - N_v)]^{1/2})$	1.65	1.49
Max and min peaks in final diff. map ($e^-/\text{\AA}^3$)	0.38 / -0.43	0.54 / -0.75

Structural data for {[DADMB]ZrCl₂}₂ (**3**).**Table 2.** Atomic coordinates and B_{iso}/B_{eq} for {[DADMB]ZrCl₂}₂ (**3**).

atom	x	y	z	B _{eq}
Zr(1)	0.58352(2)	0.04062(3)	0.55258(2)	1.664(10)
Cl(1)	0.64482(5)	-0.08708(10)	0.66341(6)	2.60(2)
Cl(2)	0.49062(4)	0.14074(9)	0.49826(6)	2.07(2)
Si(1)	0.64883(5)	-0.06918(10)	0.47343(7)	1.73(3)
Si(2)	0.64160(5)	0.2539(1)	0.68609(7)	1.90(3)
N(1)	0.6020(1)	0.0085(3)	0.4806(2)	1.75(7)
N(2)	0.6302(1)	0.1929(3)	0.6020(2)	1.77(8)
C(1)	0.5626(2)	0.0942(3)	0.4236(2)	1.69(9)
C(2)	0.5089(2)	0.0557(4)	0.3602(2)	1.94(9)
C(3)	0.4685(2)	0.1377(4)	0.3116(2)	2.21(9)
C(4)	0.4798(2)	0.2568(4)	0.3243(2)	2.5(1)
C(5)	0.5330(2)	0.2977(4)	0.3849(2)	2.27(10)
C(6)	0.5753(2)	0.2163(3)	0.4345(2)	1.49(9)
C(7)	0.6342(2)	0.2557(3)	0.4966(2)	1.84(9)
C(8)	0.6600(2)	0.2402(4)	0.5763(2)	2.13(10)
C(9)	0.7159(2)	0.2711(4)	0.6313(2)	2.24(10)
C(10)	0.7449(2)	0.3221(4)	0.6081(3)	2.6(1)
C(11)	0.7188(2)	0.3398(4)	0.5293(3)	2.7(1)
C(12)	0.6644(2)	0.3062(4)	0.4736(2)	2.06(10)
C(13)	0.6388(2)	0.3256(4)	0.3885(3)	2.8(1)
C(14)	0.5425(2)	0.4300(4)	0.3943(3)	2.8(1)
C(15)	0.7195(2)	-0.0443(4)	0.5661(3)	2.4(1)
C(16)	0.6441(2)	-0.0064(4)	0.3904(3)	2.5(1)
C(17)	0.6305(2)	-0.2319(4)	0.4546(2)	1.91(9)
C(18)	0.6336(2)	-0.2907(4)	0.5211(3)	2.8(1)
C(19)	0.6710(2)	-0.2958(4)	0.4470(3)	3.1(1)
C(20)	0.5714(2)	-0.2491(4)	0.3778(3)	3.2(1)
C(21)	0.7107(2)	0.2141(4)	0.7790(2)	2.28(10)
C(22)	0.5902(2)	0.1820(4)	0.6943(3)	2.9(1)
C(23)	0.6288(2)	0.4197(4)	0.6763(2)	2.30(10)
C(24)	0.6754(2)	0.4940(4)	0.6871(3)	3.3(1)
C(25)	0.6233(2)	0.4598(4)	0.7389(3)	3.4(1)
C(26)	0.5739(2)	0.4470(4)	0.5947(3)	3.6(1)
H(1)	0.5008	-0.0267	0.3511	2.3305
H(2)	0.4325	0.1116	0.2688	2.6497
H(3)	0.4510	0.3123	0.2915	2.9483
H(4)	0.7343	0.2569	0.6853	2.6852
H(5)	0.7825	0.3448	0.6461	3.0808
H(6)	0.7385	0.3754	0.5135	3.1873
H(7)	0.6401	0.4076	0.3797	3.3170
H(8)	0.6588	0.2816	0.3760	3.3170
H(9)	0.6013	0.2999	0.3565	3.3170
H(10)	0.5800	0.4458	0.4372	3.4009
H(11)	0.5344	0.4623	0.3479	3.4009
H(12)	0.5189	0.4651	0.4037	3.4009
H(13)	0.7214	-0.0738	0.6087	2.9035
H(14)	0.7458	-0.0846	0.5641	2.9035
H(15)	0.7274	0.0382	0.5730	2.9035
H(16)	0.6538	0.0752	0.3999	2.9840
H(17)	0.6688	-0.0477	0.3854	2.9840
H(18)	0.6073	-0.0146	0.3435	2.9840
H(19)	0.6081	-0.2532	0.5260	3.4004

H(20)	0.6246	-0.3724	0.5096	3.4004
H(21)	0.6701	-0.2829	0.5688	3.4004
H(22)	0.6623	-0.3780	0.4385	3.7180
H(23)	0.6680	-0.2639	0.4040	3.7180
H(24)	0.7077	-0.2853	0.4937	3.7180
H(25)	0.5455	-0.2130	0.3824	3.8071
H(26)	0.5687	-0.2135	0.3359	3.8071
H(27)	0.5636	-0.3315	0.3678	3.8071
H(28)	0.7148	0.1303	0.7828	2.7313
H(29)	0.7391	0.2484	0.7793	2.7313
H(30)	0.7134	0.2434	0.8223	2.7313
H(31)	0.5947	0.2128	0.7387	3.4346
H(32)	0.5537	0.1980	0.6485	3.4346
H(33)	0.5963	0.0987	0.7001	3.4346
H(34)	0.7091	0.4813	0.7381	4.0199
H(35)	0.6800	0.4706	0.6493	4.0199
H(36)	0.6659	0.5757	0.6805	4.0199
H(37)	0.6571	0.4446	0.7894	4.0362
H(38)	0.6155	0.5424	0.7334	4.0362
H(39)	0.5941	0.4174	0.7326	4.0362
H(40)	0.5667	0.5298	0.5902	4.3787
H(41)	0.5770	0.4230	0.5555	4.3787
H(42)	0.5444	0.4051	0.5881	4.3787

$$B_{eq} = 8/3 \pi^2 (U_{11}(aa^*)^2 + U_{22}(bb^*)^2 + U_{33}(cc^*)^2 + 2U_{12}(aa^*bb^*)\cos \gamma + 2U_{13}(aa^*cc^*)\cos \beta + 2U_{23}(bb^*cc^*)\cos \alpha)$$

Table 3. Anisotropic Displacement Parameters for {[DADMB]ZrCl₂}₂ (**3**).

atom	U ₁₁	U ₂₂	U ₃₃	U ₁₂	U ₁₃	U ₂₃
Zr(1)	0.0197(2)	0.0259(3)	0.0203(3)	-0.0016(2)	0.0126(2)	-0.0015(2)
Cl(1)	0.0327(6)	0.0344(6)	0.0253(6)	0.0009(5)	0.0136(5)	0.0036(5)
Cl(2)	0.0223(6)	0.0261(5)	0.0305(6)	-0.0016(5)	0.0159(5)	-0.0035(5)
Si(1)	0.0221(6)	0.0223(6)	0.0243(7)	0.0003(5)	0.0150(6)	0.0000(5)
Si(2)	0.0232(6)	0.0298(7)	0.0196(6)	-0.0024(5)	0.0126(5)	-0.0032(5)
N(1)	0.020(2)	0.021(2)	0.022(2)	0.001(1)	0.012(2)	0.003(2)
N(2)	0.022(2)	0.029(2)	0.018(2)	-0.002(2)	0.012(2)	-0.002(2)
C(1)	0.020(2)	0.024(2)	0.019(2)	0.001(2)	0.013(2)	0.000(2)
C(2)	0.028(2)	0.026(2)	0.027(2)	-0.005(2)	0.019(2)	-0.003(2)
C(3)	0.025(2)	0.030(3)	0.021(2)	-0.001(2)	0.008(2)	-0.002(2)
C(4)	0.026(3)	0.036(3)	0.026(3)	0.008(2)	0.014(2)	0.003(2)
C(5)	0.032(3)	0.024(2)	0.027(3)	0.000(2)	0.019(2)	-0.003(2)
C(6)	0.020(2)	0.025(2)	0.018(2)	-0.002(2)	0.012(2)	-0.001(2)
C(7)	0.025(2)	0.018(2)	0.026(2)	-0.002(2)	0.015(2)	-0.002(2)
C(8)	0.024(2)	0.024(2)	0.029(2)	-0.002(2)	0.016(2)	-0.006(2)
C(9)	0.028(2)	0.042(3)	0.020(2)	-0.002(2)	0.015(2)	-0.006(2)
C(10)	0.025(2)	0.052(3)	0.029(3)	-0.013(2)	0.018(2)	-0.012(2)
C(11)	0.039(3)	0.036(3)	0.042(3)	-0.014(2)	0.031(3)	-0.010(2)
C(12)	0.032(3)	0.028(2)	0.024(2)	-0.001(2)	0.020(2)	-0.003(2)
C(13)	0.046(3)	0.029(2)	0.041(3)	-0.004(2)	0.031(2)	0.004(2)
C(14)	0.040(3)	0.026(2)	0.034(3)	0.004(2)	0.017(2)	-0.001(2)
C(15)	0.028(2)	0.031(3)	0.035(3)	0.003(2)	0.019(2)	-0.001(2)
C(16)	0.036(3)	0.028(2)	0.035(3)	-0.002(2)	0.024(2)	-0.002(2)

C(17)	0.029(2)	0.021(2)	0.030(2)	-0.001(2)	0.019(2)	-0.004(2)
C(18)	0.044(3)	0.024(2)	0.038(3)	-0.001(2)	0.025(3)	0.004(2)
C(19)	0.048(3)	0.031(3)	0.051(3)	-0.002(2)	0.033(3)	-0.004(2)
C(20)	0.036(3)	0.026(2)	0.041(3)	-0.004(2)	0.017(2)	-0.006(2)
C(21)	0.030(3)	0.031(2)	0.025(2)	-0.002(2)	0.016(2)	-0.002(2)
C(22)	0.034(3)	0.048(3)	0.025(2)	-0.009(2)	0.020(2)	-0.008(2)
C(23)	0.031(3)	0.033(2)	0.026(2)	0.003(2)	0.016(2)	0.002(2)
C(24)	0.049(3)	0.033(3)	0.056(3)	0.002(2)	0.034(3)	-0.002(3)
C(25)	0.045(3)	0.044(3)	0.035(3)	0.007(2)	0.024(3)	-0.001(2)
C(26)	0.052(3)	0.044(3)	0.036(3)	0.014(3)	0.023(3)	0.002(2)

Table 4. Bond Lengths (Å) for {[DADMB]ZrCl₂}₂ (**3**).

atom	atom	distance	atom	atom	distance
Zr(1)	Cl(1)	2.412(1)	Zr(1)	Cl(2)	2.575(1)
Zr(1)	Cl(2)	2.733(1)	Zr(1)	N(1)	1.996(3)
Zr(1)	N(2)	2.063(3)	Zr(1)	C(1)	2.529(4)
Si(1)	N(1)	1.768(3)	Si(1)	C(15)	1.856(4)
Si(1)	C(16)	1.856(4)	Si(1)	C(17)	1.888(4)
Si(2)	N(2)	1.772(3)	Si(2)	C(21)	1.868(4)
Si(2)	C(22)	1.875(4)	Si(2)	C(23)	1.895(4)
N(1)	C(1)	1.441(5)	N(2)	C(8)	1.435(5)
C(1)	C(2)	1.414(5)	C(1)	C(6)	1.411(5)
C(2)	C(3)	1.375(6)	C(3)	C(4)	1.372(6)
C(4)	C(5)	1.400(6)	C(5)	C(6)	1.400(5)
C(5)	C(14)	1.509(6)	C(6)	C(7)	1.507(5)
C(7)	C(8)	1.401(5)	C(7)	C(12)	1.415(5)
C(8)	C(9)	1.400(6)	C(9)	C(10)	1.387(6)
C(10)	C(11)	1.386(6)	C(11)	C(12)	1.376(6)
C(12)	C(13)	1.513(6)	C(17)	C(18)	1.538(6)
C(17)	C(19)	1.528(6)	C(17)	C(20)	1.540(6)
C(23)	C(24)	1.545(6)	C(23)	C(25)	1.534(6)
C(23)	C(26)	1.546(6)			

Table 5. Bond Angles (°) for {[DADMB]ZrCl₂}₂ (**3**).

atom	atom	atom	angle	atom	atom	atom	angle
Cl(1)	Zr(1)	Cl(2)	132.85(4)	Cl(1)	Zr(1)	Cl(2)	84.17(4)
Cl(1)	Zr(1)	N(1)	104.51(9)	Cl(1)	Zr(1)	N(2)	96.56(9)
Cl(1)	Zr(1)	C(1)	139.16(9)	Cl(2)	Zr(1)	Cl(2)	74.59(3)
Cl(2)	Zr(1)	N(1)	119.18(9)	Cl(2)	Zr(1)	N(2)	95.14(9)
Cl(2)	Zr(1)	C(1)	86.21(9)	Cl(2)	Zr(1)	N(1)	96.56(9)
Cl(2)	Zr(1)	N(2)	166.01(9)	Cl(2)	Zr(1)	C(1)	98.69(9)
N(1)	Zr(1)	N(2)	96.8(1)	N(1)	Zr(1)	C(1)	34.7(1)
N(2)	Zr(1)	C(1)	89.9(1)	Zr(1)	Cl(2)	Zr(1)	105.41(3)
N(1)	Si(1)	C(15)	107.3(2)	N(1)	Si(1)	C(16)	108.3(2)
N(1)	Si(1)	C(17)	110.6(2)	C(15)	Si(1)	C(16)	109.6(2)
C(15)	Si(1)	C(17)	112.0(2)	C(16)	Si(1)	C(17)	109.0(2)
N(2)	Si(2)	C(21)	113.1(2)	N(2)	Si(2)	C(22)	106.6(2)

N(2)	Si(2)	C(23)	111.9(2)	C(21)	Si(2)	C(22)	104.6(2)
C(21)	Si(2)	C(23)	112.1(2)	C(22)	Si(2)	C(23)	108.0(2)
Zr(1)	N(1)	Si(1)	142.7(2)	Zr(1)	N(1)	C(1)	93.4(2)
Si(1)	N(1)	C(1)	123.6(3)	Zr(1)	N(2)	Si(2)	119.5(2)
Zr(1)	N(2)	C(8)	120.7(2)	Si(2)	N(2)	C(8)	119.2(3)
Zr(1)	C(1)	N(1)	52.0(2)	Zr(1)	C(1)	C(2)	110.7(3)
Zr(1)	C(1)	C(6)	101.1(3)	N(1)	C(1)	C(2)	119.1(3)
N(1)	C(1)	C(6)	120.8(3)	C(2)	C(1)	C(6)	119.9(4)
C(1)	C(2)	C(3)	119.9(4)	C(2)	C(3)	C(4)	120.5(4)
C(3)	C(4)	C(5)	121.0(4)	C(4)	C(5)	C(6)	119.8(4)
C(4)	C(5)	C(14)	117.9(4)	C(6)	C(5)	C(14)	122.3(4)
C(1)	C(6)	C(5)	118.8(4)	C(1)	C(6)	C(7)	119.4(4)
C(5)	C(6)	C(7)	121.7(4)	C(6)	C(7)	C(8)	121.5(4)
C(6)	C(7)	C(12)	119.1(4)	C(8)	C(7)	C(12)	119.4(4)
N(2)	C(8)	C(7)	121.1(4)	N(2)	C(8)	C(9)	119.9(4)
C(7)	C(8)	C(9)	119.1(4)	C(8)	C(9)	C(10)	120.9(4)
C(9)	C(10)	C(11)	119.7(4)	C(10)	C(11)	C(12)	120.7(4)
C(7)	C(12)	C(11)	120.1(4)	C(7)	C(12)	C(13)	121.9(4)
C(11)	C(12)	C(13)	118.0(4)	Si(1)	C(17)	C(18)	112.2(3)
Si(1)	C(17)	C(19)	109.2(3)	Si(1)	C(17)	C(20)	110.6(3)
C(18)	C(17)	C(19)	108.2(3)	C(18)	C(17)	C(20)	108.2(4)
C(19)	C(17)	C(20)	108.3(4)	Si(2)	C(23)	C(24)	114.1(3)
Si(2)	C(23)	C(25)	108.7(3)	Si(2)	C(23)	C(26)	109.2(3)
C(24)	C(23)	C(25)	107.5(4)	C(24)	C(23)	C(26)	108.4(4)
C(25)	C(23)	C(26)	108.8(4)				

Structural data for [DMBN]Zr(CH₂Ph)[η⁶-PhCH₂B(C₆F₅)₃] \cdot 3.5C₆H₆ (**7**).

Table 6. Atomic coordinates and B_{iso}/B_{eq} for [DMBN]Zr(CH₂Ph)[η⁶-PhCH₂B(C₆F₅)₃] \cdot 3.5C₆H₆ (**7**).

atom	x	y	z	B _{eq}
Zr(1)	0.05469(5)	0.25448(5)	0.32278(4)	1.96(2)
Si(1)	-0.0749(1)	0.3766(1)	0.1525(1)	2.56(5)
Si(2)	0.2366(1)	0.0210(1)	0.4027(1)	2.35(5)
F(1)	0.3860(3)	0.2973(2)	0.2673(2)	3.6(1)
F(2)	0.5297(3)	0.2677(3)	0.3387(2)	4.9(1)
F(3)	0.5665(3)	0.4123(3)	0.3503(2)	4.5(1)
F(4)	0.4558(3)	0.5906(3)	0.2846(2)	3.8(1)
F(5)	0.3026(3)	0.6239(2)	0.2207(2)	3.08(10)
F(6)	0.3931(3)	0.3698(2)	0.0911(2)	3.30(10)
F(7)	0.4752(3)	0.4170(3)	-0.0531(2)	3.9(1)
F(8)	0.4237(3)	0.5997(3)	-0.1223(2)	3.7(1)
F(9)	0.2837(3)	0.7351(3)	-0.0405(2)	3.5(1)
F(10)	0.1981(3)	0.6925(2)	0.1023(2)	2.91(9)
F(11)	0.1692(3)	0.5455(3)	0.3560(2)	3.30(10)
F(12)	-0.0093(3)	0.6694(3)	0.4090(2)	4.1(1)
F(13)	-0.1512(3)	0.7732(3)	0.3172(2)	4.5(1)
F(14)	-0.1103(3)	0.7404(3)	0.1715(2)	3.6(1)
F(15)	0.0661(3)	0.6132(2)	0.1171(2)	2.77(9)
N(1)	-0.0290(4)	0.2971(3)	0.2360(3)	2.0(1)
N(2)	0.1808(4)	0.1282(3)	0.3408(3)	2.1(1)
C(1)	-0.0214(5)	0.2035(4)	0.2430(3)	2.0(2)

C(2)	0.0730(5)	0.1313(4)	0.2329(3)	2.0(2)
C(3)	0.1701(5)	0.1476(4)	0.2080(4)	2.1(2)
C(4)	0.2243(5)	0.1398(4)	0.2604(3)	1.7(2)
C(5)	0.3174(5)	0.1503(4)	0.2350(4)	2.3(2)
C(6)	0.3539(5)	0.1718(4)	0.1584(4)	2.3(2)
C(7)	0.2984(5)	0.1834(4)	0.1024(4)	2.3(2)
C(8)	0.3349(5)	0.2063(4)	0.0225(4)	2.7(2)
C(9)	0.2830(6)	0.2118(5)	-0.0311(4)	3.6(2)
C(10)	0.1970(6)	0.1931(5)	-0.0077(4)	3.4(2)
C(11)	0.1606(5)	0.1710(5)	0.0696(4)	2.5(2)
C(12)	0.2085(5)	0.1676(4)	0.1256(4)	2.3(2)
C(13)	0.0811(5)	0.0370(4)	0.2402(3)	1.9(2)
C(14)	0.1746(5)	-0.0378(5)	0.2244(4)	2.5(2)
C(15)	0.1793(6)	-0.1266(5)	0.2290(4)	3.2(2)
C(16)	0.0911(6)	-0.1415(5)	0.2500(4)	3.3(2)
C(17)	-0.0005(6)	-0.0705(5)	0.2658(4)	3.1(2)
C(18)	-0.0086(5)	0.0209(4)	0.2610(4)	2.5(2)
C(19)	-0.1028(5)	0.0961(5)	0.2729(4)	2.4(2)
C(20)	-0.1103(5)	0.1853(5)	0.2640(4)	2.6(2)
C(21)	-0.1092(6)	0.3146(5)	0.0997(4)	3.6(2)
C(22)	0.0287(5)	0.4107(5)	0.0883(4)	2.7(2)
C(23)	-0.1949(5)	0.4872(5)	0.1704(4)	3.3(2)
C(24)	-0.2324(6)	0.5316(5)	0.0935(5)	4.0(2)
C(25)	-0.2765(6)	0.4614(5)	0.2308(5)	4.4(2)
C(26)	-0.1829(5)	0.5643(5)	0.1940(4)	3.7(2)
C(27)	0.1418(6)	-0.0326(4)	0.4430(4)	3.5(2)
C(28)	0.3490(5)	-0.0596(4)	0.3459(4)	3.0(2)
C(29)	0.2788(5)	0.0351(5)	0.4845(4)	2.7(2)
C(30)	0.1900(6)	0.0838(5)	0.5443(4)	3.6(2)
C(31)	0.3406(6)	-0.0639(5)	0.5270(4)	4.1(2)
C(32)	0.3500(6)	0.0878(5)	0.4537(4)	3.8(2)
C(33)	-0.0424(5)	0.2043(4)	0.4271(3)	2.3(2)
C(34)	-0.1442(5)	0.2535(4)	0.4729(4)	2.6(2)
C(35)	-0.1537(5)	0.2648(5)	0.5477(4)	2.4(2)
C(36)	-0.2482(6)	0.3012(5)	0.5938(4)	3.2(2)
C(37)	-0.3349(6)	0.3254(5)	0.5670(4)	3.3(2)
C(38)	-0.3278(6)	0.3152(5)	0.4928(4)	3.8(2)
C(39)	-0.2333(6)	0.2809(5)	0.4474(4)	3.4(2)
C(40)	0.2031(5)	0.4068(4)	0.2011(3)	2.1(2)
C(41)	0.1329(5)	0.3905(4)	0.2737(3)	2.2(2)
C(42)	0.1685(5)	0.3358(4)	0.3427(4)	2.7(2)
C(43)	0.0992(6)	0.3318(5)	0.4125(3)	2.3(2)
C(44)	-0.0035(5)	0.3785(5)	0.4145(4)	3.0(2)
C(45)	-0.0412(5)	0.4313(4)	0.3482(4)	2.6(2)
C(46)	0.0282(5)	0.4369(4)	0.2787(4)	2.1(2)
C(47)	0.3303(5)	0.4646(4)	0.2425(3)	2.0(2)
C(48)	0.3955(5)	0.3754(5)	0.2733(4)	2.5(2)
C(49)	0.4712(6)	0.3574(5)	0.3085(4)	3.7(2)
C(50)	0.4935(5)	0.4282(6)	0.3150(4)	3.2(2)
C(51)	0.4340(5)	0.5182(5)	0.2829(4)	2.9(2)
C(52)	0.3573(5)	0.5329(5)	0.2496(4)	2.3(2)
C(53)	0.2871(5)	0.5272(4)	0.1049(3)	1.8(2)
C(54)	0.3595(5)	0.4626(4)	0.0610(4)	2.0(2)
C(55)	0.4065(5)	0.4834(5)	-0.0132(4)	2.4(2)
C(56)	0.3802(6)	0.5767(5)	-0.0477(4)	2.6(2)
C(57)	0.3117(5)	0.6433(5)	-0.0072(4)	2.7(2)
C(58)	0.2650(5)	0.6201(4)	0.0670(3)	2.2(2)
C(59)	0.1322(5)	0.5760(4)	0.2306(3)	1.7(2)

C(60)	0.1037(5)	0.5936(5)	0.3062(4)	2.5(2)
C(61)	0.0109(5)	0.6561(5)	0.3349(4)	2.5(2)
C(62)	-0.0613(5)	0.7088(5)	0.2891(4)	2.8(2)
C(63)	-0.0386(5)	0.6924(4)	0.2150(4)	2.6(2)
C(64)	0.0537(5)	0.6277(4)	0.1898(3)	1.7(2)
C(65)	0.3092(9)	0.0601(7)	-0.2051(8)	7.6(4)
C(66)	0.2417(8)	0.0254(7)	-0.1575(6)	5.9(3)
C(67)	0.2541(8)	-0.0628(8)	-0.1589(5)	6.2(3)
C(68)	0.3365(8)	-0.1185(6)	-0.2040(6)	4.9(3)
C(69)	0.4034(7)	-0.0829(7)	-0.2511(6)	5.9(3)
C(70)	0.3904(8)	0.0063(7)	-0.2529(8)	9.0(4)
C(71)	-0.3044(9)	0.5501(9)	0.4822(8)	7.2(4)
C(72)	-0.278(1)	0.611(1)	0.4938(7)	10.0(6)
C(73)	-0.308(1)	0.698(1)	0.4515(9)	9.9(6)
C(74)	-0.361(1)	0.7231(9)	0.3975(10)	9.0(5)
C(75)	-0.3864(9)	0.659(1)	0.3801(6)	8.2(5)
C(76)	-0.356(1)	0.571(1)	0.4289(10)	7.0(4)
C(77)	0.4470(8)	-0.0794(10)	0.1149(9)	5.5(4)
C(78)	0.4004(9)	-0.0500(6)	0.0526(8)	5.2(3)
C(79)	0.3777(8)	-0.110(1)	0.0296(6)	6.8(3)
C(80)	0.4005(8)	-0.1985(9)	0.0707(9)	6.8(4)
C(81)	0.4439(9)	-0.2272(7)	0.1312(7)	5.1(3)
C(82)	0.4682(8)	-0.168(1)	0.1544(5)	5.9(3)
C(83)	-0.0123(7)	0.0899(6)	0.0001(5)	4.8(2)
C(84)	0.0533(7)	0.0120(7)	0.0422(5)	5.1(3)
C(85)	0.0669(7)	-0.0776(6)	0.0410(4)	4.8(2)
B(1)	0.2394(6)	0.4931(5)	0.1973(4)	2.0(2)
H(1)	0.355	0.142	0.272	2.712
H(2)	0.416	0.179	0.142	2.812
H(3)	0.395	0.218	0.006	3.263
H(4)	0.307	0.229	-0.084	4.278
H(5)	0.163	0.195	-0.045	4.127
H(6)	0.102	0.158	0.085	3.008
H(7)	0.235	-0.028	0.210	3.046
H(8)	0.243	-0.177	0.218	3.847
H(9)	0.095	-0.202	0.253	3.984
H(10)	-0.060	-0.082	0.280	3.769
H(11)	-0.163	0.085	0.288	2.901
H(12)	-0.175	0.235	0.272	3.111
H(13)	-0.051	0.261	0.086	4.305
H(14)	-0.133	0.356	0.055	4.305
H(15)	-0.161	0.296	0.132	4.305
H(16)	0.005	0.453	0.044	3.181
H(17)	0.048	0.440	0.115	3.181
H(18)	0.085	0.356	0.074	3.181
H(19)	-0.242	0.487	0.076	4.772
H(20)	-0.183	0.550	0.056	4.772
H(21)	-0.295	0.585	0.100	4.772
H(22)	-0.289	0.417	0.215	5.278
H(23)	-0.337	0.516	0.236	5.278
H(24)	-0.254	0.435	0.279	5.278
H(25)	-0.135	0.584	0.155	4.383
H(26)	-0.159	0.541	0.242	4.383
H(27)	-0.247	0.616	0.200	4.383
H(28)	0.170	-0.090	0.477	4.171
H(29)	0.083	0.009	0.471	4.171
H(30)	0.124	-0.044	0.402	4.171
H(31)	0.379	-0.117	0.379	3.603

H(32)	0.329	-0.070	0.306	3.603
H(33)	0.397	-0.032	0.324	3.603
H(34)	0.149	0.049	0.565	4.373
H(35)	0.215	0.087	0.585	4.373
H(36)	0.151	0.145	0.521	4.373
H(37)	0.365	-0.058	0.567	4.867
H(38)	0.298	-0.097	0.549	4.867
H(39)	0.397	-0.097	0.491	4.867
H(40)	0.407	0.054	0.419	4.608
H(41)	0.372	0.092	0.496	4.608
H(42)	0.315	0.149	0.427	4.608
H(43)	-0.051	0.158	0.411	2.803
H(44)	0.000	0.175	0.464	2.803
H(45)	-0.094	0.247	0.567	2.938
H(46)	-0.253	0.309	0.644	3.806
H(47)	-0.399	0.349	0.599	3.977
H(48)	-0.387	0.332	0.474	4.582
H(49)	-0.229	0.276	0.396	4.022
H(50)	0.262	0.350	0.197	2.512
H(51)	0.170	0.423	0.159	2.512
H(52)	0.239	0.302	0.342	3.198
H(53)	0.124	0.296	0.459	2.737
H(54)	-0.049	0.374	0.462	3.602
H(55)	-0.112	0.463	0.349	3.088
H(56)	0.002	0.474	0.233	2.524
H(57)	0.300	0.122	-0.205	9.092
H(58)	0.186	0.062	-0.123	7.122
H(59)	0.205	-0.086	-0.128	7.447
H(60)	0.347	-0.181	-0.202	5.823
H(61)	0.460	-0.121	-0.283	7.085
H(62)	0.437	0.031	-0.287	10.796
H(63)	-0.285	0.489	0.513	8.679
H(64)	-0.238	0.594	0.532	11.943
H(65)	-0.290	0.743	0.461	11.894
H(66)	-0.383	0.786	0.370	10.759
H(67)	-0.421	0.673	0.339	9.870
H(68)	-0.374	0.525	0.423	8.408
H(69)	0.464	-0.038	0.130	6.570
H(70)	0.384	0.013	0.025	6.217
H(71)	0.347	-0.090	-0.014	8.218
H(72)	0.385	-0.241	0.055	8.204
H(73)	0.458	-0.289	0.159	6.171
H(74)	0.500	-0.189	0.198	7.039
H(75)	0.089	0.021	0.072	6.113

$$B_{eq} = 8/3 \pi^2 (U_{11}(aa^*)^2 + U_{22}(bb^*)^2 + U_{33}(cc^*)^2 + 2U_{12}(aa^*bb^*)\cos \gamma + 2U_{13}(aa^*cc^*)\cos \beta + 2U_{23}(bb^*cc^*)\cos \alpha)$$

Table 7. Anisotropic Displacement Parameters
for [DMBN]Zr(CH₂Ph)[η^6 -PhCH₂B(C₆F₅)₃] \cdot 3.5C₆H₆ (7).

atom	U ₁₁	U ₂₂	U ₃₃	U ₁₂	U ₁₃	U ₂₃
Zr(1)	0.0324(4)	0.0225(4)	0.0236(4)	-0.0166(3)	-0.0025(3)	0.0026(3)
Si(1)	0.035(1)	0.033(1)	0.030(1)	-0.019(1)	-0.0095(10)	0.0069(9)
Si(2)	0.036(1)	0.025(1)	0.028(1)	-0.0147(10)	-0.0028(9)	0.0021(9)
F(1)	0.044(3)	0.028(2)	0.060(3)	-0.013(2)	-0.017(2)	0.008(2)
F(2)	0.051(3)	0.056(3)	0.069(3)	-0.019(3)	-0.028(3)	0.024(2)
F(3)	0.052(3)	0.089(4)	0.047(3)	-0.042(3)	-0.023(2)	0.010(2)
F(4)	0.051(3)	0.065(3)	0.047(3)	-0.040(2)	0.000(2)	-0.019(2)
F(5)	0.037(2)	0.032(2)	0.050(2)	-0.020(2)	-0.005(2)	-0.005(2)
F(6)	0.042(3)	0.027(2)	0.050(2)	-0.013(2)	0.001(2)	-0.007(2)
F(7)	0.042(3)	0.054(3)	0.050(3)	-0.021(2)	0.008(2)	-0.022(2)
F(8)	0.058(3)	0.071(3)	0.024(2)	-0.038(3)	0.007(2)	0.001(2)
F(9)	0.060(3)	0.038(3)	0.042(2)	-0.030(2)	-0.006(2)	0.014(2)
F(10)	0.049(3)	0.020(2)	0.036(2)	-0.016(2)	0.005(2)	-0.001(2)
F(11)	0.041(3)	0.055(3)	0.024(2)	-0.024(2)	-0.006(2)	0.000(2)
F(12)	0.053(3)	0.079(3)	0.031(2)	-0.029(3)	0.004(2)	-0.024(2)
F(13)	0.042(3)	0.062(3)	0.055(3)	-0.008(2)	-0.001(2)	-0.028(2)
F(14)	0.043(3)	0.044(3)	0.044(3)	-0.009(2)	-0.013(2)	-0.007(2)
F(15)	0.039(2)	0.038(2)	0.023(2)	-0.013(2)	-0.008(2)	-0.001(2)
N(1)	0.026(3)	0.024(3)	0.028(3)	-0.016(3)	-0.001(3)	-0.003(2)
N(2)	0.033(3)	0.021(3)	0.020(3)	-0.014(3)	0.001(3)	0.002(2)
C(1)	0.034(5)	0.024(4)	0.020(4)	-0.015(4)	-0.006(3)	0.000(3)
C(2)	0.030(4)	0.029(4)	0.019(4)	-0.021(4)	0.006(3)	0.000(3)
C(3)	0.028(4)	0.016(4)	0.032(4)	-0.014(3)	0.002(3)	-0.003(3)
C(4)	0.029(4)	0.016(4)	0.025(4)	-0.008(3)	-0.003(3)	-0.001(3)
C(5)	0.027(4)	0.019(4)	0.031(4)	-0.009(3)	-0.001(3)	-0.002(3)
C(6)	0.030(4)	0.019(4)	0.035(4)	-0.012(3)	0.000(3)	-0.004(3)
C(7)	0.039(5)	0.014(4)	0.028(4)	-0.012(3)	0.003(3)	0.001(3)
C(8)	0.038(5)	0.025(4)	0.034(4)	-0.008(4)	0.009(4)	-0.004(3)
C(9)	0.061(6)	0.037(5)	0.024(4)	-0.021(4)	0.006(4)	-0.001(3)
C(10)	0.050(5)	0.038(5)	0.025(4)	-0.011(4)	-0.008(4)	0.000(3)
C(11)	0.042(5)	0.033(4)	0.030(4)	-0.017(4)	-0.008(4)	0.007(3)
C(12)	0.034(4)	0.016(4)	0.026(4)	-0.009(3)	-0.003(3)	0.003(3)
C(13)	0.033(4)	0.025(4)	0.024(4)	-0.016(4)	-0.005(3)	-0.001(3)
C(14)	0.042(5)	0.031(4)	0.032(4)	-0.020(4)	0.003(3)	-0.005(3)
C(15)	0.048(5)	0.030(5)	0.050(5)	-0.024(4)	0.003(4)	-0.004(4)
C(16)	0.059(6)	0.033(5)	0.043(5)	-0.027(5)	0.000(4)	-0.003(4)
C(17)	0.048(5)	0.045(5)	0.033(4)	-0.030(5)	0.004(4)	-0.004(4)
C(18)	0.044(5)	0.023(4)	0.029(4)	-0.020(4)	-0.005(4)	0.001(3)
C(19)	0.036(5)	0.035(5)	0.032(4)	-0.027(4)	-0.003(3)	-0.002(3)
C(20)	0.024(4)	0.038(4)	0.034(4)	-0.014(4)	-0.001(3)	-0.010(3)
C(21)	0.049(5)	0.052(5)	0.035(4)	-0.024(4)	-0.016(4)	0.006(4)
C(22)	0.050(5)	0.036(4)	0.029(4)	-0.025(4)	-0.017(4)	0.006(3)
C(23)	0.039(5)	0.038(5)	0.045(5)	-0.026(4)	-0.008(4)	0.010(4)
C(24)	0.053(6)	0.040(5)	0.073(6)	-0.021(4)	-0.035(5)	0.011(4)
C(25)	0.039(5)	0.040(5)	0.095(7)	-0.011(4)	0.005(5)	0.001(5)
C(26)	0.038(5)	0.037(5)	0.055(5)	-0.001(4)	-0.016(4)	0.003(4)
C(27)	0.057(5)	0.022(4)	0.050(5)	-0.022(4)	-0.005(4)	0.011(4)
C(28)	0.047(5)	0.024(4)	0.049(5)	-0.012(4)	-0.013(4)	-0.004(4)
C(29)	0.041(5)	0.027(4)	0.043(5)	-0.015(4)	-0.010(4)	0.006(4)
C(30)	0.084(7)	0.037(5)	0.035(5)	-0.027(5)	-0.011(4)	-0.001(4)
C(31)	0.071(6)	0.047(5)	0.051(5)	-0.016(5)	-0.034(5)	0.005(4)
C(32)	0.073(6)	0.048(5)	0.061(6)	-0.031(5)	-0.034(5)	0.004(4)
C(33)	0.036(4)	0.028(4)	0.030(4)	-0.021(4)	0.000(3)	0.003(3)

C(34)	0.037(5)	0.019(4)	0.033(4)	-0.014(3)	-0.009(4)	0.011(3)
C(35)	0.038(5)	0.031(4)	0.041(5)	-0.023(4)	-0.006(4)	-0.005(4)
C(36)	0.038(5)	0.051(5)	0.035(4)	-0.019(4)	0.007(4)	-0.012(4)
C(37)	0.045(5)	0.050(5)	0.041(5)	-0.020(4)	0.008(4)	-0.010(4)
C(38)	0.032(5)	0.055(5)	0.042(5)	-0.008(4)	0.000(4)	-0.008(4)
C(39)	0.057(6)	0.044(5)	0.024(4)	-0.021(4)	-0.007(4)	0.006(4)
C(40)	0.029(4)	0.025(4)	0.029(4)	-0.009(3)	-0.008(3)	-0.002(3)
C(41)	0.036(4)	0.022(4)	0.019(4)	-0.017(3)	-0.007(3)	0.003(3)
C(42)	0.036(4)	0.033(4)	0.033(4)	-0.021(4)	-0.007(4)	-0.006(3)
C(43)	0.045(5)	0.035(4)	0.019(4)	-0.023(4)	-0.008(4)	0.001(3)
C(44)	0.039(5)	0.034(4)	0.035(4)	-0.024(4)	0.005(4)	-0.006(4)
C(45)	0.034(4)	0.024(4)	0.032(4)	-0.017(3)	-0.004(3)	-0.004(3)
C(46)	0.042(5)	0.013(4)	0.035(4)	-0.015(3)	-0.012(4)	0.006(3)
C(47)	0.028(4)	0.027(4)	0.018(4)	-0.014(3)	0.000(3)	0.003(3)
C(48)	0.038(5)	0.032(5)	0.042(4)	-0.025(4)	-0.009(4)	0.002(4)
C(49)	0.040(5)	0.043(5)	0.038(5)	-0.014(4)	-0.015(4)	0.013(4)
C(50)	0.033(5)	0.068(6)	0.023(4)	-0.025(5)	-0.010(4)	0.002(4)
C(51)	0.032(5)	0.054(5)	0.027(4)	-0.028(4)	0.009(4)	-0.016(4)
C(52)	0.030(4)	0.030(4)	0.026(4)	-0.016(4)	-0.003(3)	0.001(3)
C(53)	0.039(5)	0.023(4)	0.025(4)	-0.020(4)	-0.009(3)	0.002(3)
C(54)	0.037(4)	0.022(4)	0.031(4)	-0.018(4)	-0.002(3)	-0.009(3)
C(55)	0.027(4)	0.036(5)	0.037(4)	-0.013(4)	0.008(4)	-0.017(4)
C(56)	0.046(5)	0.050(5)	0.021(4)	-0.033(4)	0.009(4)	-0.006(4)
C(57)	0.035(5)	0.031(5)	0.036(4)	-0.020(4)	-0.008(4)	0.006(4)
C(58)	0.036(4)	0.026(4)	0.021(4)	-0.013(4)	0.003(3)	-0.003(3)
C(59)	0.031(4)	0.024(4)	0.024(4)	-0.022(3)	-0.003(3)	0.003(3)
C(60)	0.029(4)	0.038(4)	0.026(4)	-0.023(4)	-0.009(4)	0.005(3)
C(61)	0.035(5)	0.047(5)	0.024(4)	-0.025(4)	0.003(4)	-0.013(4)
C(62)	0.025(4)	0.037(5)	0.049(5)	-0.009(4)	0.000(4)	-0.015(4)
C(63)	0.033(5)	0.023(4)	0.033(4)	-0.005(4)	-0.016(4)	-0.003(3)
C(64)	0.046(5)	0.020(4)	0.020(4)	-0.022(4)	-0.006(3)	-0.002(3)
C(65)	0.058(8)	0.042(6)	0.20(1)	-0.012(6)	-0.008(8)	-0.025(8)
C(66)	0.095(9)	0.049(7)	0.088(8)	-0.022(6)	-0.006(6)	-0.011(6)
C(67)	0.107(9)	0.085(8)	0.045(6)	-0.053(7)	0.017(6)	-0.002(5)
C(68)	0.089(8)	0.048(6)	0.078(7)	-0.035(6)	-0.016(6)	-0.010(5)
C(69)	0.053(7)	0.055(7)	0.111(8)	-0.011(5)	-0.012(6)	-0.013(6)
C(70)	0.046(7)	0.050(7)	0.23(1)	-0.014(6)	0.024(8)	-0.003(8)
C(71)	0.089(9)	0.078(9)	0.12(1)	-0.041(7)	-0.022(8)	0.040(8)
C(72)	0.27(2)	0.18(2)	0.078(9)	-0.17(2)	-0.07(1)	0.035(9)
C(73)	0.26(2)	0.10(1)	0.13(1)	-0.11(1)	-0.06(1)	0.007(9)
C(74)	0.12(1)	0.090(10)	0.16(1)	-0.052(8)	-0.06(1)	0.071(10)
C(75)	0.077(9)	0.21(2)	0.076(8)	-0.09(1)	-0.023(7)	0.016(10)
C(76)	0.09(1)	0.10(1)	0.13(1)	-0.067(9)	0.004(8)	-0.043(9)
C(77)	0.052(7)	0.082(9)	0.12(1)	-0.036(7)	0.040(7)	-0.071(8)
C(78)	0.090(9)	0.025(6)	0.098(9)	-0.009(6)	0.021(7)	-0.008(6)
C(79)	0.079(8)	0.087(9)	0.080(8)	-0.003(7)	-0.026(6)	-0.009(7)
C(80)	0.065(8)	0.070(9)	0.13(1)	-0.036(7)	0.010(7)	-0.041(8)
C(81)	0.077(9)	0.054(7)	0.078(8)	-0.028(6)	0.022(6)	0.008(6)
C(82)	0.061(7)	0.12(1)	0.043(6)	-0.009(8)	0.015(5)	-0.025(7)
C(83)	0.095(8)	0.045(6)	0.050(5)	-0.034(6)	-0.010(5)	-0.008(5)
C(84)	0.102(8)	0.063(7)	0.065(6)	-0.037(6)	-0.039(6)	-0.005(5)
C(85)	0.090(7)	0.047(6)	0.039(5)	-0.020(5)	-0.006(5)	-0.011(4)
B(1)	0.032(5)	0.025(4)	0.018(4)	-0.016(4)	0.000(4)	-0.001(3)

The general temperature factor expression:

$$\exp(-2\pi^2(a^*2U_{11}h^2 + b^*2U_{22}k^2 + c^*2U_{33}l^2 + 2a^*b^*U_{12}hk + 2a^*c^*U_{13}hl + 2b^*c^*U_{23}kl))$$

Table 8. Bond Lengths (Å) for [DMBN]Zr(CH₂Ph)[η⁶-PhCH₂B(C₆F₅)₃]·3.5C₆H₆ (7).

atom	atom	distance	atom	atom	distance
Zr(1)	N(1)	2.083(5)	Zr(1)	N(2)	2.094(5)
Zr(1)	C(1)	2.576(6)	Zr(1)	C(4)	2.558(6)
Zr(1)	C(33)	2.250(6)	Si(1)	N(1)	1.786(5)
Si(1)	C(21)	1.876(7)	Si(1)	C(22)	1.866(7)
Si(1)	C(23)	1.915(7)	Si(2)	N(2)	1.773(5)
Si(2)	C(27)	1.868(7)	Si(2)	C(28)	1.852(7)
Si(2)	C(29)	1.892(7)	F(1)	C(48)	1.376(7)
F(2)	C(49)	1.368(8)	F(3)	C(50)	1.323(7)
F(4)	C(51)	1.365(7)	F(5)	C(52)	1.362(7)
F(6)	C(54)	1.355(7)	F(7)	C(55)	1.333(7)
F(8)	C(56)	1.365(7)	F(9)	C(57)	1.359(7)
F(10)	C(58)	1.346(7)	F(11)	C(60)	1.355(7)
F(12)	C(61)	1.365(7)	F(13)	C(62)	1.350(7)
F(14)	C(63)	1.339(7)	F(15)	C(64)	1.368(7)
N(1)	C(1)	1.444(7)	N(2)	C(4)	1.431(7)
C(1)	C(2)	1.377(8)	C(1)	C(20)	1.419(9)
C(2)	C(3)	1.518(8)	C(2)	C(13)	1.452(8)
C(3)	C(4)	1.377(8)	C(3)	C(12)	1.457(8)
C(4)	C(5)	1.415(8)	C(5)	C(6)	1.363(8)
C(6)	C(7)	1.425(9)	C(7)	C(8)	1.419(8)
C(7)	C(12)	1.410(9)	C(8)	C(9)	1.382(10)
C(9)	C(10)	1.382(10)	C(10)	C(11)	1.375(9)
C(11)	C(12)	1.391(9)	C(13)	C(14)	1.402(9)
C(13)	C(18)	1.413(9)	C(14)	C(15)	1.391(9)
C(15)	C(16)	1.382(9)	C(16)	C(17)	1.356(10)
C(17)	C(18)	1.414(9)	C(18)	C(19)	1.401(9)
C(19)	C(20)	1.367(9)	C(23)	C(24)	1.532(9)
C(23)	C(25)	1.529(9)	C(23)	C(26)	1.533(10)
C(29)	C(30)	1.523(10)	C(29)	C(31)	1.557(9)
C(29)	C(32)	1.550(10)	C(33)	C(34)	1.493(9)
C(34)	C(35)	1.396(9)	C(34)	C(39)	1.383(9)
C(35)	C(36)	1.387(9)	C(36)	C(37)	1.373(10)
C(37)	C(38)	1.389(10)	C(38)	C(39)	1.378(9)
C(40)	C(41)	1.487(8)	C(40)	B(1)	1.698(9)
C(41)	C(42)	1.418(8)	C(41)	C(46)	1.393(9)
C(42)	C(43)	1.408(8)	C(43)	C(44)	1.373(9)
C(44)	C(45)	1.382(9)	C(45)	C(46)	1.410(8)
C(47)	C(48)	1.400(9)	C(47)	C(52)	1.390(9)
C(47)	B(1)	1.623(9)	C(48)	C(49)	1.346(9)
C(49)	C(50)	1.377(10)	C(50)	C(51)	1.387(9)
C(51)	C(52)	1.354(9)	C(53)	C(54)	1.374(9)
C(53)	C(58)	1.401(8)	C(53)	B(1)	1.684(9)
C(54)	C(55)	1.372(8)	C(55)	C(56)	1.385(9)
C(56)	C(57)	1.341(9)	C(57)	C(58)	1.377(8)
C(59)	C(60)	1.403(8)	C(59)	C(64)	1.384(8)
C(59)	B(1)	1.653(10)	C(60)	C(61)	1.364(9)
C(61)	C(62)	1.377(9)	C(62)	C(63)	1.378(9)
C(63)	C(64)	1.356(8)	C(65)	C(66)	1.36(1)
C(65)	C(70)	1.37(1)	C(66)	C(67)	1.37(1)
C(67)	C(68)	1.37(1)	C(68)	C(69)	1.36(1)
C(69)	C(70)	1.37(1)	C(71)	C(72)	1.30(2)

C(71)	C(76)	1.30(2)	C(72)	C(73)	1.35(2)
C(73)	C(74)	1.31(2)	C(74)	C(75)	1.40(2)
C(75)	C(76)	1.41(2)	C(77)	C(78)	1.37(1)
C(77)	C(82)	1.36(1)	C(78)	C(79)	1.36(1)
C(79)	C(80)	1.36(1)	C(80)	C(81)	1.31(1)
C(81)	C(82)	1.37(1)	C(83)	C(84)	1.39(1)
C(83)	C(85)	1.37(1)	C(84)	C(85)	1.38(1)

Table 9. Bond Angles ($^{\circ}$) for [DMBN]Zr(CH₂Ph)[η^6 -PhCH₂B(C₆F₅)₃] \cdot 3.5C₆H₆ (**7**).

atom	atom	atom	angle	atom	atom	atom	angle
N(1)	Zr(1)	N(2)	126.1(2)	N(1)	Zr(1)	C(1)	34.1(2)
N(1)	Zr(1)	C(4)	100.3(2)	N(1)	Zr(1)	C(33)	103.1(2)
N(2)	Zr(1)	C(1)	97.8(2)	N(2)	Zr(1)	C(4)	34.0(2)
N(2)	Zr(1)	C(33)	91.1(2)	C(1)	Zr(1)	C(4)	84.2(2)
C(1)	Zr(1)	C(33)	86.3(2)	C(4)	Zr(1)	C(33)	121.2(2)
N(1)	Si(1)	C(21)	108.3(3)	N(1)	Si(1)	C(22)	108.7(3)
N(1)	Si(1)	C(23)	116.4(3)	C(21)	Si(1)	C(22)	108.8(3)
C(21)	Si(1)	C(23)	105.1(3)	C(22)	Si(1)	C(23)	109.3(3)
N(2)	Si(2)	C(27)	108.0(3)	N(2)	Si(2)	C(28)	109.3(3)
N(2)	Si(2)	C(29)	113.4(3)	C(27)	Si(2)	C(28)	108.4(3)
C(27)	Si(2)	C(29)	109.5(3)	C(28)	Si(2)	C(29)	108.0(3)
Zr(1)	N(1)	Si(1)	150.8(3)	Zr(1)	N(1)	C(1)	92.0(3)
Si(1)	N(1)	C(1)	114.6(4)	Zr(1)	N(2)	Si(2)	148.2(3)
Zr(1)	N(2)	C(4)	91.0(3)	Si(2)	N(2)	C(4)	119.7(4)
Zr(1)	C(1)	N(1)	53.9(3)	Zr(1)	C(1)	C(2)	85.0(4)
Zr(1)	C(1)	C(20)	129.4(4)	N(1)	C(1)	C(2)	119.3(6)
N(1)	C(1)	C(20)	120.3(6)	C(2)	C(1)	C(20)	120.3(6)
C(1)	C(2)	C(3)	122.3(6)	C(1)	C(2)	C(13)	119.6(6)
C(3)	C(2)	C(13)	118.0(6)	C(2)	C(3)	C(4)	122.1(5)
C(2)	C(3)	C(12)	118.2(6)	C(4)	C(3)	C(12)	119.7(6)
Zr(1)	C(4)	N(2)	54.9(3)	Zr(1)	C(4)	C(3)	84.3(4)
Zr(1)	C(4)	C(5)	127.4(4)	N(2)	C(4)	C(3)	118.6(6)
N(2)	C(4)	C(5)	120.7(6)	C(3)	C(4)	C(5)	120.5(6)
C(4)	C(5)	C(6)	121.1(6)	C(5)	C(6)	C(7)	120.0(6)
C(6)	C(7)	C(8)	120.7(6)	C(6)	C(7)	C(12)	120.2(6)
C(8)	C(7)	C(12)	119.0(6)	C(7)	C(8)	C(9)	119.7(7)
C(8)	C(9)	C(10)	120.7(6)	C(9)	C(10)	C(11)	120.1(7)
C(10)	C(11)	C(12)	121.2(7)	C(3)	C(12)	C(7)	118.2(6)
C(3)	C(12)	C(11)	122.6(6)	C(7)	C(12)	C(11)	119.2(6)
C(2)	C(13)	C(14)	122.1(6)	C(2)	C(13)	C(18)	118.9(6)
C(14)	C(13)	C(18)	119.0(6)	C(13)	C(14)	C(15)	120.7(6)
C(14)	C(15)	C(16)	119.8(7)	C(15)	C(16)	C(17)	120.8(7)
C(16)	C(17)	C(18)	121.1(7)	C(13)	C(18)	C(17)	118.6(6)
C(13)	C(18)	C(19)	119.5(6)	C(17)	C(18)	C(19)	121.9(6)
C(18)	C(19)	C(20)	121.5(6)	C(1)	C(20)	C(19)	120.2(6)
Si(1)	C(23)	C(24)	106.5(5)	Si(1)	C(23)	C(25)	110.1(5)
Si(1)	C(23)	C(26)	116.9(5)	C(24)	C(23)	C(25)	109.1(6)
C(24)	C(23)	C(26)	105.4(6)	C(25)	C(23)	C(26)	108.5(6)
Si(2)	C(29)	C(30)	112.6(5)	Si(2)	C(29)	C(31)	108.6(5)
Si(2)	C(29)	C(32)	111.2(5)	C(30)	C(29)	C(31)	106.8(6)
C(30)	C(29)	C(32)	110.2(6)	C(31)	C(29)	C(32)	107.2(6)
Zr(1)	C(33)	C(34)	132.7(4)	C(33)	C(34)	C(35)	120.7(6)

C(33)	C(34)	C(39)	122.3(6)	C(35)	C(34)	C(39)	116.7(7)
C(34)	C(35)	C(36)	121.2(6)	C(35)	C(36)	C(37)	120.4(7)
C(36)	C(37)	C(38)	119.8(7)	C(37)	C(38)	C(39)	118.9(7)
C(34)	C(39)	C(38)	123.1(7)	C(41)	C(40)	B(1)	113.5(5)
C(40)	C(41)	C(42)	122.0(6)	C(40)	C(41)	C(46)	120.8(5)
C(42)	C(41)	C(46)	116.9(6)	C(41)	C(42)	C(43)	120.1(6)
C(42)	C(43)	C(44)	120.9(6)	C(43)	C(44)	C(45)	120.7(6)
C(44)	C(45)	C(46)	118.4(6)	C(41)	C(46)	C(45)	122.9(6)
C(48)	C(47)	C(52)	110.7(6)	C(48)	C(47)	B(1)	128.9(6)
C(52)	C(47)	B(1)	120.3(6)	F(1)	C(48)	C(47)	119.9(6)
F(1)	C(48)	C(49)	114.9(6)	C(47)	C(48)	C(49)	125.3(7)
F(2)	C(49)	C(48)	121.2(7)	F(2)	C(49)	C(50)	117.4(7)
C(48)	C(49)	C(50)	121.4(7)	F(3)	C(50)	C(49)	122.4(7)
F(3)	C(50)	C(51)	121.3(7)	C(49)	C(50)	C(51)	116.2(7)
F(4)	C(51)	C(50)	118.7(6)	F(4)	C(51)	C(52)	121.2(7)
C(50)	C(51)	C(52)	120.2(7)	F(5)	C(52)	C(47)	118.2(6)
F(5)	C(52)	C(51)	115.6(6)	C(47)	C(52)	C(51)	126.1(7)
C(54)	C(53)	C(58)	113.4(6)	C(54)	C(53)	B(1)	120.7(5)
C(58)	C(53)	B(1)	125.7(6)	F(6)	C(54)	C(53)	120.5(5)
F(6)	C(54)	C(55)	114.3(6)	C(53)	C(54)	C(55)	125.2(6)
F(7)	C(55)	C(54)	122.1(6)	F(7)	C(55)	C(56)	119.5(6)
C(54)	C(55)	C(56)	118.4(6)	F(8)	C(56)	C(55)	119.8(7)
F(8)	C(56)	C(57)	120.9(6)	C(55)	C(56)	C(57)	119.3(6)
F(9)	C(57)	C(56)	120.1(6)	F(9)	C(57)	C(58)	118.9(6)
C(56)	C(57)	C(58)	120.9(6)	F(10)	C(58)	C(53)	121.4(5)
F(10)	C(58)	C(57)	115.8(6)	C(53)	C(58)	C(57)	122.8(6)
C(60)	C(59)	C(64)	111.7(6)	C(60)	C(59)	B(1)	124.7(6)
C(64)	C(59)	B(1)	123.0(5)	F(11)	C(60)	C(59)	120.0(6)
F(11)	C(60)	C(61)	116.1(6)	C(59)	C(60)	C(61)	123.9(6)
F(12)	C(61)	C(60)	119.6(6)	F(12)	C(61)	C(62)	119.5(6)
C(60)	C(61)	C(62)	120.8(6)	F(13)	C(62)	C(61)	120.3(6)
F(13)	C(62)	C(63)	122.0(6)	C(61)	C(62)	C(63)	117.8(7)
F(14)	C(63)	C(62)	118.0(6)	F(14)	C(63)	C(64)	122.9(6)
C(62)	C(63)	C(64)	119.1(6)	F(15)	C(64)	C(59)	119.2(6)
F(15)	C(64)	C(63)	114.3(6)	C(59)	C(64)	C(63)	126.5(6)
C(66)	C(65)	C(70)	120.3(9)	C(65)	C(66)	C(67)	119.3(9)
C(66)	C(67)	C(68)	121.1(9)	C(67)	C(68)	C(69)	118.7(9)
C(68)	C(69)	C(70)	121.2(9)	C(65)	C(70)	C(69)	119.3(9)
C(72)	C(71)	C(76)	121(1)	C(71)	C(72)	C(73)	119(1)
C(72)	C(73)	C(74)	121(1)	C(73)	C(74)	C(75)	120(1)
C(74)	C(75)	C(76)	113(1)	C(71)	C(76)	C(75)	122(1)
C(78)	C(77)	C(82)	119(1)	C(77)	C(78)	C(79)	120.4(10)
C(78)	C(79)	C(80)	118(1)	C(79)	C(80)	C(81)	121(1)
C(80)	C(81)	C(82)	120(1)	C(77)	C(82)	C(81)	119(1)
C(84)	C(83)	C(85)	119.3(7)	C(83)	C(84)	C(85)	121.0(8)
C(83)	C(85)	C(84)	119.6(8)	C(40)	B(1)	C(47)	116.4(5)
C(40)	B(1)	C(53)	108.7(5)	C(40)	B(1)	C(59)	102.9(5)
C(47)	B(1)	C(53)	103.5(5)	C(47)	B(1)	C(59)	113.3(5)
C(53)	B(1)	C(59)	112.3(5)				

Table 10. Least Squares Planes for [DMBN]Zr(CH₂Ph)[η^6 -PhCH₂B(C₆F₅)₃] \cdot 3.5C₆H₆ (7).

Atoms defining plane

Distance

C(41)	0.003(6)
C(42)	-0.009(6)
C(43)	0.007(6)
C(44)	0.002(7)
C(45)	-0.007(6)
C(46)	0.004(6)
Additional Atoms	Distance
Zr(1)	-2.325
mean deviation	χ^2
0.0055	5.8